Early Palaeogene planktic foraminiferal assemblages in Australasian sequences: links to past changes in climate and carbon cycling.

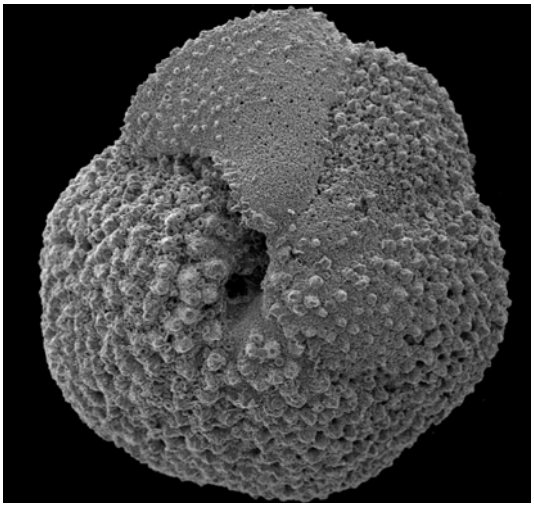

SEM micrograph of the Late Paleocene

planktic foraminifera Igorina albeari

Thesis submitted by

Haidi Jean Louise HANCOCK BVA *University of Newcastle*, BSc *University of Newcastle*, BSc (Honours) *James Cook University*

in April, 2005

Thesis submitted in partial fulfilment of the requirements for the

Degree of Doctor of Philosophy in the Department of Earth Sciences at James Cook University of North Queensland.

STATEMENT OF ACCESS

I, the undersigned, the author of this thesis, understand that James Cook University of North Queensland will make it available for use within the University Library and, by microfilm or other means, allow access to users in other approved libraries. All users consulting this thesis will have to sign the following statement:

> In consulting this thesis I agree not to copy or closely paraphrase it in whole or in part without the written consent of the author; and to make proper public written acknowledgment for any assistance which I have obtained from it.

Substantial portions of this thesis may be submitted for publication by my primary thesis supervisor (Dr Gerald Dickens) as long as I am given first authorship.

Beyond this, I do not wish to place any restriction on access to this thesis.

…… ……

(……..) *(Date)*

STATEMENT OF SOURCES DECLARATION

I declare that this thesis is my own work and has not been submitted in any form for another degree or diploma at any university or other institution of tertiary education. Information derived from the published or unpublished work of others has been acknowledged in the text and a list of references is given.

…… ……

(……..) *(Date)*

STATEMENT OF SOURCES DECLARATION (ELECTRONIC COPY)

I, the undersigned, the author of this work, declare that the electronic copy of this thesis provided to the James Cook University Library is an accurate copy of the print thesis submitted, within the limits of the technology available.

…… ……

(……..) *(Date)*

PREFACE

In August/October, 2001, I sailed as a scientist/sedimentologist on the *JOIDES Resolution* Ocean Drilling Program Leg 198 to the Shatsky Rise, central-west Pacific. The cruise objectives targeted rapid intervals of global warming in the generally warm periods of the Cretaceous and Palaeogene, with obvious applications to modern climate problems. This thesis contributes a new body of knowledge derived from a dataset acquired during Leg 198, which documents carbonate dissolution episodes in the Paleocene and Eocene and is a major contribution to the leg's objectives. Furthermore, it represents the first study of this kind focused on the Paleocene and Eocene.

Two consecutive field seasons were spent with the New Zealand geological survey logging stream sections and collecting samples from early Palaeogene strata in the Clarence Valley, Marlborough, south island of New Zealand. Specific skills exercised included field mapping and targeting techniques in mountainous terrain, section logging, magnetometer reading, hard rock sample collection for planktic foraminiferal biostratigraphy and isotope analysis and working within a tight-knit team of professionals. One month after each of two field seasons was spend at the Institute of Geological and Nuclear Sciences (IGNS), Lower Hutt (NZ) laboratories preparing hard rock samples for foraminifera and isotope analysis and working with other members of the palaeontological department on the Marlborough projects.

A three month summer project was undertaken at the Woods Hole Oceanographic Institute (WHOI), Massachusetts, (US) with Dr. Richard Norris investigating a coiling reversal in the Late Paleocene planktic foraminifera *Igorina albeari.* In the process I learnt to identify critical Late Paleocene planktic foraminifera under key workers in the field, including researchers affiliated with petroleum companies.

The publication "Early Palaeogene planktic foraminiferal and carbon isotope stratigraphy, Hole 762C, Exmouth Plateau, northwest Australian margin", is based on a

dataset collected for my BSc (Honours) thesis. However, minor additions were made to the data set as well preparing a manuscript for publication as part of my doctoral program. Consequently the published paper is included with this thesis as an appendix.

ACKNOWLEDGMENTS

Thanks go to my primary and secondary PhD supervisors, Gerald Dickens and Robert Henderson, for their continual encouragement, guidance, support, discussions and reviews related to chapters in this thesis. Thanks go to the IGNS Marlborough Project members: Chris Hollis, Percy Strong, and Brad Field, for their field support and for making facilities available at the Lower Hutt laboratories. Thanks go to the ODP for giving me a berth as a scientist on Leg 198 to the Shatsky Rise, and to all of the crew members, especially the co-chiefs Tim Bralower, Isabella Premoli-Silva and chief scientist Mitch Malone. Thanks go to WHOI for providing me with a three month internship and use of facilities and to Richard Norris for project guidance and discussions. Thanks go to Ellen Thomas for helpful discussions and benthic foraminiferal identifications. William Berggren, Brian Huber, Richard Olsson, Frederique Quillevere are also thanked for their invaluable help with planktic foraminiferal species identifications.

This PhD was funded by the James Cook University (JCU) Prestigious Postgraduate Research Scholarship, the JCU Doctoral Merit Research Scheme (WHOI project), and a JCU completion scholarship. The Dee Stream project was funded by student grants from the Mid-American Paleontological Society (MAPS), Paleontological Society, and the *Journal of Foraminiferal Research*, Palaeobiology Department, Smithsonian Institute.

ABSTRACT

The early Palaeogene (65-45 million years ago (Ma)) is of great interest to the earth science community, as significant perturbations in climate and carbon cycling marked this time interval clearly evidenced by major turnovers in biota, and profound variations in global carbon isotope ($\delta^{13}C$) records. The most prominent of these $\delta^{13}C$ changes include an interval of extreme ^{13}C-enrichement, the Paleocene Carbon Isotope Maximum (PCIM) (~59-57 Ma), a fairly rapid and extraordinary decline at the Basal Eocene Thermal Maximum (BETM) (~55.5 Ma), and an interval of very low $\delta^{13}C$ that initiated the Early Eocene Climatic Optimum (EECO).

Although the climate and carbon cycling perturbations in the early Palaeogene are global, most records come from the Northern Hemisphere and Atlantic Ocean and relatively few from the Indian and Pacific Oceans, especially in the Southern Hemisphere. Biotic and sedimentary response to the climate and carbon cycle perturbations in the early Palaeogene is just being appreciated. This thesis addresses these issues.

Chapter 2 examines seafloor carbonate dissolution in the central Pacific Ocean during the Paleocene and Eocene. Ocean Drilling Program (ODP) Holes 1209A (2387 m water depth) and 1211A (2907 m water depth) recovered 115 and 65 m-thick sections of nannofossil ooze of this age respectively, on Shatsky Rise. Carbonate content, coarse size fraction (>38 μm), benthic foraminifer abundance (BENTH), and planktic foraminifer fragmentation ratio (FRAG) were measured to create a record of dissolution. There are three intervals where dissolution parameters indicate prominent dissolution episodes for both holes between 65 and 33.7 Ma: during the middle Paleocene (~59 Ma), during the BETM (~55.5 Ma), and during the Middle to Late Eocene (~37-33.7 Ma). Enhanced preservation of planktic foraminiferal assemblages marks the start of both the Paleocene and Eocene epochs. Of the dissolution indices, BENTH and FRAG are the most reliable indicators. The dissolution record at Holes

1209A and 1211A provides the first detailed dissolution record for the Paleocene and Eocene in the Pacific Ocean.

In Chapter 3, the middle Paleocene (~59 Ma) dissolution episode is further investigated, especially to determine coeval oceanographic changes. Planktic foraminiferal assemblages were examined for their biozonation, isotope record and coiling direction in *Igorina albeari*. I show that the dissolution episode is widespread throughout the central Pacific and that it is associated with a coiling shift from dextral to sinistral in the Late Paleocene planktic foraminifera *Igorina albeari*. It coincides with a ~+0.5‰ $\delta^{13}C$ excursion near the base of the PCIM suggesting a link to enhanced carbon burial at this time. The coiling shift at the Pacific sites closely approximates the first appearance of *Globanomalina pseudomenardii*, the zonal marker for planktic foraminiferal Zone P4.

Chapter 4 examines carbonate contents in a section offshore eastern New Zealand. The abyssal ODP Hole 1121B, north-east of Campbell Plateau, contains a 30 m-thick interval of siliceous nannofossil ooze sediment deposited during the Late Paleocene. The presence of carbonate is unusual given present and past water depths, and suggests a drop in the carbonate compensation depth (CCD). Carbonate contents were analyzed to better document and understand this interval. When combined with age data, carbonate accumulation correlates temporally with the early part of the PCIM, and deposition of the Waipawa Formation, an organic rich unit, which is widely represented in New Zealand Palaeogene basins. It is likely that high surface water productivity led to an expanded oxygen minimum zone, and a deepening of the CCD.

Chapter 5 examines the stratigraphy of an expanded early Palaeogene section on South Island, New Zealand. Dee Stream, in Clarence Valley of Marlborough, cuts Muzzle Group, a sequence of well-bedded siliceous limestones and marls deposited from the late Cretaceous to the middle Eocene. An ~100 m thick portion of this sequence was mapped and logged, and samples were collected for planktic foraminiferal biostratigraphy and bulk carbon isotope analyses. The section spans planktic foraminiferal biozones Zone P4 to Subzone P6b in the global sub-tropical scheme or the *Subbotina triloculinoides* to *Pseudohastigerina wilcoxensis* zones of the New Zealand scheme. Bulk carbon isotopes through the section show $\delta^{13}C$ trends very similar to those

observed in global compilations. This includes a 1 m thick interval across the BETM, where a -1.5‰ decrease in $\delta^{13}C$ corresponds to an anomalous presence of *Morozovella aequa* and a major benthic foraminiferal extinction event (BFEE). The Teurian/Waipawan boundary corresponds to the BETM, which is a globally recognized event. Overall, the Dee Stream section together with other stream sections in the region, are important sites for understanding environmental change at high latitude continental margins in the Southern Hemisphere during the early Palaeogene.

In Chapter 6, another early Palaeogene interval of anomalous deep-sea carbonate accumulation is investigated. Deep Sea Drilling Project (DSDP) Site 259 on the Perth Abyssal Plain, southwestern Australian margin, contains a ~30 m-thick unit of carbonate-rich sediment sandwiched between zeolitic clay and indicating a deepening of the CCD at this time. Carbonate contents, planktic and benthic foraminiferal assemblages, carbon and oxygen isotopes, and non-carbonate mineralogy were analyzed to further investigate the timing and nature of early Palaeogene carbonate deposition at Site 259. Carbonate content ranges from 3 to 80%, and generally exceeds 50% between 35 and 57 metres below sea floor (mbsf). The section spans planktic foraminiferal Zones P4c through P6b (~57-52 Ma) and contains a BETM interval. The BETM occurs across a clay-rich interval and is characterized by a significant BFEE, and an influx of large *Acarinina* planktic foraminifera. The $\delta^{13}C$ records of bulk carbonate and *Nuttallides* spp. carbon isotopes exhibit trends similar to those observed in Upper Paleocene-Lower Eocene sediment (~57-52 Ma) from other locations. Two successive decreases in $\delta^{13}C$ of 0.5‰ and 1.0‰ start at the BFEE. The mineralogy of the non-carbonate fraction of sediment consistently comprises expanding clay, quartz, heulandite (zeolite), pyrolusite (MnO_2), feldspar and minor mica. The uniformity of this assemblage suggests that Site 259 experienced continuity in sediment provenance and that the sediment record reflects a drop in the CCD from ~57 to 52 Ma.

TABLE OF CONTENTS

LIST OF FIGURES

CHAPTER 5

CHAPTER 6

APPENDIX A

LIST OF PLATES

LIST OF TABLES

APPENDIX A

APPENDIX B

APPENDIX C

CHAPTER 1

INTRODUCTION

EARLY PALAEOGENE CLIMATES AND CARBON CYCLING

The Paleocene and Eocene epochs of the early Paleogene (65-33.7 Ma, *sensu* Berggren *et al.*, 1995; **Fig. 1**) are characterized by generally warm earth surface temperatures and high levels of atmospheric CO_2 relative to present-day (e.g., Shackleton, 1986; Wise *et al.*, 1992; Pearson and Palmer, 2000; Zachos *et al.*, 2001; Tyrrell and Zeebe, 2003). Warm intervals have generally been viewed as stable in the past, however, recent work over the last decade highlights a series of profound changes from the Paleocene through the Eocene over both long and short time scales (e.g., Kennett and Stott, 1991; Zachos *et al.*, 1993; Corfield and Norris, 1998; Zachos *et al.*, 2001). Crucial in this regard has been the construction of detailed benthic foraminiferal oxygen isotope $\delta^{18}O$ records (**Fig. 1**), which track deep-ocean temperatures and presumably high latitude surface temperatures where deep waters form (e.g., Zachos *et al.*, 2001).

Both stable isotope (**Fig. 1**) and biotic assemblage records indicate major long term fluctuations in global temperatures during the early and middle Palaeogene (Estes, 1988; Stott and Kennett, 1990; Wing, 1998; Zachos *et al.*, 2001; Gingerich, 2003). Temperatures in the early Paleocene *ca*. 65-58 Ma were relatively cool. Benthic foraminiferal $\delta^{18}O$ ratios were relatively high (i.e., enriched in ^{18}O). Narrow growth rings in Danian fossil wood from the northern Antarctic Peninsula indicate a cool climate (Francis and Poole, 2002). Both leaf fossil assemblages and an increase in biosiliceous productivity in the South Island of New Zealand, which can be linked to sea-level falls recorded in Europe and North and Central America, suggest cool-temperate conditions for the early Paleocene (Hollis, 2003; Kennedy, 2003). Terrestrial and marine ostracode assemblages of this age from northern Alaska were adapted to cool temperature, seasonal, low-light conditions, and geographic isolation (Brouwers and de Decker, 1993).

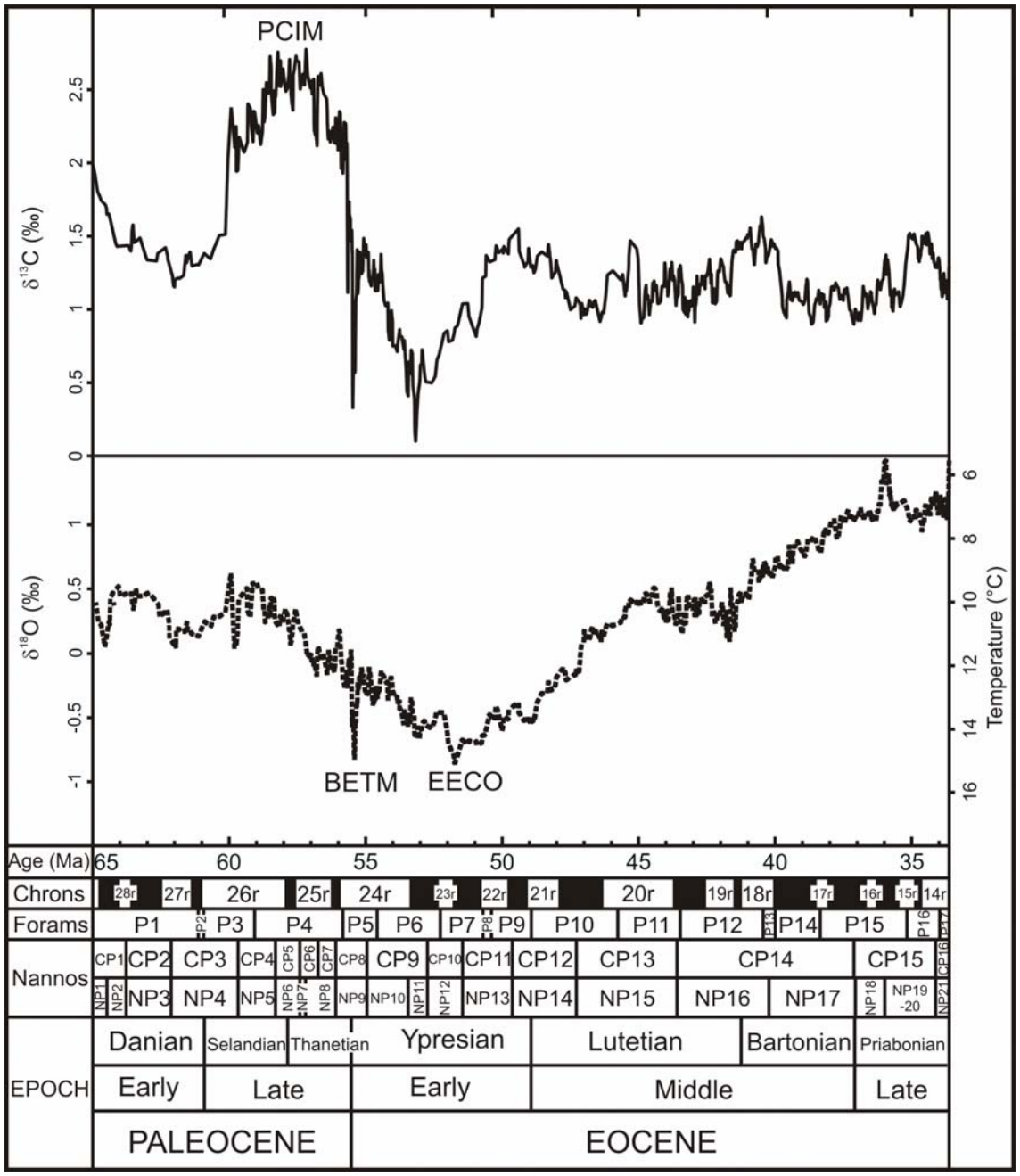

Figure 1. Paleocene and Eocene geochronology (following Berggren *et al.*, 1995) with global carbon and oxygen isotope curves constructed using benthic foraminiferal isotope data (adapted from Zachos *et al.*, 2001). Three key intervals of changing climate and carbon cycling are noted: PCIM = Paleocene Carbon Isotope Maximum, BETM = Basal Eocene Thermal Maximum, EECO = Early Eocene Climatic Optimum.

Beginning in the middle Paleocene *ca*. 58 Ma, global temperatures rose, reaching a peak at the Early Eocene Climatic Optimum (EECO) from about 53 to 50 Ma. This warming is manifested as a long term 1.5‰ decrease in benthic foraminifera $\delta^{18}O$ records (Zachos *et al.*, 2001), and as major shifts in biotic assemblages, especially at high latitudes. Strongly evergreen/thermophilic floral species were located at high latitude and broad-leaved deciduous forest in the polar regions (Collinson and Hooker, 2003). Floral patterns show that in the mid latitudes of central North America and southern Australia, plant species were dominated by broad leafed varieties, typical of warm low latitudes (Greenwood and Wing, 1995; Wing and Harrington, 1999). Warm polar regions and land connections between Asia and America during the Early Eocene (Estes and Hutchison, 1980) led to a rapid rise in turtle diversity in western North America (Hutchison, 1998). The Early Eocene record of crocodilians shows a similar pattern of migration into the high latitude North American continental interior (Novacek *et al.*, 1991).

Following the EECO, global temperatures generally cooled for the next 17 m.y. This cooling trend is marked by a 1.5‰ rise in benthic foraminiferal $\delta^{18}O$ records (Zachos *et al.*, 2001). Late Middle Eocene floras reflect an increase in temperate and deciduous or sclerophyllous species, which replaced the paratropical and subtropical floras of the Early Eocene (Collinson and Hooker, 2003). At the Middle/Late Eocene boundary dramatic cooling, which coincided with the India/Asia collision and the opening of the Tasman gateway, brought about a long-term turnover in microfossils and mollusks with new taxanomic groups supplanting antecedent forms (Prothero, 1994), including the extinction of a number of warm-adapted molluscs, nannofossils, planktic foraminifera, benthic foraminifera and large nummulitids. For high southern latitudes, ostracode abundance declined from the middle Eocene to the end of the Palaeogene, a trend which may have resulted from increased oceanic ventilation dissolution with declining temperatures and $CaCO_3$ availability (Majoran and Dingle, 2002). Floral patterns from Antarctica suggest a cooling trend during the Eocene, with middle to late Eocene seasonal, cool-temperate, rainy climates and increased latitudinal gradients (Reguero *et al.*, 2002).

Superimposed on these long-term thermal changes were at least one and possibly numerous, rapid and transient global warming events. The most conspicuous

example is the Basal Eocene Thermal Maximum (BETM), which began at the Paleocene/Eocene Boundary *ca*. 55.5 Ma (see supplementary note, below). During the BETM, benthic foraminifera $\delta^{18}O$ records suggest that deep waters warmed by ~5ºC (Kennett and Stott, 1991; Koch *et al.*, 1992; Sloan and Thomas, 1998; Norris and Röhl, 1999; Zachos *et al.*, 2001). A major temperature rise is also inferred from the $\delta^{18}O$ and Mg/Ca ratios of planktic foraminifera across the BETM (Zachos *et al.*, 2003).

The cause of generally high Earth surface temperatures during the early Palaeogene remains debatable, and could be attributed to a number of different factors. Atmospheric ρCO2 was likely to have been very high, perhaps because of increased seafloor spreading rates and reorganization of oceanic circulation (Berger and Crowell, 1982; Owen and Rea, 1985), or changing outputs such as limestone formation and organic carbon burial (Berger and Vincent, 1986; Raymo and Ruddiman, 1992). Atmospheric methane may also have been high (Sloan and Huber, 2001). Larger-scale orbital parameters including reduced planetary obliquity have also been invoked to explain a generally warm Earth with reduced temperature gradients (Sewall and Sloan, 2004). The complex nature of global climate change in the Paleocene and Eocene suggests that there is more than one factor involved.

Although the precise causes for warming remain open issues, records of stable carbon isotopes ($\delta^{13}C$) clearly indicate that significant fluctuations in global carbon cycling occurred during the early Palaeogene. The exogenic carbon cycle has long been recognised as containing three major inputs due to silicate weathering, organic oxidation and volcanism and two major outputs represented by the accumulation of carbonate and organic matter. Because two stable isotopes of carbon exist in nature, and different types of carbon compounds have different isotopic signatures, we can track carbon transfers between terrestrial, atmospheric and oceanic reservoirs and estimate masses and fluxes within the climate system (Ruddiman, 2001).

The largest and longest sustained positive $\delta^{13}C$ excursion of the Cenozoic occurred during the Late Paleocene from ~59 to 56 Ma (**Fig. 1**). This broad high in $\delta^{13}C$, referred to as the Paleocene Carbon Isotope Maximum (PCIM) in this thesis, is characterized by a rapid increase in $\delta^{13}C$ commonly at *ca*. 59 Ma, a ~3 m.y interval of

generally high $\delta^{13}C$ values, and a rapid decline in $\delta^{13}C$ at *ca*. 56 Ma. Thus, it broadly coincides with the start of the long-term, Late Paleocene temperature rise. The PCIM probably signifies anomalously high rates of organic carbon burial in either the terrestrial realm (Oberhansli and Perch-Nielsen, 1990; Kurtz *et al.*, 2003) or marine realm (Corfield and Cartlidge, 1992; Hollis *et al.*, 2005). Certainly, there is evidence for elevated primary productivity in Late Paleocene surface waters. Deep-sea sediments deposited at this time contain rich assemblages of surface dwelling microfossils (Berggren and Norris, 1997; Olsson *et al.*, 1999), and high accumulations of biogenic barite (Thompson and Schmitz, 1997). A substantial difference between the $\delta^{13}C$ of planktic and benthic foraminifera is also apparent, indicating enhanced productivity in surface waters (Shackleton *et al.*, 1985; Corfield and Cartlidge, 1992).

Global carbon isotope records show a remarkable negative carbon isotope excursion (CIE) across the BETM (Kennett and Stott, 1991; Koch *et al.*, 1992; Bralower *et al.*, 1995; Koch *et al.*, 1995; Kaiho *et al.*, 1996; Thomas and Shackleton, 1996; Hollis *et al.*, 2005). The overall shape and magnitude of the CIE suggests a rapid and massive injection of ^{13}C-depleted carbon into the ocean and atmosphere. The source for this carbon input has been attributed to increased volcanism (Eldholm and Thomas, 1993), impact of a comet (Kent *et al.*, 2003), or catastrophic release of methane from gas hydrates on continental slopes (Dickens *et al.*, 1995; Dickens *et al.*, 1997). More recently, Svensen *et al.* (2004) suggested that intrusion of voluminous mantle-derived magma into North Atlantic sedimentary basins induced the release of hydrocarbons. Irrespective of source, massive carbon input during the BETM should have dissolved calcium carbonate on the seafloor (Dickens *et al.*, 1997; Dickens, 2000). This has been observed in deep marine sedimentary records as a sharp dissolution layer (e.g., Katz *et al.*, 1999; Thomas and Shackleton, 1996; Zachos *et al.*, 2004).

After the CIE, and a short-term rebound to prior conditions, global $\delta^{13}C$ records plunge to a broad low that coincides with the onset of peak Cenozoic temperatures on land and in the ocean, a time referred to as the Early Eocene Climatic Optimum (EECO) (~52-50 Ma). The $\delta^{13}C$ low lacks a satisfactory explanation, although it must denote a major perturbation in carbon inputs or outputs from the ocean-atmosphere system (Shackleton and Hall, 1984; Kump and Arthur, 1999).

EARLY PALAEOGENE PLANKTIC FORAMINIFERA

The Order Foraminiferida is a group of microscopic, marine protozoans of the Phylum Sarcodina whose tests form an important component of chalk and many deep-sea oozes. Foraminifera live in a wide range of marine environments and are partitioned into two distinct ecological groups. Benthic foraminifera live on the sea floor whereas planktic foraminifera live in the upper few hundred metres of the water column. The tests of all planktic and most benthic foraminifera are composed of calcite. The mineralized test facilitates their preservation in the sedimentary record.

Planktic foraminiferal tests deposited in deep-sea sedimentary strata are not only useful stratigraphic tools but record changes in ocean chemistry and temperature and consequently the Earth's climate and global geochemical cycles. Planktic foraminifera are used in a variety of ways as palaeoclimate proxies. Tests of foraminifera are precipitated in equilibrium with surrounding seawater inclusive of isotopic signatures. They provide important insights into the fractionation of isotopes between and within global reservoirs. The carbon and oxygen isotopic signatures of foraminiferal tests also provide information on the preferred habitat of individual morphotypes, including water depth and palaeogeographic range. Knowledge of the preferred habitat of foraminifera can help identify the prevailing palaeoenvironmental conditions of the water mass in which they lived, including water temperature and nutrient availability. The preservation state of planktic foraminifera, assessed by test fragmentation and benthic to planktic ratios, helps constrain the position of the carbonate compensation depth (CCD), which in turn has palaeoclimatic implications.

The planktic foraminifera have an extensive palaeontologic record dating back to the Middle Jurassic when they first appeared in strata on the northern margin of Tethys and in the epicontinental basins of Europe (Lipps, 1993). They characteristically have diverse shell morphologies, short time ranges, and a planktic habit that makes them extremely useful stratigraphic tools (Berggren *et al.*, 1995).

There is a rich record of planktic foraminifera from the early and middle Paleocene. Subbotina (1953) was the first comprehensive use of Palaeogene planktic foraminifera as a stratigraphic tool, an endeavour undertaken to solve stratigraphic

problems in oil and gas exploration in the northern foothills of the Caucasus Mountains during the 1930's. A second detailed subdivision of the Palaeogene was developed in the Caribbean region (Bolli, 1957b, a) and quickly expanded into other regions of petroleum exploration (Stainforth *et al.*, 1975; Blow, 1979; Toumarkine and Luterbacher, 1985). The most current zonal scheme is the low latitude biozonation of Berggren *et al.* (1995) which is integrated with Cenozoic magnetobiochronologic time scale based on Berggren and Miller (1988). This is the principal biostratigraphic scheme used in the present study. Olsson *et al.* (1999) and Berggren and Norris (1997) utilized the zonation of Berggren *et al.* (1995) and provide current information on the classification of Paleocene foraminifera, their ranges and zonal boundaries, and palaeohabitats. For Early Eocene biostratigraphy the schemes of Toumarkine and Luterbacher (1985) and Blow (1979) are used. The supraspecific classification of foraminifera utilized here follows Loeblich and Tappan (1988).

Planktic foraminifera underwent a series of extinctions and radiations beginning immediately after the Cretaceous/Tertiary (K/T) boundary mass extinction event through to the end of the Eocene. In general, extinctions and radiations were responsive to episodes of biotic and climatic change including variations in nutrient cycling. Their timing and expression are briefly summarized below.

Following the K/T boundary impact event and mass extinction (Alvarez *et al.*, 1980) the earliest Paleocene saw the biotic recovery of whole new ecosystems, which arose from low diversity assemblages (Zachos, 1989; Sole *et al.*, 2002).

Only a few planktic foraminiferal genera including the *Hedbergella*, *Guembelitria, Rectoguembelina*, and *Zeauvigerina* survived the K/T boundary mass extinction. In the earliest Paleocene, planktic foraminifera were small in size with assemblages being nearly monospecific (Olsson *et al.*, 1999), in stark contrast to the large and heavily ornamented and morphologically diverse assemblages of the latest Cretaceous (Caron, 1985). One of the most significant morphological innovations to occur in planktic foraminifera during the Cenozoic was the introduction of the cancellate wall structure, thought to be an evolutionary response to changing water mass conditions in the earliest Paleocene (Olsson *et al.*, 1999).

Marine biotic communities recovered to their former diversity and productivity levels and were flourishing by the Late Paleocene (Berggren and Norris, 1997; Olsson *et al.*, 1999). Marine productivity also reached its maximum in the Late Paleocene, *ca.* 57 Ma, coinciding with the peak of the PCIM (Shackleton *et al.*, 1985; Corfield and Cartlidge, 1992; Zachos *et al.*, 1993; Corfield, 1994; Schmitz *et al.*, 1997).

Planktic foraminifera in the Late Paleocene were characterized by diverse assemblages. Diversity peaked during the PCIM with the rapid evolutionary radiation of the muricate planktic foraminifera *Acarinina* and *Morozovella*, which were the major surface-dwelling groups (Olsson *et al.*, 1999; Norris, 2000). Evidence from stable isotopes and palaeogeography suggest that *Morozovella* inhabited oligotrophic waters, dominating assemblages in tropical regions and warm water excursions into the high latitudes (Boersma and Premoli Silva, 1983; Hallock *et al.*, 1991). *Acarinina* show similar $\delta^{18}O$ values to those of *Morozovella* and slightly lighter carbon isotope ratios (Boersma *et al.*, 1979; Shackleton *et al.*, 1985), suggesting more mesotrophic surface water habitats. The Late Paleocene *Acarinina* radiation may have resulted from the opening of new geographic provinces, and perhaps also through the availability of more nutrient rich waters from cooler regions (Quillevere and Norris, 2003).

The Paleocene/Eocene (P/E) boundary marks another dramatic turnover in biota. In the deep-sea, benthic foraminifera underwent a major change with 35-50% of deep-sea species becoming extinct (Thomas, 2003). Massive release of methane from the dissociation of methane hydrate at the CIE is thought to have led to a build up of CO_2 in bottom waters, acidifying them and depleting oxygen concentrations, with major benthic foraminifera extinction as a consequence (Kaiho *et al.*, 1996; Thomas, 1998). In continental margin regions, post-extinction faunas were dominated by thin-walled, elongate taxa, typical of low oxygen environments (Kaiho *et al.*, 1996). High latitude nannoplankton assemblages underwent a dramatic change that show cold, eutrophic conditions were replaced by warm, oligotrophic conditions at the BETM (Bralower, 2002). In the terrestrial realm, high-latitude warming opened corridors for mammalian orders that included primates, perissodactyls, and artiodactyls to immigrate from Asia into North America and Europe (Clyde and Gingerich, 1998; Hooker, 1998; Bowen *et al.*, 2002; Gingerich, 2003).

At the same time, planktic foraminifera diversified at low latitudes and genera typical of the low latitudes since the Late Paleocene made their first appearance at high latitudes (Huber, 1991; Kelly *et al.*, 1996; Boersma *et al.*, 1998; Kelly, 2002). BETM "excursion taxa" were first identified by Kelly *et al* (1996) and include *Acarinina africana*, *Acarinina sibaiyaensis* and *Morozovella allisonensis*. At high latitude Southern Ocean ODP Site 690 the onset of the CIE is coeval with the first occurrence of heavily calcified *Acarinina* and rare *Morozovella aequa* (Kelly, 2002). The onset of the CIE recorded in planktic foraminifera predates the onset of the CIE in bulk carbonate, indicating that changes in microplankton began prior to the BFEE (benthic foraminifera extinction event, which suggests that the surface ocean/atmosphere was affected before the deep-sea (Kelly, 2002; Thomas *et al.*, 2002).

During the EECO the biotic realm is characterized by similar patterns seen at the BETM, including the presence of thermophilic taxa at high latitudes, indicating warm polar regions (Novacek *et al.*, 1991; Hutchison, 1998). Planktic foraminiferal assemblages during the EECO are dominated by *Morozovella* and *Acarinina*, indicating a continuance of the expansion of oligotrophic waters into high latitudes that was initiated in the Late Paleocene. At high southern latitudes, *Morozovella* dominate Early Eocene assemblages but they were rare to absent in this region during the Paleocene (Strong *et al.*, 1995; Boersma *et al.*, 1998; Hollis *et al.*, 2005).

As noted by Prothero (1994) the abrupt cooling event at the Late/Middle Eocene boundary, which coincided with the India/Asia collision and opening of the Tasman gateway, induced a mass extinction in the marine realm. The warm circumequatorial Tethyan belt had at this time cooled and narrowed, and experienced the extinction of a number of warm-adapted molluscs, nannofossils, planktic foraminifera, benthic foraminifera and large nummulitids (Prothero, 1994; Coccioni *et al.*, 2001).

A significant biotic turnover in planktic foraminifera occurred at the Late/Middle Eocene boundary with a dramatic reduction in *Acarinina* and the extinction the *Morozovella* lineage (Wade, 2004). There is no direct link between temperature and the decline of these surface dwellers. The faunal patterns are perhaps the result of increased surface water productivity and the deterioration of photosymbiotic relationships (Wade, 2004).

OUTSTANDING ISSUES

The general trends in climate and carbon cycling are well known for the Paleocene and Eocene. Less clear are the causes and consequences of these changes. As emphasized above, however, the global biota, inclusive of planktic foraminifera, was very clearly affected.

Over the last several decades, considerable advances have been made in understanding Plio-Pleistocene climate change (e.g., Shackleton, 1997). To a large degree, this has resulted from three factors: (1) numerous stratigraphic records with high temporal resolution are available from widespread locations; (2) Earth surface boundary conditions are reasonably well-constrained, and (3) multiple records of different processes have been constructed at the same location. As highlighted in various parts of this thesis, a general lack of control in terms of these factors currently hinders our understanding of the Paleocene and Eocene world.

Much of the work on Paleocene and Eocene palaeoenvironments has come from drill cores in the open ocean or from exposed terrestrial sections in the Northern Hemisphere. By comparison, records from the Southern Hemisphere are poor. For example, until recently the only record of the BETM in the South Pacific region was at Tawanui, southeastern North Island (Kaiho *et al.*, 1996; Crouch *et al.*, 2000; Crouch, 2001).

Coupled ocean-atmosphere models need boundary constraints to understand carbon cycle perturbations. One obvious component is carbonate dissolution in the deep sea. The CCD is the depth where carbonate dissolution exceeds carbonate supply so that no carbonate accumulates on the seafloor (Murray and Renard, 1891; Bramlette, 1961). The water column above the CCD where the preservation of carbonate decreases noticeably (commonly some 2 km across) is termed the lysocline (Berger, 1971). The CCD and lysocline are prone to change over geological time in response to variations in carbonate supply and properties of deep ocean waters (Berger, 1974; Farrell and Prell, 1989; Berger, 1992; Le and Shackleton, 1992; LaMontagne *et al.*, 1996). The pattern of change is not adequately known for the Paleocene and Eocene.

Perturbations in early Palaeogene stable oxygen and carbon isotope records are generally interpreted as representing changes in temperatures and carbon cycling. There is a need for the collection of multiple palaeoenvironmental proxy records across sequences representing this period of time to improve our knowledge of global change. This has been accomplished for some intervals, particularly the BETM. For most intervals of the early Palaeogene, however, isotopic perturbations, and by inference, episodes of global oceanographic change are not well correlated with records of deep-sea carbonate dissolution or records of planktic foraminiferal evolution.

Coiling reversals in planktic foraminifera appear to be an evolutionary response to some ecological parameter (Bandy, 1959; Ericson, 1959; Kucera and Kennett, 2002). They are commonly used as biostratigraphic markers and in reconstructions of palaeoenvironmental conditions during the Neogene. However, there is a paucity of such studies for the Palaegoene (Pearson, 1993; Norris and Nishi, 2001).

STUDY OBJECTIVES

The aim of this thesis is to contribute to the broad understanding of early Palaeogene global change by examining various aspects of sedimentary sections in the Australasian region (**Fig. 2**). In general, planktic foraminiferal assemblages and carbon isotopes are used to date previously undocumented sections, carbonate contents and dissolution indices are used to establish changes in deep-sea carbonate preservation, and all of these parameters are used to constrain the causes and consequences of global change.

In this work carbon and oxygen signatures of depth specific planktic foraminiferal shells provide information on preferred habitat of individual morphotypes, including water depth and palaeogeographic range, and at larger scale, global climatic conditions and carbon cycling.

Perturbations in the carbon and oxygen isotope curves for the Palaeogene are generally interpreted as representing profound changes in early Cenozoic bottom water temperatures and global carbon cycling. For most intervals of the Palaeogene, isotopic perturbations, and by inference episodes of global oceanographic change, are not

sufficiently well correlated with records of deep-sea carbonate dissolution or linked to evolution within the planktic foraminifera. The intention of this study is to advance knowledge of these relationships.

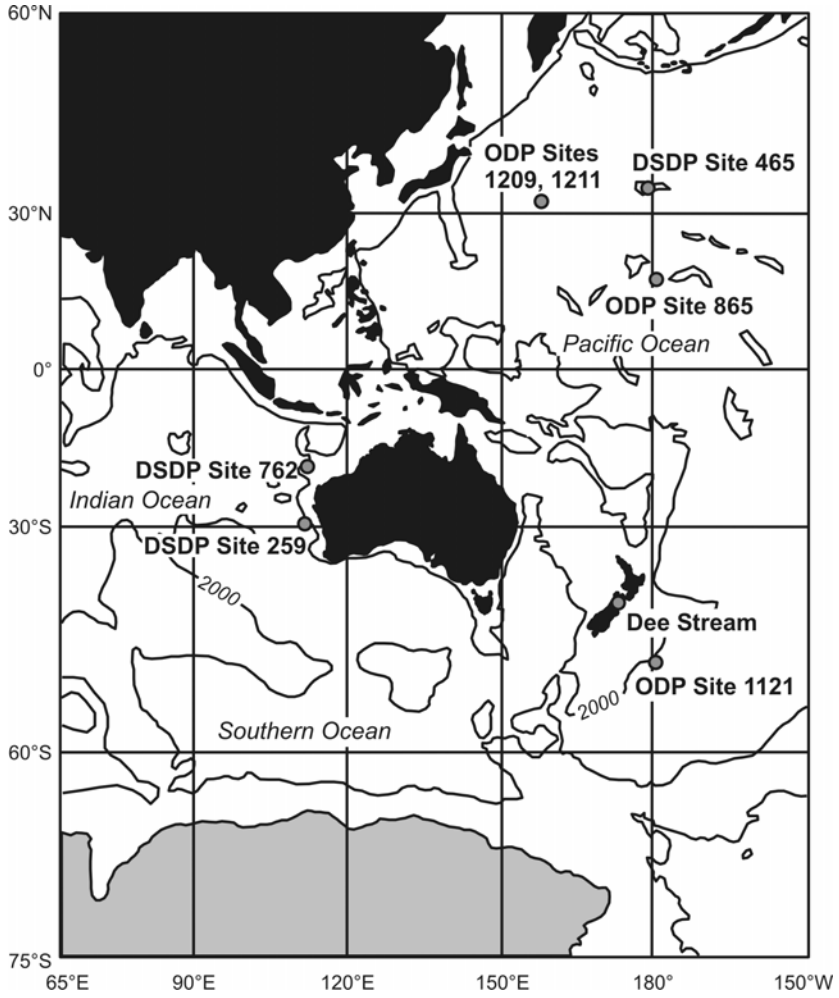

Figure 2. Location map of study areas employed in this study including Ocean Drilling Program (ODP) and Deep Sea Drilling Program (DSDP) sites.

Characterizing the effect of CO_2-induced acidification on the production, dissolution and preservation of carbonate in the modern oceans is an important task for the future (e.g., Feely *et al.*, 2004). Ocean Drilling Program (ODP) Leg 198 drilled a series of boreholes on Shatsky Rise in the central-west Pacific. Several of these boreholes penetrated nearly continuous sections of Paleocene and Eocene sediment buried at relatively shallow depths. The intention of this study is to construct a long-term carbonate dissolution profile for the Paleocene and Eocene from sediment

recovered from the Shatsky Rise providing insight into the mid Pacific history of the CCD during this time (Chapter 2).

Major changes in deep-sea carbonate dissolution, if global, should manifest at other locations throughout the oceans. In particular, one might expect oscillations in the CCD and the existence of abyssal carbonate 'plugs', intervals of relatively high carbonate content within abyssal clays and formed during times of a lowered CCD. The significance of unusual carbonate 'plugs' that accumulated at abyssal depths during the early Palaeogene are investigated at Deep Sea Drilling Project (DSDP) Site 259 and ODP Site 1121 (Chapters 4, 6), in the context of change in the CCD during the Paleocene-Eocene interval.

Coiling reversals in planktic foraminifera provide valuable information for palaeoenvironmental reconstructions. This study addresses the deficiency of coiling data in the Palaeogene planktic foraminifera (Chapter 3). *Igorina albeari* experienced a coiling switch in the middle Paleocene at Site 865 in the central Pacific (Norris and Nishi, 2001). Coiling data was collected at two additional sites located in the central Pacific (Sites 465 and 1209), and a mid-latitude site located on the northwestern Australian margin (Site 762), to evaluate whether the reversal was a widespread event or confined to a specific region. The relation between carbon and oxygen isotope patterns in depth-specific foraminifera, specifically in the early part of the PCIM, and the coiling pattern in *Igorina albeari*, was identified as a specific research target.

On the South Island of New Zealand, in the Clarence Valley, several streams bisect uplifted and tilted Palaeogene strata. The region presents a unique opportunity to study exposed continental margin strata, a rarity in the Southern Hemisphere for this period of significant global change (Chapter 5). When this study was undertaken the Paleocene/Eocene boundary lacked a global stratotype subsequently established in Egypt (see Supplementary Note below). Reconnaissance studies (Strong *et al.*, 1995) located the approximate position of the Paleocene-Eocene boundary. It was the intention of this study to document and further resolve events during the BETM for this high latitude Southern Hemisphere sequence.

SUPPLEMENTARY NOTE

The BETM is where vertebrate palaeontologists have traditionally placed the P/E boundary because this is where a major turnover in mammal orders occurred (Gingerich, 2003). Indeed, the Paleocene Epoch was first recognized as distinct from the Eocene Epoch from the late nineteenth century when fieldwork in the Paris Basin revealed distinctive mammalian skeletons representing a quite different fauna from that of succeeding strata and now placed as Paleocene (Gervais, 1877). However, until recently, there has been controversy amongst Cenozoic stratigraphers as to where to place the Paleocene/Eocene boundary (Aubry *et al.*, 2003). Planktic foraminiferal specialists commonly used the P5/P6 zonal boundary and calcareous nannofossil specialists prefered the NP9/NP10 boundary (Berggren *et al.*, 1995). Both zonal boundaries post-date the BETM, a brief and pronounced interval of global environmental change (Thomas and Shackleton, 1996). The BETM is a short-lived (~150-200 k.y.) globally recognized event in terms of climate change, biotic evolution and carbon cycling and its global isochrony makes it a powerful stratigraphic tool. The Global Standard Stratotype-section (GSSP) for the Paleocene/Eocene (P/E) boundary has recently been selected in the Dababiya Quarry Section, near Luxor in Egypt, in the lower part of the Esna Shale Formation where the base of the CIE is recorded (Dupius *et al*., 2003).

REFERENCES

Alvarez, L.W., Alvarez, W., *et al.*, 1980. Extraterrestrial cause for the Cretaceous-Tertiary extinction. *Science*, 4448:1095-1108.

Aubry, M.P., Berggren, W.A., *et al.*, 2003. Chronostratigraphic terminology at the Paleocene/Eocene boundary. *In* Wing, S.L., Gingerich, P.D., Schmitz, B., *et al.*, (Eds), *Causes and consequences of the globally warm climates in the early Paleogene*, The Geological Society of America, Spec. Paper 369, 551-566.

Bandy, O.L., 1959. Geologic significance of coiling ratios in the foraminifer Globigerina pachyderma (Ehrenberg) (California). *Geological Society of America Bulletin*, 70:1708.

Berger, W.H., 1971. Sedimentation of planktonic foraminifera. *Marine Geology*, 11:325-358.

Berger, W.H., 1974. Plate stratigraphy and the fluctuating carbonate line. *Spec. Publs. Int. Ass. Sediment*, 1:11-48.

Berger, W.H., 1992. Pacific carbonate cycles revisited: arguments for and against productivity control. *In* Ishizaki, K., and Saito, T., (Eds), *Centenary ofJapanese Micropaleontology*: Tokyo Terra Scientific Publishing Company, 15-25.

Berger, W.H., and Crowell, J.C., 1982. *Climate in earth-history*: Washington, D.C., National Academy Press, 212 p.

Berger, W.H., and Vincent, E., 1986. Deep-sea carbonates; reading the carbon-isotope signal. *Geologische Rundschau*, 75:249-269.

Berggren, W.A., Kent, D.V., *et al.*, 1995. A revised Cenozoic geochronology and chronostratigraphy. *In* Berggren, W.A., Kent, D.V., Aubry, M.P., *et al.*, (Eds), *Geochronology, time scales and global stratigraphic correlation*, SEPM Special Publication 54, 129-212.

Berggren, W.A., and Miller, K.G., 1988. Paleogene tropical planktonic foraminiferal biostratigraphy and magnetobiochronology. *Micropaleontology*, 34:362-380.

Berggren, W.A., and Norris, R.D., 1997. *Biostratigraphy, phylogeny and systematics of Paleocene trochospiral planktonic Foraminifera*: New York, (American Museum of Natural History), 116 p.

Blow, W.H., 1979. *The Cainozoic Globigerinida; a study of the morphology, taxonomy, evolutionary relationships and the stratigraphical distribution of some Globigerinida (mainly Globigerinacea)*: Leiden, E. J. Brill, 752 p.

Boersma, A., and Premoli Silva, I., 1983. Paleocene planktonic foraminiferal biogeography and the paleoceanography of the Atlantic Ocean. *Micropaleontology*, 29:355-381.

Boersma, A., Premoli Silva, I., *et al.*, 1998. Trophic models for the well-mixed and poorly mixed warm oceans across the Paleocene/Eocene epoch boundary. *In* Aubry, M.P., Lucas, S.G., and Berggren, W.A., (Eds), *Late Paleocene-early Eocene climatic and biotic events in the marine and terrestrial records*: New York, NY Columbia University Press, 204-213.

Boersma, A., Shackleton, N.J., *et al.*, 1979. Carbon and oxygen isotope records at DSDP Site 384 (North Atlantic) and some Paleocene paleotemperatures and carbon isotope variations in the Atlantic Ocean. *In* Tucholke, B.E., and Vogt, P.R., (Eds), *Proc. DSDP*, 43: Washington (US Government Printing Office), 695-717.

Bolli, H.M., 1957a. The genera *Globigerina* and *Globorotalia* in the Paleocene-Lower Eocene Lizard Springs Formation of Trinidad, B. W. I. *In* Loeblich, A.R., Jr., Tappan, H.N., Beckmann, J.-P., *et al.*, (Eds), *Loeblich, A R , Jr , Studies in Foraminifera*: Washington (US Government Printing Office), 61-81.

Bolli, H.M., 1957b. Planktonic foraminifera from the Eocene Navet and San Fernando formations of Trinidad, B. W. I. *In* Loeblich, A.R., Jr., Tappan, H.N., Beckmann, J.-P., *et al.*, (Eds), *Loeblich, A R , Jr , Studies in Foraminifera*: Washinton (US Government Printing Office), 155-172.

Bowen, G.J., Clyde, W.C., *et al.*, 2002. Mammalian dispersal at the Paleocene/Eocene boundary. *Science*, 295:2062-2065.

Bralower, T.J., 2002. Evidence of surface water oligotrophy during the Paleocene-Eocene thermal maximum: Nannofossil assemblage data from Ocean Drilling Program Site 690, Maud Rise, Weddell Sea. *Paleoceanography*, VOL. 17, NO. 2, 1023, doi:10.1029/2001PA000662, 200.

Bralower, T.J., Zachos, J.C., *et al.*, 1995. Late Paleocene to Eocene paleoceanography of the Equatorial Pacific Ocean; stable isotopes recorded at Ocean Drilling Program Site 865, Allison Guyot. *Paleoceanography*, 10:841-865.

Bramlette, M.N., 1961. Pelagic Sediments. *In* Sears, M., (Ed.) *Oceanography*, 67 AAAS, 345-366.

Brouwers, E.M., and de Decker, P., 1993. Late Maastrichtian and Danian ostracode faunas from northern Alaska: reconstructions of environment and paleogeography. *Palaios*, 8:140-154.

Caron, M., 1985. Cretaceous planktic foraminifera. *In* Bolli, H.M., Saunders, J.B., and Perch-Nielsen, K., (Eds), *Plankton stratigraphy*: Cambridge (Cambridge University Press), 17-86.

Clyde, W.C., and Gingerich, P.D., 1998. Mammalian community response to the latest Paleocene thermal maximum; an isotaphonomic study in the northern Bighorn Basin, Wyoming. *Geology*, 26:1011-1014.

Coccioni, R., Basso, D., *et al.*, 2001. Marine biotic signals across a late Eocene impact layer at Massignano, Italy: evidence for long term environmental perturbations? *Terra Nova*, 12:258-263.

Collinson, M.E., and Hooker, J.J., 2003. Paleogene vegetation of Eurasia: framework for mammalian faunas. *In* Reumer, J.W.F., and Wessels, W., (Eds), *Distribution*

and migration of Tertiary mammals in Eurasia. A volume in honour of Hans de Bruijn, 10: Deinsea, 41-83.

Corfield, R.M., 1994. Palaeocene oceans and climate; an isotopic perspective. *Earth-Science Reviews*, 37:225-252.

Corfield, R.M., and Cartlidge, J.E., 1992. Oceanographic and climate implications of the Paleocene carbon isotope maximum. *Terra Nova*, 4:443-455.

Corfield, R.M., and Norris, R.D., 1998. The oxygen and carbon isotopic context of the Paleocene/Eocene epoch boundary. *In* Aubry, M.-P., Lucas, S.G., and Berggren, W.A., (Eds), *Late Paleocene-early Eocene climatic and biotic events in the marine and terrestrial records*: New York, NY Columbia University Press, 124-137.

Crouch, E.M., 2001. *Environmental change at the time of the Paleocene-Eocene biotic turnvoer*, LPP Contribution Series No. 14: Utrecht, Utrecht University, 216 p.

Crouch, E.M., Bujak, J.P., *et al.*, 2000. Southern and northern Hemisphere dinoflagellate cyst assemblage changes in association with the late Paleocene thermal maximum. *GFF*, 122:40-41.

Dickens, G.R., 2000. Methane oxidation during the late Palaeocene thermal maximum. *Bulletin de la Societe Geologique de France*, 171:37-49.

Dickens, G.R., Castillo, M.M., *et al.*, 1997. A blast of gas in the latest Paleocene; simulating first-order effects of massive dissociation of oceanic methane hydrate. *Geology*, 25:259-262.

Dickens, G.R., O'Neil, J.R., *et al.*, 1995. Dissociation of oceanic methane hydrate as a cause of the carbon isotope excursion at the end of the Paleocene. *Paleoceanography*, 10:965-971.

Dupius, C., Ouda, K., *et al*., 2003. The Dababiya Quarry Section: Lithostratigraphy, clay mineralogy, geochemistry and paleontology. *Micropaleontology*, 49, Supplement 1:1-59

Eldholm, E., and Thomas, E., 1993. Environmental impact of volcanic margin formation. *Earth and Planetary Science Letters*, 117:319-329.

Ericson, D.B., 1959. Coiling direction of *Globigerina pachyderma* as a climatic index. *Science*, 130:219-220.

Estes, R., 1988. Lower vertebrates from the Golden Valley Formation, early Eocene of North Dakota. *Acta Zoologica Cracoviana*, 31:541-562.

Estes, R., and Hutchison, J.H., 1980. Eocene lower vertebrates from Ellesmere Island, Canadian Arctic Archipelago. *Palaeogeography, Palaeoclimatology, Palaeoecology*, 30:325-347.

Farrell, J.W., and Prell, W.L., 1989. Climatic change and $CaCO_3$ preservation: an 800 000 year bathymetric reconstruction from the central equatorial Pacific Ocean. *Paleoceanography*, 4:447-466.

Feely, R.A., Sabine, C.L., *et al.*, 2004. Impact of anthropogenic CO_2 on the $CaCO_3$ system in the oceans. *Science*, 305:362-366.

Francis, J.E., and Poole, I., 2002. Cretaceous and early Tertiary climates of Antarctica: Evidence from fossil wood. *Palaeogeography, Palaeoclimatology, Palaeoecology*, 182:47-64.

Gervais, P., 1877. Enumeration de quelques ossements d'animaux vertebres recueillis aux environs de Reims par M. Lemoine. *Journal de Zoologie*, 6:74-79.

Gingerich, P.D., 2003. Mammalian responses to climate change at the Paleocene-Eocene boundary: Polecat Bench record in the northern Bighorn Basin, Wyoming. *In* Wing, S.L., Gingerich, P.D., Schmitz, B., *et al.*, (Eds), *Causes and consequences of globally warm climates in the early Paleogene*, The Geological Society of America, Spec. Paper 369, 463-478.

Greenwood, D.R., and Wing, S.L., 1995. Eocene continental climates and latitudinal temperature gradients. *Geology (Boulder)*, 23:1044-1048.

Hallock, P., Premoli Silva, I., *et al.*, 1991. Similarities between planktonic and larger foraminiferal evolutionary trends through Paleogene paleoceanographic changes. *The oceans of the Paleogene Palaeogeography, Palaeoclimatology, Palaeoecology*, 83:49-64.

Hollis, C.J., 2003. The Cretaceous/Tertiary boundary event in New Zealand: Profiling mass extinction. *New Zealand Journal of Geology and Geophysics*, 46:307-321.

Hollis, C.J., Dickens, G.R., *et al.*, 2005. The Paleocene-Eocene transition at Mead Stream, New Zealand: a southern Pacific record of early Cenozoic global change. *Palaeogeography, Palaeoclimatology, Palaeoecology,* 215:313-343.

Hooker, J.J., 1998. Mammalian faunal change across the Paleocene-Eocene transition in Europe. *In* Aubry, M.P., Lucas, S.G., and Berggren, W.A., (Eds), *Late Paleocene-early Eocene climatic and biotic events in the marine and terrestrial records*: New York, NY Columbia University Press, 428-450.

Huber, B.T., 1991. Paleogene and early Neogene planktonic foraminifer biostratigraphy of sites 738 and 744, Kerguelen Plateau (southern Indian Ocean). *Proceedings of the Ocean Drilling Program scientific results*, 119:427-449.

Hutchison, J.H., 1998. Turtles across the Paleocene/Eocene epoch boundary in west-central North America. *In* Aubry, M.P., Lucas, S.G., and Berggren, W.A., (Eds), *Late Paleocene-early Eocene climatic and biotic events in the marine and terrestrial records*: New York, NY Columbia University Press, 401-408.

Kaiho, K., Arinobu, T., *et al.*, 1996. Latest Paleocene benthic foraminiferal extinction and environmental changes at Tawanui, New Zealand. *Paleoceanography*, 11:447-465.

Katz, M.E., Pak, D.K., *et al.*, 1999. The source and fate of massive carbon input druing the latest Paleocene thermal maximum. *Science*, 286:1531-1533.

Kelly, D.C., 2002. Response of Antarctic (ODP Site 690) planktonic foraminifera to the Paleocene-Eocene thermal maximum; faunal evidence for ocean/climate change. *Paleoceanography*, 17 (4), 1071, doi:10.1029/2002PA000761.

Kelly, D.C., Bralower, T.J., *et al.*, 1996. Rapid diversification of planktonic foraminifera in the tropical Pacific (ODP Site 865) during the late Paleocene thermal maximum. *Geology*, 24:423-426.

Kennedy, E.M., 2003. Late Cretaceous and Paleocene terrestrial climates of New Zealand: Leaf fossil evidence from South Island assemblages. *New Zealand Journal of Geology and Geophysics*, 46:295-306.

Kennett, J.P., and Stott, L., 1991. Abrupt deep-sea warming, palaeoceanographic changes and benthic extinctions at the end of the Paleocene. *Nature*, 353:225-229.

Kent, D.V., Wright, J.D., *et al.*, 2003. A case for a comet impact trigger for the Paleocene/Eocene thermal maximum and carbon isotope excursion. *Earth and Planetary Science Letters*, 211:13-26.

Koch, P.L., Zachos, J., *et al.*, 1992. Correlation between isotope records in marine and continental carbon reservoirs near the Paleocene/Eocene boundary. *Nature*, 358:319-322.

Koch, P.L., Zachos, J.C., *et al.*, 1995. Stable isotope stratigraphy and paleoclimatology of the Paleogene Bighorn Basin (Wyoming, USA). *Palaeogeography, Palaeoclimatology, Palaeoecology*, 115:61-89.

Kucera, M., and Kennett, J.P., 2002. Causes and consequences of a middle Pleistocene origin of the modern planktonic foraminifer Neogloboquadrina pachyderma sinistral. *Geology*, 30:539-542.

Kump, L.R., and Arthur, M.A., 1999. Interpreting carbon-isotope excursions; carbonates and organic matter. *Chemical Geology*, 161:181-198.

Kurtz, A., Kump, L.R., *et al.*, 2003. Early Cenozoic decoupling of the global carbon and sulfur cycles. *Paleoceanography*, 18(4), 1090, doi:10.1029/2003PA000908.

LaMontagne, R.W., Murray, R.W., *et al.*, 1996. Decoupling of carbonate preservation, carbonate concentration, and biogenic accumulation: A 400-kyr record from the central equatorial Pacific Ocean. *Paleoceanography*, 11:553-562.

Le, J., and Shackleton, N.J., 1992. Carbonate dissolution fluctuations in the western equatorial Pacific during the late Quaternary. *Paleoceanography*, 7:21-42.

Lipps, J.H., 1993. Fossil prokaryotes and protists: Boston, Blackwell Scientific Publications, p. 342.

Loeblich, A.R., Jr., and Tappan, H.N., 1988. *Foraminiferal genera and their classification*: New York, Von Nostrand and Reinhold Company, 970 p.

Majoran, S., and Dingle, R.V., 2002. Cenozoic deep-sea ostracods from Maud Rise, Weddell Sea, Antarctica (ODP Site 689): A palaeoceanographical perspective. *Geobios*, 35:137-152.

Murray, J., and Renard, A.F., 1891. *Deep-sea deposits based on the specimens collected during the voyage of H.M.S. Challenger in the years 1872 to 1876*: London, Longmans, 525 p.

Norris, R.D., 2000. Pelagic species diversity, biogeography, and evolution *Pelagic biogeography and speciation*.

Norris, R.D., and Nishi, H., 2001. Evolutionary trends in coiling of tropical Paleogene planktic foraminifera. *Paleobiology*, 27:327-347.

Norris, R.D., and Röhl, U., 1999. Carbon cycling and chronology of climate warming during the Palaeocene/Eocene transition. *Nature*, 401:775-778.

Novacek, M.J., Ferrusquia-Villafranca, K., *et al.*, 1991. Wasatchian (ealry Eocene) mammals and other vertebrates from Baja California, Mexico: The Lomas las Tetas de Cabra fauna. *Bulletin of the American Museum of Natural History*, 208:88 pp.

Oberhansli, H., and Perch-Nielsen, K., 1990. The Paleocene ^{13}C-event: Was it due to changes in the storage rate of terrestrial biomass? *Veroff. Ubersee Mus. Bremen Reihe A*,, A10:99–112.

Olsson, R.K., Hemleben, C., *et al.*, 1999. *Atlas of Paleocene planktonic Foraminifera*: Washington, DC, Smithsonian Institution, 252 p.

Owen, R.M., and Rea, D.K., 1985. Sea floor hydrothermal activity links climate to tectonics: the Eocene carbon dioxide greenhouse. *Science*, 227:166-169.

Pearson, P.N., 1993. A lineage phylogeny for the Paleogene planktonic foraminifera. *Micropaleontology*, 39:193-232.

Pearson, P.N., and Palmer, M.R., 2000. Atmospheric carbon dioxide concentrations over the past 60 million years. *Nature*, 406:659-699.

Prothero, D.R., 1994. *The Eocene-Oligocene transition: paradise lost*: New York, Columbia University Press, 291 p.

Quillevere, F., and Norris, R.D., 2003. Ecological development of acarininids (planktonic Foraminifera) and hydrographic evolution of Paleocene surface waters. *In* Wing, S.L., Gingerich, P.D., Schmitz, B., *et al.*, (Eds), *Causes and consequences of globally warm climates in the early Paleogene*, The Geological Society of America, Spec. Paper 369, 223-238.

Raymo, M.E., and Ruddiman, W.F., 1992. Tectonic forcing of late Cenozoic climate. *Nature*, 359:117-122.

Reguero, M.A., Marenssi, S.A., *et al.*, 2002. Antarctic Peninsula and South America (Patagonia) Paleogene terrestrial faunas and environments: Biogeographic relationships. *Palaeogeography, Palaeoclimatology, Palaeoecology*, 179:189-210.

Ruddiman, W.F., 2001. *Earth's climate: past and future*: New York, W.H. Freeman, 465 p.

Schmitz, B., Charisi, S.D., *et al.*, 1997. Barium, SiO_2 (excess), and P_2O_5 as proxies of biological productivity in the Middle East during the Palaeocene and the latest Palaeocene benthic extinction event. *Terra Nova*, 9:95-99.

Sewall, J.O., and Sloan, L.C., 2004. Less ice, less tilt, less chill; the influence of a seasonally ice-free Arctic Ocean and reduced obliquity on early Paleogene climate. *Geology (Boulder)*, 32:477-480.

Shackleton, N.J., 1986. Paleogene stagle isotope events. *Palaeogeography, Palaeoclimatology, Palaeoecology*, 57:91-102.

Shackleton, N.J., 1997. The deep-sea sediment record and the Pliocene-Pleistocene boundary. *Quaternary International*, 40:33-35.

Shackleton, N.J., Corfield, R.M., *et al.*, 1985. Stable isotope data and the ontogeny of Paleocene planktonic foraminifera, Cushman Foundation for Foraminiferal Research, Ithaca, NY, p. 321-336.

Shackleton, N.J., and Hall, M.A., 1984. Carbon isotope data from Leg 74 sediments. *In* Moore, J., T. C., Rabinowitz, P.D., Boersma, A., *et al.*, (Eds), *Init. Repts. DSDP*, 74: Washington US Government Printing Office, 613-619.

Sloan, L., and Huber, B.T., 2001. North Atlantic climate variability in early Palaeogene time: A climate modelling sensitivity study. *Geological Society of America Special Publication*, 183:253-272.

Sloan, L.C., and Thomas, E., 1998. *Global climate of the late Paleocene epoch; modeling the circumstances associated with a climatic "event"*: New York, NY.

Sole, R.V., Montoya, J.M., *et al.*, 2002. Recovery after mass extinction: evolutionary assembly in large-scale biosphere dynamics. *Phil. Trans. R. Soc. Lond. B*, 357:697-707.

Stainforth, R.M., Lamb, H., *et al.*, 1975. Cenozoic planktonic foraminiferal zonation and characteristics of index forms. *University of Kansas Paleontological Contributions, Article*, 62:425 p.

Stott, L.D., and Kennett, J.P., 1990. Antarctic Paleogene planktonic foraminifer biostratigraphy; ODP Leg 113, Sites 689 and 690. *In* Barker, P.F., Kennett, J.P., and et al., (Eds), *Proc. ODP, Sci. Results,* 113: College Station, TX Ocean Drilling Program, 549-565.

Strong, C.P., Hollis, C.J., *et al.*, 1995. Foraminiferal, radiolarian, and dinoflagellate biostratigraphy of Late Cretaceous to middle Eocene pelagic sediments (Muzzle Group), Mead Stream, Marlborough, New Zealand. *New Zealand Journal of Geology and Geophysics*, 38:171-209.

Subbotina, N.N., 1953. Fossil foraminifera of the USSR (Globigerinidae, Hantkeninidae and Globotorotaliidae. *VNIGRI*, 76:296 p.

Svensen, H., Planke, S., *et al.*, 2004. Release of methane from a volcanic basin as a mechanism for initial Eocene global warming. *Nature*, 429:542-545.

Thomas, D., Zachos, J.C., *et al.*, 2002. Warming the fuel for the fire: evidence for the thermal dissociation of methane hydrate during late Paleocene-Eocene thermal maximum. *Geology*, 30:1067-1070.

Thomas, E., 1998. The biogeography of the late Paleocene benthic foraminiferal extinction. *In* Aubry, M.P., Lucas, S.G., and Berggren, W.A., (Eds), *Late Paleocene-early Eocene climatic and biotic events in the marine and terrestrial records*: New York, NY Columbia University Press, 214-243.

Thomas, E., 2003. Extinction and food at the seafloor: a high resolution benthic foraminiferal record across the Initial Eocene Thermal Maximum, Southern Ocean Site 690. *In* Wing, S.L., Gingerich, P.D., Schmitz, B., *et al.*, (Eds), *Causes and consequences of the globally warm climates in the early Paleogene,* The Geological Society of America, Spec. Paper 369, 319-332.

Thomas, E., and Shackleton, N.J., 1996. The Paleocene-Eocene benthic foraminiferal extinction and stable isotope anomalies. *In* Knox, R.W.O.B., Corfield, R.M., and Dunay, R.E., (Eds), *Correlation of the early Paleogene in Northwest Europe,* 101 Geological Society London Special Publication, 401-441.

Thompson, E.I., and Schmitz, B., 1997. Barium and the late Paleocene $\delta^{13}C$ maximum: evidence of increased marine surface producitivity. *Paleoceanography*, 12:239-254.

Toumarkine, M., and Luterbacher, H.-P., 1985. Paleocene and Eocene planktic foraminifera. *In* Bolli, H.M., Saunders, J.B., and Perch-Nielsen, K., (Eds), *Plankton stratigraphy*: Cambridge Cambridge University Press, 87-154.

Tyrrell, T., and Zeebe, R.E., 2003. History of carbonate ion concentration over the last 100 million years. *Geochimica et Cosmochimica Acta,* 68:3521-3530.

Wade, B.S., 2004. Planktonic foraminiferal biostratigraphy and mechanisms in the extinction of *Morozovella* in the late middle Eocene. *Marine Micropaleontology*, 51:23-38.

Wing, S.L., 1998. Late Paleocene-early Eocene floral and climatic change in the Bighorn Basin, Wyoming. *In* Aubry, M.P., Lucas, S.G., and Berggren, W.A., (Eds), *Late Paleocene-early Eocene climatic and biotic events in the marine and terrestrial records*: New York, NY Columbia University Press, 380-400.

Wing, S.L., and Harrington, G.J., 1999. Floral response to rapid global warming near the Paleocene-Eocene boundary *Geological Society of America, 1999 annual meeting,* 31: Anonymous Geological Society of America (GSA), 121-122.

Wise, S.W., Jr., Breza, J.R., *et al.*, 1992. Paleogene glacial history of Antarctica in light of Leg 120 drilling results. *In* Wise, S.W., and Schlich, R., (Eds), *Proc. ODP Sci. Res.*, 120: College Station, TX (Ocean Drilling Program), 1001-1030.

Zachos, J.C., 1989. Geochemical evidence for suppression of pelagic marine productivity at the Cretaceous/Tertiary boundary. *Nature*, 337:61-64.

Zachos, J.C., Kroon, D., *et al.*, 2004. *Proc. ODP, Init. Repts.*, Volume 208 [Online], Available from World Wide Web: http://www-odp.tamu.edu/publications/208_IR/208ir.htm.

Zachos, J.C., Pagani, M., *et al.*, 2001. Trends, rhythms, and aberrations in global climate 65 Ma to present. *Science*, 292:686-693.

Zachos, J.C., Petrizzo, M.R., *et al.*, 2003. A transient rise in tropical sea surface temperature during the Paleocene-Eocene thermal maximum. *Science*, 302:1551-1554.

Zachos, J.C., Walker, J.C.G., *et al.*, 1993. Abrupt climate change and transient climates during the Paleogene: A marine perspective. *Journal of Geology*, 101:191-213.

CHAPTER 2

CARBONATE DISSOLUTION EPISODES IN PALEOCENE AND EOCENE SEDIMENT, SHATSKY RISE, WEST-CENTRAL PACIFIC.

Abstract. Holes 1209A and 1211A on Southern High, Shatsky Rise contain expanded, nearly continuous records of carbonate-rich sediment deposited in deep water of the equatorial Pacific Ocean during the Paleocene and Eocene. In this study, we document intervals of carbonate dissolution in these records by examining temporal changes in four parameters: carbonate content, coarse size fraction (>38 μm), benthic foraminiferal abundance, and planktic foraminiferal fragmentation ratio. Carbonate content is not a sensitive indicator of carbonate dissolution in the studied sections, although rare intervals of low carbonate may reflect times of relatively high dissolution. The proportion of coarse size fraction does not accurately record carbonate dissolution either because the relative abundance of nannofossils largely determines the grain-size distribution. Benthic abundance and fragmentation covary (r^2 = 0.77), and are probably the best indicators for carbonate dissolution. For both holes, records of these parameters indicate two episodes of prominent dissolution. The first of these occurs in the Upper Paleocene (~59-58 Ma) and the second, in the Middle to Upper Eocene (~45-33.7 Ma). Other intervals of enhanced carbonate dissolution are located in the Upper Paleocene (~56 Ma) and in the upper Lower Eocene (~51 Ma). The transient dissolution episode that occurred during the BETM was not preserved in these holes. Enhanced preservation of planktic foraminiferal assemblages marks the start of both the Paleocene and Eocene epochs.

INTRODUCTION

Calcite and aragonite produced by plankton sinks toward the seafloor throughout the oceans. At some depth, depending on mineralogy, this carbonate begins to dissolve because of unfavorable physiochemical conditions. The carbonate compensation depth (CCD) is the depth where carbonate dissolution exceeds carbonate supply so that no carbonate accumulates on the seafloor (Murray and Renard, 1891; Bramlette, 1961). The water column above the CCD where the preservation of carbonate decreases noticeably (often some 2 km in depth) is the lysocline (Berger, 1971). Early experiments evaluating the lysocline involved measuring weight loss in suspended calcite spheres (Peterson, 1966). When samples of foraminiferal ooze are suspended in the lysocline, thin-walled planktic tests preferentially dissolve and shell fragmentation increases (Berger, 1967).

The CCD and lysocline at a given location may change over geological time in response to variations in carbonate supply and properties of deep ocean waters (e.g., Berger, 1974, 1992; Farrell and Prell, 1989; Le and Shackleton, 1992; LaMontagne *et al*., 1996). Stable oxygen and carbon isotope records constructed using benthic foraminifera display a series of large-amplitude excursions during the Paleocene and Eocene at ~65-33.7 Ma, especially spanning the Late Paleocene, the Basal Eocene Thermal Maximum (BETM), and the Early Eocene Climatic Optimum (EECO) (**Fig. 1**). These perturbations in $\delta^{18}O$ and $\delta^{13}C$ of deep-sea carbonate are generally interpreted as representing profound changes in early Cenozoic deep water temperatures and global carbon cycling. As such, they might also correspond to times of significant depth variation in the CCD and lysocline. Enhanced deep-sea carbonate dissolution clearly coincided with a prominent -3‰ excursion in the $\delta^{13}C$ of benthic foraminifera at the BETM (Kennett and Stott, 1991; Schmitz *et al*., 1996; Thomas and Shackleton, 1996; Zachos *et al*., 2001), both phenomena signifying a rapid, massive input of carbon to the ocean and atmosphere (Dickens *et al*., 1997; Dickens, 2000). For most intervals of the Paleocene and Eocene, however, established records of deep-sea carbonate dissolution (van Andel, 1975; Lyle, Wilson, Janacek, *et al*., 2002) are not sufficiently well constrained for correlation with isotopic perturbations and, by inference, episodes of global oceanographic change.

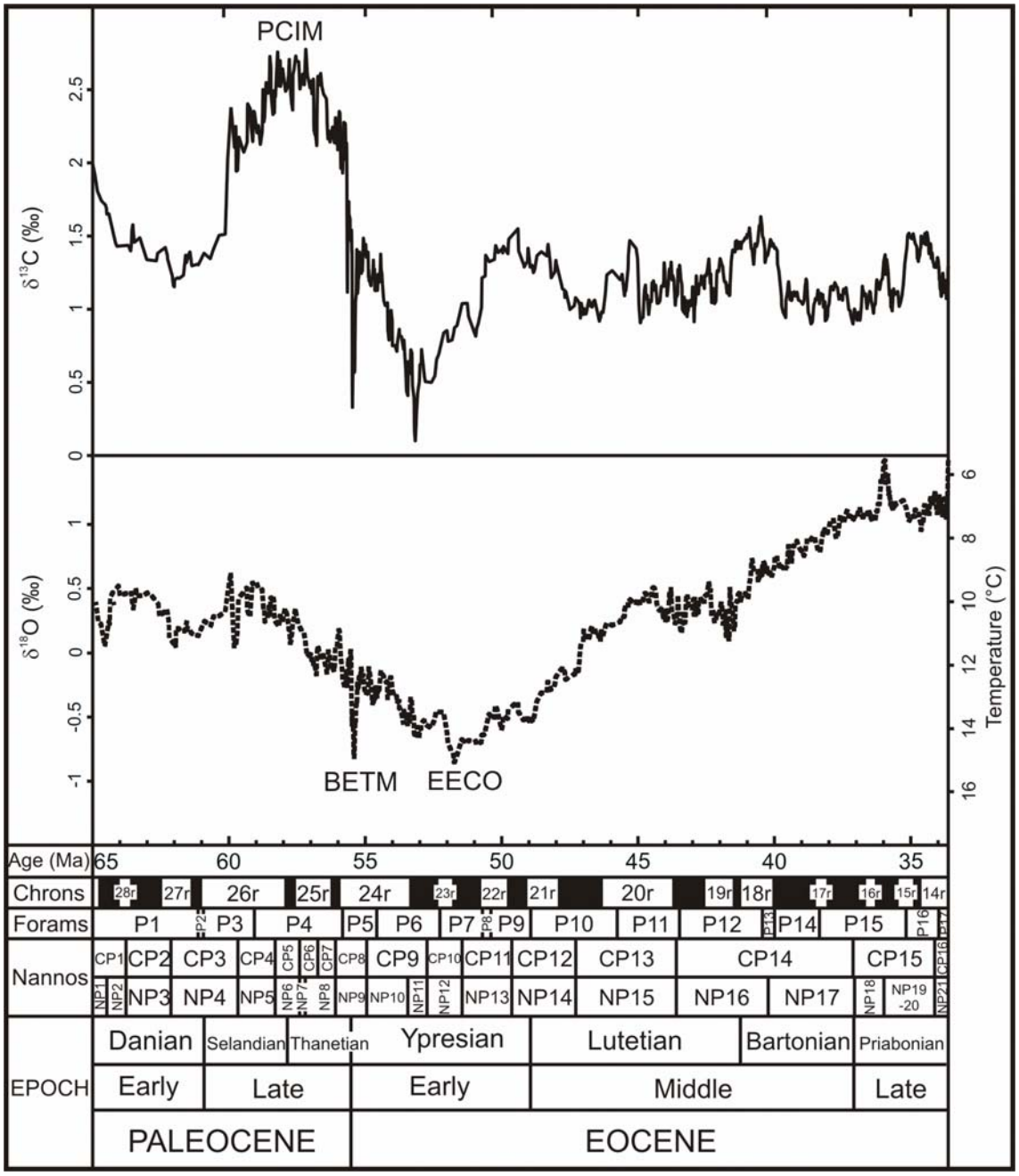

Figure 1. Paleocene and Eocene geochronology (following Berggren *et al.*, 1995) with global carbon and oxygen isotope curves constructed using benthic foraminiferal isotope data (adapted from Zachos *et al.*, 2001). Three key intervals of changing climate and carbon cycling are noted: PCIM = Paleocene Carbon Isotope Maximum, BETM = Basal Eocene Thermal Maximum, EECO = Early Eocene Climatic Optimum.

ODP Leg 198 cored a series of locations on Shatsky Rise in the North Pacific (**Fig. 2**) to evaluate the record of Cretaceous and Palaeogene oceanographic change (Shipboard Scientific Party, 2002). During the Paleocene and Eocene, the crest of Shatsky Rise was nominally at 1500 m water depth (Ito and Clift, 1998; Sager *et al*., 1999). The relatively thick and complete Palaeogene sedimentary successions down the flanks of Shatsky Rise (Krasheninnikov, 1981; Sliter and Brown, 1993) should, therefore, hold a record of past fluctuations in carbonate dissolution. In this study, carbonate content, coarse size fraction, benthic foraminiferal abundance and planktic foraminiferal fragmentation were measured in samples of Paleocene and Eocene sediment from Holes 1209A and 1211A on the Southern High of Shatsky Rise (**Fig. 2**). Our primary aim was to document intervals of enhanced dissolution between 65 and 33.7 Ma. We also compare our records to the Palaeogene CCD curve recently published for the Equatorial Pacific Ocean (Lyle, Wilson, Janacek, *et al*., 2002).

Figure 2. Map showing the location of Sites 1209 and 1211 on the Southern High, Shatsky Rise (adapted from Shipboard Scientific Party, 2002).

SITES AND SAMPLES

Shatsky Rise is a large igneous province in the northwest Pacific that rises from surrounding abyssal plains to a present-day water depth of 2000 m. This feature originally formed in the central equatorial Pacific at ~148 Ma, and subsequently moved south and then northwest to its present-day position (Sager *et al*., 1999; Shipboard Scientific Party, 2002). During the Paleocene and Eocene, Shatsky Rise lay at ~20˚N (Larson *et al*., 1992; Shipboard Scientific Party, 2002). Thermal subsidence models (Ito and Clift, 1998) and rudist fossils dredged from the south edge of the Southern High (Sager *et al*., 1999) indicate that Shatsky Rise was subaerially exposed during and immediately after eruption. During the Palaeogene, however, Shatsky Rise submerged to water depths between 1500 and 4000 m (Ito and Clift, 1998; Sager *et al*., 1999). Importantly, Shatsky Rise received little siliceous material during the Paleocene and Eocene and has always been distant from a continental margin and associated terrigenous inputs (Bralower, Premoli Silva, Malone *et al*., 2002). These factors simplify interpretations of the sedimentary record.

Eight sites were drilled on Shatsky Rise (Shipboard Scientific Party, 2002). Boreholes at two of these sites were chosen for this study. Site 1209 is located close to the top of the Southern High at 32˚39.10’N, 158˚30.36’E (2387 m water depth), and Site 1211 is located 100 km to the southwest on the southern flank of the Southern High at 32˚00.13’N, 157˚51.00’E (2907 m water depth) (**Fig. 2**). The two sites thus comprise a depth transect of 520 m. Site 1211 was drilled at the location of Deep Sea Drilling Project (DSDP) Site 305 (Larson, Moberly, *et al*., 1975). According to thermal subsidence curves (Ito and Clift, 1998), Site 305 (and, hence, Site 1211) lay beneath ~2.5 km of water during the Paleocene and Eocene. Site 1209 was under ~2.0 km of water during this time, assuming a similar depth offset between Sites 1209 and 1211 throughout the Cenozoic. The CCD in the equatorial Pacific was probably between 3 and 4 km for good portions of the Paleocene and Eocene (van Andel *et al*., 1975; Lyle, Wilson, Janacek, *et al*., 2002)**.** Sites 1209 and 1211 should, therefore, be ideal locations to monitor fluctuations in the early Palaeogene lysocline.

Three holes were cored at each of Sites 1209 and 1211. These holes extend to ~320 metres below seafloor (mbsf) at Site 1209, and ~180 mbsf at Site 1211 (Shipboard

Scientific Party, 2002). By splicing together sections from the holes, composite logs were constructed for both sites (Shipboard Scientific Party, 2002). Depths on these logs and in this study are thus reported in metres composite depth (mcd). Apparently continuous Paleocene and Eocene sections occur from ~140 to 255 mcd at Site 1209, and from ~85 to 150 mcd at Site 1211 (Shipboard Scientific Party, 2002) (**Fig. 3**). Paleocene and Eocene sediment at both sites is primarily very pale orange nannofossil and moderate yellowish-brown clayey nannofossil ooze, commonly showing dm- to m-scale cyclicity. Interestingly, this cyclicity is more pronounced at the shallower Site 1209. Paleocene and Eocene sediments at Sites 1209 and 1211 were dated using planktic foraminiferal assemblages (Petrizzo, pers. comm., 2004), using age datums provided by Berggren *et al*. (1995). This biostratigraphy is fairly similar to that suggested on the ship (Bralower, Premoli Silva, Malone, *et al*., 2002) and renders average Paleocene-Eocene sedimentation rates of 1.5 and 3 m/m.y. in Holes 1211A and 1209A, respectively (Shipboard Scientific Party, 2002, p. 121). Values are typical for plateaus in open-ocean, deep-water settings (Kennett, 1982).

Sediment deposited during several critical episodes of Palaeogene climate evolution (**Fig. 1**) was recovered in both Holes 1209A and 1211A (**Fig. 2**). These episodes include the Eocene/Oligocene transition, the EECO and the BETM, as well as a mid Paleocene biotic event characterized by the FO of the nannolith *Heliolithus kleinpellii* (58.4 Ma) and primitive *Discoasters*, both of which are important, and often dominant, components of Late Paleocene and younger nannoplankton assemblages. Sediment deposited during this biotic event also contains a low-diversity planktic foraminiferal assemblage dominated by *Igorina tadjikastanensis* (Shipboard Scientific Party, 2002; Petrizzo, 2005).

An increase in carbonate content and a lack of colour cycles highlights the Eocene/Oligocene transition. Although no obvious lithological changes characterize the EECO, a thin claystone marks the BETM, and a phillipsite-rich, carbonate-poor horizon containing abundant fish teeth and manganese-coated foraminifera marks the mid Paleocene biotic event (Shipboard Scientific Party, 2002). Additionally, intervals of low sedimentation rate are found in Middle to Upper Eocene sediment between 33.7 and 45 Ma in both holes (Petrizzo, pers. comm., 2004).

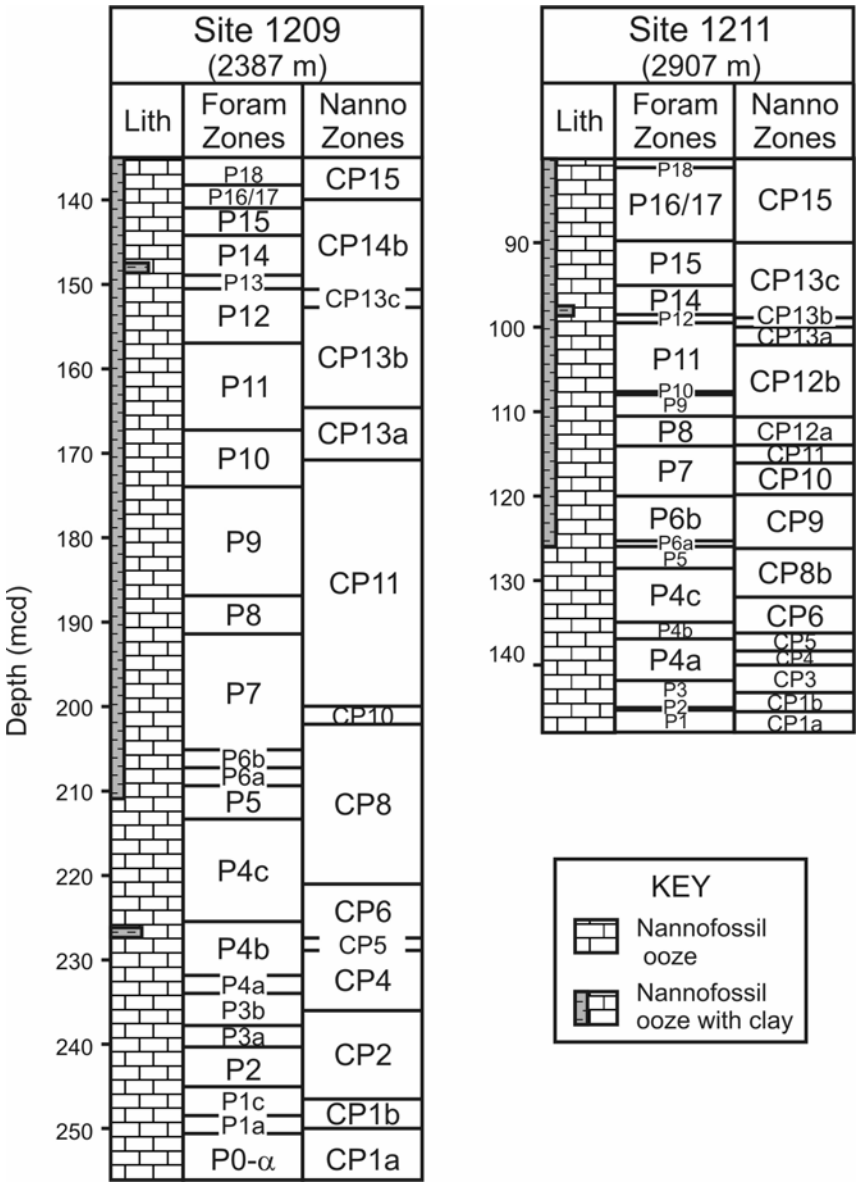

Figure 3. Lithologic logs for Sites 1209 and 1211 with planktonic foraminifer (Petrizzo, pers. comm., 2004) and nannofossil datums (Bralower, pers. comm., 2004).

For this study, we collected 134 sediment samples of 10 cm^3 from 137.56 to 251.38 mcd in Hole 1209A, and 99 sediment samples of 10 cm^3 from 84.60 to 147.46 mcd in Hole 1211A (**Fig. 3**). Samples were initially taken on board ship at a resolution of three per core. In order to examine a potential relationship between sediment cycles and dissolution, one sample was also taken from obvious light and dark layers. Additional samples were collected every 10 to 20 cm over suspected dissolution episodes. On average and from each hole, there are about four samples for every 1 m.y. of sediment deposition.

METHODS

Preparation

All samples were freeze-dried to remove water and divided into two portions. The first ~2 cm^3 portion was crushed and used to determine bulk carbonate content. The other ~5 cm^3 portion was weighed, wet sieved at 38 μm, and used to determine coarse size fraction, benthic foraminiferal abundance and foraminiferal fragmentation. All four of these parameters have been used in previous investigations to make inferences about carbonate dissolution (e.g., Le and Shackleton, 1992; LaMontagne *et al*., 1996). In studies of Quaternary foraminiferal assemblages, the >63 μm size fraction has generally been used for dissolution studies because it conveniently coincides with the sand size fraction (e.g., Broecker and Clark, 1999, 2001). However, 38μm was chosen to delineate coarse fraction in this study as Paleocene foraminifera are commonly small.

Carbonate content

Approximately 100 mg of dried, crushed sample was analyzed for carbonate content according to the "Karbonate-Bomb" method (Mueller and Gastner, 1971). Sample aliquots were reacted with ~3 mL of 10% HCl to produce CO_2 gas in a closed vessel attached to a water-filled cylinder marked with 0.1 mL graduations. Carbonate content was determined by comparing the volume of CO_2 gas generated to that produced from known masses of laboratory-grade $CaCO_3$. Each sample was analyzed twice to ensure analytical precision. These replicate analyses were consistently within 2wt%, and reported carbonate contents are the average of both measurements. A sample of Palaeogene siliceous limestone (JCU Sample MS14) with a known carbonate content of 72wt% was also analyzed twice to evaluate accuracy and precision. The measured carbonate content of MS14 was 71wt% ± 2wt%.

Coarse size fraction and microsplitting

After wet sieving, the coarse (>38 μm) component of the second sample portion was dried and weighed. This mass divided by bulk sample mass rendered the coarse

(>38 μm) size fraction. Carbonate dissolution within the lysocline commonly leads to fragmentation of foraminifera tests, which decreases the coarse size fraction of bulk sediment (Berger, *et al*., 1982; Broecker and Clark, 1999). However, we were unsure if and how this proxy would register dissolution in Palaeogene sediment from Shatsky Rise because nannofossils are the dominant contributors (>90wt%) to the sediment (see "Visual Core Description" in Bralower, Premoli Silva, Malone, *et al*., 2002). Changes in the relative abundances of nannofossils and foraminifera could certainly give variations in grain size unrelated to dissolution.

A microsplitter was then used to separate at least 300 foraminifera and fragments from the coarse fraction onto a marked slide. Care was taken to distribute material evenly over the microsplitter to avoid sampling bias. The number of fragments, benthic foraminifera, and planktic foraminifera were recorded. Where the sample was highly fragmented, and whole foraminifera rare, at least 50 counts of whole foraminifera were made.

Benthic abundance (BENTH)

The relative abundance of benthic foraminifera (BENTH) is expressed as a ratio of benthic foraminifera to the sum of benthic and planktic foraminifera. Benthics are less susceptible to dissolution than planktic foraminifera because the latter typically have porous chamber walls designed to maintain buoyancy in surface waters. Thus, the relative abundance of benthic foraminifera may serve as an index for carbonate dissolution at deep-water sites (Schlanger and Douglas, 1973; Thunell, 1976).

Foraminiferal fragmentation (FRAG)

A foraminiferal fragment (F) is defined here and elsewhere (Berger *et al*., 1982) as a test portion less than two-thirds of its original size. The fragmentation index (FRAG) for each sample was calculated according to the following equation (Williams *et al*., 1985; Malmgren, 1987):

FRAG = (F/8) / [(F/8) + whole planktic foraminifera]

The number of fragments is divided by eight because, on average, one foraminifer breaks into this number of fragments and it is the proportion of fragmented foraminifera, rather than the number of fragments themselves, that has a near-linear relationship with dissolution (Le and Shackleton, 1992, p. 30). Benthic foraminifera are not included in the whole foraminifera count as their tests are more resistant to dissolution than planktic foraminifera.

RESULTS

Carbonate content across all samples varies from 64wt% to 100wt%. Values generally exceed 85wt%, which is consistent with shipboard data (Bralower, Premoli Silva, Malone, *et al.*, 2002) (**Appendix 1, Tables 1, 2; Fig. 4**). Fluctuations between low and high carbonate content are more periodic at the shallower Site 1209, especially in Middle to upper Lower Eocene sediment. For Hole 1209A, the lowest carbonate contents were found in Upper Paleocene sediment deposited at the base of planktic foraminiferal Zone P4 (~59 Ma) and in Middle Eocene sediment deposited at the base of Zone P14 (~40 Ma) (**Fig. 4**). For Hole 1211A, the lowest carbonate contents were found in Middle Eocene sediment deposited at the base of Zone P12 (~43 Ma) (**Fig. 4**). The Upper Paleocene sediment samples with low carbonate content contain abundant phillipsite, fish teeth, manganese-coated planktic foraminifera, and residual foraminiferal assemblages dominated by thick-walled species.

Grain size throughout both studied sequences is generally fine, with the coarse fraction varying from <1wt% to 40wt%, but averaging 5wt% (**Appendix 1, Tables 1, 2; Fig. 5**). The typically small grain size is consistent with shipboard lithological descriptions, which classified the recovered Paleocene and Eocene sediment as nannofossil ooze (Bralower, Premoli Silva, Malone, *et al.*, 2002). There are, however, several intervals particularly enriched in coarse-grained sediment. For both holes, the >38-μm fraction surpasses 31wt% and 13wt% at the start of the Paleocene and Eocene, respectively (**Fig. 5**).

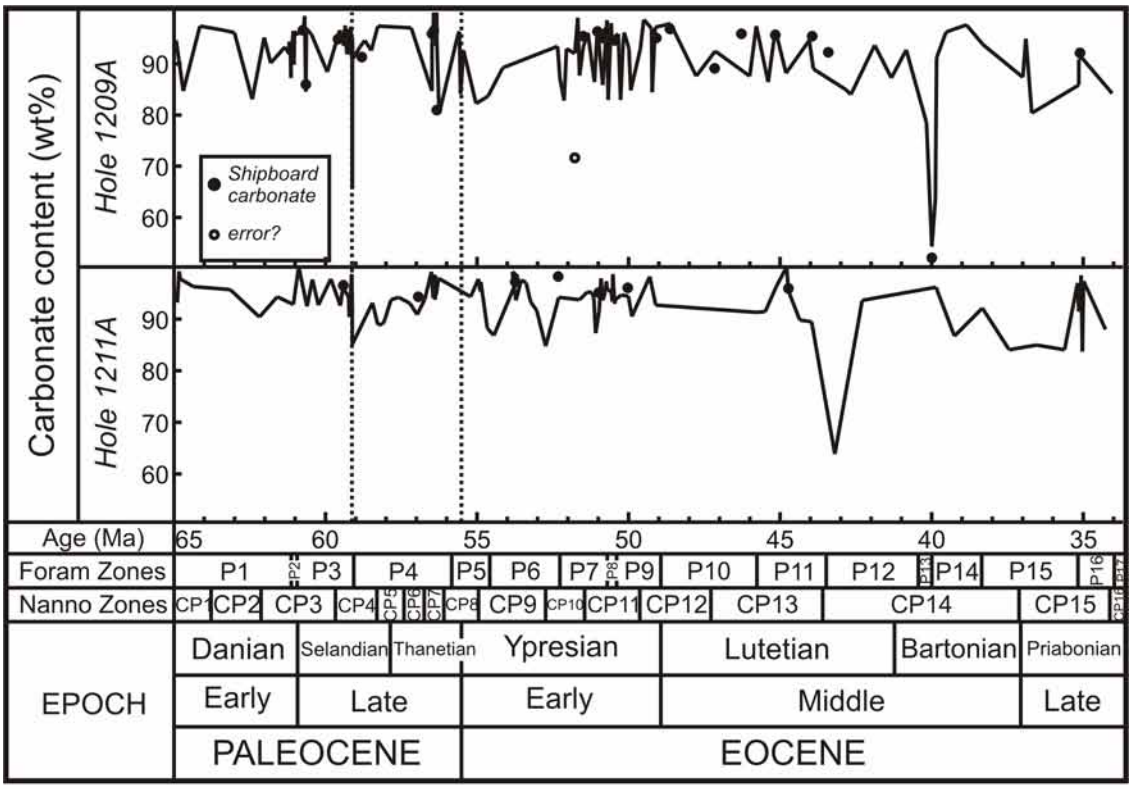

Figure 4. Carbonate content (wt%) in Paleocene and Eocene sediment at Holes 1209A and 1211A.

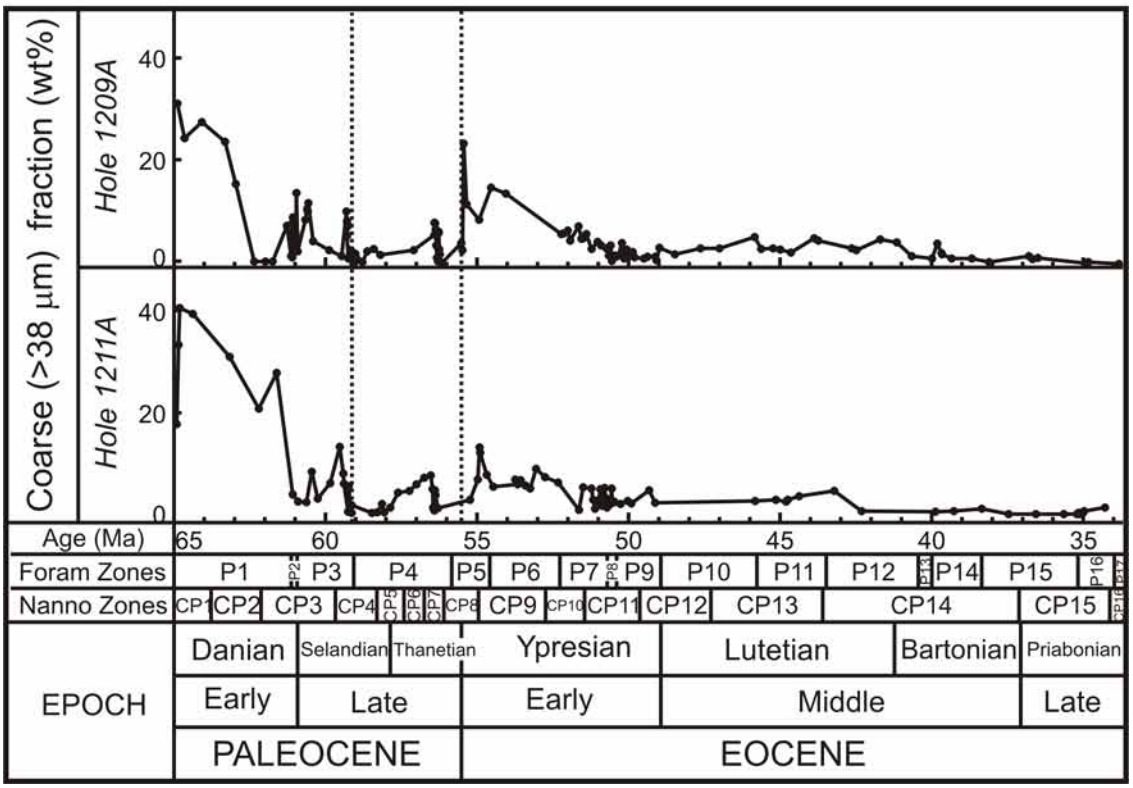

Figure 5. Coarse (>38 μm) fraction of sediment (wt%) in Paleocene and Eocene sediment at Holes 1209A and 1211A.

Benthic foraminiferal abundance varies considerably in the samples studied, ranging from <1% to 100% (**Appendix 1, Tables 1, 2; Fig. 6**). In both holes, BENTH usually averages 20%, implying that planktic species generally dominate Paleocene and Eocene foraminiferal assemblages. A wide range in BENTH occurs, however, because foraminiferal assemblages are comprised mostly of benthic species across several specific intervals, notably in planktic foraminiferal Zone P4 (~59-58 Ma and 56 Ma) and during the Middle and Late Eocene in Zones P12 to P16 (specifically ~40 and 37-33.7 Ma) in both holes.

The fragmentation index varies from <1% to 100% but averages ~25% and is generally <10% for both sites (**Appendix 1, Tables 1, 2; Fig. 7**). However, significant increases in FRAG were found in Zone P4 (~59-58 and 56 Ma) and during the Middle and Late Eocene (~37-33.7 Ma) for both holes. At Hole 1209A, FRAG also increases in the Middle Eocene (~43 and 41 Ma), and at Hole 1211A, FRAG also increases in the late Early Eocene (~51 Ma) and in the Middle Eocene (~45 Ma).

RELIABILITY OF DISSOLUTION INDICES

Of the dissolution indices examined, FRAG and BENTH record greater-amplitude and higher-frequency variations than carbonate content or the proportion of coarse fraction (**Figs. 4-7**). Presumably, FRAG and BENTH are more sensitive measures of carbonate dissolution because they can be high where carbonate content is high (e.g., LaMontagne *et al*., 1996), such as within the upper lysocline (Berger, 1967).

Plots between the various indices, such as FRAG versus each of carbonate content, size faction and BENTH (**Fig. 8A-C**), show some insights and complexities facing dissolution interpretations. Trends of FRAG and BENTH display a good correlation ($r^2 = 0.77$) across the sample set, and both probably provide good indicators of carbonate dissolution, at least for most samples in this study. However, planktic and benthic counts are far less time consuming than fragmentation counts, so BENTH is a much easier measurement. A bivariate plot of FRAG and carbonate content shows a broad relationship of high carbonate content with low FRAG, but with weak correlation ($r^2 = 0.03$). At moderate to low carbonate content (<70wt% for this study), FRAG may become problematic because significant numbers of fragments may have been

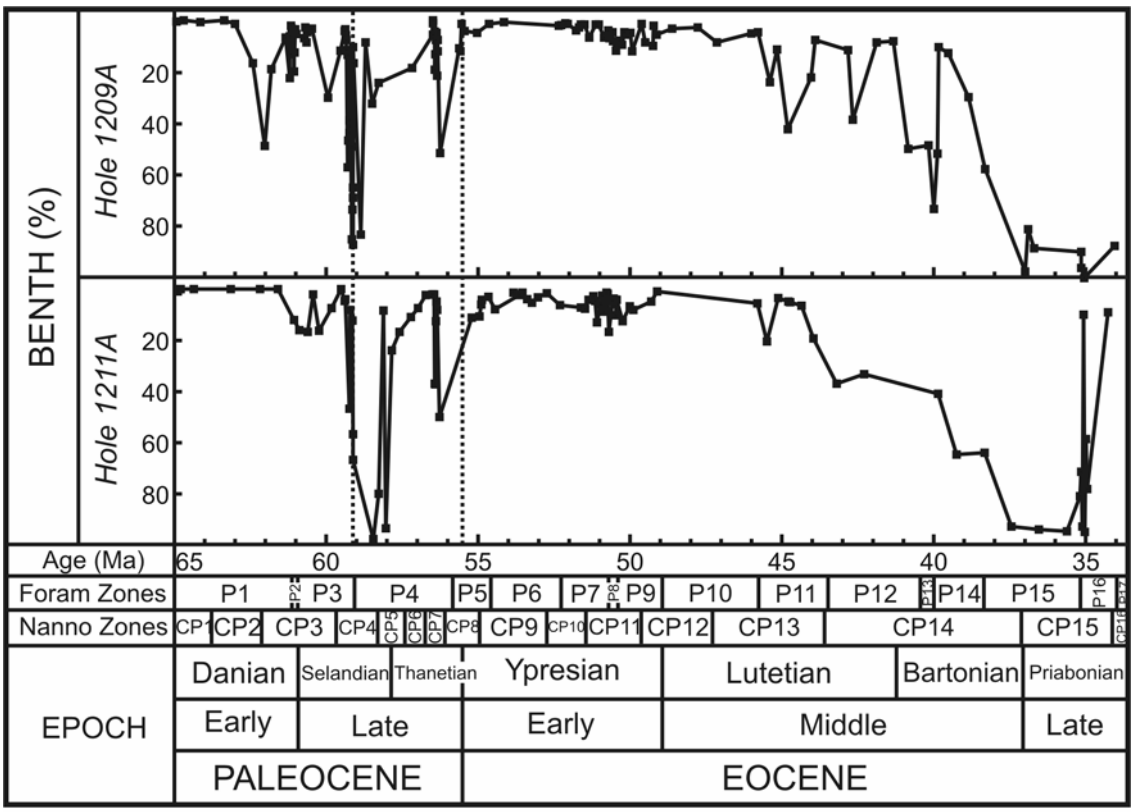

Figure 6. The dissolution proxy BENTH (%) in Paleocene and Eocene sediment at Holes 1209A and 1211A.

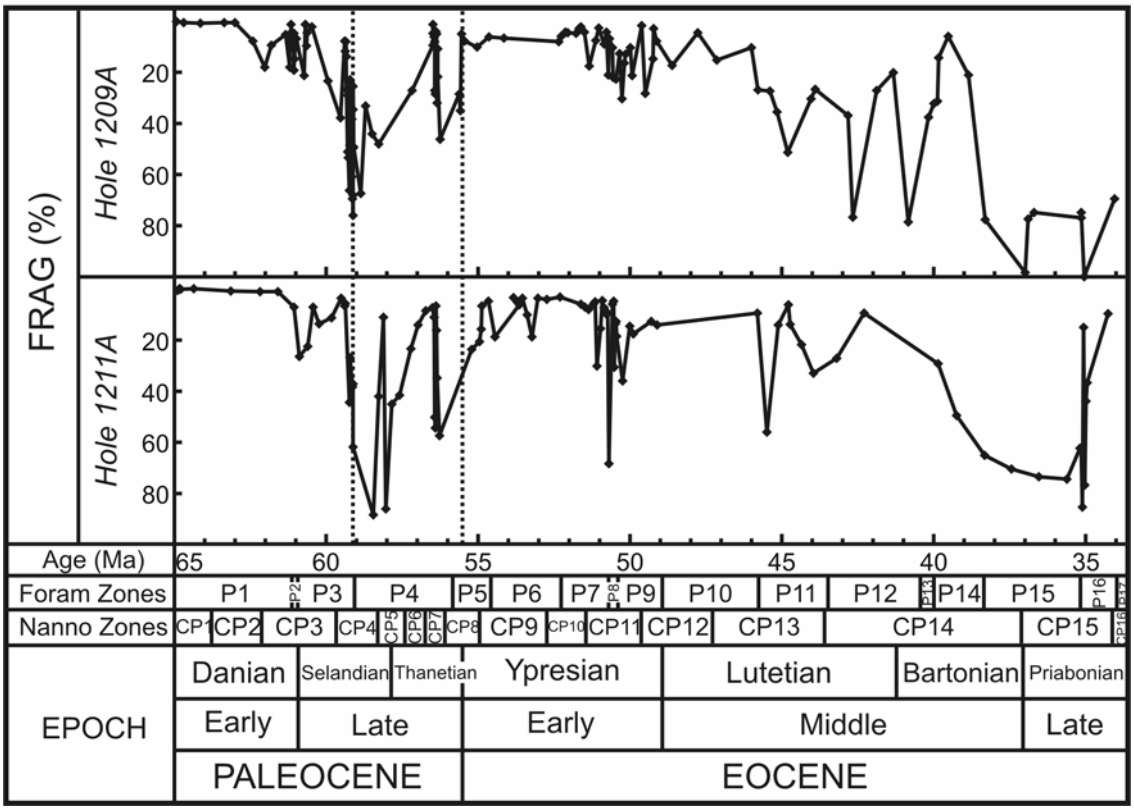

Figure 7. The dissolution proxy FRAG (%) in Paleocene and Eocene sediment at Holes 1209A and 1211A.

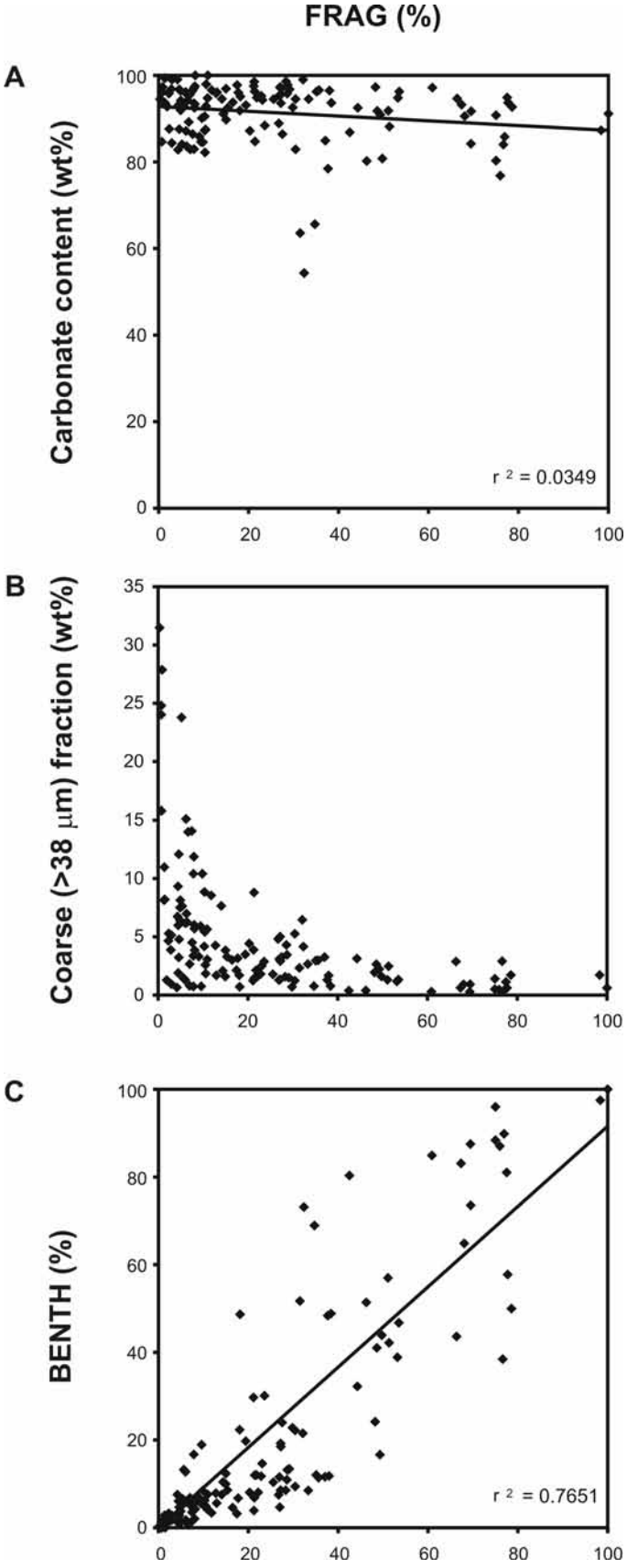

Figure 8. Bivariant plots of potential dissolution indices. A. FRAG (%) versus carbonate content (wt%). B. FRAG (%) versus coarse (>38 μm) fraction (wt%). C. FRAG (%) versus BENTH (%).

dissolved, and the residual assemblage can contain resistant tests. Post-burial dissolution and fragmentation of foraminiferal shells complicates FRAG. A plot of FRAG against coarse fraction shows that FRAG varies widely (0%-80%) when fine-grained material dominates bulk sediment (<10wt% coarse), but is fairly constant when coarse-grained material comprises a significant fraction. As mentioned previously, the relative abundance of nannofossils complicates grain size interpretations in these sediments.

DISSOLUTION EPISODES

Paleocene and Eocene sediment sections at Sites 1209 and 1211 are relatively expanded and complete (**Fig. 3**). As suggested by the various proxy records for dissolution (**Figs. 4-7**), this probably reflects a history where the two sites remained above the lysocline for good portions of the early Palaeogene. Given estimated palaeodepths of 2.0 and 2.5 km for Sites 1209 and 1211, respectively, this is consistent with a Pacific CCD greater than 3.0 km during most of the Paleocene and Eocene (van Andel, 1975; Lyle, Wilson, Janacek, *et al*., 2002).

However, intervals of carbonate dissolution do punctuate the Paleocene and Eocene sediment sections on Shatsky Rise. When all four dissolution indices are examined collectively, prominent dissolution occurred at both sites during the Late Paleocene (lower Zone P4; ~59-58 Ma), and during the Middle to Late Eocene (Zone P11-P16, ~45-33.7 Ma). We discuss these two "dissolution episodes" below, but note that intervals of enhanced carbonate dissolution also occurred during the Late Paleocene (upper Zone P4, ~56 Ma), and the late Early Eocene (Zone P7, ~51 Ma). The first of these other dissolution intervals precedes the BETM. Interestingly, however, the BETM does not stand out in our records, as discussed below. In other deep marine sedimentary records, a transient dissolution episode has been observed during the BETM (e.g., Thomas and Shakleton, 1996; Katz *et al*., 1999; Zachos *et al*., 2004).

Considering the entire time interval examined, times of dissolution generally seem longer and more pronounced at Hole 1211A compared to Hole 1209A (**Figs. 4-7**). This is consistent with the depth positions of the two sites.

Late Paleocene (~59-58 Ma)

Beginning close to the boundary between the P3 and P4 foraminiferal biozones (~59.1 Ma), and continuing for 1 to 2 m.y. afterwards, BENTH and FRAG are unusually high at both Site 1209 and Site 1211 (**Figs. 6, 7**). There are also noticeable decreases in the carbonate content and coarse fraction of bulk sediment (**Figs. 4, 5**). At both sites, the dissolution episode closely coincides with the mid Paleocene biotic event (**Figs. 4-7**). Note that Petrizzo (2005) dated the mid Paleocene biotic event at ~58.4 Ma whereas the planktic foraminiferal biostratigraphy used in this study (Berggren *et al*., 1995; Petrizzo, pers. comm., 2004) gives an age of ~59.1 Ma. The biotic event is characterized by high magnetic susceptibility, high abundances of phillipsite and manganese coated foraminifera, and residual foraminiferal assemblages (Shipboard Scientific Party, 2002; Petrizzo, 2005). These sedimentological features further support carbonate dissolution and reduced sedimentation rates (Shipboard Scientific Party, 2002; Petrizzo, 2005). Thus, all information suggests that the lysocline shoaled significantly during this time.

Importantly, carbonate dissolution as measured in our study extends several metres beyond the biotic event as defined by obvious lithological change. For example, at Hole 1209A, the zone of high magnetic susceptibility and phillipsite spans from about 212.30 to 211.85 mbsf, whereas BENTH and FRAG generally exceed 25% from 215.80 to 210.90 mbsf. Thus, it appears that the biotic event marks a brief extreme within the context of a longer, 1-2 m.y. interval of unusual conditions. The relatively long time supports the view of Petrizzo (2005) that the biotic event and its coeval carbonate dissolution were somehow linked to a change in ocean circulation, rather than a massive input of carbon such as occurred at the BETM. We note that an unusual black shale facies closely corresponds to the start of the P4 foraminiferal biozone in sections deposited off the east coast of New Zealand, and that this also has been attributed to a change in Pacific circulation (Hollis *et al*., 2005).

Middle to Late Eocene (~45-33.7 Ma)

All indices for dissolution also suggest a relative shoaling of the lysocline in the Late Eocene beginning at about 45 Ma, and becoming particularly prominent between

37 and 33.7 Ma. Support for such dissolution on Shatsky Rise comes from sedimentation rates, which drop significantly through this interval at Sites 1209, 1210, 1211, and 1212 (Bralower, Premoli Silva, Malone, *et al*., 2002). In Hole 1209A carbonate (wt%) drops precipitously at ~40 Ma but there is no corresponding drop in the deeper record, which is possibly an artefact of inadequate sampling.

Site 711 on Madingley Rise in the Central Indian Ocean also contains a condensed interval of low carbonate accumulation during the Late Eocene (Peterson *et al*., 1992). This may hint at a correlative shoaling of the lysocline in this basin. Furthermore, existing CCD records for the Pacific and Indian Oceans (van Andel, 1975; Lyle, Wilson, Janacek, *et al*., 2002) indicate an anomalously shallow CCD of about 3.2 km for the Late Eocene. Although the exact shapes of the CCD and lysocline profiles through the early Palaeogene remain poorly constrained, both probably shoaled between 45 and 33.7 Ma, perhaps to minimum depths between 37 and 33.7 Ma.

The magnitude and longevity of this Middle to Late Eocene dissolution interval suggests a change in the ocean carbonate budget, which may ultimately relate to alkalinity and Ca inputs. Interestingly, this time interval was characterized by significant cooling and the first ephemeral ice sheets on Antarctica (Zachos *et al*., 1994, 2001).

Initial Eocene Thermal Maximum (~55.5 Ma)

At Sites 1209 and 1211, the BETM (~55.5 Ma in this study) is marked by an ~12 cm-thick layer of clayey nannofossil ooze with a sharp basal contact, a mm-thick clay layer, and a gradational upper contact (Shipboard Scientific Party, 2002). Additionally, nannofossil preservation decreases toward the base of this unit (Shipboard Scientific Party, 2002). The lysocline probably shoaled significantly and rapidly during the BETM on Shatsky Rise (Colosimo *et al*., in press) and in all regions of the ocean in response to massive carbon addition (Dickens *et al.,* 1997; Dickens 2000).

Our records do not express this lysocline shoaling very well, probably for two related reasons. First, the BETM is poorly represented in Holes 1209A and 1211A (e.g., core recovery and splitting appears to have disturbed the clay seam in Hole 1209A)

(Shipboard Scientific Party, 2002). Second, we did not examine the base of the interval with appropriate sample resolution. Interestingly, though, BENTH and FRAG both drop significantly within 10 to 20 cm above the start of the BETM (**Figs. 6, 7**). This interval also has a corresponding influx of well-preserved planktic foraminifera, which increase the >38 μm fraction (**Fig. 5**). Together, these observations may indicate a deepening of the lysocline immediately following the initial lyscoline shoaling and carbon addition. Carbon cycle models that include a weathering feedback, where increased CO_2 in the atmosphere accelerates continental weathering, predict such a change in the lysocline (Dickens *et al*., 1997).

SUMMARY AND CONCLUSIONS

Indices for carbonate dissolution were examined in lower Palaeogene sediment (65 to 33.7 Ma) recovered from two boreholes (1209A, 1211A) on Shatsky Rise. The two best measures for carbonate dissolution are probably FRAG and BENTH, which indicate the relative abundance of foraminifera test fragmentation and benthic foraminifera, respectively. These proxies display good covariance across the sample set and similar downhole patterns at Holes 1209A and 1211A.

For Holes 1209A and 1211A, all indices suggest two significant early Palaeogene dissolution episodes. The first of these occurred in the early Late Paleocene at ~59-58 Ma (lower part of planktic foraminifera Zone P4), and coincides with a recently identified biotic event. We suspect that the biotic event and accompanying seafloor carbonate dissolution relate to a change in deep ocean circulation. The second dissolution episode is more protracted, beginning in the Middle Eocene at ~45 Ma (P11) but reaches a maximum during the Late Eocene at ~37-33.7 Ma (P15-P16). This is probably the most prominent interval of carbonate dissolution recorded in Palaeogene sediments from Shatsky Rise, and may represent a time of shallow lysoclines and CCDs throughout the oceans. Other intervals of enhanced carbonate dissolution occurred in the Late Paleocene ~56 Ma (upper Zone P4) and in the late Early Eocene ~51 Ma (Zone P7). The BETM interval was not really investigated in this study, but the lysocline may have first shoaled then deepened.

ACKNOWLEDGMENTS

Tim Bralower and Maria Rose Petrizzo are thanked for making biostratigraphic data available prior to publication. Tim Bralower, David Rea and Mitch Lyle are thanked for their helpful reviews that improved the paper. This research used samples and data provided by the Ocean Drilling Program (ODP). ODP is sponsored by the U.S. National Science Foundation (NSF) under management of Joint Oceanographic Institutions (JOI), Inc. Funding for this research was provided by Australian ODP.

REFERENCES

van Andel, T.H., 1975. Mesozoic/Cenozoic calcite compensation depth and the global distribution of calcareous sediments. *Earth and Planetary Science Letters*, 26:187-194.

Berger, W.H., 1967. Foraminiferal ooze: solution at depths. *Science*, 156:383-385.

Berger, W.H., 1971. Sedimentation of planktonic foraminifera. *Marine Geology*, 11:325-358.

Berger, W.H., 1974. Plate stratigraphy and the fluctuating carbonate line. *Special Publication of the International Association of Sedimentologists*, 1:11-48.

Berger, W.H., Bonneau, M.C. and Parker, F.L., 1982. Foraminifera on the deep-sea floor; lysocline and dissolution rate. *Oceanologica Acta*, 5(2):249-258.

Berger, W.H., 1992. Pacific carbonate cycles revisited: arguments for and against productivity control. *In* Ishizaki, K. and Saito, T., (Eds.), *Centenary of Japanese Micropaleontology*, 15-25.

Berggren, W.A., Kent, D.V., Swisher, C.C., III, *et al*., 1995. A revised Cenozoic geochronology and chronostratigraphy. *In* Berggren, W.A., Kent, D.V., Aubry, M.-P. and Hardenbol, J. (Eds.), *Geochronology, time scales and global stratigraphic correlation*, Special Publication- Society Economic Paleontology and Mineralogy. (Soc. Sediment. Geol.), 54:129-212.

Bralower, T.J., Premoli Silva, I., Malone, M.J., *et al*., 2002. *Proc. ODP, Init. Repts*, 198 [CD-ROM]. Available from: Ocean Drilling Program, Texas A&M University, College Station TX 77845-9547, USA.

Bramlette, M.N., 1961. Pelagic sediments. *In* Turekian, K.K., (Ed), *Oceanography*. Publs. Am. Ass. Advmt Sci., 67:345-366.

Broecker, W.S. and Clark, E., 1999. $CaCO_3$ size distribution: A paleocarbonate ion proxy? *Paleoceanpgoraphy*, 14(5):596-604.

Broecker, W.S. and Clark, E., 2001. Reevaluation of the $CaCO_3$ size index paleocarbonate ion proxy. *Paleoceanography*, 16(6):669-671.

Dickens, G.R., Castillo, M.M. and Walker, J.C.G., 1997. A blast of gas in the latest Paleocene; simulating first-order effects of massive dissociation of oceanic methane hydrate. *Geology*, 25(3):259-262.

Dickens, G.R., 2000. Methane oxidation during the Late Palaeocene Thermal Maximum. *Bull. Soc. Geol. Fr.*, 171:37-49

Farrell, J.W. and Prell, W.L., 1989. Climatic change and $CaCO_3$ preservation: An 800 000 year bathymetric reconstruction from the central equatorial Pacific Ocean. *Paleoceanography*, 4(4):447-466.

Hollis, C.J., Dickens, G.R., Field, B.C., Jones, C.M., and Strong, C.P., 2005. The Paleocene-Eocene transition at Mead Stream, New Zealand: a southern Pacific record of early Cenozoic global change. *Palaeogeography, Palaeoclimatology, Palaeoecology*, 215:313-343, 2005.

Ito, G. and Clift, P.D., 1998. Subsidence and growth of Pacific Cretaceous plateaus. *Earth and Planetary Science Letters,*, 161(1-4):85-100.

Katz, M.E., Pak, D.K., *et al.*, 1999. The source and fate of massive carbon input druing the latest Paleocene thermal maximum. *Science*, 286:1531-1533.

Kennett, J. P., 1982. *Marine geology*. Prentice-Hall, Englewood Cliffs, NJ, 813 pp.

Kennett, J.P. and Stott, L., 1991. Abrupt deep-sea warming, paleoceanographic changes and benthic extinctions at the end of the Paleocene. *Nature*, 353:225-229.

Kobashi, T., Grossman, E. L., Dockery III, D. T. and Ivany, L. C., 2004. Water mass stability reconstructions from greenhouse (Eocene) to icehouse (Oligocene) for the northern Gulf Coast continental shelf (USA), *Paleoceanography, 19*, PA1022, doi:10.1029/2003PA000934.

Krasheninnikov, V.A., 1981. Paleogene planktonic foraminifers from Deep Sea Drilling Project Leg 62 sites and adjacent areas of the Northwest Pacific. *In* Thiede, J. and Vallier, T.L. (Eds.), *Init. Repts. DSDP*. Washington (U.S. Govt. Printing Office), 62:365-376.

LaMontagne, R.W., Murray, R.W., Wei, K.-Y., *et al.*, 1996. Decoupling of carbonate preservation, carbonate concentration, and biogenic accumulation: a 400-kyr

record from the central equatorial Pacific Ocean. *Paleoceanography*, 11(5):553-562.

Larson, R.L., Moberly, R., *et al*., 1975. *Init. Repts. DSDP*, 32: Washington (U.S. Govt. Printing Office).

Larson, R.L., Steiner, M.B., Erba, E., *et al*., 1992. Paleolatitudes and tectonic reconstructions of the oldest portion of the Pacific Plate: a comparative study. *In* Larson, R.L. and Lancelot, Y. (Eds.), *Proc. ODP, Init. Repts., 129*. College Station, TX (Ocean Drilling Program), 615-631.

Le, J. and Shackleton, N.J., 1992. Carbonate dissolution fluctuations in the western equatorial Pacific during the late Quaternary. *Paleoceanography*, 7(1):21-42.

Lyle, M., Wilson, P.A., Janecek, T.R., *et al*., 2002. *Proc. ODP, Init. Repts.*, 199 [CD-ROM]. Available from: Ocean Drilling Program, Texas A&M University, College Station TX 77845-9547, USA.

Malmgren, B.A., 1987. Differential dissolution of Upper Cretaceous planktonic foraminifera from a temperate region of the South Atlantic Ocean. *Marine Micropaleontology*, 11(4):251-271.

Mueller, G. and Gastner, M., 1971. The "Karbonate-Bombe", a simple device for the determination of the carbonate content in sediments, soils, and other materials. *Neues Jahrbuch fuer Mineralogie Monatshefte*, 10:466-469.

Murray, J. and Renard, A.F., 1891. Deep-sea deposits based on the specimens collected during the voyage of H.M.S. Challenger in the years 1872 to 1876. *Rep. Voy. Challenger*, Longmans, London, 525 pp. (Johnson reprint, London 1965).

Peterson, L.C., Murray, D.W., Ehrmann, W.U., *et al*., 1992. Cenozoic carbonate accumulation and compensation depth changes in the Indian Ocean. *Geophysical Monograph*, 70:311-333.

Peterson, M.N.A., 1966. Calcite: rates of dissolution in a vertical profile in the central Pacific. *Science*, 154:15422-1544.

Petrizzo, 2005. An early late Paleocene event on Shatsky Rise, northwest Pacific Ocean (ODP Leg 198): evidence from planktonic foraminiferal assemblages. *In* Bralower, T.J., Premoli Silva, I., and Malone, M.J. (Eds.), *Proc. ODP, Sci. Results*, 198, 1-29 [Online}. Available from World Wide Web: <http://www-odp.tamu.edu/publications/198_SR/VOLUME/CHAPTERS/102.PDF>.

Sager, W.W., Kim, J., Klaus, A., *et al.*, 1999. Bathymetry of Shatsky Rise, Northwest Pacific Ocean; implications for ocean plateau development at a triple junction. *Journal of Geophysical Research*, 104(4):7557-7576.

Schlanger, S.O. and Douglas, R.G., 1973. Porosity and textural changes related to the ooze-chalk-limestone transition. *European Geophys. Soc. Meet. Abstracts*, 1:92.

Schmitz, B., Speijer, R.P. and Aubry, M.P., 1996. Latest Paleocene benthic extinction event on the southern Tethyan shelf (Egypt): foraminiferal stable isotopic ($\delta^{13}C$ and $\delta^{18}O$) records. *Geology*, 24:347-350.

Shipboard Scientific Party, 2002. Leg 198 summary. *In* Bralower, T.J., Premoli Silva, I., Malone, M.J., *et al.*, *Proc. ODP, Init. Repts.*, 198: College Station TX (Ocean Drilling Program), 1-148.

Sliter, W.V., and Brown, G.R., 1993. Shatsky Rise: seismic stratigraphy and sedimentary record of Pacific paleoceanography since the Early Cretaceous. *In* Natland, J.H., Storms, M.A., *et al.*, *Proc. ODP, Sci. Results*, 132: College Station, TX (Ocean Drilling Program), 3-13.

Thomas, E. and Shackleton, N.J., 1996. The Paleocene-Eocene benthic foraminiferal extinction and stable isotope anomalies. *In* Knox, R.W.O.B., Corfield, R.M. and Dunay, R.E., (Eds.), *Correlation of the Early Paleogene in Northwest Europe.* Special Publication of the Geological Society of London, 101:401-441.

Thunell, R.C., 1976. Optimum indices of calcium carbonate dissolution in deep-sea sediments. *Geology*, 4(9):525-528.

Williams, D.F., Healy-Williams, N. and Leschak, P., 1985. Dissolution and water-mass patterns in the Southeast Indian Ocean; Part I, Evidence from Recent to late Holocene foraminiferal assemblages. *Geological Society of America Bulletin*, 96(2):176-189.

Zachos, J.C., Stott, L.D. and Lohmann, K.C., 1994. Evolution of early Cenozoic marine temperatures. *Paleoceanography*, 9(2):353-387.

Zachos, J., Pagani, M., Sloan, L., *et al.*, 2001. Trends, rhythms, and aberrations in global climate 65 Ma to present. *Science*, 292(5517):686-693.

Zachos, J.C., Kroon, D., *et al.*, 2004. *Proc. ODP, Init. Repts.*, Volume 208 [Online], Available from World Wide Web: http://www-odp.tamu.edu/publications/208_IR/208ir.htm.

APPENDIX 1. Dissolution indices for Holes 1209A and 1211A.

Table 1. Dissolution indices for Hole 1209A.

Hole	Core	Type	Sct	Top (cm)	Bot (cm)	Depth (mbsf)	Depth (mcd)	Age (Ma)	FRAG (%)	BENTH (%)	Coarse Fraction (>38µm) (wt%)	Carbonate Content (wt%)
1209A	14	H	5	67	69	128.87	139.06	34.04	69.4	87.5	0.3	84.2
	14	H	6	67	69	130.37	140.56	35.04	100.0	100.0	0.6	91.2
	14	H	6	82	84	130.52	140.71	35.13	75.0	96.0	0.5	90.8
	15	H	1	67	69	132.37	140.68	35.13	76.9	89.8	0.4	85.8
	15	H	2	67	69	133.87	142.18	36.69	75.0	88.4	1.4	80.3
	15	H	2	85	87	134.05	142.36	36.88	77.5	81.0	1.1	94.9
	15	H	2	95	97	134.15	142.46	36.99	98.4	97.5	1.7	87.3
	15	H	3	67	69	135.37	143.68	38.30	77.7	57.8	0.6	93.7
	15	H	4	69	71	136.89	145.20	38.86	21.1	29.7	1.2	97.5
	15	H	5	122	124	138.92	147.23	39.52	6.0	12.8	1.3	96.1
	15	H	6	72	74	139.92	148.23	39.84	14.4	10.4	2.1	91.1
	15	H	6	80	82	140.00	148.31	39.87	31.5	51.7	2.3	63.6
	15	H	7	20	22	140.40	148.71	40.00	32.4	73.1	4.2	54.3
	15	H	CC	2	4	140.98	149.29	40.17	37.7	48.4	1.3	78.4
	16	H	1	45	47	141.65	151.22	40.83	78.6	50.0	1.7	92.7
	16	H	2	67	69	142.66	152.23	41.33	20.3	8.1	4.4	87.2
	16	H	3	27	29	143.76	153.33	41.87	27.2	8.6	5.0	93.6
	16	H	4	36	38	145.35	154.92	42.66	76.6	38.5	2.9	84.0
	16	H	4	67	69	145.66	155.23	42.81	37.1	11.6	3.3	84.9
	16	H	6	67	69	148.66	158.23	43.90	26.7	7.5	4.8	88.9
	16	H	7	30	32	149.29	158.86	44.03	30.4	22.2	5.3	94.5
	17	H	1	55	57	151.25	162.49	44.80	51.3	42.2	2.5	88.2
	17	H	2	67	69	152.87	164.11	45.14	35.6	11.4	3.0	96.6
	17	H	3	32	34	154.02	165.26	45.39	27.5	24.0	3.3	86.4
	17	H	4	67	69	155.87	167.11	45.78	27.0	4.7	3.1	97.3
	17	H	4	117	119	156.37	167.61	45.99	10.4	5.1	5.4	87.5
	17	H	6	67	69	158.87	170.11	47.13	15.3	8.6	3.3	92.5
	17	H	7	55	57	160.25	171.49	47.76	4.6	2.8	3.2	87.6
	18	H	2	67	69	162.37	173.35	48.61	17.5	3.2	2.1	97.8
	18	H	3	107	109	164.27	175.25	49.12	7.8	5.5	3.4	97.0
	18	H	4	47	49	165.17	176.15	49.22	2.9	2.1	0.9	84.4
	18	H	4	69	71	165.39	176.37	49.24	15.0	10.0	1.6	96.9
	18	H	6	73	75	167.72	178.70	49.50	28.3	8.5	1.6	98.6
	18	H	7	20	22	168.69	179.67	49.61	1.9	1.4	1.3	92.8
	19	H	1	30	32	170.00	182.53	49.93	21.4	12.0	1.5	84.7
	19	H	1	85	87	170.55	183.08	49.99	10.5	4.8	2.6	92.9
	19	H	2	70	72	171.90	184.43	50.14	13.0	5.6	1.7	96.1
	19	H	2	105	107	172.25	184.78	50.18	16.5	4.6	3.0	93.8
	19	H	3	21	23	172.91	185.44	50.25	30.4	9.4	1.2	82.9
	19	H	3	92	94	173.62	186.15	50.33	12.8	7.9	4.3	95.9
	19	H	4	69	71	174.89	187.42	50.46	22.8	11.8	1.8	95.3
	19	H	5	22.5	24.5	175.93	188.46	50.54	22.2	8.1	1.6	95.2
	19	H	5	62.5	64.5	176.32	188.86	50.58	10.6	4.7	1.8	97.9
	19	H	6	31	33	177.51	190.04	50.68	7.0	6.8	0.8	82.9
	19	H	6	73	75	177.93	190.46	50.71	21.2	3.9	3.9	98.5
	19	H	7	42	44	178.62	191.15	50.77	4.5	6.1	1.9	93.1
	20	H	1	63	65	179.83	191.98	50.85	9.1	6.8	3.3	85.9
	20	H	2	67	69	181.37	193.52	51.02	2.8	1.7	3.9	96.8
	20	H	3	25	27	182.45	194.60	51.13	7.6	1.7	4.5	86.4
	20	H	4	66	68	184.36	196.51	51.34	17.7	6.7	3.2	96.0
	20	H	5	72	74	185.92	198.07	51.50	4.5	1.5	6.0	93.2
	20	H	6	28	30	186.98	199.13	51.62	2.3	1.5	5.3	87.6
	20	H	6	72	74	187.42	199.57	51.66	3.0	2.8	5.1	99.0
	20	H	7	15	17	188.35	200.50	51.76	4.9	3.8	7.5	91.9
	21	H	1	120	122	189.90	203.11	52.04	4.7	1.4	4.8	92.9
	21	H	2	40	42	190.60	203.81	52.12	4.3	1.2	6.7	82.8
	21	H	3	15	17	191.85	205.06	52.25	6.1	1.8	6.2	87.1
	21	H	3	61	63	192.31	205.52	52.33	8.0	2.0	6.0	93.4
	21	H	4	67	69	193.87	207.08	54.14	6.7	0.7	14.0	89.2
	21	H	5	67	69	195.37	208.58	54.63	6.2	1.5	15.1	83.6
	21	H	6	30	32	196.50	209.71	55.03	10.3	4.9	8.9	82.2
	21	H	6	140	142	197.60	210.81	55.43	7.9	4.1	11.9	92.5
	21	H	7	19	21	197.89	211.10	55.54	5.2	1.5	23.8	84.1
	21	H	7	29	31	197.99	211.20	55.57	35.1	12.0	3.0	96.3
	21	H	7	40	42	198.10	211.31	55.61	28.6	11.0	4.3	95.8
	22	H	1	66	68	198.86	213.06	56.25	46.3	51.4	0.4	80.2
	22	H	2	22.5	24.5	199.93	214.13	56.32	21.8	12.0	2.1	94.9
	22	H	2	68	70	200.38	214.58	56.32	10.9	7.6	3.1	100.0

Table 1. cont.

Hole	Core	Type	Sct	Top (cm)	Bot (cm)	Depth (mbsf)	Depth (mcd)	Age (Ma)	FRAG (%)	BENTH (%)	Coarse Fraction (>38 μm) (wt%)	Carbonate Content (wt%)
1209A	22	H	3	42	44	201.62	215.82	56.34	32.1	21.5	6.5	99.0
	22	H	3	132	134	202.52	216.72	56.36	5.1	4.9	6.2	93.5
	22	H	4	70	71	203.40	217.60	56.38	4.2	7.6	0.7	99.0
	22	H	5	37.5	39.5	204.57	218.78	56.40	28.7	13.2	3.5	97.8
	22	H	5	141.5	143.5	205.62	219.82	56.41	27.2	19.2	1.4	95.6
	22	H	6	69	71	206.39	220.59	56.43	8.1	4.3	3.9	100.0
	22	H	7	50	52	207.20	221.40	56.44	6.3	6.0	7.0	95.6
	23	H	1	20	22	207.90	223.55	56.48	4.9	1.3	8.1	94.2
	23	H	1	38	40	208.08	223.73	56.48	1.5	0.0	8.2	93.4
	23	H	1	80	82	208.50	224.15	56.49	9.5	5.6	5.9	84.6
	23	H	2	66	68	209.86	225.51	57.17	27.2	18.5	2.9	97.0
	23	H	3	21	23	210.91	226.56	58.26	48.2	24.2	2.0	97.3
	23	H	3	42	44	211.12	226.77	58.48	44.3	32.3	3.1	92.5
	23	H	3	62	64	211.32	226.97	58.69	33.3	8.5	2.7	94.5
	23	H	3	77.5	79.5	211.48	227.13	58.85	67.3	83.1	0.6	93.2
	23	H	3	100	102	211.70	227.35	59.08	49.3	16.7	2.2	90.9
	23	H	3	110	112	211.80	227.45	59.10	25.6	10.4	1.8	94.5
	23	H	3	120	122	211.90	227.55	59.11	49.7	43.9	1.6	80.8
	23	H	3	130	132	212.00	227.65	59.11	34.7	68.9	0.8	65.6
	23	H	3	140	142	212.10	227.75	59.12	76.0	87.0	0.5	76.8
	23	H	3	147.5	149.5	212.18	227.83	59.12	68.0	64.9	0.9	90.6
	23	H	4	11	13	212.31	227.96	59.13	69.5	73.5	0.9	91.7
	23	H	4	48	50	212.68	228.33	59.14	38.4	48.9	0.8	93.7
	23	H	4	67	69	212.87	228.52	59.15	60.9	84.9	0.3	97.2
	23	H	5	21	23	213.91	229.56	59.20	23.1	14.6	2.5	94.3
	23	H	5	41.5	43.5	214.12	229.77	59.21	48.6	41.0	2.7	91.8
	23	H	5	80	82	214.50	230.15	59.23	53.2	38.9	1.2	94.8
	23	H	5	102.5	104.5	214.73	230.38	59.24	66.4	43.6	2.9	94.6
	23	H	6	20	22	215.40	231.05	59.27	53.5	46.7	1.3	96.3
	23	H	6	60	62	215.80	231.45	59.29	29.1	13.4	1.5	96.8
	23	H	6	67	69	215.87	231.52	59.29	51.1	57.0	1.3	91.8
	23	H	6	140	142	216.60	232.25	59.32	26.9	11.6	1.3	95.4
	23	H	7	58	60	217.28	232.93	59.35	8.1	5.7	5.7	97.5
	24	H	1	10	12	217.30	232.33	59.33	14.1	7.6	7.7	94.6
	24	H	1	85	87	218.05	233.08	59.36	11.8	3.4	8.6	96.6
	24	H	1	135	137	218.55	233.58	59.38	7.9	4.1	10.4	93.5
	24	H	2	65	67	219.35	234.38	59.53	38.0	11.8	1.7	96.5
	24	H	3	47.5	49.5	220.68	235.71	59.94	23.6	30.1	2.9	88.4
	24	H	4	66	68	222.36	237.39	60.47	2.3	3.3	4.7	95.8
	24	H	5	5	7	223.25	238.28	60.63	4.6	4.7	12.1	96.8
	24	H	5	11	13	223.31	238.34	60.64	9.9	8.5	10.4	84.6
	24	H	5	30	32	223.50	238.53	60.67	1.4	2.9	11.0	99.3
	24	H	6	62.5	64.5	225.32	238.85	60.73	21.3	6.8	8.8	96.3
	24	H	6	67	69	225.37	240.40	60.98	7.0	5.3	2.7	95.6
	24	H	6	121.5	123.5	225.91	240.95	61.02	7.5	3.5	14.1	96.4
	24	H	7	17	19	226.37	241.40	61.04	15.0	12.4	3.8	89.8
	24	H	7	35	37	226.55	241.58	61.05	10.9	4.2	5.7	94.7
	24	H	7	52.5	54.5	226.73	241.76	61.06	19.4	19.8	3.5	93.1
	24	H	7	68	70	226.88	241.91	61.06	4.9	3.7	6.4	96.4
	25	H	1	35	37	227.05	243.33	61.13	10.2	6.2	5.5	90.5
	25	H	1	50	52	227.20	243.48	61.13	4.4	3.1	9.3	93.0
	25	H	1	65	67	227.35	243.63	61.14	10.3	6.3	4.2	87.3
	25	H	1	82.5	84.5	227.52	243.81	61.15	1.3	2.1	8.2	93.8
	25	H	1	100	102	227.70	243.98	61.15	5.6	13.3	1.5	92.8
	25	H	2	17.5	19.5	228.38	244.66	61.18	6.4	6.3	6.3	94.3
	25	H	2	32.5	34.5	228.52	244.81	61.19	18.1	22.4	1.7	91.9
	25	H	2	75	77	228.95	245.23	61.33	5.3	6.6	7.6	93.2
	25	H	3	7.5	9.5	229.77	246.06	61.80	9.6	18.9	0.8	90.1
	25	H	3	47.5	49.5	230.18	246.46	62.02	18.2	48.7	0.7	95.1
	25	H	3	115	117	230.85	247.13	62.41	7.9	16.7	0.7	83.0
	25	H	4	70	72	231.90	248.18	63.00	0.7	1.4	15.8	96.0
	25	H	4	130	132	232.50	248.78	63.35	0.7	0.0	24.0	96.5
	25	H	5	85	87	233.55	249.83	64.13	0.9	0.8	27.9	97.3
	25	H	6	10	12	234.30	250.58	64.69	0.7	0.0	24.8	84.7
	25	H	6	90	92	235.10	251.38	64.92	0.3	0.5	31.5	94.5

Table 2. Dissolution indices for Hole 1211A.

Hole	Core	Type	Sct	Top (cm)	Bot (cm)	Depth (mbsf)	Depth (mcd)	Age (Ma)	FRAG (%)	BENTH (%)	Coarse Fraction (>38 µm) (wt%)	Carbonate Content (wt%)
1211A	9	H	6	67	69	77.47	84.60	34.26	9.8	9.0	1.6	87.9
	10	H	1	20	22	79.00	88.15	34.95	36.7	78.1	0.8	96.8
	10	H	1	40	42	79.20	88.35	34.99	44.0	58.6	0.5	97.2
	10	H	1	60	62	79.40	88.55	35.03	76.8	94.8	0.4	83.7
	10	H	1	80	82	79.60	88.75	35.07	15.0	10.1	0.2	98.3
	10	H	1	100	102	79.80	88.95	35.11	85.3	92.9	0.4	92.8
	10	H	1	120	122	80.00	89.15	35.15	62.8	71.4	0.5	91.3
	10	H	1	140	142	80.20	89.35	35.19	62.4	81.0	0.3	96.8
	10	H	2	67	69	80.97	90.12	35.62	74.4	94.7	0.3	83.9
	10	H	3	70	72	82.50	91.65	36.54	73.6	94.0	0.2	85.0
	10	H	4	67	69	83.97	93.12	37.43	70.4	92.9	0.2	84.0
	10	H	5	65	67	85.45	94.60	38.33	65.2	64.0	1.2	92.1
	10	H	6	68	70	86.98	96.13	39.25	49.6	64.7	0.8	86.6
	10	H	7	67	69	87.97	97.12	39.85	29.3	40.9	0.7	96.0
	11	H	1	42	44	88.72	98.21	42.29	9.5	33.3	0.8	93.5
	11	H	1	66	68	88.96	98.45	43.19	27.2	36.9	4.8	63.8
	11	H	2	67	69	90.47	99.96	43.95	33.0	19.3	.	89.4
	11	H	3	71.5	73.5	92.01	101.51	44.35	21.8	6.5	3.7	89.8
	11	H	4	69	71	93.49	102.98	44.72	14.0	5.1	3.0	95.4
	11	H	4	90	92	93.70	103.19	44.77	6.2	4.8	2.7	100.0
	11	H	5	73	75	95.03	104.52	45.11	14.3	3.4	3.0	96.3
	11	H	6	72	74	96.52	106.01	45.49	56.0	20.4	.	91.4
	11	H	7	43	45	97.73	107.22	45.79	9.5	5.5	2.8	91.3
	12	H	1	20	22	98.00	107.92	49.10	14.2	1.0	2.4	92.7
	12	H	1	64	66	98.44	108.36	49.30	12.7	4.9	4.8	98.2
	12	H	2	40.5	42.5	99.71	109.63	49.88	17.7	8.1	2.4	90.4
	12	H	2	67	69	99.97	109.89	50.00	14.6	6.8	2.8	94.4
	12	H	2	118	120	100.48	110.40	50.24	36.1	12.5	2.2	94.6
	12	H	3	26.5	28.5	101.07	110.99	50.43	18.6	4.3	2.6	93.6
	12	H	3	48	50	101.28	111.20	50.46	12.9	10.2	2.7	92.9
	12	H	3	63	65	101.43	111.35	50.48	13.8	4.3	2.6	94.7
	12	H	3	88	90	101.68	111.60	50.51	30.7	5.9	2.7	98.6
	12	H	3	107	109	101.87	111.79	50.54	4.9	3.7	5.3	93.3
	12	H	3	138	140	102.18	112.10	50.58	6.1	4.6	2.2	95.5
	12	H	4	69	71	102.99	112.91	50.69	68.4	16.7	1.6	95.4
	12	H	4	103	105	103.33	113.25	50.73	9.6	1.8	3.4	97.2
	12	H	4	122	124	103.52	113.44	50.76	10.1	1.4	5.3	95.1
	12	H	5	23	25	104.03	113.95	50.85	7.5	8.8	1.9	93.6
	12	H	5	41	43	104.21	114.13	50.90	4.7	2.5	5.1	97.8
	12	H	5	67	69	104.47	114.39	50.97	15.7	6.1	3.0	91.5
	12	H	5	108	110	104.88	114.80	51.08	30.1	13.0	1.3	87.2
	12	H	5	133	135	105.13	115.05	51.14	5.0	4.6	3.0	94.0
	12	H	6	8	10	105.38	115.30	51.21	6.1	2.7	5.3	95.0
	12	H	6	67	69	105.97	115.89	51.36	8.1	4.1	.	95.2
	12	H	6	113	115	106.43	116.35	51.48	7.2	7.6	5.5	94.4
	12	H	7	10	12	106.90	116.82	51.61	6.0	7.2	1.1	93.7
	13	H	1	67	69	107.97	119.46	52.30	3.4	6.2	6.4	94.1
	13	H	1	89	91	108.19	119.68	52.72	4.2	1.7	7.4	84.7
	13	H	2	67	69	109.47	120.96	53.03	3.6	3.2	9.0	91.6
	13	H	3	10	12	110.40	121.89	53.22	18.9	5.4	5.2	93.3
	13	H	3	67	69	110.97	122.46	53.37	10.3	3.9	5.8	96.9
	13	H	3	112.5	114.5	111.43	122.92	53.53	3.6	1.5	6.9	97.5
	13	H	4	12	14	111.92	123.41	53.72	5.1	2.2	7.0	93.5
	13	H	4	68	70	112.48	123.97	53.82	3.6	1.4	.	99.0
	13	H	4	100	102	112.80	124.29	53.64	6.2	2.4	6.0	98.0
	13	H	5	67	69	113.97	125.46	54.43	18.8	7.9	5.6	86.8
	13	H	5	100	102	114.30	125.79	54.65	4.9	3.0	7.9	88.1
	13	H	6	3	5	114.68	126.17	54.86	6.8	4.1	12.2	97.2
	13	H	6	10	12	114.75	126.24	54.90	15.8	5.9	13.2	95.2
	13	H	6	20	22	114.85	126.34	54.95	20.7	10.7	7.0	97.7
	13	H	6	68	70	115.33	126.82	55.21	23.8	11.1	3.1	94.3
	13	H	7	64	66	116.79	128.28	56.27	57.5	50.0	1.4	97.8
	14	H	1	45.5	47.5	117.25	130.26	56.34	35.0	8.2	4.0	94.6
	14	H	1	110	112	117.90	130.90	56.36	16.2	5.0	4.9	95.2
	14	H	2	13	15	118.43	131.43	56.38	6.7	12.6	0.9	93.7
	14	H	2	67	69	118.97	131.97	56.39	54.4	37.3	1.3	98.4
	14	H	3	21.5	23.5	120.01	133.02	56.43	50.2	37.0	1.5	95.5
	14	H	3	67	69	120.47	133.47	56.45	11.2	2.2	5.1	94.0
	14	H	4	65	67	121.95	134.95	56.50	7.5	2.1	7.8	99.1
	14	H	4	96.5	98.5	122.26	135.27	56.72	8.7	2.2	7.3	93.8
	14	H	4	118	120	122.48	135.48	56.97	14.2	7.5	6.0	90.8

Table 2. cont.

Hole	Core	Type	Sct	Top (cm)	Bot (cm)	Depth (mbsf)	Depth (mcd)	Age (Ma)	FRAG (%)	BENTH (%)	Coarse Fraction (>38 µm) (wt%)	Carbonate Content (wt%)
1211A	14	H	4	138.5	140.5	122.68	135.69	57.21	23.6	10.9	4.7	93.0
	14	H	5	21	23	123.01	136.01	57.58	41.6	16.7	4.4	94.1
	14	H	5	42	44	123.22	136.22	57.83	45.1	24.0	1.5	93.7
	14	H	5	60.5	62.5	123.40	136.41	58.04	86.0	93.5	0.6	89.9
	14	H	5	67	69	123.47	136.47	58.12	11.1	8.3	2.2	88.9
	14	H	5	80.5	82.5	123.61	136.61	58.27	42.0	80.0	0.6	88.8
	14	H	5	96	98	123.76	136.76	58.45	88.4	97.6	0.5	93.1
	14	H	6	5	7	124.35	137.35	59.10	61.8	66.7	2.0	85.0
	14	H	6	16	18	124.46	137.46	59.11	37.2	56.8	0.5	92.5
	14	H	6	66	69	124.96	137.96	59.14	38.4	12.4	0.6	98.7
	14	H	7	42.5	44.5	126.22	139.23	59.21	27.0	8.1	5.7	90.3
	14	H	7	59	61	126.39	139.39	59.22	44.3	46.7	0.7	94.2
	15	H	1	23	25	126.53	141.79	59.37	5.9	3.9	6.2	95.5
	15	H	1	43	45	126.73	141.99	59.38	6.8	4.7	8.1	97.4
	15	H	1	90	92	127.20	142.46	59.50	3.7	0.0	13.3	92.5
	15	H	1	130	132	127.60	142.86	59.82	11.4	7.4	6.2	97.7
	15	H	2	36	38	128.16	143.42	60.23	13.6	16.4	3.3	92.6
	15	H	2	67	69	128.47	143.73	60.43	7.3	2.1	8.5	97.5
	15	H	2	93	95	128.73	143.99	60.61	22.4	16.7	2.6	92.4
	15	H	2	133	135	129.13	144.39	60.87	26.5	16.2	2.6	100.0
	15	H	3	23	25	129.53	144.79	61.06	7.3	12.2	4.1	92.8
	15	H	3	98	100	130.28	145.54	61.59	1.0	0.0	27.8	94.3
	15	H	3	130	132	130.60	145.86	62.18	1.2	0.0	20.8	90.3
	15	H	4	28	30	131.08	146.34	63.14	0.9	0.0	30.9	95.6
	15	H	4	58	60	131.38	146.64	64.36	0.0	0.0	39.3	96.2
	15	H	4	95	97	131.75	147.01	64.78	0.1	0.0	40.4	97.7
	15	H	4	118	120	131.98	147.24	64.83	0.0	0.0	33.3	99.2
	15	H	4	140	142	132.20	147.46	64.88	0.7	1.0	17.7	93.1

CHAPTER 3

COILING SHIFTS AND STABLE ISOTOPE CHANGES IN THE LATE PALEOCENE PLANKTIC FORAMINIFERA *Igorina albeari*: EXPRESSION AND SIGNIFICANCE.

Abstract. In a cluster of central Pacific sites, the Late Paleocene planktic foraminifera *Igorina albeari* undergoes a coiling reversal from dextral to sinistral dominated populations at the base of Zone P4 (~59.2 Ma) in DSDP Hole 465 (Hess Rise), ODP Hole 1209A (Shatsky Rise), and ODP Hole 865B (Allison Guyot). In contrast, populations of *I. albeari* at mid latitude site ODP Hole 762C on Exmouth Plateau remain dominated by the dextral morph. Carbon and oxygen isotope values for sinistral and dextral coiling morphs are similar and there is no clear correlation between coiling reversal and isotope events. Thus, the shift to sinistral coiling mode did not involve a significant shift in depth ecology or photosymbiosis. We speculate that the coiling reversal results instead from a relative decline in the dextral morph at the tropical localities, due to a change in some other ecological parameter, for example, nutrient availability, while the dextral morph remains the dominant form at the mid latitude location. A possibly analogous situation is the modern presence of sinistral *Globorotalia truncatulinoides* in the gyres and dextral *G. truncatulinoides* in the equatorial oceans. An episode of dissolution occurs ~100kyr after the coiling shift is a dissolution layer at both localities occurring ~100 kyr after its onset. This can be at least partially correlated with an extended cooling episode (~59.2 to 58.1 Ma; ~1.2 myr) in Hole 865. The isotope record from the dissolution layer in Hole 465 shows a gradual cooling of ~0.5ºC and ~2ºC in benthic and deep thermocline water, up to +0.7‰ shift in $\delta^{13}C$ in benthic and surface dwelling foraminifera and an increase in $\Delta\delta^{13}C$ at both low latitude sites. This dissolution layer represents a profound change in oceanic circulation and can be correlated to a cooling event at high latitude characterized by high southern latitude organic and biogenic rich sedimentation. We show that the first marked shift to

sinsitrally dominated populations occurred at multiple locations in the central Pacific, and that this coiling shift corresponds to a prominent rise in the $\delta^{13}C$ of the global carbon cycle. However, we also show that the other coiling shifts recorded in Hole 865B do not occur at our Pacific sites and that the range of *I. albeari* in Holes 865B and 762C are extended. Stable isotopes of *I. albeari* specimens suggest that both the sinistrally and dextrally coiled morphotypes occupied similar water masses. The exact cause of the coiling reversal remains an open issue.

INTRODUCTION

Many invertebrates precipitate coiled shells (or tests) that from a given reference frame, spiral to the left or to the right. For planktic foraminifera in spiral view, sinistral coiling means addition of successive chambers towards the left, while dextral coiling means the opposite. Large collections of morphologically defined planktic foraminifera species often display proportionate coiling, where the population has a nominally 50:50 ratio of sinistral and dextral tests. In some cases, however, populations show a distinct preference for one coiling direction.

For some morphologically defined planktic foraminifera species, shifts in preferred coiling direction have been found in sedimentary records (Bolli, 1950; Ericson *et al.*, 1955; Bandy, 1959; Bolli, 1971; Saito, 1976; Pearson, 1993; Xu *et al.*, 1995; Norris and Nishi, 2001). An excellent example is *Neogloboquadrina pachyderma*, which displays coiling shifts in Quaternary and late Neogene sediment cores (Kucera and Kennett, 2002; Bauch *et al.*, 2003). Sinistrally coiled *Neogloboquadrina pachyderma* has a modern polar distribution while the dextrally coiled form has a subpolar affinity. Thus, the ratio of the two coiling morphs is a powerful tool for reconstructing past climate conditions, in particular to track glacial/interglacial cycles (e.g., Ericson, 1959; Bandy, 1972; CLIMAP Project Members, 1976; Bond *et al.*, 1993; Ufkes and Zachariasse, 1993). Recent genetic evidence demonstrates that sinistral and dextral morphospecies of modern *N. pachyderma* are separate species (Darling *et al.*, 2000; Bauch *et al.*, 2003). Morphometric and stable isotopic analyses further suggest that the modern sinistral form originated in the middle Pleistocene (Kucera and Kennett, 2002). Despite this complexity, coiling shifts can be used for stratigraphic correlation and palaeoenvironmental interpretations (above references).

As highlighted by stable isotope records of marine carbonate (**Fig. 1**), the Late Paleocene and Early Eocene (~60–50 Ma) were characterized by a series of profound global environmental perturbations (e.g., Zachos *et al.*, 2001), some which clearly affected the distribution of marine microfossils (Aubry, 1998; Quillevere *et al.*, 2001; Hollis, 2002; Kelly, 2002; Quillevere and Norris, 2003; Thomas, 2003). Among the microfossil changes, prominent shifts in coiling direction may have occurred in one easily identified, morphologically defined planktic foraminifera species. *Igorina albeari* (Cushman and Bermúdez, 1949) (**Appendix 1**) is found in Upper Paleocene sediment deposited at relatively low latitudes (Stott and Kennett, 1990; Olsson *et al.*, 1999). Its range spans from the base of planktic foraminiferal Zone P3b (where it serves as the zonal marker) to planktic foraminiferal Zone P5 (~55.9-60 Ma) (Berggren and Norris, 1997). Interestingly, in core from Ocean Drilling Program (ODP) Site 865, located on Allison Guyot, central Pacific Ocean (**Fig. 2**), Norris and Nishi (2001) documented several changes in the coiling direction of *I. albeari* (**Fig. 3**). Populations of *I. albeari* were proportionately coiled in the early part of its range but rapidly became dominated by sinistral forms soon after the first appearance datum (FAD) of the nannofossil *Heliolithus kleinpelli* (~58.4 Ma) (Berggren *et al.*, 1995). At least two additional coiling shifts in *I. albeari* populations occurred at Site 865 before its extinction.

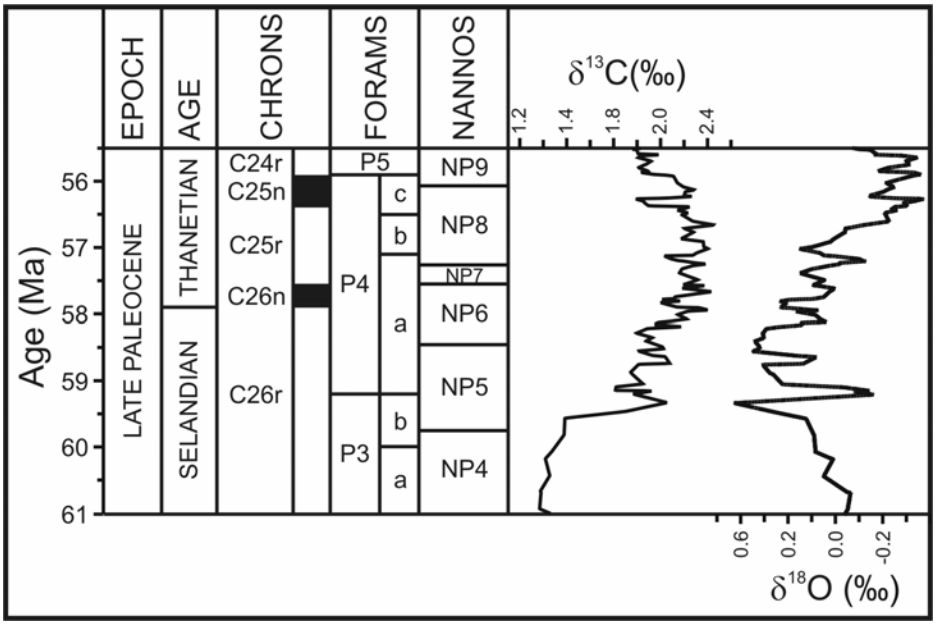

Figure 1. Late Paleocene timescale (following Berggren *et al*., 1995) with global carbon and oxygen isotope curves constructed from benthic foraminifer isotope data (adapted from Zachos *et al*., 2001, p. 688).

Late Paleocene coiling shifts in *Igorina albeari*, like those of other planktic foraminifera, could relate to significant changes in surface water conditions. In particular, the first coiling shift might coincide with (and provide constraints to) a fairly rapid ~0.7‰ increase in the $\delta^{13}C$ of the global carbon cycle (**Fig. 1**), and a recently identified "biotic event" in the north Pacific Ocean (Shipboard Scientific Party, 2002; Petrizzo, 2005). Sediments deposited on Shatsky Rise ~0.50 m above the FAD of *H. kleinpelli* (**Fig. 3**) contain a short (<1 m) interval characterized by carbonate dissolution, abundant fish teeth and numerous tests of *I. tadjikastanensis* (Shipboard Scientific Party, 2002; Petrizzo, 2005; Hancock and Dickens, 2005). To date, however, Site 865 is the only location where coiling shifts in *I. albeari* have been documented. It is also uncertain whether *I. albeari* lived in surface or thermocline waters (Pearson, 1993; Olsson *et al.*, 1999).

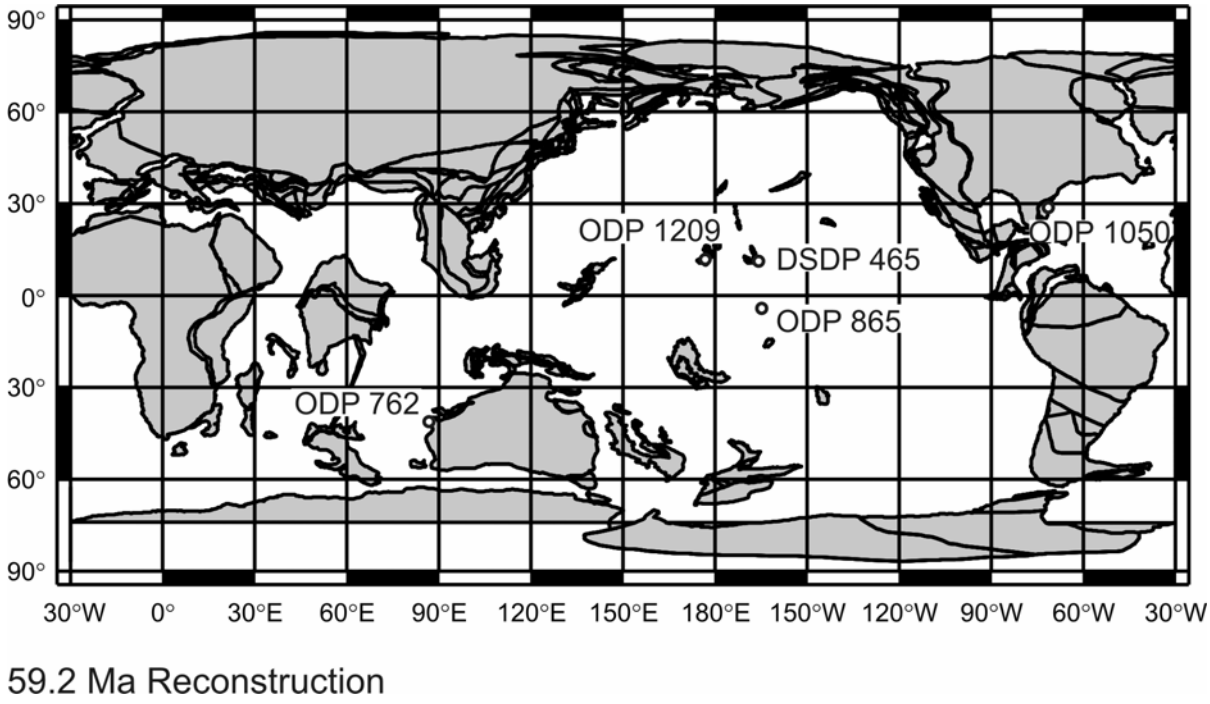

Figure 2. Palaeogeographic map for the Late Paleocene (~59.2 Ma) showing palaeopositions of DSDP Site 465 (Hess Rise), and ODP Sites 762 (Exmouth Plateau), 865 (Alison Guyot), 1209 (Shatsky Rise) and 1050 (Blake Nose). Map and site locations were made using the Ocean Drilling Stratigraphic network (www.odsn.de).

In this study, we investigate the timing, extent and palaeoceanographic significance of *Igorina albeari* coiling shifts by examining Upper Paleocene sections at four locations in the Indo-Pacific region (**Fig. 2**). We determine changes in the coiling direction of *I. albeari*, quantify the relative abundance of *I. tadjikistanensis*, measure stable carbon and oxygen isotopes of foraminifera tests (including *I. albeari*), and quantify the amount of carbonate dissolution. We show that the initial coiling shift of *I. albeari* occurred at multiple locations in the central Pacific, and corresponds to an obvious increase in the abundance of *I. tadjikistanensis*, a prominent rise in surface and deep water $\delta^{13}C$, and deep-sea carbonate dissolution. Although exact causes of the coiling reversal and contemporaneous oceanographic phenomena remain open issues, something clearly changed in surface waters of the central Pacific during the global step in $\delta^{13}C$ (~59 Ma) (Zachos *et al.*, 2001).

SECTIONS AND SAMPLES

Sediment samples were collected from two cores recovered from holes within 2800 km of Hole 865B (18˚26.418'N, 179˚33.348'W), located in the central Pacific on Allison Guyot in 1516 m water depth (**Fig. 2**). Deep Sea Drilling Project (DSDP) Hole 465 was drilled on Hess Rise (33°49'N; 178°55'E) in 2161 m of water (Thiede *et al.*, 1981), and ODP Hole 1209A was drilled on Shatsky Rise (32˚39.10'N, 158˚30.36'E) in 2387 m of water (Shipboard Scientific Party, 2002). The third hole, ODP Hole 762C, is located on Exmouth Plateau off the northwest Australian margin (19˚53.24'S, 112˚15.24'E) in 1360 m of water (Haq *et al.*, 1990). Cores from the other two holes were chosen because they make thick Upper Paleocene stratigraphic sections (**Fig. 3**), which contain abundant, well-preserved foraminifera (Hancock *et al.*, 2002; Hancock and Dickens, 2005). Presumably, the additional Pacific holes are sufficiently close to Hole 865B (**Fig. 2**) so that they would contain coiling shifts in *Igorina albeari*, even if the event was regionally restricted.

Upper Paleocene nannofossil ooze was recovered between 100 and 135 mbsf in Hole 865B (**Fig. 3**). Within this interval, the FAD of the nannofossil *Heliolithus kleinpelli* occurs at 129.7 mbsf (Bralower and Mutterlose, 1995). Other than aforementioned work, stable carbon and oxygen isotopes have been measured on

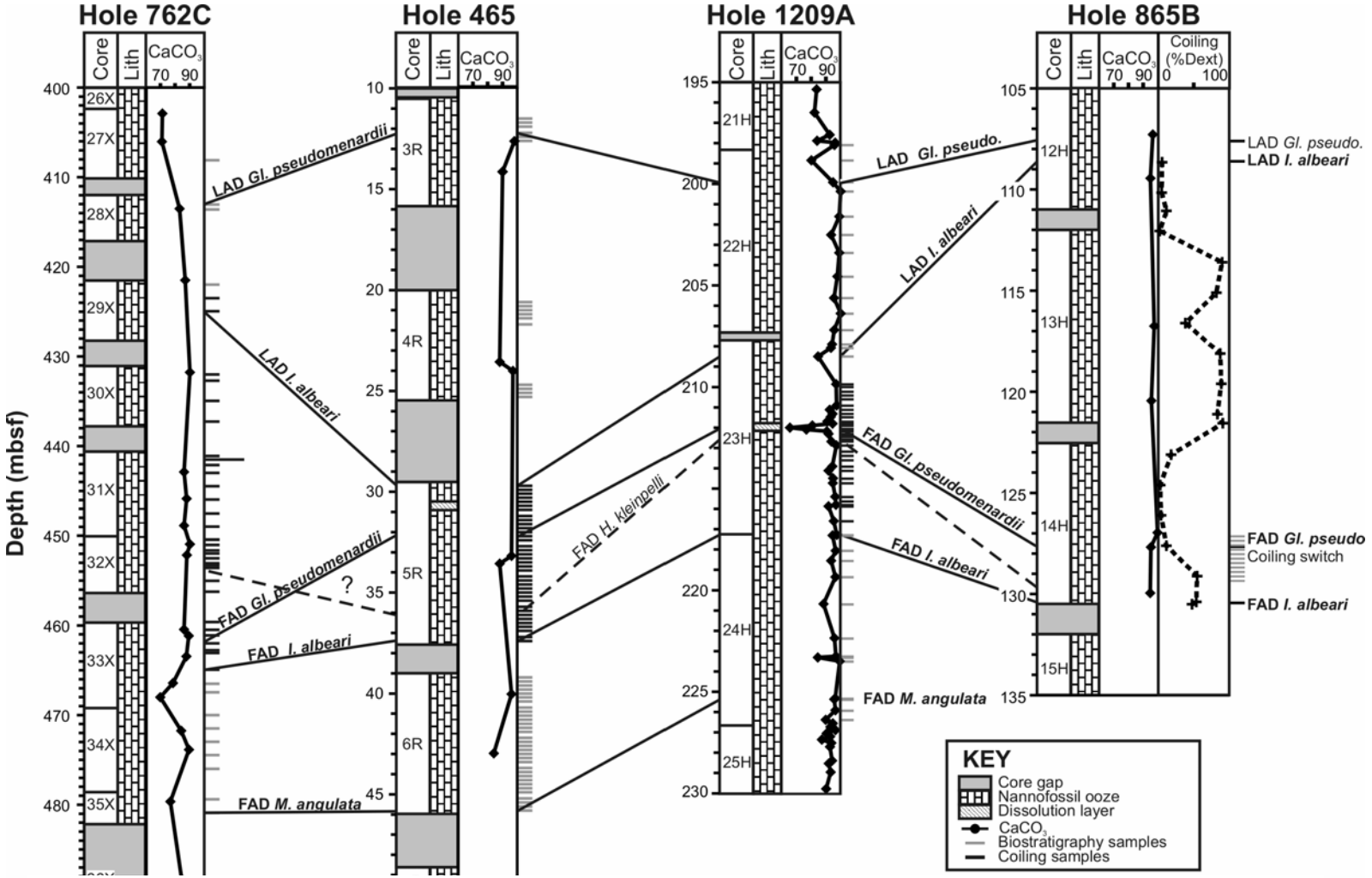

Figure 3. Lithologic logs and key stratigraphic datums for Upper Paleocene sections DSDP Sites 465 and ODP Sites 762, 865, and 1209. Data used to make this figure comes from the Initial Reports Volumes (Shipboard Scientific Party, 1981; Shipboard Scientific Party, 1990; Shipboard Scientific Party, 1993; Shipboard Scientific Party, 2002), other selected works (Bralower *et al*., 1995; Norris and Nishi, 2001; Hancock *et al*., 2002), and this study. Those datums identified in this study are shown in **Boldface**. Also shown is the initial coiling record of *Igorina albeari* at Site 865 (Norris and Nishi, 2001).

planktic foraminifera from 37 samples (Bralower *et al.*, 1995). A further eleven samples were obtained between 127.20 and 129.32 mbsf at 20 cm spacing for higher resolution carbon and oxygen isotope and coiling data over the observed coiling shift (Norris and Nishi, 2001).

The Upper Paleocene record in Hole 465 comprises "highly disturbed" nannofossil ooze between 10 and 45 mbsf (**Fig. 3**). Eighty-five samples were examined to: 1) refine planktic foraminiferal zonal boundaries, in particular the base of Zone P3b, delineated in previous studies (Boersma, 1981; Berggren and Norris, 1997; Quillevere, 2000), and 2) to determine the range, coiling and isotope composition of *Igorina albeari*. Samples were generally taken at 20 cm spacing from 25 to 46 mbsf, although this includes 4.4 and 1.5 m core gaps. (The range of *I. albeari* does not extend above 29.7 mbsf so only selected samples were collected above this depth).

A nearly contemporaneous section of nannofossil ooze accumulated in Hole 1209A between 200 and 225 mbsf (**Fig. 3**). Unlike at Holes 865B and 465, a prominent 20 cm thick, dark brown clay-rich layer from 211.9 to 212.1 mbsf punctuates the sequence. This horizon, representing the "biotic event" and characterized by carbonate dissolution (Hancock and Dickens, 2005) occurs 58 cm above the FAD of *Heliolithus kleinpelli* (Shipboard Scientific Party, 2002). The latter datum implies that the biotic event closely corresponds to the initial coiling shift documented in Hole 865B (**Fig. 3**). Sixty-two samples were obtained from between 198.1 and 226.4 at a typical spacing of 45 cm, but at higher resolution over the dissolution layer. As for other sites, the main focus was the interval characterized by the common occurrence of *Igorina albeari*.

The Upper Paleocene section in Hole 762C consists of nannofossil ooze between 410 and 480 mbsf (**Fig. 3**). Previous work at this site showed that the FAD *of Heliolithis kleinpelli* occurs at 452.8 mbsf (Seisser and Bralower, 1992), and that *Igorina albeari* commonly occurs between 424 and 465 mbsf (Hancock *et al.*, 2002). Hence, 49 samples were collected from 408.0 to 488.2 mbsf to span this range. Unfortunately, four significant (2.5-4.3 m) coring gaps exist between Cores 28X and 33X, making the record discontinuous. Disregarding these core gaps, samples were spaced about every 1.5 m.

METHODS

Planktic Foraminifera

All bulk sediment samples collected were washed over a 63 µm sieve. Residues were dried, and examined under a reflected light microscope for their planktic foraminiferal content.

Rather than solely relying on preexisting biostratigraphic data (compiled by different workers at different sites and at different resolution over many years (Boersma, 1981; Berggren and Norris, 1997; Quillevere, 2000; Norris and Nishi, 2001; Hancock *et al.*, 2002), the biostratigraphy across all holes was reassessed using planktic foraminifera. All sieved assemblages were scanned for species that mark Late Paleocene zonal boundaries at sub-tropical locations (Berggren *et al.*, 1995; Olsson *et al.*, 1999). These are (**Table 1**): FAD of *Morozovella angulata* (P2/P3a), FAD of *Igorina albeari* (P3a/P3b), FAD of *Globanomalina pseudomenardii* (P3b/P4), FAD of *Acarinina soldadoensis* (P4b/P4c), and last appearance datum (LAD) of *Gl. pseudomenardii* (P4/P5). Note that the P4a and P4b foraminiferal biozones are merged in this study because the zonal marker, LAD of *Ac. subsphaerica*, has a diachronous range (Berggren *et al.*, 2000; Hancock *et al.*, 2002). Additionally, according to our taxonomic concepts, *I. albeari* has a biconvex, tumid shape with a distinct keel extending to the final chamber (**Appendix 1**), and *Gl. pseudomenardii, sensu stricto*, has a biconvex shape, a sharp keel that extends to the final chamber, and flush sutures (Bolli, 1957) (**Plates 1, 2, 3**). These "taxa" have inappropriately long ranges with less strict taxonomic concepts.

Between 50 and 100 specimens of *Igorina albeari* were then examined for each sieved sample to determine the proportion of dextral forms (**Appendix 1**). To assess analytical precision, five replicate samples from DSDP Hole 465 were re-sieved and recounted. Analyses of these replicates (**Table 2**) suggest that reported *I. albeari* coiling ratios are within 4% (absolute). A sample from the same depth as one of the samples in the Norris and Nishi (2001) dataset was sieved and counted, and the *I. albeari* coiling ratio was found to be within 1% (absolute) (**Table 2**).

As previously mentioned, the number of *Igorina tadjikistanensis* tests dramatically increases in sediment deposited on Shatsky Rise (including in Hole 1209A) during the Late Paleocene biotic event (Shipboard Scientific Party, 2002). Selected foraminiferal assemblages at all four holes were examined for the relative abundance of this microfossil to see if this phenomenon occurs elsewhere. The >63 µm size fraction was poured into a microsplitter, and processed to obtain a sample of nominally 300 planktic foraminifera. Between 250 and 300 counts of planktic foraminifera were then made to determine the relative abundance of *I. tadjikastensis*. Note that *I. tadjikistanensis* is readily distinguished from *Igorina albeari* (**Appendix 1**). Three samples were also examined to evaluate analytical precision. On the basis of these replicate analyses (**Table 2**) reported abundances are within 3% (absolute).

Stable Isotopes

Stable carbon and oxygen isotopes have been measured on some morphologically defined planktic foraminifera genera or species over some intervals of the Upper Paleocene in Hole 465 (Berggren and Norris, 1997; Quillevere, 2000), Hole 762C (Thomas *et al.*, 1992; Hancock *et al.*, 2002) and Hole 865B (Bralower *et al.*, 1995). A bulk stable isotope record has also been constructed for Upper Paleocene sediment in Hole 762C (Thomas *et al.*, 1992). To complement these existing records, and to better understand the ecology of *Igorina albeari*, we collected additional suites of planktic foraminifera from sediment sieved at 210 to 260 µm. The size fraction was restricted because foraminiferal ontogenesis and photosymbionts can affect stable isotope composition (Hemleben *et al.*, 1989; Spero and Lea, 1993; D'Hondt *et al.*, 1994).

For all four holes, multiple aliquots, each containing 30 to 40 specimens of a morphologically defined species (or sub-species) were picked from numerous samples and analyzed (**Table 3**). The selected species varied across sites but included *Morozovella velascoensis, M. occlusa, M. acutispira, Subbotina triangularis* or *Igorina albeari* (both sinistral and dextral morphologies). Beyond relating *I. albeari* coiling shifts to Paleocene carbon isotope changes (**Fig. 1**), our rationale for making these analyses was as follows. Stable isotopes suggest that *M. velascoensis* dwelled in surface waters (Boersma *et al.*, 1987; Corfield and Cartlidge, 1991; D'Hondt *et al.*, 1994; Kelly *et al.*, 1996), while *S. triangularis* inhabited thermocline waters (Boersma *et al.*, 1987;

Corfield and Cartlidge, 1991; Pearson and Shackleton, 1996; Berggren and Norris, 1997). Such work has not been extended to *I. albeari*, dextral or sinistral.

To correlate our records to the widely-cited global benthic foraminiferal $\delta^{13}C$ curve (**Fig. 1**), the benthic foraminifera *Nuttallides truempyi* was also picked from samples in Hole 465 for stable isotope analyses. Samples were sieved at a smaller and wider size fraction of 125 to 250 μm because of the rarity of benthic foraminifera specimens. The 19 aliquots contained between 40 and 50 specimens each.

Most aliquots of single-species foraminifera were analyzed for stable isotopes at the Research School of Earth Sciences, Australian National University, using an automated individual carbonate reaction (Kiel) device coupled with a Finnigan MAT-251 mass spectrometer. Samples were reacted at 90°C in 103% orthophosphoric acid. The $\delta^{18}O$ and $\delta^{13}C$ values were calculated as per mil (‰) deviations relative to Vienna Peedee Belemnite (V-PDB), following calibration with the National Bureau of Standards NBS-19 ($\delta^{18}O$ = -2.20‰, $\delta^{13}C$ = 1.95‰) and NBS-18 ($\delta^{18}O$ = -23.0‰, $\delta^{13}C$ = -5.0‰). The standard deviation for a typical 200 μg aliquot of NBS-19 was 0.03‰ for $\delta^{18}O$ (n = 33) and 0.01‰ for $\delta^{13}C$ (n = 33). The aliquots of *Morozovella* from Hole 762C were analyzed at the stable isotope laboratory in the School of Earth Science, University of California, Santa Cruz, employing similar methods.

Carbonate Dissolution

With data available before this study, the initial coiling shift of *Igorina albeari* in Hole 865B appeared coincident with the biotic event in Hole 1209A (**Fig. 3,** ~212 mbsf). A horizon of carbonate dissolution, characterized by high benthic foraminifera concentration and planktonic foraminifera test fragmentation, marks this event on Shatsky Rise (Hancock and Dickens, 2005). Changes in foraminiferal test preservation can be quantified by two parameters: BENTH = (#benthics) / (#benthics + #planktics); and FRAG = (#fragments/8) / [(#fragments/8) + # whole planktic foraminifers] (e.g., Le and Shackleton, 1992; LaMontagne *et al.*, 1996). One test breaks into ~8 fragments so we divide by 8 to produce a linear relationship between fragmentation and depth (see Le

and Shackleton, 1992, p.30). To test for a short interval of carbonate dissolution in Hole 465, BENTH and FRAG were determined on bulk samples sieved at >63 µm.

RESULTS

Revised Stratigraphy

Upper Paleocene sediment was moderately well constrained in the time domain in all four holes prior to our work (**Fig. 3**). Of particular interest, the FAD of the nannofossil *Heliolithus kleinpelli* lies at 36.1 mbsf, 212.65 mbsf, 129.70 mbsf, and 452.8 mbsf in Holes 465**,** 1209A, 865B and 762C, respectively (**Table 1**).

Table 1. Planktic foraminiferal zones (mbsf), LAD *I. ableari* (italicised), and linear sedimentation rates in Holes 465, 1209A, 865B and 762C. *Ages follow Berggren *et al*. (1995).

Zonal Marker	Pacific Sites			Indian Site	Zonal Boundary	Age (Ma)*	Zone	Linear Sedimentation Rates (cm/kyr)			
	465	1209A	865B	762C				465	1209A	865B	762C
LAD *Gl. pseudomenardii*	12.20	199.93	107.50	413.04	P4c/P5	55.9					
			108.65	*424.96*			P4c	1.5	0.9	1.5	2.0
FAD *Ac. soldadoensis*	21.00	205.62	116.60	424.96	P4a-b/P4c	56.5					
	29.70	*208.50*					P4a-b	0.4	0.2	0.4	1.4
FAD *Gl. pseudomenardii*	32.20	212.18	127.60	462.00	P3b/P4a-b	59.2					
							P3b	0.7	0.6	0.4	0.4
FAD *H. kleinpelli*	36.10	212.65	129.70	452.80	NP5/NP6	58.4					
FAD *I. albeari*	37.40	217.28	130.49	464.95	P3a/P3b	60.0					
							P3a	0.8	0.8	-	1.6
FAD *M. angulata*	45.80	225.32	-	480.92	P2/3a	61.0					

Key datums defining Late Paleocene planktic foraminiferal biozones were identified in all four holes (**Table 1**). These datums generally agree with available stratigraphy, but allow more precise age placements and better inter-hole correlations. The FAD of *Globanomalina pseudomenardii* is particularly important. Given its age (59.2 Ma, Berggren *et al*., 1995), this event must have occurred very close to the initial *Igorina albeari* coiling shift in Hole 865, and the biotic changes found in Hole 1209A. In fact, the FAD of *Gl. pseudomenardii* lies within the originally documented coiling reversal in Hole 1209A, 8 cm below the base of the clay-rich layer (**Table 1; Fig. 3**).

The foraminiferal biozones can be used to estimate average sedimentation rates through the Late Paleocene in each hole (**Table 1**). These range from 0.2 to 2.0 cm/kyr,

which are common for pelagic sequences. Hole 762C has the highest overall sedimentation rates. In general, sedimentation is also high across Zone P4c and low across Zone P4a-b. This may indicate poorly constrained ages in global chronostratigraphy during this interval (Berggren *et al.*, 1995). However, the near-coincidence of the FADs of *Heliolithus kleinpelli* and *Gl. pseudomenardi* with a dissolution horizon in Hole 1209A suggests a concatenation of the record at this site.

Igorina albeari *and its coiling*

The LAD of *Igorina albeari* does not represent an isochronous event (**Table 1**). *Igorina albeari* can be found until 56.0 Ma in Hole 865B, and 56.5 Ma in Hole 762C. At Hole 1209A, however, the species only occurs until 57.7 Ma. *Igorina albeari* also has a short range in Hole 465, although a core gap truncates its full extent (**Fig. 3**).

When found, *Igorina albeari* makes a common component of the foraminiferal assemblages in Holes 465, 865 and 1209. In Hole 762C, however, it is fairly common at its FAD but relatively rare above. Given the tropical to subtropical affinity of *I. albeari* (Olsson *et al.*, 1999), this may reflect the moderately high palaeolatitude of Site 762 (**Fig. 1**). Importantly, though, the high numbers of *I. albeari* mean that coiling ratios are not biased from low specimen counts.

Marked shifts in coiling direction occur in *Igorina albeari* populations in Hole 465 (**Table 2a; Fig. 4**). At its FAD, populations slightly favour the dextral morph (50% to 60% dextral). Over the next 5.6 m (~900 kyr), the population becomes increasingly dextral, reaching 80% of this morph at 31.8 mbsf, 40 cm above the FAD of *Globanomalina pseudomenardii* (59.2 Ma). Coiling then reverses within 60 cm (~140 kyr), so that <30% of specimens are dextrally coiled. For the next 1.5 m, the population becomes increasingly sinistral, attaining 90% of this morph by the LAD of *I. albeari*.

Populations of *Igorina albeari* display a fairly similar coiling history in Hole 1209A (**Table 2b; Fig. 4**). At its FAD, the coiling mode is nearly proportionate, slightly favoring the dextral morph (50% to 60% dextral). Over the next 4.9 m (~800 kyr), the population gradually becomes dextral, reaching 76% of this morph by 212.4 mbsf. From this depth, there is a rapid reversal to sinistral coiling over 22 cm. The FAD of

Globanomalina pseudomenardii occurs at the start of the coiling shift at 212.18 mbsf. Assuming a coincident and identical coiling reversal occurred in Late Paleocene waters above Hole 465 and Hole 1209A, the shortened length of the reversal in the latter hole suggests a condensed interval, as expected given other aforementioned stratigraphic relationships (**Fig. 3**) and the evidence for dissolution (Shipboard Scientific Party, 2002; Hancock and Dickens, 2005). From the FAD of *Gl. Pseudomenardii* to the LAD *I. albeari* (210 mbsf), the population becomes completely sinistral.

Higher-resolution sampling at Hole 865B shows that the population starts off proportionately coiled (~60.0 Ma) and becomes increasingly sinistral over ~100 kyr, which agrees with original coiling data from Norris and Nishi (2001) (**Table 2c; Fig. 4**). The FAD of *H. kleinpelli* occurs <1 m below the start of the coiling shift at 129.70 mbsf. However, the FAD of *Globanomalina pseudomenardii* at 127.60 mbsf occurs relatively late within the coiling shift, compared to the other Pacific sites, when populations are already significantly sinistrally dominated (12% dextrals).

The coiling record of *Igorina albeari* in Hole 762C differs significantly from those constructed at sites in the central Pacific Ocean (**Table 2d; Fig. 4**). When it first appears, coiling is nearly proportionate, slightly favoring the dextral morph (50% to 60% dextral). Although *I. albeari* is relatively rare in Hole 762C, populations of *I. albeari* do not show a major coiling shift. Instead, the populations consistently have a strong dextral coiling bias, averaging 81% of the dextral morph, except at the base of planktic foraminiferal Zone P4 where populations slightly favor the sinistral coiling mode. Interestingly, the sample below this consists of heavily dissolved carbonate with severe secondary calcification hampering foraminiferal identification.

Igorina tadjikastanensis *abundance*

The abundance of *Igorina tadjikasatensis* increases markedly across the coiling shift in Holes 465 and 1209A (**Tables 2b, 2c; Fig. 4**). In both of these holes, *I. tadjikastanensis* is rare in sieved samples (<5%) below the initial coiling reversal of *I. albeari*. The numbers of *I. tadjikasatensis* then rapidly rise, comprising over 85% of the total planktic foraminiferal assemblage. Within about 100 kyr, however, *I. tadjikastanensis* abundance reverts to <5%.

Table 2a. Coiling direction and *Igorina tadjikastanensis* abundance for Hole 465.

Site, Section, Sample (cm)	Depth (mbsf)	Age (Ma)	Coiling (%Dextral)	Replicate Analyses	*Igorina tadjikastanensis* abundance	Replicate Analyses
465-4H-4, 80-82	25.30	57.54			7.8	9.9
465-5H-1, 20-22	29.70	58.60	11.0		78.9	
465-5H-1, 40-42	29.90	58.65	10.3		51.8	
465-5H-1, 60-62	30.10	58.69	13.5		54.1	54.3
465-5H-1, 80-82	30.30	58.74	12.0	10.0	63.9	
465-5H-1, 100-102	30.50	58.79	31.1		85.5	
465-5H-1, 120-122	30.70	58.84	24.3	29.0	86.3	
465-5H-1, 140-142	30.90	58.89	31.0		2.1	
465-5H-2, 20-22	31.20	58.96	29.7	27.0	0.8	
465-5H-2, 40-42	31.40	59.01	56.4		5.2	
465-5H-2, 60-62	31.60	59.06	67.6	64.0	2.7	
465-5H-2, 80-82	31.80	59.10	78.8		4.0	
465-5H-2, 100-102	32.00	59.15	70.3		4.5	
465-5H-2, 120-122	32.20	59.20	69.0		11.9	
465-5H-2, 140-142	32.40	59.23	69.0			
465-5H-3, 20-22	32.70	59.28	76.0		9.0	7.1
465-5H-3, 40-42	32.90	59.31	60.8	58.0		
465-5H-3, 60-62	33.10	59.34	67.0			
465-5H-3, 80-82	33.30	59.37	76.0			
465-5H-3, 100-102	33.50	59.40	65.0		1.6	
465-5H-3, 120-122	33.70	59.43	72.0			
465-5H-3, 140-142	33.90	59.46	69.0			
465-5H-4, 20-22	34.20	59.51	63.0			
465-5H-4, 40-42	34.40	59.54	64.0			
465-5H-4, 60-62	34.60	59.57	66.0			
465-5H-4, 80-82	34.80	59.60	68.0			
465-5H-4, 100-102	35.00	59.63	61.2			
465-5H-4, 120-122	35.20	59.66	61.0			
465-5H-4, 140-142	35.40	59.69	63.0			
465-5H-5, 20-22	35.70	59.74	61.8			
465-5H-5, 40-42	35.90	59.77	50.0			
465-5H-5, 60-62	36.10	59.80	51.3			
465-5H-5, 80-82	36.30	59.83	54.5			
465-5H-5, 100-102	36.50	59.86	58.3			
465-5H-5, 120-122	36.70	59.89	53.3			
465-5H-5, 140-142	36.90	59.92	63.9			
465-5H-6, 20-22	37.20	59.97	48.9			
465-5H-6, 40-42	37.40	60.00	60.9			

Table 2b. Coiling direction and *Igorina tadjikastanensis* abundance for Hole 1209A.

Hole, Section, Sample (cm)	Depth (mbsf)	Age (Ma)	Coiling (%Dextral)	*Igorina tadjikastanensis* abundance
1209A-23H-1, 80-82	208.50	57.69		4.8
1209A-23H-2, 66-68	209.86	58.25		9.6
1209A-23H-2, 80-82	210.00	58.30	0.0	
1209A-23H-2, 103-105	210.23	58.40	6.0	
1209A-23H-2, 121-123	210.41	58.47	10.0	
1209A-23H-2, 140-142	210.60	58.55	6.0	2.4
1209A-23H-3, 21-23	210.91	58.68	10.2	
1209A-23H-3, 42-44	211.12	58.72	2.0	46.6
1209A-23H-3, 62-64	211.32	58.76	3.4	
1209A-23H-3, 77.5-79.5	211.48	58.80	21.2	96.0
1209A-23H-3, 100-102	211.70	58.84	8.1	92.3
1209A-23H-3, 110-112	211.80	58.86	4.9	
1209A-23H-3, 120-122	211.90	58.88	19.0	97.4
1209A-23H-3, 130-132	212.05	58.90	12.5	
1209A-23H-3, 140-142	212.1	58.92	24.4	52.4
1209A-23H-3, 147.5-149.5	212.18	58.94	18.0	20.1
1209A-23H-4, 11-13	212.31	59.22	66.2	23.3
1209A-23H-4, 11-22	212.365	59.23	-	
1209A-23H-4, 20-22	212.40	59.23	76.0	
1209A-23H-4, 24-26	212.44	59.24	70.9	10.2
1209A-23H-4, 37-39	212.57	59.26	68.0	
1209A-23H-4, 48-50	212.68	59.28	67.3	3.5
1209A-23H-4, 67-69	212.87	59.31	71.4	
1209A-23H-4, 96.5-98.5	213.17	59.35	61.8	
1209A-23H-4, 118-120	213.38	59.39	68.0	
1209A-23H-4, 140-142	213.60	59.42	80.0	
1209A-23H-5, 21-23	213.91	59.47	72.3	3.6
1209A-23H-5, 41.5-43.5	214.12	59.5	54.5	
1209A-23H-5, 80-82	214.50	59.56	64.0	
1209A-23H-5, 102.5-104.5	214.73	59.60	72.0	3.6
1209A-23H-6, 20-22	215.40	59.71	68.0	
1209A-23H-6, 42-44	215.62	59.74	50.0	
1209A-23H-6, 60-62	215.80	59.77	50.0	
1209A-23H-6, 67-69	215.87	59.78	60.0	
1209A-23H-6, 140-142	216.6	59.89	52.8	
1209A-23H-7, 58-60	217.28	60	45.0	

Table 2c. Coiling direction for Hole 865B.

Hole, Section, Sample (cm)	Depth (mbsf)	Age (Ma)	Coiling (%Dextral)
865B-14H-4, 20-22	127.20	59.10	6.00
865B-14H-4, 40-42	127.40	59.15	7.69
865B-14H-4, 60-62	127.60	59.20	12.00
865B-14H-4, 80-82	127.80	59.26	11.29
865B-14H-4, 98-100	127.98	59.31	5.36
865B-14H-4, 118-120	128.18	59.36	22.00
865B-14H-4, 140-142	128.40	59.42	12.00
865B-14H-5, 23-25	128.73	59.51	36.00
865B-14H-5, 42-44	128.92	59.57	35.29
865B-14H-5, 62-64	129.12	59.62	49.21
865B-14H-5, 82-84	129.32	59.68	40.38

Table 2d. Coiling direction for Hole 762C.

Hole, Section, Sample (cm)	Depth (mbsf)	Age (Ma)	Coiling (%Dextral)
762C-29X-3, 46-50	424.96	56.50	90.5
762C-30X-1, 101-105	432.01	57.01	88.0
762C-30X-2, 20-24	432.70	57.06	93.5
762C-30X-3, 96-100	434.96	57.23	90.2
762C-30X-4, 66-70	437.26	57.40	80.8
762C-31X-1, 60-64	441.10	57.68	94.0
762C-31X-1, 100-104	441.50	57.71	85.1
762C-31X-2, 10-14	442.10	57.75	92.0
762C-31X-2, 100-104	443.00	57.82	91.4
762C-31X-3, 97-101	444.47	57.92	87.5
762C-31X-4, 97-101	445.97	58.03	83.6
762C-31X-5, 101-105	447.51	58.14	83.7
762C-31X-6, 97-101	448.97	58.25	74.5
762C-32X-1, 50-53	450.50	58.4	85.5
762C-32X-1, 101-105	451.01	58.40	66.0
762C-32X-2, 100-104	452.50	58.51	92.0
762C-33X-1, 100-104	460.50	59.09	59.3
762C-33X-2, 20-23	461.20	59.14	64.1
762C-33X-2, 100-104	462.00	59.20	48.0
762C-33X-4, 95-99	464.95	60.00	62.1

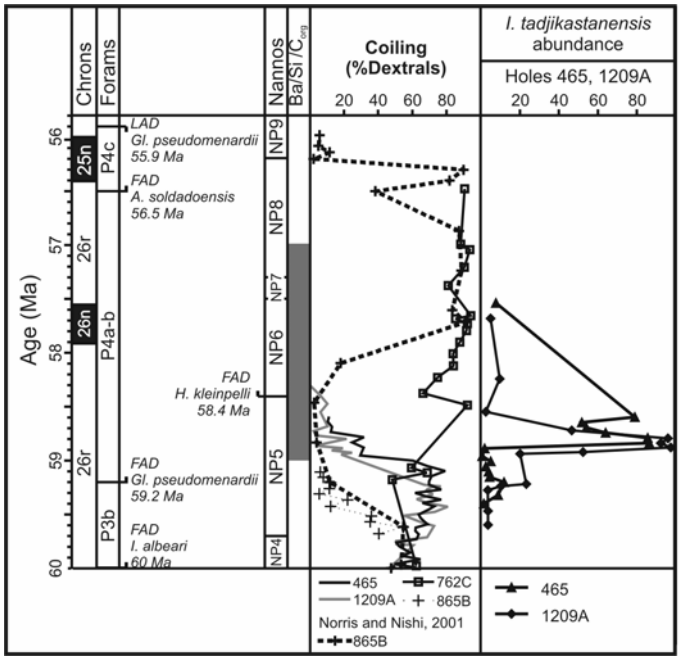

Figure 4. *I. albeari* coiling data and *I. tadjikastanensis* abundance for Holes 465 and 1209A.

Carbon Isotopes

The carbon isotope curves for Hole 465 show a significant ramping episode (**Table 3a; Fig. 5**). Both coiling morphs *Igorina albeari* and *Morozovella velascoensis* show $\delta^{13}C$ values averaging 3.6‰ up until 30.7 mbsf (58.8 Ma) where $\delta^{13}C$ values increase by ~0.5‰ to ~4.1‰. These higher values are maintained until the end of the sampled section. *Subbotina triangularis* $\delta^{13}C$ values remain at ~2.8‰ throughout so that $\Delta\delta^{13}C$ between surface and deep thermocline dwellers increases in the top part of the section. *Nuttallides* average 1.3‰ and ramp up by to1.6‰ at 30.7 mbsf (58.8 Ma) also, stabilizing at these higher values for the remainder of the section.

Hole 1209A shows a similar pattern to above. *Igorina albeari* $\delta^{13}C$ values average 3.6‰ (**Table 3b; Fig. 5**). From 212.18 mbsf (59.2 Ma) to 211.7 mbsf (59.0 Ma) $\delta^{13}C$ values increase by 0.4‰ to ~4.0‰ and remain high for the remainder of the section. A highly dissolved layer occurs at 212.1 mbsf (59.2 Ma), but was devoid of collectable material (**Fig. 5**). As with Hole 465, $\Delta\delta^{13}C$ increases towards the top of the section. *Subbotina triangularis* $\delta^{13}C$ values remain at ~2.7‰ until 211.7 mbsf (58.8 Ma) where $\delta^{13}C$ decreases from 2.7‰ to 2.2‰ simultaneous with the increase in *I. albeari*.

Supplementary data in Hole 865B shows during the initial coiling shift mixed *Igorina albeari* $\delta^{13}C$ average 3.8‰ and *Subbotina triangularis* 2.8‰ (**Table 3c; Fig. 5**).

For Hole 762C *Morozovella spp.* $\delta^{13}C$ values average 3.5‰. Although sparse over the coiling interval $\delta^{13}C$ values show a general increase similar in value to the other sites (~0.5‰) (**Table 3d; Fig. 5**). *Subbotina triangularis* $\delta^{13}C$ values average 2.3‰.

Oxygen Isotopes

The oxygen isotope record for Hole 465 shows some significant variations associated with the sinistrally dominated populations of *Igorina albeari* (**Table 3a; Fig. 6**). Sinistral and dextral *I. albeari* $\delta^{18}O$ values are very similar, averaging -1.3‰. *Morozovella velascoensis* $\delta^{18}O$ values average -1.2‰, *Subbotina triangularis* values average -0.9 ‰ and *Nuttallides* 0.4‰. At the base of the coiling reversal at ~31.6 mbsf (~59.1 Ma) there is a small, sharp decrease in all planktic foraminifera $\delta^{18}O$ of ~0.3‰ over 20 cm (~33 kyr). *S. triangularis* $\delta^{18}O$ reaches its minimum value at 30.7 mbsf (58.8 Ma) (1.0‰) and approaches the *M. velascoensis* curve, while there is a small decrease (0.3‰) in dextrally coiled *I. albeari*. Over the next 1 m (~250 kyr) *S. triangularis* $\delta^{18}O$ increases 0.3‰. At 29.7 mbsf (58.6 Ma) (last sample before core gap) there is a rapid decrease in *Nuttallides* $\delta^{18}O$ (0.4‰) and *S. triangularis* (0.2‰).

Oxygen isotopes for Hole 1209A mixed morphs show a similar overall trend to above (**Table 3b; Fig. 6**). Mixed *Igorina albeari* $\delta^{18}O$ average -1.0 ‰. *Subbotina triangularis* and *I. albeari* values are similar (~-0.8‰) from 212.44 mbsf (59.2 Ma) to 210.91mbsf (58.7 Ma), a pattern repeated in Hole 465. However there was no obvious increase in *S. triangularis* values after the coiling shift at 1209A.

The *Igorina albeari* mixed morphs oxygen isotope record for Hole 865B show that during the initial coiling reversal *Igorina albeari* (mixed) $\delta^{18}O$ values average -1.3‰ and *Subbotina triangularis* -0.4‰ (**Table 3c; Fig. 5**). There is a marked increase of 0.6‰ at the FAD of *Globanomalina pseudomenardii* at 127.65 mbsf (~59.2 Ma).

The *Morozovella spp.* oxygen isotope record for Hole 762C is sparse over the correlative P3a/P4 boundary interval but shows a general small decline similar to that seen at the Pacific sites (**Table 3d; Fig. 6**). *Morozovella spp.* $\delta^{18}O$ values average -1.2 ‰ for the sampled interval. *Subbotina triangularis* $\delta^{18}O$ values average -0.88‰.

Table 3a. Coiling direction and carbon and oxygen isotopes for Hole 465.

Site, Section, Sample (cm)	Depth (mbsf)	Age (Ma)	Coiling (%Dextral)	*Igorina albeari* (sinistral) $\delta^{13}C$ (‰)	*Igorina albeari* (sinistral) $\delta^{18}O$ (‰)	*Igorina albeari* (dextral) $\delta^{13}C$ (‰)	*Igorina albeari* (dextral) $\delta^{18}O$ (‰)	*Subbotina triangularis* $\delta^{13}C$ (‰)	*Subbotina triangularis* $\delta^{18}O$ (‰)	*Morozovella velascoensis* $\delta^{13}C$ (‰)	*Morozovella velascoensis* $\delta^{18}O$ (‰)	*Nuttallides* $\delta^{13}C$ (‰)	*Nuttallides* $\delta^{18}O$ (‰)
465-5H-1, 20-22	29.70	58.60	11.0	3.93	-1.47	4.09	-1.32	2.88	-0.91	4.04	-1.07	1.69	0.15
465-5H-1, 40-42	29.90	58.65	10.3	4.08	-1.43	4.09	-1.36	2.74	-0.71	4.13	-1.06	1.63	0.45
465-5H-1, 60-62	30.10	58.69	13.5	4.00	-1.20	4.02	-1.23	2.84	-0.68	4.12	-1.05	1.67	0.50
465-5H-1, 80-82	30.30	58.74	12.0	4.10	-1.30	4.13	-1.25	2.84	-0.91	4.17	-1.29	1.65	0.51
465-5H-1, 100-102	30.50	58.79	31.1	4.02	-1.27	3.75	-1.47	2.83	-0.88	4.09	-1.09	1.67	0.41
465-5H-1, 120-122	30.70	58.84	24.3	3.92	-1.30	3.93	-1.26	2.93	-1.01	4.08	-1.09	1.51	0.46
465-5H-1, 140-142	30.90	58.89	31.0	3.58	-1.29	3.50	-1.19	2.89	-1.01	3.72	-1.20	1.18	0.40
465-5H-2, 20-22	31.20	58.96	29.7	3.54	-1.23	3.55	-1.26	2.74	-1.20	3.66	-1.20	1.25	0.40
465-5H-2, 40-42	31.40	59.01	56.4	3.46	-1.25	3.63	-1.24	2.83	-1.01	3.70	-1.18	1.25	0.40
465-5H-2, 60-62	31.60	59.06	67.6	3.58	-1.41	3.60	-1.35	2.83	-0.89	3.78	-1.19	1.11	0.44
465-5H-2, 80-82	31.80	59.10	78.8	3.54	-1.23	3.57	-1.22	2.84	-0.97	3.64	-1.13	1.14	0.44
465-5H-2, 100-102	32.00	59.15	70.3	3.70	-1.26	3.44	-1.21	2.85	-0.91	3.61	-1.12	1.21	0.43
465-5H-2, 120-122	32.20	59.20	69.0	-	-	-	-	-	-	-	-	-	-
465-5H-2, 140-142	32.40	59.23	69.0	-	-	-	-	-	-	-	-	-	-
465-5H-3, 20-22	32.70	59.28	76.0	-	-	-	-	-	-	-	-	-	-
465-5H-3, 40-42	32.90	59.31	60.8	3.52	-1.17	3.64	-1.30	2.87	-0.85	3.74	-1.26	1.20	0.45
465-5H-3, 60-62	33.10	59.34	67.0	-	-	-	-	-	-	-	-	-	-
465-5H-3, 80-82	33.30	59.37	76.0	-	-	-	-	-	-	-	-	-	-
465-5H-3, 100-102	33.50	59.40	65.0	3.59	-1.29	3.59	-1.28	2.80	-0.99	3.62	-1.29	1.21	0.52
465-5H-3, 120-122	33.70	59.43	72.0	-	-	-	-	-	-	-	-	-	-
465-5H-3, 140-142	33.90	59.46	69.0	-	-	-	-	-	-	-	-	-	-
465-5H-4, 20-22	34.20	59.51	63.0	-	-	-	-	-	-	-	-	-	-
465-5H-4, 40-42	34.40	59.54	64.0	3.74	-1.35	3.71	-1.35	2.81	-0.89	3.76	-1.39	1.35	0.56
465-5H-4, 60-62	34.60	59.57	66.0	-	-	-	-	-	-	-	-	-	-
465-5H-4, 80-82	34.80	59.60	68.0	-	-	-	-	-	-	-	-	-	-
465-5H-4, 100-102	35.00	59.63	61.2	3.69	-1.37	3.59	-1.32	3.05	-0.98	3.77	-1.14	1.34	0.53
465-5H-4, 120-122	35.20	59.66	61.0	-	-	-	-	-	-	-	-	-	-
465-5H-4, 140-142	35.40	59.69	63.0	-	-	-	-	-	-	-	-	-	-
465-5H-5, 20-22	35.70	59.74	61.8	-	-	-	-	-	-	-	-	-	-
465-5H-5, 40-42	35.90	59.77	50.0	3.86	-1.19	3.80	-1.23	2.97	-0.82	3.78	-1.11	1.39	0.46
465-5H-5, 60-62	36.10	59.80	51.3	-	-	-	-	-	-	-	-	-	-
465-5H-5, 80-82	36.30	59.83	54.5	-	-	-	-	-	-	-	-	-	-
465-5H-5, 100-102	36.50	59.86	58.3	3.61	-1.36	3.77	-1.23	2.79	-0.78	3.71	-1.02	1.32	0.43
465-5H-5, 120-122	36.70	59.89	53.3	-	-	-	-	-	-	-	-	-	-
465-5H-5, 140-142	36.90	59.92	63.9	-	-	-	-	-	-	-	-	-	-
465-5H-6, 20-22	37.20	59.97	48.9	-	-	-	-	-	-	-	-	-	-
465-5H-6, 40-42	37.40	60.00	60.9	3.51	-1.05	3.59	-1.15	2.68	-0.54	3.50	-1.00	-	-

Table 3b. Coiling direction and carbon and oxygen isotopes for Hole 1209A.

Hole, Section, Sample (cm)	Depth (mbsf)	Age (Ma)	Coiling (%dextral)	*I. albeari* (mixed) $\delta^{13}C$ (‰)	*I. albeari* (mixed) $\delta^{18}O$ (‰)	*Subbotina triangularis* $\delta^{13}C$ (‰)	*Subbotina triangularis* $\delta^{18}O$ (‰)
1209A-23H-2, 80-82	210.00	58.30	0.0	4.07	-1.05	3.03	-0.65
1209A-23H-2, 103-105	210.23	58.40	6.0	4.07	-1.13	2.97	-0.73
1209A-23H-2, 121-123	210.41	58.47	10.0	4.05	-1.10	2.98	-0.71
1209A-23H-2, 140-142	210.60	58.55	6.0	4.03	-1.03	2.85	-0.49
1209A-23H-3, 21-23	210.91	58.68	10.2	3.81	-1.11	2.23	-1.02
1209A-23H-3, 42-44	211.12	58.72	2.0	3.65	-1.02	-	-
1209A-23H-3, 62-64	211.32	58.76	3.4	3.82	-1.23	-	-
1209A-23H-3, 77.5-79.5	211.48	58.80	21.2	3.69	-1.03	-	-
1209A-23H-3, 100-102	211.70	58.84	8.1	3.78	-1.01	2.67	-0.90
1209A-23H-3, 110-112	211.80	58.86	4.9	3.72	-0.93	-	-
1209A-23H-3, 120-122	211.90	58.88	19.0	3.58	-1.04	2.77	-0.75
1209A-23H-3, 130-132	212.05	58.90	12.5	3.52	-0.96	2.82	-0.92
1209A-23H-3, 140-142	212.1	58.92	24.4	-	-	-	-
1209A-23H-3, 147.5-149.5	212.18	58.94	18.0	3.39	-1.06	2.75	-0.81
1209A-23H-4, 11-13	212.31	59.22	66.2	3.40	-1.06	-	-
1209A-23H-4, 11-22	212.365	59.23	-	-	-	2.60	-0.63
1209A-23H-4, 20-22	212.40	59.23	76.0	3.41	-1.09	-	-
1209A-23H-4, 24-26	212.44	59.24	70.9	3.29	-0.84	2.67	-0.80
1209A-23H-4, 37-39	212.57	59.26	68.0	3.35	-0.94	2.64	-0.61
1209A-23H-4, 48-50	212.68	59.28	67.3	3.42	-1.04	2.79	-0.66
1209A-23H-4, 67-69	212.87	59.31	71.4	-	-	-	-
1209A-23H-4, 96.5-98.5	213.17	59.35	61.8	3.52	-1.07	2.75	-0.69
1209A-23H-4, 118-120	213.38	59.39	68.0	-	-	-	-
1209A-23H-4, 140-142	213.60	59.42	80.0	3.41	-1.08	2.74	-0.54
1209A-23H-5, 21-23	213.91	59.47	72.3	-	-	-	-
1209A-23H-5, 41.5-43.5	214.12	59.5	54.5	-	-	-	-
1209A-23H-5, 80-82	214.50	59.56	64.0	3.55	-0.99	2.92	-0.72
1209A-23H-5, 102.5-104.5	214.73	59.60	72.0	3.52	-0.96	2.83	-0.77
1209A-23H-6, 20-22	215.40	59.71	68.0	-	-	2.70	-0.68
1209A-23H-6, 42-44	215.62	59.74	50.0	3.45	-0.99	2.61	-0.61
1209A-23H-6, 60-62	215.80	59.77	50.0	3.59	-0.84	2.69	-0.57
1209A-23H-6, 67-69	215.87	59.78	60.0	-	-	-	-
1209A-23H-6, 140-142	216.6	59.89	52.8	-	-	-	-
1209A-23H-7, 58-60	217.28	60	45.0	-	-	-	-

Table 3c. Coiling direction, carbon and oxygen isotopes for Hole 865B.

Hole, Section, Sample (cm)	Depth (mbsf)	Age (Ma)	Coiling (%Dextral)	*Igorina albeari* (mixed) $\delta^{13}C$ (‰)	*Igorina albeari* (mixed) $\delta^{18}O$ (‰)	*Subbotina triangularis* $\delta^{13}C$ (‰)	*Subbotina triangularis* $\delta^{18}O$ (‰)
865B-14H-4, 20-22	127.20	59.10	6.00	3.74	-1.36	-	-
865B-14H-4, 40-42	127.40	59.15	7.69	3.79	-1.33	2.49	-0.33
865B-14H-4, 60-62	127.60	59.20	12.00	-	-	-	-
865B-14H-4, 80-82	127.80	59.26	11.29	3.79	-1.37	-	-
865B-14H-4, 98-100	127.98	59.31	5.36	3.83	-1.42	2.53	-0.54
865B-14H-4, 118-120	128.18	59.36	22.00	3.74	-1.29	-	-
865B-14H-4, 140-142	128.40	59.42	12.00	3.84	-1.38	2.42	-0.71
865B-14H-5, 23-25	128.73	59.51	36.00	3.68	-1.24	-	-
865B-14H-5, 42-44	128.92	59.57	35.29	3.57	-1.22	2.43	-0.69
865B-14H-5, 62-64	129.12	59.62	49.21	-	-	-	-
865B-14H-5, 82-84	129.32	59.68	40.38	3.73	-1.29	-	-

Table 3d. Coiling direction, carbon and oxygen isotopes for Hole 762C.

Hole, Section, Sample (cm)	Depth (mbsf)	Age (Ma)	Coiling (%Dextral)	*Subbotina triangularis* $\delta^{13}C$ (‰)	*Subbotina triangularis* $\delta^{18}O$ (‰)	*Morozovella spp.*	$\delta^{13}C$ (‰)	$\delta^{18}O$ (‰)
762C-28X-1, 104-107	413.04	55.90	-	-	-	*M. occlusa*	3.61	-1.26
762C-28X-2, 10-12	413.60	55.93	-	-	-	*M. occlusa*	3.64	-1.27
762C-29X-1, 48-52	421.98	56.35	-	-	-	*M. occlusa*	3.74	-1.12
762C-29X-2, 49-53	423.49	56.43	-	-	-	*M. occlusa*	4.25	-1.17
762C-29X-3, 46-50	424.96	56.50	90.48	-	-	*M. occlusa*	4.31	-1.34
762C-30X-1, 101-105	432.01	57.01	88.00	-	-	-	-	-
762C-30X-2, 20-24	432.70	57.06	93.48	-	-	-	-	-
762C-30X-3, 96-100	434.96	57.23	90.20	-	-	-	-	-
762C-30X-4, 66-70	437.26	57.40	80.77	-	-	-	-	-
762C-31X-1, 60-64	441.10	57.68	94.00	-	-	-	-	-
762C-31X-1, 100-104	441.50	57.71	85.14	-	-	*M. acutispira*	3.62	-1.19
762C-31X-2, 10-14	442.10	57.75	92.00	-	-	-	-	-
762C-31X-2, 100-104	443.00	57.82	91.38	-	-	*M. acutispira*	3.70	-1.10
762C-31X-3, 97-101	444.47	57.92	87.50	-	-	*M. acutispira*	3.57	-1.01
762C-31X-4, 97-101	445.97	58.03	83.65	-	-	*M. acutispira*	3.26	-1.33
762C-31X-5, 101-105	447.51	58.14	83.72	-	-	*M. acutispira*	3.57	-1.18
762C-31X-6, 97-101	448.97	58.25	74.51	-	-	*M. acutispira*	3.73	-1.17
762C-32X-1, 20-23	450.20	58.34	-	-	-	*M. acutispira*	2.95	-1.16
762C-32X-1, 50-53	450.50	58.36	85.50	2.34	-0.73	*M. acutispira*	3.46	-1.11
762C-32X-1, 101-105	451.01	58.40	66.00	-	-	*M. acutispira*	3.67	-1.11
762C-32X-2, 20-23	451.70	58.45	-	-	-	*M. acutispira*	3.50	-1.10
762C-32X-2, 55-58	452.05	58.47	-	2.33	-0.69	*M. acutispira*	3.34	-1.07
762C-32X-2, 100-104	452.50	58.51	92.00	-	-	*M. acutispira*	3.43	-1.07
762C-32X-3, 15-18	453.15	58.55	-	1.95	-0.85	*M. acutispira*	3.04	-1.15
762C-32X-3, 35-38	453.35	58.57	-	-	-	*M. acutispira*	3.07	-1.23
762C-32X-3, 66-69	453.66	58.59	-	-	-	*M. acutispira*	3.24	-1.23
762C-32X-4, 60-63	455.10	58.70	-	2.38	-1.00	*M. acutispira*	3.02	-1.53
762C-32X-CC, 32-35	456.32	58.79	-	-	-	*M. acutispira*	3.22	-1.21
762C-33X-1, 20-23	459.70	59.03	-	2.25	-1.00	-	-	-
762C-33X-1, 100-104	460.50	59.09	59.26	-	-	-	-	-
762C-33X-2, 20-23	461.20	59.14	64.10	2.28	-0.91			
762C-33X-2, 100-104	462.00	59.20	48.00	-	-	-	-	-
762C-33X-3, 35-38	462.85	59.43	-	2.27	-0.87	-	-	-
762C-33X-3, 66-69	463.16	59.51	-	2.22	-0.95	-	-	-
762C-33X-4, 60-63	464.60	59.91	-	-	-	-	-	-
762C-33X-4, 95-99	464.95	60.00	62.07	-	-	*M. acutispira*	2.98	-1.39

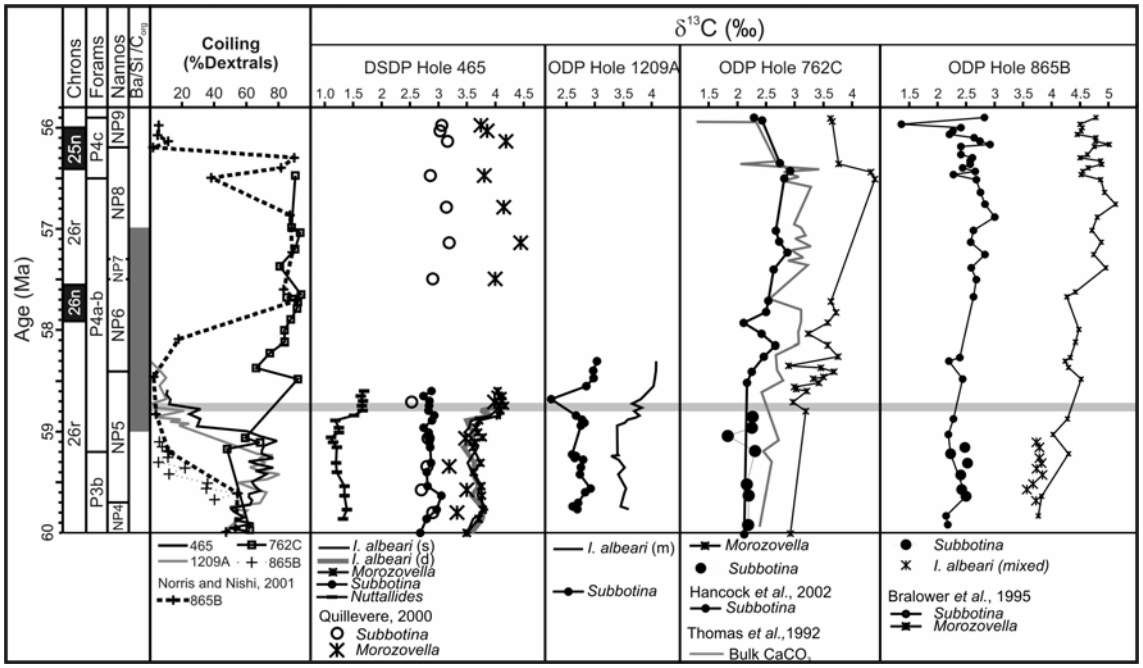

Figure 5. Chronostratigraphy, planktic foraminifera and nannofossil biostratigraphy, Ba export (Thompson and Schmitz, 1997) and Waipawa Formation (Hollis 2002; Hollis *et al*., 2005) (grey block), coiling data and carbon isotopes for Holes 465, 1209A, 762C and 865B. S = sinistral, D = dextral, M = mixed. Grey band represents interval of highly dissolved sediment in Holes 465 and 1209A.

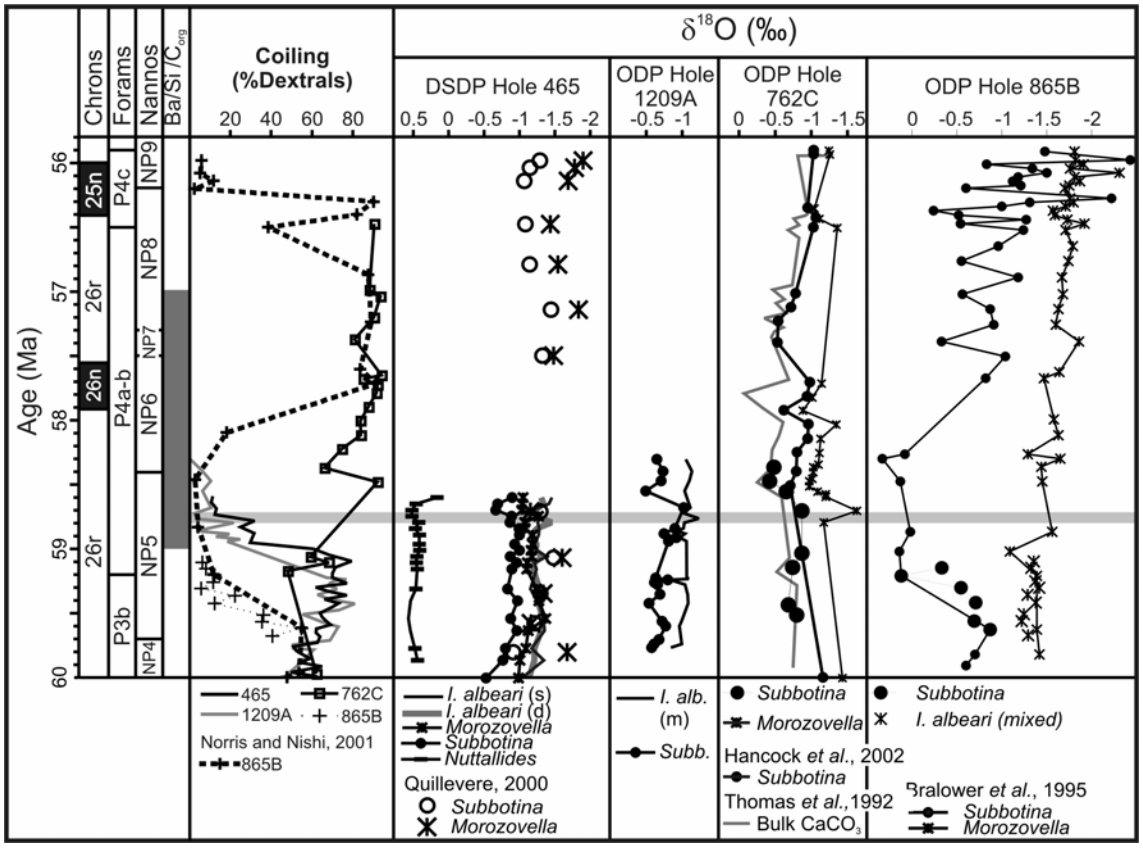

Figure 6. Chronostratigraphy, planktic foraminifera and nannofossil biostratigraphy, Ba export (Thompson & Schmitz, 1997) and Waipawa Formation (Hollis 2002; Hollis *et al*., 2005) (grey block), coiling data and oxygen isotopes for Holes 465, 1209A, 762C and 865B. S = sinistral, D = dextral, M = mixed. Grey band represents interval of highly dissolved sediment in Holes 465 and 1209A.

Carbonate Dissolution

Carbonate dissolution is a prominent feature associated with the coiling shift and isotope changes in Holes 465 and 1209A. For Hole 465-BENTH is generally very low, below 10%, but increases to an anomalous spike of 35% at 30.7 mbsf (58.8 Ma) 90 cm above the base of the coiling shift (**Table 4a; Fig. 7**), coincident with the ramping episode in $\delta^{13}C$ (**Fig. 5**). FRAG is generally below 20% but also increases to 28% at 30.7 mbsf.

For Hole 1209A, BENTH is generally below 40%. From 212.30 mbsf (59.2 Ma) to 212.10 mbsf (59.1 Ma) BENTH increases to ~85% at. This interval corresponds to the coiling shift and the 20 cm thick clay-rich dissolution layer (**Table 4b; Fig. 7**). FRAG is generally above 50% and peaks at 75% at 212.10 mbsf.

As mentioned above, an extremely poorly preserved and heavily recrystallized sample occurs at 463.50 (~59.2 Ma) in Hole 762C where there is a slight bias towards sinistral populations of *Igorina albeari.*

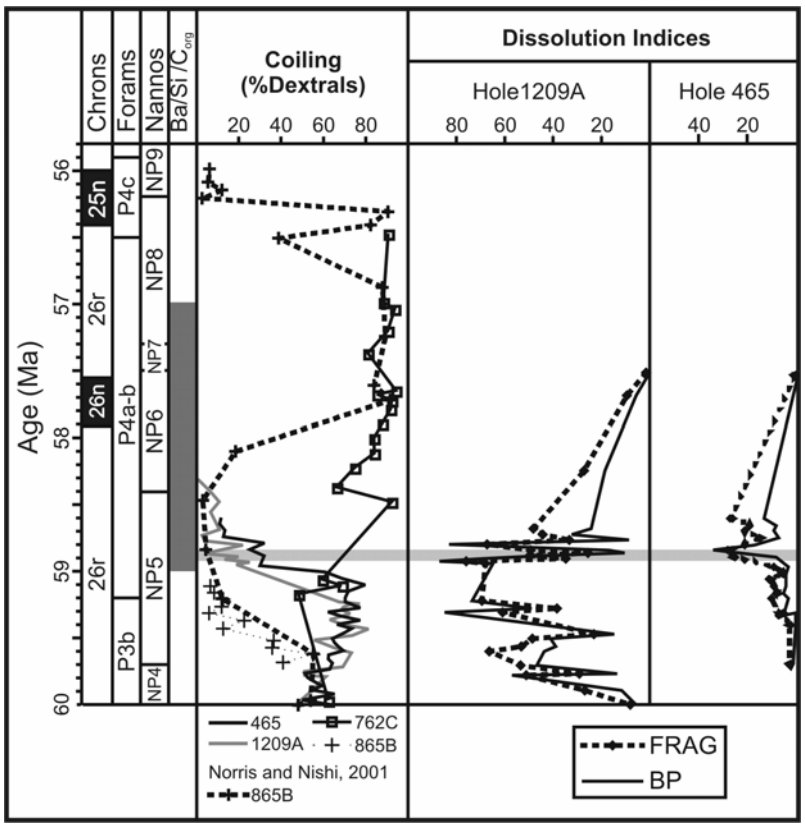

Figure 7. Dissolution indices including FRAG and BENTH for Holes 465 and 1209A.

Table 4a. Dissolution indices for Hole 465. Shaded area is peak dissolution in Hole 465.

Hole, Section, Sample (cm)	Depth (mbsf)	Age (Ma)	B/P	FRAG
465-5H-1, 20-22	29.70	58.60	13.11	27.02
465-5H-1, 40-42	29.90	58.65	9.02	19.49
465-5H-1, 60-62	30.10	58.69	10.00	21.45
465-5H-1, 80-82	30.30	58.74	7.22	15.09
465-5H-1, 100-102	30.50	58.79	17.98	21.51
465-5H-1, 120-122	30.70	58.84	34.67	27.94
465-5H-1, 140-142	30.90	58.89	8.82	25.64
465-5H-2, 20-22	31.20	58.96	4.07	9.67
465-5H-2, 40-42	31.40	59.01	4.17	6.03
465-5H-2, 60-62	31.60	59.06	4.23	11.27
465-5H-2, 80-82	31.80	59.10	4.30	9.76
465-5H-2, 100-102	32.00	59.15	6.04	8.42
465-5H-3, 40-42	32.90	59.31	0.76	6.14

Table 4b. Dissolution indices for Hole 1209A. Shaded area is peak dissolution in Hole 1209A.

Hole, Section, Sample (cm)	Depth (mbsf)	Age (Ma)	B/P	FRAG
1209A-22H-5, 141.5-143.5	205.62	56.50	27.17	19.23
1209A-22H-6, 69-71	206.39	56.82	8.13	4.33
1209A-22H-7, 50-52	207.20	57.15	6.31	5.99
1209A-23H-1, 20-22	207.90	57.44	4.93	1.26
1209A-23H-1, 38-40	208.08	57.51	1.49	0.00
1209A-23H-1, 80-82	208.50	57.69	9.46	5.59
1209A-23H-2, 66-68	209.86	58.25	27.23	18.50
1209A-23H-3, 21-23	210.91	58.68	48.21	24.19
1209A-23H-3, 42-44	211.12	58.76	44.28	32.26
1209A-23H-3, 62-64	211.32	58.85	33.33	8.51
1209A-23H-3, 77.5-79.5	211.48	58.91	67.35	83.10
1209A-23H-3, 100-102	211.70	59.00	49.28	16.67
1209A-23H-3, 110-112	211.80	59.04	25.56	10.38
1209A-23H-3, 120-122	211.90	59.08	49.73	43.90
1209A-23H-3, 130-132	212.00	59.13	34.72	68.93
1209A-23H-3, 140-142	212.10	59.17	75.97	87.04
1209A-23H-3, 147.5-149.5	212.18	59.20	68.05	64.86
1209A-23H-4, 11-13	212.31	59.22	69.49	73.53
1209A-23H-4, 48-50	212.68	59.28	38.39	48.85
1209A-23H-4, 67-69	212.87	59.31	60.87	84.92
1209A-23H-5, 21-23	213.91	59.47	23.08	14.63
1209A-23H-5, 41.5-43.5	214.12	59.50	48.60	41.03
1209A-23H-5, 80-82	214.50	59.56	53.19	38.89
1209A-23H-5, 102.5-104.5	214.73	59.60	66.35	43.64
1209A-23H-6, 20-22	215.40	59.71	53.50	46.74
1209A-23H-6, 60-62	215.80	59.77	29.11	13.43
1209A-23H-6, 67-69	215.87	59.78	51.07	56.98
1209A-23H-6, 140-142	216.60	59.89	26.90	11.57
1209A-23H-7, 58-60	217.28	60.00	8.07	5.69

DISCUSSION

The coiling shift in *Igorina albeari* is abrupt and slightly diachronous at three low latitude Pacific sites. It occurs at the FAD of *Globanomalina pseudomenardii* (59.2 Ma) in Hole 1209A, 1.3 m below this datum in Hole 865B and 80 cm above it in Hole 465. The FAD of the nannofossil *Heliolithis kleinpelli* occurs below the coiling shift in Holes 1209A (47 cm) (Bralower, pers. comm.) and 865B (2.1 m) (Bralower and Mutterlose, 1995) (**Fig. 4**). In Holes 465 and 1209A *I. albeari* shifts its coiling direction once. In Hole 865B, the populations reverse to sinistral coiling twice (Norris and Nishi, 2001).

At all sites the FAD of *Heliolithis kleinpelli* (58.4 Ma) occurs ***below*** the FAD of *Globanomalina p*seudomenardii (59.2 Ma). Our ages are based on the planktic foraminiferal zonation following Berggren et al. (1995). Berggren et al. (1995) point out the possible errors in their dating of the FAD of *Gl. pseudomenardii*. Irrespective of the accuracy of these dates, between the FADs of *H. kleinpelli* and *Gl. pseudomenardii* there is a profound change in ocean temeperatures and the carbon cycle. Holes 865B and 465 have the best preserved and most expanded P3b/P4 boundary interval. The base of the coiling shift in Holes 865B and 465 corresponds to a warming of the surface layer, seen as a small decrease in $\delta^{18}O$, which may have triggered a divergence of the two coiling morphs (**Fig. 4**). In Hole 465 at 30.7 mbsf (58.8 Ma), where 72% of specimens are sinistrally coiled, *Igorina albeari* and *Morozovella velascoensis* $\delta^{18}O$ values are similar suggesting an expansion of the surface layer. At the same time at both locations, $\delta^{13}C$ increases sharply and the difference between surface and deeper dwellers, $\Delta\delta^{13}C$, becomes more marked (**Fig. 5**). This is immediately followed by cooling of bottom and deep thermocline waters by ~0.5ºC and ~2ºC respectively for the duration of the coiling reversal. In Hole 865 an extended cooling period is preserved from ~59.2 to 58.1 Ma (~1.1 myr) and at the base of Zone P4 there is anomalous increase in oxygen isotope values of ~0.5‰ (**Fig. 6**). If the cooling interval is caused by increased productivity then a negative feedback effect may have occurred whereby atmospheric CO_2 drawdown during periods of increased productivity has the effect of cooling the surface and thermocline layers. A global cooling episode (~59-57 Ma) correlated with the lower part of the Paleocene Carbon Isotope Maximum (PCIM) (Zachos *et al.,* 2001) supports this idea. Hole 865B records a period of cooling in the

deep thermocline coincident with sinistrally dominated populations in lower Zone P4 (~59.2-58.1 Ma) (**Fig. 4**). Changes in *Subbotina* $\delta^{18}O$ values were not observed in Hole 1209A, due to the condensed nature of the section there.

The cooling interval in both Holes 465 and 1209A spans a highly dissolved layer with very high BENTH and FRAG, and at 1209A also an abundance of fish teeth and manganese coated foraminifera (Shipboard Scientific Party, 2002; Hancock and Dickens, 2005). The Leg 198 Shipboard Scientific Party (2002) recorded this clay-rich layer at several of the Southern High sites, including Hole 1209A and described it as an important biotic event (~58 Ma) close to the evolutionary first appearance of the nannofossil *Discoaster*, a dominant Cenozoic genus, and characterized by a planktic foraminifera assemblage dominated by *Igorina tadjikastanensis* (Petrizzo, 2005). At Site 465 there is also an abundance of *I. tadjikistansis* in the dissolution layer. At Sites 1267 and 1262 on the Walvis Ridge, a similar mid Paleocene biotic event is coincident with a sharp magnetic susceptibility spike near the FAD of *Heliolithus kleinpellii* at the base of Zone NP6 (Zachos *et al.*, 2004).

The highest values of $\delta^{13}C$ of the Cenozoic denote the PCIM. Rich assemblages of plankton and an increasing $\Delta\delta^{13}C$ between surface and bottom dwelling foraminifera plus high Ba and Si export suggest that the PCIM was a period of high productivity in surface waters (Shackleton *et al.*, 1985; Corfield and Cartlidge, 1992; Thompson and Schmitz, 1997; Hollis, 2002) (**Figs. 1, 5**). Strengthening of vertical carbon and oxygen isotope gradients in the water column shortly after the coiling reversal in the Pacific Ocean is correlative with the lower part of the PCIM, also associated with a high latitude cooling episode expressed in global oxygen isotope records at ~59-57 Ma (Zachos *et al.*, 2001) and a contemporaneous drop in global sea level (Haq *et al.*, 1987; Killops *et al.*, 2000). Our *Nuttallides* and *Subbotina* oxygen isotope data for Hole 465 show a minor cooling event of ~0.5ºC and ~2ºC in bottom and deep thermocline waters coincident with increasing $\delta^{13}C$ and supports the occurrence of a high latitude cooling event during the mid Paleocene. A 60 m thick, richly biosiliceous/calcareous deposit in Hole 1121B, Campbell Plateau, South-west Pacific Ocean has recently been correlated with the PCIM. Here at the base of radiolarian zone RP6 compacted sediment accumulation rates double largely due to an increase in radiolarian and larger diatom

accumulation rates (Hollis, 2002). ODP Hole 761B and DSDP Hole 208 also show a significant increase in biosiliceous productivity, which is correlative to the mid Paleocene cooling event (~59-57 Ma) apparent in global benthic foraminiferal records (Zachos *et al.*, 2001). High latitude, Southern Ocean Leg 113 sites from the Maud Rise, Weddell Sea record an increase in *Subbotina* and benthic foraminifera $\delta^{18}O$ of ~1‰, equivalent to a decline of 4ºC in deep thermocline and bottom waters during middle Late Paleocene (middle Zone P4) (Corfield and Cartlidge, 1992). The Waipawa Formation is a diachronous (~58-57 Ma) organic-rich formation present in numerous New Zealand basins. It has been interpreted as a transgressive continental margin succession that was influenced by an expanded oxygen minimum zone at the shelf-slope break (Hollis, 2002; Hollis *et al.*, 2005) (**Fig. 4**). Perhaps, vigorous oceanic circulation during a mid Paleocene cooling episode led to increased surface water productivity and an expanded oxygen minimum zone. There is further evidence supporting a mid Paleocene cooling episode. The palaeogeographical range of the planktic foraminifera *Acarinina* expanded from the mid-high latitudes into the tropics along with nutrient rich water during the mid Paleocene (Quillevere *et al.*, 2001; Quillevere and Norris, 2003). Mid Paleocene floral compositions and $\delta^{18}O$ values of aragonite mollusk fossils from the Bighorn and Green River and Bighorn Basins, Wyoming demonstrate that continental interiors were cool (Dettman and Lohmann, 2000; Wilf, 2000).

For *Igorina albeari*, a coiling shift at the base of Zone P4 is registered in the central Pacific Basin and also in the Atlantic Basin in sediment from Site 1050, Blake Ridge (Hancock, pers. observ.), and not at mid latitude sites, implying that populations with different coiling ratios exist in different parts of the ocean at the same time. A possibly analogous situation is the contemporary presence of sinistral *Globorotalia truncatulinoides* in the central nutrient depleted oceanic gyres and dextral *G. truncatulinoides* in the equatorial ocean (Thiede, 1971; de Vargas *et al.*, 2001). At Site 865 the range of *I. albeari* is extended ~6.1 m.y. compared to ~3.5 m.y. in Holes 465 and 1209A) and there are at least two additional coiling shifts higher up the column that do not occur at the other Pacific sites. The higher accumulation rates at Site 865 at its palaeolatitude during the Upper Paleocene (**Fig. 2**) indicate that the site was positioned in the equatorial divergence. Water mass boundaries can restrict gene flow and lead to reproductive isolation (Brummer and Kroon, 1988). Such a hydrographic barrier between Site 865 and the other Pacific sites may have induced speciation and resulted in

the differences seen in the range of *I. albeari* and its sinistral coiling morph. For *Igorina albeari*, the similarity between sinistral and dextral isotope values suggests that whatever the genetic or ecological differences are between the two morphs, they are not correlated to temperature, depth ecology or photosymbiosis (as a control on $\delta^{13}C$). These data leave open the possibility that other ecological differences in sinistral and dextral morphs of *I. albeari* exist, perhaps comparable to those observed for *G. truncatulinoides*. Other ecological differences between the two coiling morphs may include feeding ecology, rates of maturation or ecological preferences in terms of the strength of thermocline stratification, as suggested by the reduction in surface to deep thermocline $\delta^{18}O$ gradients apparent in Hole 465.

CONCLUSIONS

Populations of *Igorina albeari* showed prominent changes in preferred coiling direction within Upper Paleocene sediment at ODP Site 865 in the central Pacific Ocean. This study examined the nature, extent and cause of these coiling shifts by constructing records of *I. albeari* coiling direction and foraminiferal stable isotope composition. We draw the following conclusions:

(1) A prominent coiling reversal occurred in populations of *Igorina albeari* that inhabited low latitudes of the Pacific and Atlantic Ocean during the Late Paleocene. This shift is from dominantly dextral morphs to dominantly sinistral morphs beginning at the P3b/P4 boundary interval at ~59.2 to 59.1 Ma. We did not find a second coiling shift at Holes 465 and 1209A.

(2) The coiling shift provides an important biomarker for the Late Paleocene. It occurs between the FADs of *the nannofossil Heliolithis kleinpelli* (58.2 Ma) and *Globanomalina pseudomenardii* sensu stricto (59.2 Ma) at the Pacific sites. The FAD of the *H. kleinpelli* occurs close to the FAD of *Gl. pseudomenardii* in Holes 1209A (47 cm) and 865B (2.1 m) (Bralower, pers. comm., 2004). As can be seen there is an obvious age discrepancy between the planktic foraminifera and nannofossil datums, as the nannofossil makes its first appearance ***first*** even though it is given a younger age. The base of the coiling shift is slightly diachronous. In Hole 865 (the most expanded and complete section) the coiling shift begins 1.3 m below the FAD of *Gl.*

pseudomenardii. In Hole 465 the coiling shift begins at or just above (60 cm or ~140 kyrs) the FAD of *Gl. pseudomenardii* and in Hole 1209A it occurs at the FAD of *Gl. pseudomenardii*. This diachroneity suggests some kind of separation between the water masses that bathed Hole 865B from those that bathed Holes 465 and 1209A.

(3) Carbon and oxygen isotope values for *Igorina albeari* are similar to *Morozovella velascoensis* establishing it as a surface dweller. *Igorina albeari* has a thick, pustulose test, which is more dissolution resistant than *Morozovella* making it important for reconstructing surface water conditions during intervals of high dissolution.

(4) Populations of *Igorina albeari* in Hole 865B begin with proportionate coiling and shift to sinistral coiling. At Holes 465, 1209A and 762C they begin with proportionate coiling and progressively become more dextrally dominated until they either reverse coiling direction as at 465and 1209A, or remain dextrally dominated in the mid-high latitude Hole 762C. A modern analogy is *Globorotalia truncatulinoides* with sinistral populations in the gyres and dextral populations in the equatorial oceans.

(5) In Holes 465 and 865B oxygen isotopes indicate a small warming episode of ~0.5˚C from surface and deeper dwelling *Igorina albeari*, *Morozovella velascoensis* and *Subbotina triangularis* at the base of the coiling shift (~59.1 Ma).

(6) In Hole 865 the *Subbotina triangularis* oxygen isotope data suggests warming in the deep thermocline by expansion of the surface layer during the coiling shift. During the coiling shift in Hole 465 oxygen isotope values for *Subbotina triangularis* approach *Igorina albeari* and *Morozovella velascoensis* (~58.8 Ma) suggesting an expansion of the surface layer.

(7) At the same time there is a rapid increase in $\delta^{13}C$ of surface dwellers of ~0.5‰ and $\Delta\delta^{13}C$ between surface and deep-thermocline species increases.

(8) Over the next 200 kyr benthic and deep thermocline waters cooled ~0.5˚C and ~2ºC respectively. Oxygen isotope data from Hole 865B shows that this cooling period continued for the duration of sinistrally dominated populations in lower Zone P4 (~59.2 to 58.1 Ma). This cooling episode is preserved in Holes 465 and 1209A in a highly

dissolved layer reflected in high FRAG and BENTH ratios and abundance of the thick-walled, solution resistant *Igorina tadjikastansis*. It is most prominent at 1209A, where there is a 20 cm thick clay-rich layer showing a magnetic susceptibility spike.

(9) No obvious causal relationship between coiling shift and isotopes and no significant offset between sinistrally and dextrally coiled morphologies of *Igorina albeari s*uggests that there was no spatial partitioning between the two morphologies, although it may yet be possible that the two are separate species.

10) There may be other ecological differences between sinistrals and dextrals, such as different seasonal timing of population growth, feeding ecology, rates of maturation or ecological preferences in terms of the strength of thermocline stratification.

ACKNOWLEDGMENTS

Special thanks go to Dick Norris and the Woods Hole Oceanographic Institute for providing a place for me over a three month period at WHOI where I could work on this project with world leaders in the field. This research was funded by the Doctoral Merit Research Scheme, James Cook University, North Queensland.

REFERENCES

Aubry, M.-P., 1998. Early Paleogene calcareous nannoplankton evolution; a tale of climatic amelioration. *In* Aubry, M.-P., Lucas, S.G., and Berggren, W.A., (Eds), *Late Paleocene-early Eocene climatic and biotic events in the marine and terrestrial records*: New York, NY Columbia University Press, 158-203.

Bandy, O.L., 1959. Geologic significance of coiling ratios in the foraminifer Globigerina pachyderma (Ehrenberg) (California). *Geological Society of America Bulletin*, 70:1708.

Bandy, O.L., 1972. Origin and development of *Glororotalia (Turborotalia) pachyderma* (Ehrenberg). *Micropaleontology*, 18:294-318.

Bauch, D., Darling, K.F., *et al.*, 2003. Palaeoceanographic implications of genetic variation in living North Atlantic *Neogloboquadrina pachyderma*. *Nature*, 424:299-302.

Berggren, W.A., Aubry, M.P., *et al.*, 2000. Integrated Paleocene calcareous plankton magnetobiochronology and stable isotope stratigraphy; DSDP Site 384 (NW Atlantic Ocean). *Palaeogeography, Palaeoclimatology, Palaeoecology*, 159:1-51.

Berggren, W.A., Kent, D.V., *et al.*, 1995. A revised Cenozoic geochronology and chronostratigraphy. *In* Berggren, W.A., Kent, D.V., Aubry, M.P., *et al.*, (Eds), *Geochronology, time scales and global stratigraphic correlation*, SEPM Special Publication 54, 129-212.

Berggren, W.A., and Norris, R.D., 1997. *Biostratigraphy, phylogeny and systematics of Paleocene trochospiral planktonic Foraminifera*: New York, (American Museum of Natural History), 116 p.

Boersma, A., 1981. Cretaceous and early Tertiary foraminifers from Deep Sea Drilling Project Leg 62 sites in the central Pacific. *In* Boersma, A., Stout, L.N., Thiede, J., *et al.*, (Eds), *Init. Repts. DSDP*, 62: College Station, TX (Ocean Drilling Program), 377-396.

Boersma, A., Premoli Silva, I., *et al.*, 1987. Atlantic Eocene planktonic foraminiferal paleohydrographic indicators and stable isotope paleoceanography. *Paleoceanography*, 2:287-331.

Bolli, H.M., 1950. The direction of coiling in the evolution of some Globorotaliidae. *Contributions from the Cushman Foundation for Foraminiferal Res.*, 1:82-89.

Bolli, H.M., 1957. The genera *Globigerina* and *Globorotalia* in the Paleocene-Lower Eocene Lizard Springs Formation of Trinidad, B. W. I. *In* Loeblich, A.R., Jr., Tappan, H.N., Beckmann, J.-P., *et al.*, (Eds), *Loeblich, A R , Jr , Studies in Foraminifera*: Washington (US Government Printing Office), 61-81.

Bolli, H.M., 1971. The direction of coiling in planktonic foraminifera. *In* Funnell, B.M., and Reidel, W.R., (Eds), *The micropaleontology of oceans*: Cambridge Cambridge University Press, 639-648.

Bond, G.C., Broecker, W.S., *et al.*, 1993. Correlations between climate records for North Atlantic sediments and Greenland ice. *Nature*, 365:143-147.

Bralower, T.J., and Mutterlose, J., 1995. Calcareous nannofossil biostratigraphy of ODP Site 865, Allison Guyot, Central Pacific Ocean: a tropical Paleogene reference section. *In* Winterer, E.L., Sager, W.W., Firth, J.V., *et al.*, (Eds), *Proc. ODP, Sci. Res.*, 143 College Station TX (Ocean Drilling Program), 31-74.

Bralower, T.J., Parrow, M., *et al.*, 1995. *Data Report:* stable isotopic stratigraphy of the Paleogene cap at Site 865, Allison Guyot. *In* Batiza, R., Storms, M.A., and Allan, J.F., (Eds), *Proc. ODP, Sci. Results*, 142 College Station TX (Ocean Drilling Program), 581-586.

Brummer, G.J.A., and Kroon, D., 1988. Genetically controlled planktonic foraminiferal coiling ratios as tracers of past ocean dynamics. *In* Brummer, G.J.A., and Kroon, D., (Eds), *Planktonic Foraminifera as tracers of ocean-climate history: ontology, relationships and preservation of modern species and stable isotopes, phenotypes and assemblage distribution in different water masses*: Amsterdam Free University Press, 293-297.

CLIMAP Project Members, 1976. The surface of the ice-age Earth. *Science*, 191:1131-1137.

Corfield, R.M., and Cartlidge, J.E., 1991. Isotopic evidence for the depth stratification of fossil and Recent Globigerinina; a review. *Historical Biology*, 5:37-63.

Corfield, R.M., and Cartlidge, J.E., 1992. Oceanographic and climate implications of the Paleocene carbon isotope maximum. *Terra Nova*, 4:443-455.

Cushman, J.A., and Bermúdez, P.J., 1949. Some Cuban species of *Globorotalia*. *Contributions from the Cushman Foundation for Foraminiferal Res.*, 25:26-45.

Darling, K.F., Wade, C.M., *et al.*, 2000. Molecular evidence for genetic mixing of Arctic and Antarctic subpolar populations of planktonic foraminifers. *Nature*, 405:43-47.

de Vargas, C., Renaud, S., *et al.*, 2001. Pleistocene adaptive radiation in *Globorotalia truncatulinoides*: genetic, morphologic, and environmental evidence. *Paleobiology*, 27:104-125.

Dettman, D.L., and Lohmann, K.C., 2000. Oxygen isotope evidence for high-altitude snow in the Laramide Rocky Mountains of North America during the Late Cretaceous and Paleogene. *Geology*, 28:243-246.

D'Hondt, S., Zachos, J.C., *et al.*, 1994. Stable isotopic signals and photosymbiosis in late Paleocene planktic foraminifera. *Paleobiology*, 20:391-406.

Ericson, D.B., 1959. Coiling direction of *Globigerina pachyderma* as a climatic index. *Science*, 130:219-220.

Ericson, D.B., Wollin, G., *et al.*, 1955. Coiling direction of Globorotalia truncatulinoides in deep-sea cores. *Deep-Sea Research*, 2:152-158.

Hancock, H.J.L., Chaproniere, G.C., *et al.*, 2002. Early Palaeogene planktic foraminiferal and carbon isotope stratigraphy, Hole 762C, Exmouth Plateau, northwest Australian margin. *Journal of Micropalaeontology*, 21:29-42.

Hancock, H.J.L. and Dickens, G.R., 2005. Carbonate dissolution episodes in Paleocene and Eocene sediment, Shatsky Rise, west-dentral Pacific. *In* Bralower, T.J., Premoli Silva, I., and Malone, M.J. (Eds), *Proc. ODP, Sci. Results*, 198 [Online]. Available from World Wide Web: <http://www-odp.tamu.edu/publications/198_SR/116/116.htm>. [Cited 2005-09-02]

Haq, B.U., Hardenbol, J., *et al.*, 1987. Chronology of fluctuating sea levels since the Triassic. *Science*, 235:1156-1167.

Haq, B.U., von Rad, U., *et al.*, 1990. *Prod. ODP, Init. Repts.*, 122: College Station TX, (Ocean Drilling Program), 826 p.

Hemleben, C., Spindler, M., *et al.*, 1989. *Modern planktonic foraminifera*: New York, Springer.

Hollis, C.J., 2002. Biostratigraphy and paleoceanographic significance of Paleocene radiolarians from offshore eastern New Zealand. *Marine Micropal.*, 46:265-316.

Hollis, C.J., Dickens, G.R., *et al.*, 2005. The Paleocene-Eocene transition at Mead Stream, New Zealand: a southern Pacific record of early Cenozoic global change. *Palaeogeography, Palaeoclimatology, Palaeoecology*, 215:313-343.

Kelly, D.C., 2002. Response of Antarctic (ODP Site 690) planktonic foraminifera to the Paleocene-Eocene thermal maximum; faunal evidence for ocean/climate change. *Paleoceanography*, 17 (4), 1071, doi:10.1029/2002PA000761.

Kelly, D.C., Arnold, A.J., *et al.*, 1996. Paedomorphosis and the origin of the Paleogene planktonic foraminiferal genus *Morozovella*. *Paleobiology*, 22:266-281.

Killops, S.D., Hollis, C.J., *et al.*, 2000. Paleoceanographic significance of late Paleocene dysaerobia at the shelf/slope break around New Zealand. *Palaeogeography, Palaeoclimatology, Palaeoecology*, 156:51-70.

Kucera, M., and Kennett, J.P., 2002. Causes and consequences of a middle Pleistocene origin of the modern planktonic foraminifer Neogloboquadrina pachyderma sinistral. *Geology*, 30:539-542.

LaMontagne, R.W., Murray, R.W., *et al.*, 1996. Decoupling of carbonate preservation, carbonate concentration, and biogenic accumulation: A 400-kyr record from the central equatorial Pacific Ocean. *Paleoceanography*, 11:553-562.

Le, J., and Shackleton, N.J., 1992. Carbonate dissolution fluctuations in the western equatorial Pacific during the late Quaternary. *Paleoceanography*, 7:21-42.

Norris, R.D., and Nishi, H., 2001. Evolutionary trends in coiling of tropical Paleogene planktic foraminifera. *Paleobiology*, 27:327-347.

Olsson, R.K., Hemleben, C., *et al.*, 1999. *Atlas of Paleocene planktonic Foraminifera*: Washington, DC, Smithsonian Institution, 252 p.

Pearson, P.N., 1993. A lineage phylogeny for the Paleogene planktonic foraminifera. *Micropaleontology*, 39:193-232.

Pearson, P.N., and Shackleton, N.J., 1996. Stable isotopes and the enigma of planktonic foraminifer evolution *Sixth North American paleontological convention*, 8: Repetski, John E. The Paleontological Society at the University of Tennessee Dept. of Geological Sciences, 304.

Petrizzo, M.R., 2005. An early late Paleocene event on Shatsky Rise, northwest Pacific Ocean (ODP Leg 198): evidence from planktonic foraminiferal assemblages, *in* Bralower, T.J., Premoli Silva, I., and Malone, M.J., eds., *Proc. ODP, Sci. Results*, Volume 198, 1-29 [Online]. Available from World Wide Web: <http://www-odp.tamu.edu/publications/198_SR/VOLUME/CHAPTERS/102.PDF>.

Quillevere, F., 2000. Etude morphometrique et isotopique ($\delta^{18}O$, $\delta^{13}C$) de la diversification paleocene du genre *Acarinina* (foraminifere planctonique): implications paleoceanographiques [Doctorale thesis], University Montpellier II.

Quillevere, F., and Norris, R.D., 2003. Ecological development of acarininids (planktonic Foraminifera) and hydrographic evolution of Paleocene surface waters. *In* Wing, S.L., Gingerich, P.D., Schmitz, B., *et al.*, (Eds), *Causes and*

consequences of globally warm climates in the early Paleogene, The Geological Society of America, Spec. Paper 369, 223-238.

Quillevere, F., Norris, R.D., *et al.*, 2001. Role of photosymbiosis and biogeography in the diversification of early Paleogene acarininids (planktonic Foraminifera). *Paleobiology*, 27:311-326.

Saito, T., 1976. Geologic significance of coiling direction in the planktonic foraminifera Pulleniatina. *Geology*, 4:305-309.

Seisser, W.G., and Bralower, T.J., 1992. Cenozoic calcareous nannofossil biostratigraphy on the Exmouth Plateau, eastern Indian Ocean. *In* von Rad, U., Haq, B.U., and al., e., (Eds), *Proc. ODP, Sci. Results*, 122 College Station, TX (Ocean Drilling Program), 601-631.

Shackleton, N.J., Corfield, R.M., *et al.*, 1985. Stable isotope data and the ontogeny of Paleocene planktonic foraminifera, Cushman Foundation for Foraminiferal Research, Ithaca, NY, p. 321-336.

Shipboard Scientific Party, 1981. Site 465: Southern Hess Rise. *In* Thiede, J., and Vallier, T.L., (Eds), *Init. Repts. DSDP*, 62: Washington (U.S. Govt. Printing Office), 107-154.

Shipboard Scientific Party, 1990. Site 762. *In* Haq, B.U., von Rad, U., O'Connell, S., *et al.*, (Eds), *Proc. ODP, Init. Repts*, 122: (College Station, TX) Ocean Drilling Program, 213-289.

Shipboard Scientific Party, 1993. Site 865. *In* Sager, W.W., Winterer, E.L., Firth, J.V., *et al.*, (Eds), *Proc. ODP Init. Repts.*, 143 College Station TX (Ocean Drilling Program), 111-180.

Shipboard Scientific Party, 2002. Leg 198 Summary. *In* Bralower, T.J., Premoli Silva, I., and Malone, M.J., (Eds), *Proc. ODP, Init. Repts.*, 198 College Station TX (Ocean Drilling Program), 1-148.

Spero, H.J., and Lea, D.W., 1993. Intraspecific stable isotope variability in the planktic foraminifera Globigerinoides sacculifer; results from laboratory experiments. *Marine Micropaleontology*, 22:221-234.

Stott, L.D., and Kennett, J.P., 1990. Antarctic Paleogene planktonic foraminifer biostratigraphy; ODP Leg 113, Sites 689 and 690. *In* Barker, P.F., Kennett, J.P., and et al., (Eds), *Proc. ODP, Sci. Results*, 113: College Station, TX Ocean Drilling Program, 549-565.

Thiede, J., 1971. Variations in coiling ratios of Holocene planktonic foraminifera. *Deep-Sea Research*, 18:823-831.

Thiede, J., Vallier, T.L., *et al.*, 1981. *Init. Repts. DSDP*, 62: Washington, (U.S. Govt. Printing Office).

Thomas, E., 2003. Extinction and food at the seafloor: a high resolution benthic foraminiferal record across the Initial Eocene Thermal Maximum, Southern Ocean Site 690. *In* Wing, S.L., Gingerich, P.D., Schmitz, B., *et al.*, (Eds), *Causes and consequences of the globally warm climates in the early Paleogene,* The Geological Society of America, Spec. Paper 369, 319-332.

Thomas, E., Shackleton, N.J., *et al.*, 1992. Data report; Carbon isotope stratigraphy of Paleogene bulk sediments, Hole 762C (Exmouth Plateau, eastern Indian Ocean). *Proc. ODP, Sci. Res.*, 122:897-901.

Thompson, E.I., and Schmitz, B., 1997. Barium and the late Paleocene $\delta^{13}C$ maximum: evidence of increased marine surface producitivity. *Paleoceanography*, 12:239-254.

Ufkes, E., and Zachariasse, W.J., 1993. Origin of coiling differences in living neogloboquadrinids in the Walvis Bay region, off Namibia, Southwest Africa. *Micropaleontology*, 39:283-287.

Wilf, P., 2000. Late Paleocene-early Eocene climate changes in southwestern Wyoming; paleobotanical analysis. *Geological Society of America Bulletin*, 112:292-307.

Xu, X., Kimoto, K., *et al.*, 1995. Predominance of left-coiling *Globorotalia truncatulinoides* (d'Orbigny) between 115,000 and 50,000 yrs BP; a latest foraminiferal biostratigraphic event in the western North Pacific. *Daiyonki-Kenkyu = Quaternary Research*, 34:39-47.

Zachos, J., Pagani, M., *et al.*, 2001. Trends, rhythms, and aberrations in global climate 65 Ma to present. *Science*, 292:686-693.

Zachos, J.C., Kroon, D., *et al.*, 2004. *Proc. ODP, Init. Repts.*, Volume 208 [Online], Available from World Wide Web: http://www-odp.tamu.edu/publications/208_IR/208ir.htm.

APPENDIX 1. Taxonomic Notes on *Igorina albeari*

The *Igorina* lineage can be traced back to *Praemurica uncinata* and proceeded with the development of thick pustules on the test wall, elongate oval-shaped changes and an elevated trochospire (Olsson *et al.*, 1999). *Igorina albeari* developed along with *I. tadjikistanensis* from *I. pusilla* in the Late Paleocene (Olsson *et al.*, 1999). *Igorina* evolved around the same time as the appearance of the first *Morozovella*.

***Igorina albeari* Systematics**

Family **Truncorotaloididae** Loeblich and Tappan 1961

Genus ***Igorina*** Davidzon, 1976

Igorina albeari Cushman & Bermúdez (1949)

(**Plates 1-3**)

Globorotalia albeari Cushman and Bermúdez, 1949:33, pl. 6: figs. 13-15 [holotype].

Globorotalia (Globorotalia) albeari Cushman and Bermúdez.—Blow, 1979:883, pl. 92: figs. 4, 8, 9, pl. 93: figs. 1-4.

Igorina albeari (Cushman and Bermúdez).—Olsson, Hemleben, Berggren and Huber, 1999:69, pl. 56: figs. 1-16.

DIAGNOSIS.—In Holes 865B, 465-1209A and 762C the test is small, oval to circular and biconvex with strongly recurved chambers well visible on the dorsal side. There are 5 to 9 chambers in the final whorl that increase gradually in size. Aperture is an umbilical-extraumbilical slitted arch not quite reaching the peripheral margin. Test surface is cancellate and pustulose with the peripheral margin distinctly carinate on the final chambers giving the impression of a flattened keel.

REMARKS.—*Igorina albeari* is a distinct species at the central Pacific sites with its heavily pustulose test, strongly recurved spiral sutures and flattened and carinate final chambers. It is rare in Hole 762C.

This species is distinct from *Igorina "trichotrocha"* (Loeblich & Tappan) 1957, which is circular, plano-convex and has a deep umbilicus (See Berggren & Norris, 1997, p. 62; Plate 1, Figs. 3-6). It is also distinct from *Igorina tadjikistanensis* (Byokova) 1953, which has a more evolute coiling and does not have a flattened final chamber with a distinct keel (**Plate 2, Figs. F, G**).

STRATIGRAPHIC RANGE.— In Holes 465 and 1209A *I. albeari* ranges from the P3a/P3b boundary to the top of P4b. In Holes 865B and 762C the range of *I. albeari* extends from the P3a/P3b boundary to the base of P5.

Plate 1. Scanning Electron Microscope (SEM) photographs of *Igorina albeari* (Cushman & Bermúdez, 1949) at Holes 465 and 1209A. (S) = sinistral. (D) = dextral. **A,** *I. albeari*, (S); ventral view (465-5H-2, 20-22 cm). **B,** *I. albeari*, (D); ventral view (465-5H-2, 20-22 cm). **C,** *I. albeari*, (D); ventral view (465-5H-2, 60-62 cm). **D,** *I. albeari*, (D); spiral view (465-5H-2, 60-62 cm). **E,** *I. albeari*, (D); spiral view (5H2, 120-122 cm). **F,** *I. albeari*, (S); ventral view (5H2, 60-62 cm). **G,** *I. albeari*, (S); ventral view (1209A-23H-6, 67-69 cm). **H,** *I. albeari*, (S); side view (1209A-23H-6, 67-69 cm). **I,** *I. albeari*, (S); ventral view (1209A-23H-6, 67-69 cm). **J,** *I. albeari*, (S); side view (1209A-23H-6, 67-69 cm). **K,** *I. albeari*, (D); ventral view (1209A-23H-6, 67-69 cm). **L,** *I. albeari*, (D); side view (1209A-23H-6, 67-69 cm). **M,** *I. albeari*, (D); ventral view (1209A-23H-6, 67-69 cm). N**,** *I. albeari*, (D); side view (1209A-23H-6, 67-69 cm).

Plate 2. Scanning Electron Microscope (SEM) photographs of *Igorina albeari* Cushman & Bermúdez (1949) and *Igorina tadjikastanensis* (Byokova) 1953 at Holes 1209A and 762C. **A,** *I. albeari*, (S); ventral view (1209A-23H-2, 140-142 cm). **B,** *I. albeari*, (S); side view (1209A-23H-2, 140-142 cm). **C,** *I. albeari*, (S); spiral view (1209A-23H-2, 140-142 cm). **D,** *I. albeari*, (D); ventral view (1209A-23H-6, 20-22 cm). **E,** *I. albeari*, (D); side view (1209A-23H-6, 20-22 cm). **F,** *I. tadjikastanensis*; ventral view (1209A-23H-3, 21-23 cm). **G,** *I. tadjikastanensis*; side view (1209A-23H-3, 21-23 cm). **H,** *I. albeari*, (D); ventral view (762C-30X-2, 40-44 cm). **I,** *I. albeari*, (D); side view (762C-30X-2, 40-44 cm). **J,** *I. albeari*, (D); ventral view (762C-31X-5, 101-105 cm). **K,** *I. albeari*, (D); spiral view (762C-31X-5, 101-105 cm). **L,** *I. albeari*, (S); ventral view (762C-31X-5, 101-105 cm). **M,** *I. albeari*, (D); ventral view (762C-31X-5, 101-105 cm). **N,** *I. albeari*, (D); ventral view (762C-33X-4, 95-99 cm). **O,** *I. albeari*, (D); spiral view (762C-33X-4, 95-99 cm).

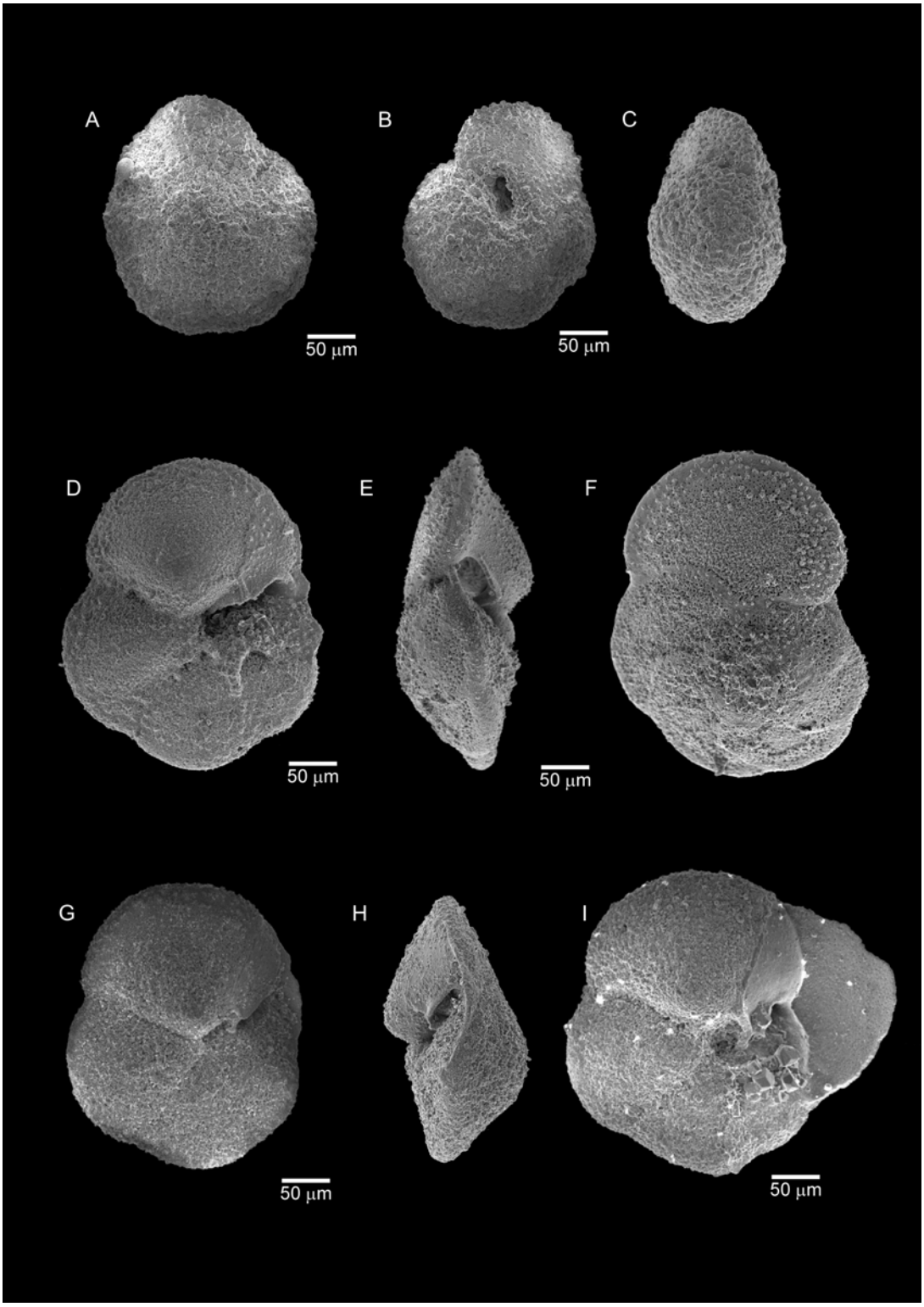

Plate 3. Scanning Electron Microscope (SEM) photographs of *Igorina albeari* and *Globanomalina pseudomenardii* Bolli (1957) at Holes 762C and 1209A. **A,** *I. albeari*, (S); ventral view (762C-31X-3, 97-101 cm). **B,** *I. albeari*, (D); ventral view (762C-31X-3, 97-101 cm). **C,** *I. albeari*, (D); side view (762C-31X-3, 97-101). **D,** *Gl. pseudomenardii*; ventral view (1209A-23H-2, 80-82 cm). **E,** *Gl. pseudomenardii*; side view (1209A-23H-3, 147.5-149.5 cm). **F,** *Gl. pseudomenardii*; spiral view (1209A-23H-3, 147.5-149.5 cm). **G,** *Gl. pseudomenardii*; spiral view (762C-30X-3, 96-100 cm). **H,** *Gl. pseudomenardii*; side view (762C-30X-3, 96-100 cm). **I,** *Gl. pseudomenardii*; ventral view (762C-31X-3, 97-101 cm).

CHAPTER 4

CARBONATE CONCENTRATIONS OF PALAEOGENE SEDIMENT IN HOLE 1121B, CAMPBELL "DRIFT".

INTRODUCTION

Site 1121 is located southeast of New Zealand on the Campbell "Drift" (50°53.876'S; 176°59.862'E) at a water depth of 4487.90 m below sea level (mbsl) (**Fig. 1**). The site was drilled to recover an expanded sediment sequence from a Neogene contourite drift (Shipboard Scientific Party, 1999). Unexpectedly, the sequence between 32 and 132 m below seafloor (mbsf) is composed of Palaeogene siliceous and nannofossil bearing ooze and chalk (Shipboard Scientific Party, 1999). This finding is intriguing because the location was probably fairly deep (>3 800 mbsl) during the Palaeogene (Shipboard Scientific Party, 1999), suggesting a carbonate compensation depth (CCD) lower than that expected from Cenozoic CCD curves (van Andel *et al.*, 1975). Thirty-nine samples of sediment were taken from Hole 1121B to construct a more detailed carbonate record through this lithologic unit.

METHODS

Carbonate concentrations for all samples were analyzed using the "Karbonate-Bombe" method (Mueller and Gastner, 1971). All 39 samples were freeze-dried to remove pore water and crushed to a fine powder. Approximately 200 mg of powdered sample was then placed in a sealed chamber and reacted with HCl to produce CO_2 gas. The resulting gas volume was measured using water displacement in a burette and related to carbonate mass by comparison to a standard curve constructed by measuring volumes of gas produced from known masses of laboratory grade $CaCO_3$. All samples were analyzed twice. A sample of Palaeogene siliceous limestone (JCU sample MS14)

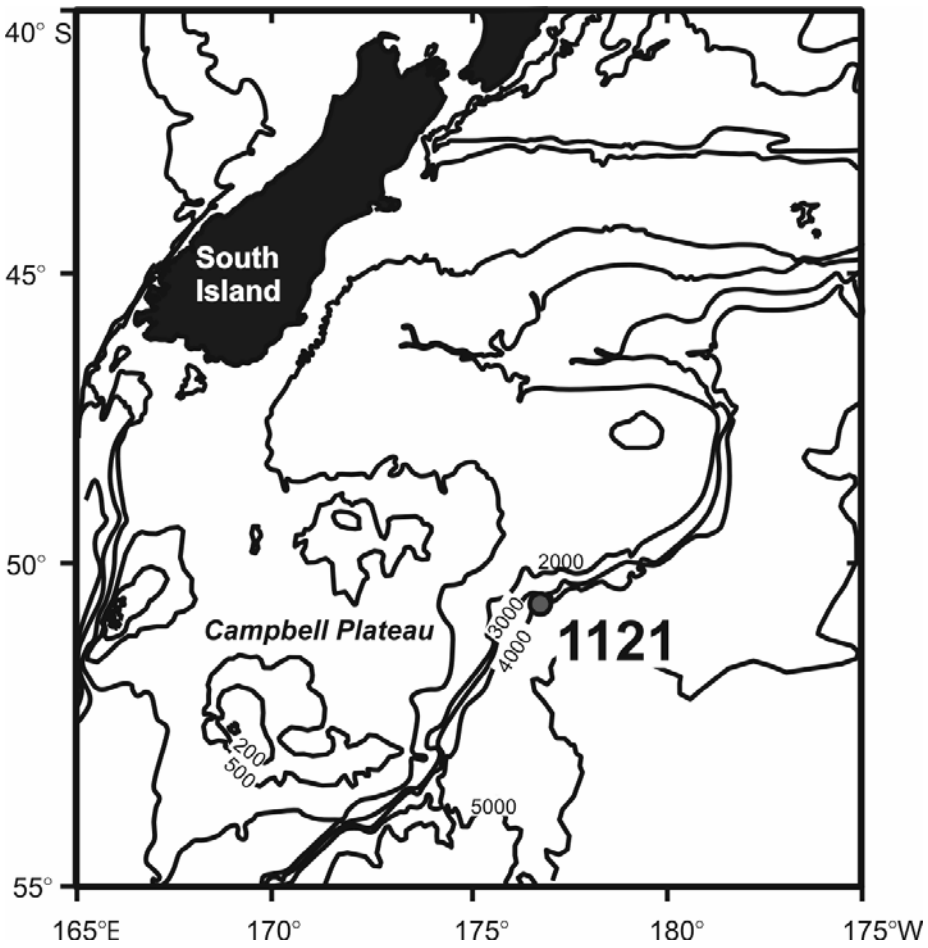

Figure 1. Location map for Site 1121 offshore east coast New Zealand.

with a known $CaCO_3$ concentration of 72 wt% was also analyzed three times to evaluate accuracy and precision. Replicate analyses of the Site 1121 samples were consistently within 1.1 wt%. The measured $CaCO_3$ concentration of MS14 was 71.9 wt% ± 1.5 wt%.

RESULTS

Bulk carbonate concentrations vary significantly between 3.7 wt% and 51.4 wt% and average 31 wt% (**Table 1; Fig. 2**). These results are consistent with shipboard carbonate concentrations which, over a similar depth, vary between 0.6 wt% and 52 wt% and average 30 wt% (**Fig. 2**). Although carbonate concentrations are moderately high (~30-50 wt%) between 32.9 mbsf and 131.7 mbsf, a marked low occurs at 74.4 mbsf (6.4 wt%). Carbonate concentrations are <5 wt% below 132 mbsf.

Table 1. Hole 1121B Carbonate (wt%). * Average of two replicate samples

Sample Hole, Section, Interval (cm)	Depth (mbsf)	Carbonate (wt%)*
1121B-6X-1, 20-22	32.90	43.63
1121B-6X-2, 21-23	34.41	50.65
1121B-6X-3, 20-22	35.90	37.76
1121B-7X-1, 20-22	42.50	27.96
1121B-7X-2, 20-22	44.00	29.49
1121B-7X-3, 20-22	45.50	40.16
1121B-7X-4, 20-22	47.00	41.87
1121B-7X-5, 20-22	48.50	40.65
1121B-8X-1, 20-22	52.20	48.47
1121B-8X-2, 20-22	53.70	40.46
1121B-8X-3, 20-22	55.20	21.23
1121B-8X-4, 20-22	56.70	20.23
1121B-8X-5, 20-22	58.20	27.52
1121B-8X-6, 20-22	59.55	31.17
1121B-8X-6, 39-41	59.74	24.40
1121B-9X-1, 20-22	61.80	38.46
1121B-9X-2, 20-22	63.30	32.98
1121B-9X-3, 20-22	64.80	39.24
1121B-9X-4, 20-22	66.30	32.00
1121B-9X-5, 20-22	67.80	37.81
1121B-9X-6, 20-22	69.30	27.59
1121B-10X-1, 20-22	71.40	31.21
1121B-10X-2, 20-22	72.90	19.87
1121B-10X-3, 20-22	74.40	6.41
1121B-10X-4, 20-22	75.69	27.87
1121B-11X-1, 20-22	81.10	32.58
1121B-11X-2, 20-22	82.60	37.35
1121B-11X-3,18-20	84.08	34.63
1121B-11X-4, 20-22	85.60	35.01
1121B-12X-1, 20-22	90.70	33.14
1121B-12X-2, 20-22	92.20	38.63
1121B-12X-3, 20-22	93.70	51.43
1121B-15X-1, 20-22	119.60	32.26
1121B-15X-2, 18-20	121.08	20.15
1121B-16X-1, 20-22	126.20	30.79
1121B-17X-1, 20-22	130.20	18.28
1121B-17X-2, 20-22	131.70	29.67
1121B-17X-3, 20-22	133.20	3.65
1121B-17CC, 10-12	134.27	4.95

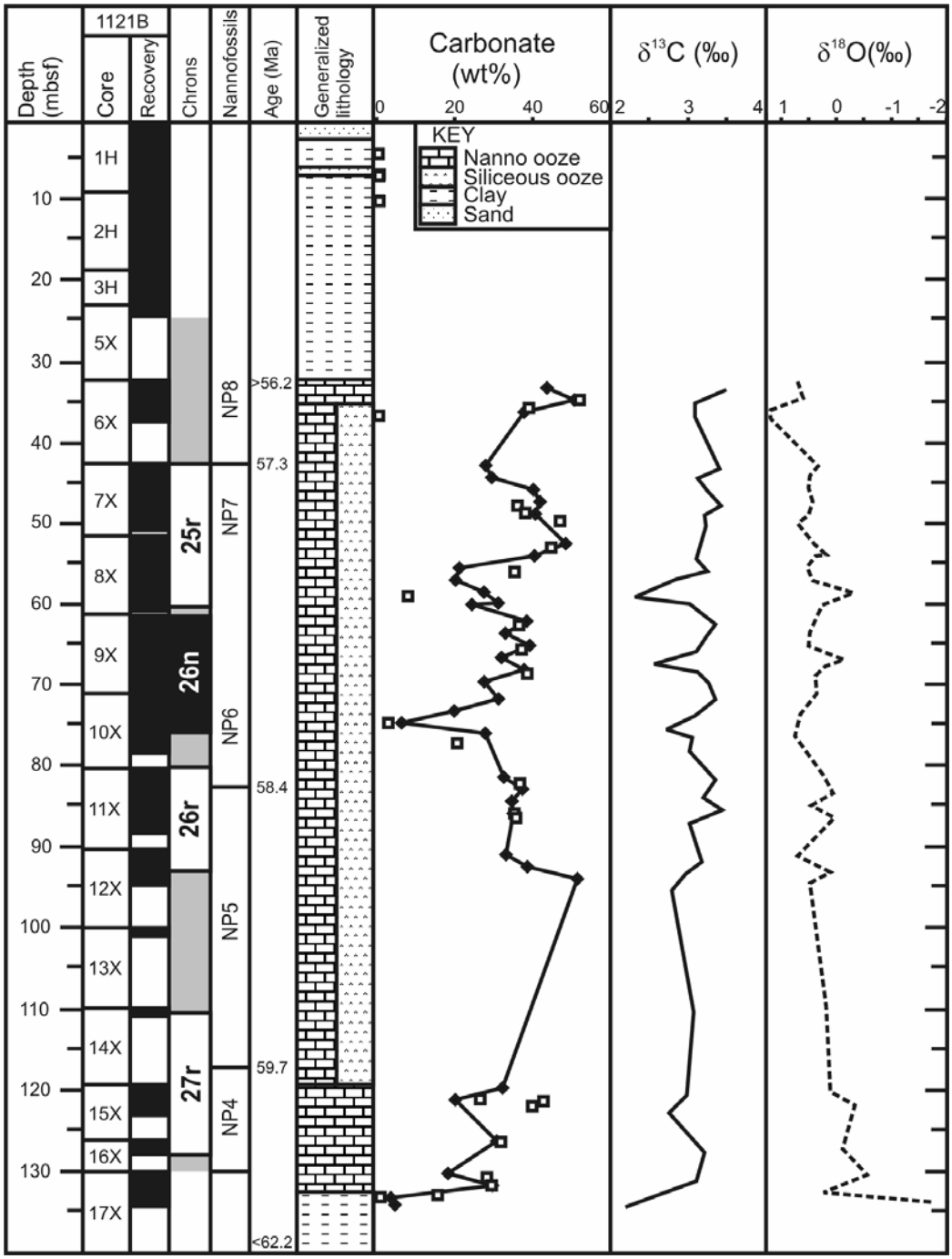

Figure 2. Summary log for Hole 1121B including geochronology (Carter *et al.*, 2004, fig. 19), lithology, carbonate content (wt%) from this study (filled diamonds) and Shipboard Scientific Party (1999) (open squares), and carbon and oxygen isotopes (adapted from Carter *et al.*, 2004, fig. 19).

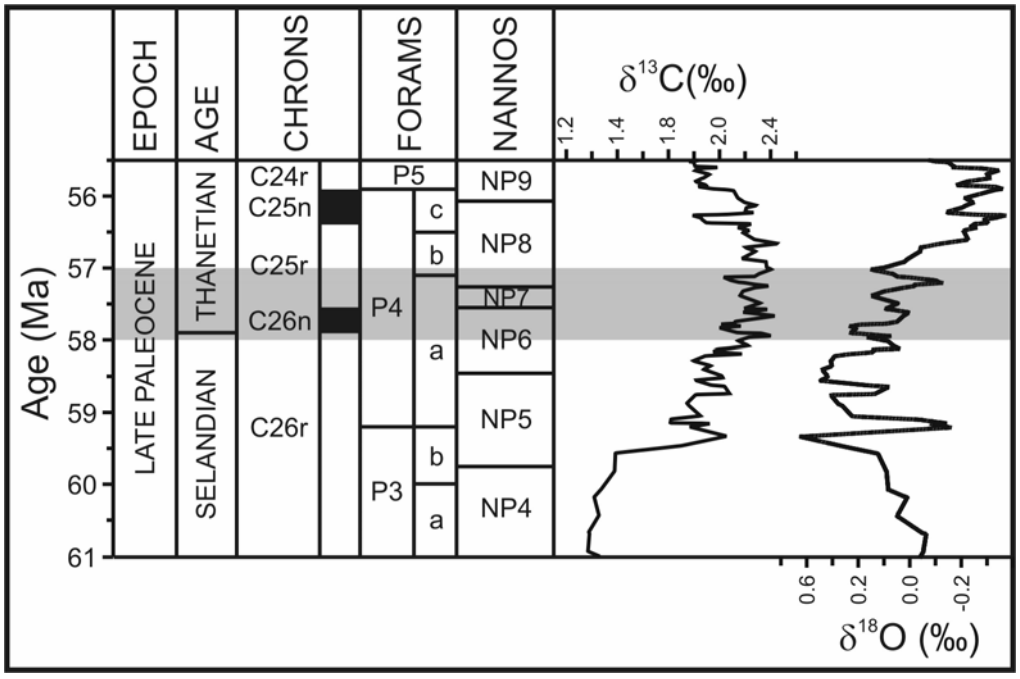

Figure 3. Late Paleocene timescale (following Berggren *et al*., 1995) with global carbon and oxygen isotope curves constructed from benthic foraminiferal isotope data (adapted from Zachos *et al*., 2001, p. 688). Shaded area is temporal correlation of Waipawa Formation, an organic-rich deposit found in numerous New Zealand basins.

CONCLUSIONS

Site 1121 was located at abyssal depths during the Late Paleocene (>3 800 mbsl) (Shipboard Scientific Party, 1999). Unusally high carbonate concentrations for this depth suggest a drop in the CCD not shown in global CCD reconstructions (van Andel *et al.*, 1975). The increase in both carbonate and silica deposition indicate high surface water productivity. A mid Paleocene cooling episode leading to vigorous oceanic circulation might explain the abundance of cool-water siliceous biota.

The biostratigraphy and carbon isotope stratigraphy (Carter *et al.*, 2004) (**Fig. 2**) show that carbonate and silica deposition at Hole 1121B is temporally correlative with the Waipawa Formation, a diachronous (~58-57 Ma) organic rich formation in numerous New Zealand basins in the lower part of the PCIM and (**Fig. 3**) (Hollis, 2002). It has been interpreted as a transgressive succession that resulted from the intersection of an expanded oxygen minimum zone with the shelf-slope break depositing organic rich material (Hollis, 2002; Hollis *et al.*, 2005).

REFERENCES

van Andel, T.H., 1975. Mesozoic/Cenozoic calcite compensation depth and the global distribution of calcareous sediments. *Earth and Planetary Science Letters*, 26:187-194.

Carter, R.M., McCave, I.N., *et al.*, 2004. Leg 181 synthesis: fronts, flows, drifts, volcanoes, and the evolution of the southwestern gateway to the Pacific Ocean, Eastern New Zealand. *In* Richter, C., (Ed.) *Proc. ODP, Sci. Results*, 181 College Station TX (Ocean Drilling Program), 1-112.

Hollis, C.J., 2002. Biostratigraphy and paleoceanographic significance of Paleocene radiolarians from offshore eastern New Zealand. *Marine Micropaleontology*, 46:265-316.

Hollis, C.J., Dickens, G.R., *et al.*, 2005. The Paleocene-Eocene transition at Mead Stream, New Zealand: opening the window on early Cenozoic global environmental change in the high-latitude Pacific. *Palaeogeography, Palaeoclimatology, Palaeoecology*, 215:313-343.

Mueller, G., and Gastner, M., 1971. The "Karbonate-Bombe", a simple device for the determination of the carbonate content in sediments, soils, and other materials. *Neues Jahrbuch fuer Mineralogie Monatshefte*, 10:466-469.

Shipboard Scientific Party, 1999. Site 1121: The Campbell "Drift". *In* Carter, R.M., McCave, I.N., Richter, C., *et al.*, (Eds), *Proc. ODP, Init. Repts.*, 181: College Station, TX 77845-9547, U.S.A. Ocean Drilling Program, Texas A&M University, 1-112 [CD-ROM].

CHAPTER 5

FORAMINIFERAL AND CARBON ISOTOPE STRATIGRAPHY THROUGH THE PALEOCENE-EOCENE TRANSITION AT DEE STREAM, MARLBOROUGH, NEW ZEALAND.

Abstract. Dee Stream in the Clarence River valley of New Zealand bisects a well-exposed section of marine sedimentary rocks deposited in the early Palaeogene at high southern latitudes. One hundred metres of strata lying within this section and comprising cm-dm well-bedded, siliceous limestone with marly partings was mapped, logged, and sampled to establish a detailed foraminiferal and carbon isotope stratigraphy and to examine environmental changes across the Basal Eocene Thermal Maximum (BETM). Although low abundance and poor preservation of planktic and benthic foraminifers characterizes much of the Paleocene, foraminifera and carbon isotopes clearly show that the section spans the Upper Paleocene to Lower Eocene, planktic foraminiferal zones from Zone P4 to Subzone P6b, and the *Subbotina triloculinoides* to *Pseudohastigerina wilcoxensis* Zones. The $\delta^{13}C$ record correlates closely to $\delta^{13}C$ curves generated from other key early Palaeogene carbonate sequences. The Dee Stream logged section contains a 1 m thick BETM interval at 26.5 m in upper Zone P5, or the *Morozovella velascoensis* Subzone. Here, benthic foraminifera undergo significant extinction, *Morozovella aequa* makes its first appearance, and the $\delta^{13}C$ of carbonate decreases by 2‰. The benthic foraminifer *Bulimina tuxpamensis* dominates benthic assemblages immediately following the onset of the BETM interval, suggesting dysoxic bottom waters during this event. In conjunction with other recently examined sections from the Marlborough region, the thick and apparently continuous Palaeogene record at Dee Stream provides an important site for understanding environmental change on high-latitude continental margins during the Palaeogene, including the BETM.

INTRODUCTION

Over a 200 000 yr interval at ~55 Ma, high-latitude sea-surface and deep-ocean temperatures soared by 4 to 7°C (Bralower *et al*., 1995; Katz *et al*., 1999; Kennett and Stott, 1991; Thomas and Shackleton, 1996). This abrupt warming event, now known as the initial Eocene thermal maximum (BETM), coincided with, among other phenomena, a major benthic foraminifera extinction event (BFEE), a rapid diversification of planktic foraminifera, and an extraordinary -2 to -3‰ excursion in the isotopic composition of the global carbon budget (e.g., above references and (Bains *et al*., 1999; Kaiho *et al*., 1996; Kelly *et al*., 1996; Koch *et al*., 1992; Norris and Röhl, 1999). The carbon isotope excursion (CIE) reflects a massive input of ^{13}C-depleted carbon to the ocean and atmosphere, probably through release of microbially generated methane from buried gas hydrates on continental slopes (Bains *et al*., 1999; Dickens, 2000; Dickens *et al*., 1997; Dickens *et al*., 1995; Kaiho *et al*., 1996; Katz *et al*., 1999; Norris and Röhl, 1999). Understanding geological, chemical, and biotic changes before, during, and after the BETM is important because the interval may serve as a past analogue for how Earth systems respond to extreme warmth and massive carbon input (Dickens, 1999; Norris and Röhl, 1999).

Elevated surface temperatures and atmospheric CO_2 during the BETM may have significantly impacted continental margins as continental weathering, sediment and nutrient delivery to the coast all increased (Bains *et al*., 2000; Beerling, 2000; Kaiho *et al*., 1996; Zachos and Dickens, 2000). These manifestations of abrupt environmental change are thought to have been maximised at high latitudes (Bralower *et al*., 1995; Peters and Sloan, 2000). However, while there is some evidence for increased riverine discharge and enhanced productivity during the BETM in high-latitude marine sections (Bains *et al*., 2000; Crouch *et al*., 2001; Kaiho *et al*., 1996; Robert and Kennett, 1992), there is a general paucity of sections with a well-defined BETM.

New Zealand margins accumulated thick, marine, sedimentary sequences between 50 and 60°S latitude during the early Palaeogene, and in several places these have been uplifted and exposed ((Field and Browne, 1989; Killops *et al*., 2000; King *et al*., 1999). Until recently, the only record of the BETM in the South Pacific region was at Tawanui, southeastern North Island (Crouch, 2001; Crouch *et al*., 2000; Kaiho *et al*.,

1996). However, low carbonate concentrations and an unusually shaped CIE complicate interpretation of the BETM record at this site. Moreover, the section appears to be a fortuitous, isolated record of the BETM in eastern North Island. In other, possibly shallower sections in the region, the early Palaeogene is truncated by an unconformity (Field & Uruski *et al*., 1997).

The Clarence River valley in the northeast South Island (**Fig. 1**) presents a special opportunity for studying high-latitude continental margins during and adjacent to the BETM. Here, the Muzzle Group, a thick sequence of biogenic marine sedimentary rocks deposited during the Late Cretaceous (late Haumurian = Maastrichtian) to late Middle Eocene (Bortonian = Bartonian), has been uplifted and tilted to form a 35 km long, steeply dipping strike ridge (Reay, 1993). A series of streams cut this ridge roughly perpendicular to strike (**Fig. 1**), exposing a range of depositional environments from outer shelf in the southwest to slope in the northeast (**Fig. 2**).

Figure 1. Location map for Dee Stream and other streams that dissect the Muzzle Group in eastern Marlborough (adapted from Strong *et al*. 1995); geology from Lensen (1962).

Figure 2. Facies relationships in the Mead Hill Formation, Amuri Limestone and upper Seymour Group (adapted from Reay, 1993).

Prior to widespread recognition of the BETM and its significance, a reconnaissance-scale biostratigraphic study of foraminifera, radiolarians, and dinoflagellates within Muzzle Group strata was undertaken at Mead Stream (**Fig. 1**) (Strong *et al*., 1995). An initial effort to pinpoint the BETM at Mead Stream focused too low in the section (Hollis *et al*., 2000a), but more recent microfossil and carbon isotope studies indicate a greatly expanded (~5 m) BETM interval at this location (Hollis *et al*., 2000b)). This presents a unique opportunity to locate and study the BETM across a range of depositional environments in the Clarence valley. Dee Stream cuts through the middle portion of the Muzzle Group ~6 km southwest of Mead Stream (**Fig. 1**), presumably exposing rocks deposited at a somewhat shallower water depth (**Fig. 2**). Here, we describe the Dee Stream lithostratigraphy, foraminiferal assemblages, and carbon isotopes of bulk carbonate to establish a detailed early Palaeogene stratigraphy at this location. Finally, we locate and discuss the BETM within this framework.

GENERAL LITHOSTRATIGRAPHY AND LOCATION

The Muzzle Group (Reay, 1993) consists of well-bedded, pelagic limestone and marl deposited during the Late Cretaceous (late Haumurian) to late Middle Eocene (Bartonian). The group is composed of two formations, Mead Hill Formation and Amuri Limestone, previously described in detail at Mead Stream (Strong *et al*., 1995).

The Mead Hill Formation is mostly dm-bedded, greenish-grey siliceous limestone rhythmically interbedded with mm-bedded, medium grey marl. Limestone beds display a characteristic knobbly bedding texture toward the top. Based on planktonic foraminiferal assemblages, the base of the Mead Hill Formation is Haumurian (Maastrichtian) at Mead Stream, and the top of the formation is Teurian (Paleocene). The Amuri Limestone is mostly cm-dm bedded, light greenish-grey siliceous limestone interbedded with mm-cm bedded, greenish-grey marl. However, the relative proportion of limestone and marl varies significantly, forming the basis of subdivision into four informal units: lower limestone, lower marl, upper limestone and upper marl (**Fig. 2**). The upper contact of the Mead Hill Formation is, at least in part, unconformable with the base of the Amuri Limestone becoming younger to the south. Upper Paleocene or Lower Eocene Amuri Limestone unconformably overlies the Cretaceous Mead Hill Formation in the southern Clarence valley, with the basal unit consisting of greensand (Teredo Limestone Member). North of Dee Stream, at Mead Stream, the Amuri Limestone conformably overlies the Mead Hill Formation, with the basal unit consisting of dark grey siliceous mudstone. This mudstone unit (= "Black Siltstone" of Strong *et al*. 1995) has been shown to be the lateral equivalent of the Waipawa Formation in the eastern North Island (Hollis *et al*., 2001; Hollis *et al*., 2000a; Hollis *et al*., 2000b; Killops *et al*., 2000; Strong *et al*., 1995). Calcareous nannofossils at Mead Stream and Tawanui (Hawke's Bay, North Island) indicate that the formation is mid-Late Paleocene age (mid-late Teurian) (Hollis *et al*., 2000a, b).

At least 120 m of the upper Mead Hill Formation and lower Amuri Limestone crop out along Dee Stream on two walls of a prominent gorge ~1.6 km upstream of Dee Hut (**Fig. 3**). Although neither the west nor east face contains an entire section, the stratigraphy on both overlaps, and exposure on each exceeds 90%. Well-bedded rocks on both faces strike northeast (40-50°) and dip northwest (45-55°). The base of a prominent and distinctive 30 cm thick, greenish-grey siliceous limestone bed on the west face provides the 0.0 m datum for the section, which was logged through the Paleocene-Eocene transition with tape and compass. Our log spans the section from –9.0 to +94.0 m (**Fig. 4**).

Figure 3. Tape and compass survey of Dee Stream section showing survey points, sample locations and key geographic, lithologic and structural features. Inset shows location of Dee Stream section on 1:50 000 topographic map (P30 Clarence, NZMS 260, sourced from Land Information New Zealand, Crown copyright reserved).

SAMPLES AND METHODS

Seventy-nine representative samples were collected from the closely logged Dee Stream section routinely at ~3 m intervals, but in detail as required. These included 36 samples from hard, limestone layers and 45 samples from softer, marly layers. Additional limestone samples were collected across obvious changes in lithology. Marly interbeds were sampled where sufficiently thick (>5 mm). Marl horizons between 28.7 and 52.2 m were too thin to sample.

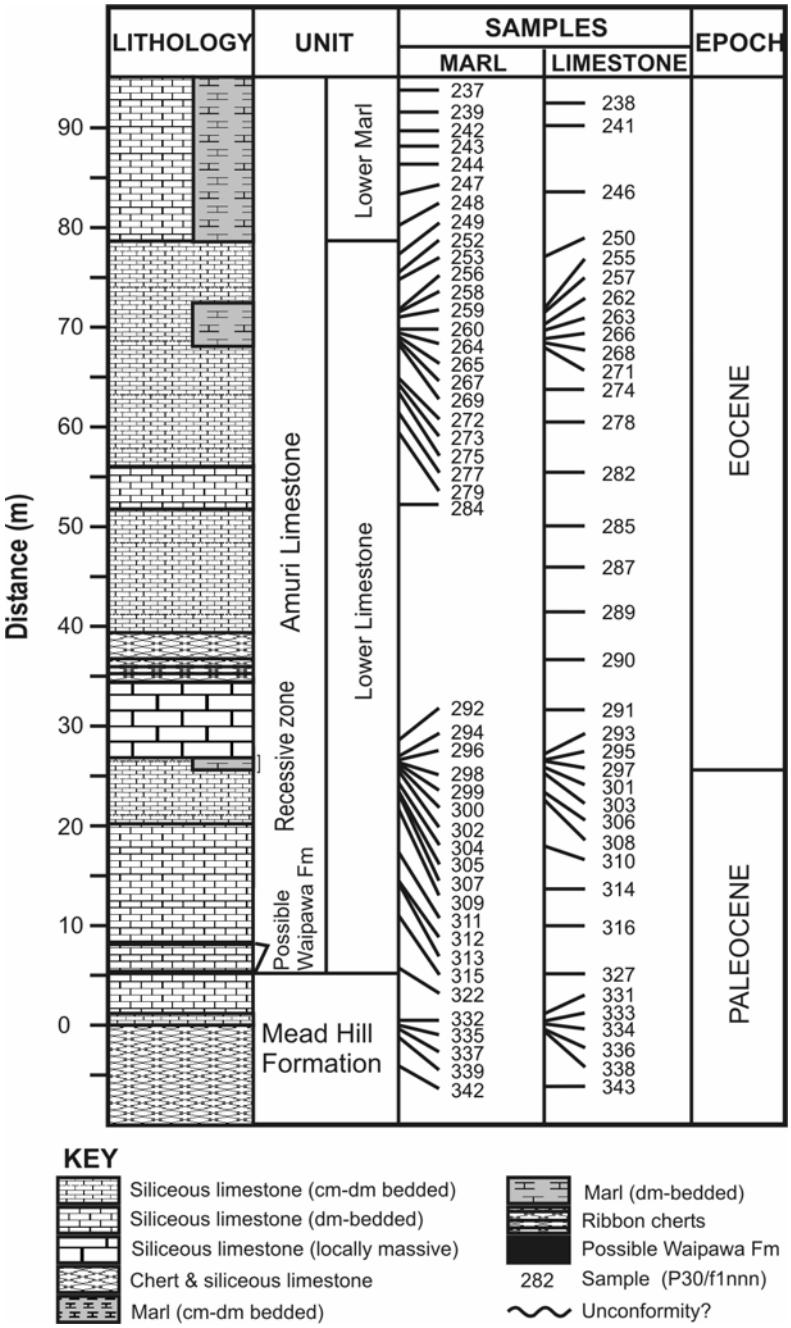

Figure 4. Lithostratigraphy of the Dee Stream section and sample locations.

A portion of each marl sample was lightly crushed, treated with hydrogen peroxide, and sieved at 63 µm. Planktic and benthic foraminiferal tests were picked from the >63 µm fraction. The abundance of both planktic and benthic foraminifera in each sample was estimated as a percentage of the total bulk sediment (>63 µm) and classified accordingly as ‘rare’ (<1%), ‘few’ (2-5%), ‘common’ (5-10%), or ‘abundant’ (>10%).

Foraminiferal species were identified using both a stereomicroscope and a scanning electron microscope (SEM). Approximately 100 specimens (less if preservation was poor) from each sample were picked to represent the total foraminiferal assemblage. Overall test preservation in each sample was classified as 'good', 'moderate', or 'poor' on the following criteria. Tests with good preservation, although often infilled with secondary calcite, can be identified to the species level. Tests with moderate preservation are typically encrusted with significant secondary calcite, making species identification only tentative. Tests with poor preservation are difficult to classify to the species and sometimes to genus levels. Most of the poorly preserved tests occur below 26.2 m.

Bulk rock samples were analyzed for stable isotopes in the Earth Science Department at the University of California, Santa Cruz, according to methods outlined by Billups *et al*. (1998; 2002). Approximately 20 g of each sample was crushed to a fine powder and reacted with H_3PO_4 at 90°C to produce CO_2, which was analyzed with a Prism gas source mass spectrometer. Carbon isotope values were calibrated to the Peedee belemnite (PDB) standard and converted to conventional delta notation ($\delta^{13}C$). Analytical precision is within ± 0.08‰.

LITHOLOGIC TYPES

At Dee Stream, from –9.0 to 0.0 m, the dominant lithology is strongly indurated, dm-bedded, greenish-grey siliceous limestone, with abundant chert nodules and a knobly bedding texture (**Fig. 5A**). This lithology is similar to the upper Mead Hill Formation at Mead Stream. Above the green-grey siliceous limestone bed (**Fig. 5A**) are ~25 m of strongly indurated, cm-dm thick, light greenish-grey siliceous limestone and interbedded mm-thick, light grey marl (**Fig. 5A**). This lithology is similar to that of the lower limestone at Mead Stream. Based on these general lithologic features, the Mead Hill Formation/Amuri Limestone contact is provisionally placed at zero datum, i.e. at the base of the green-grey siliceous limestone bed. Neither the Teredo Limestone nor the Waipawa Formation, the two units that define the base of the Amuri Limestone in other sections (Reay 1993, Strong *et al*., 1995, Killops *et al*., 2001), have been identified at Dee Stream, despite careful searching. Two thin, dark-grey mudstone beds occur at 5.8 and 8.0 m (**Fig. 5B**), respectively, but further biostratigraphic and

Figure 5A. Very strongly indurated, dm-bedded, greenish-grey siliceous limestone with abundant chert nodules giving rise to a knobbly, bedding texture (left of arrow). Mead Hill Formation (~3 to 0 m). The base of a green-grey siliceous limestone bed defines zero datum (arrow points to base) and marks possible base of Amuri Limestone Formation (lower limestone). Strongly indurated, cm-dm thick, light greenish-grey siliceous limestone interbedded with mm-thick, light grey marl (right of arrow). Lower limestone (0 to ~4 m). Southwest bank of stream.

Figure 5B. The first of two, thin, dark-grey mudstone beds separated by 2.2 m (arrow points to base). Lower limestone (5.8 m). Southwest bank of stream.

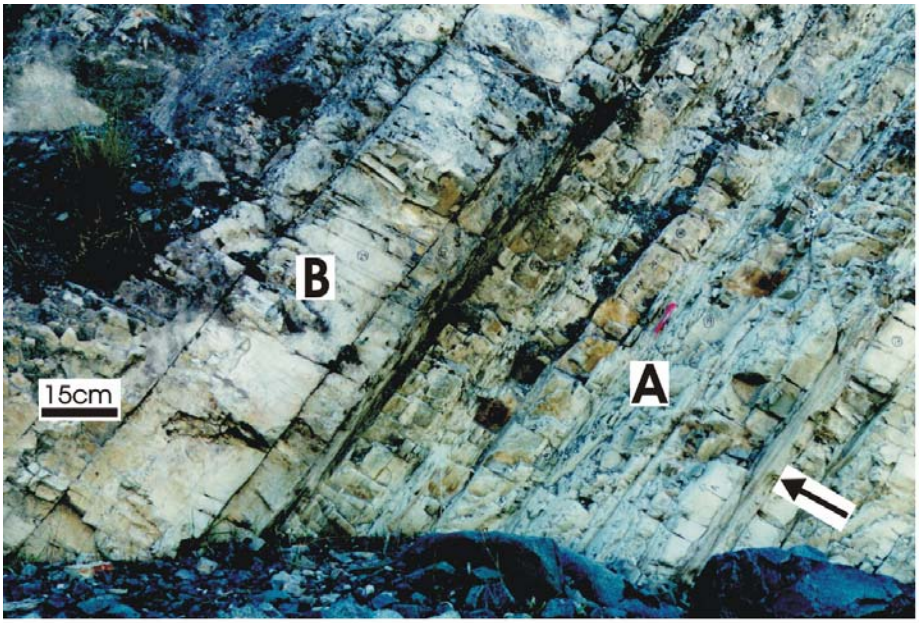

Figure 5C. (A) Strongly indurated, cm-dm bedded, light greenish-grey siliceous limestone, with 1 m thick, marl-rich recessive unit (arrow points to base of recessive unit). (B) Locally massive, strongly indurated, dm-bedded, light greenish-grey siliceous limestone. Lower limestone (~25-28 m). Northeast bank of stream.

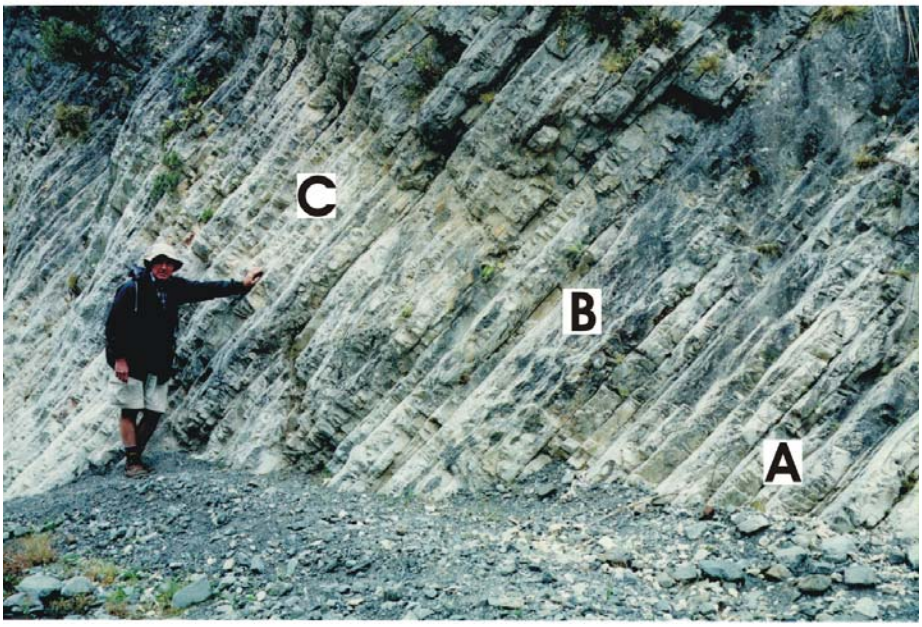

Figure 5D. (A) Strongly indurated, thick (dm-bedded), light greenish-grey siliceous limestone. (B) Five metres of strongly indurated, cm-dm bedded, light greenish-grey siliceous limestone with ribbon chert. (C) Strongly indurated cm-dm bedded, light greenish-grey siliceous limestone. Lower limestone. (~30-45 m). Northeast bank of stream.

Figure 5E. Indurated cm-dm bedded, light greenish-grey siliceous limestone with mm-cm bedded light greenish-grey marl interbeds. Lower limestone (~68 to 73 m). Northeast bank of stream.

Figure 5F. Indurated >dm-thick, interbedded, light greenish-grey siliceous limestone (60%) and marl (40%). Lower marl (~ 85 m). Northeast bank of stream.

geochemical study is required to determine if these beds correlate with the two mudstone units within the Waipawa Formation at Mead Stream.

By matching marker beds within the ~25 m thick siliceous limestone unit, a small fault offset has been accounted for and the measured section continued on the northeast bank of the stream (**Fig. 3**). An apparently continuous, recessed interval of cm-dm bedded siliceous limestone with marly partings occurs between 26 and 27 m (**Fig. 5C**). A similar but thicker recessive interval marks the BETM at Mead Stream (Hollis *et al*., 2000b). Approximately 7 m of locally massive, dm-bedded, light greenish-grey siliceous limestone and 5 m of cm-dm bedded, light greenish-grey siliceous limestone with ribbon cherts overlie the recessive interval between 27.0 and 39.4 m (**Fig. 5C, 5D**). Above this unit lies ~30 m of cm-dm bedded, light greenish-grey siliceous limestone with light greenish-grey, marl interbeds that increase in abundance from 63.5 to 94.0 m (**Fig. 5D, 5E**). The section contains dm-bedded, interbedded, light greenish-grey siliceous limestone (60%) and marl (40%) from 78.0 to 94.0 m (**Fig. 5F**). This part of the section forms seven rhythmically interbedded siliceous limestone and marl packages, a lithology strikingly similar to that of the lower marl at Mead Stream. A fault immediately above the section has truncated the upper part of the lower marl.

With the exception of uncertain correlation of the units marking the base of the formation, the stratigraphic succession within the Amuri Limestone at Dee Stream (**Fig. 4**) is very similar to that at Mead Stream (Strong *et al*., 1995).

BIOSTRATIGRAPHY

A planktic foraminiferal biostratigraphy was constructed at Dee Stream by comparing observed fauna to established zonal schemes for the early Palaeogene (**Fig. 6**). We have endeavored to correlate the assemblages to both the Cenozoic, tropical-subtropical zonal scheme of Berggren *et al*. (1995) and the high-latitude New Zealand zonal scheme of Jenkins (1966, 1974, with modifications following Hornibrook *et al*., 1989, Table 4, p. 146). As the New Zealand Late Paleocene stratigraphic record is the richest in the South Pacific, a secondary aim of our study is to reconcile these two schemes in the Late Paleocene and Early Eocene. Ages for tropical-subtropical zonal boundaries are based on Berggren *et al*. (1995). The correlation of New Zealand local

stages with the international time scale (Berggren *et al*., 1995) is based on (Morgans *et al*., 1996) (**Fig. 6**).

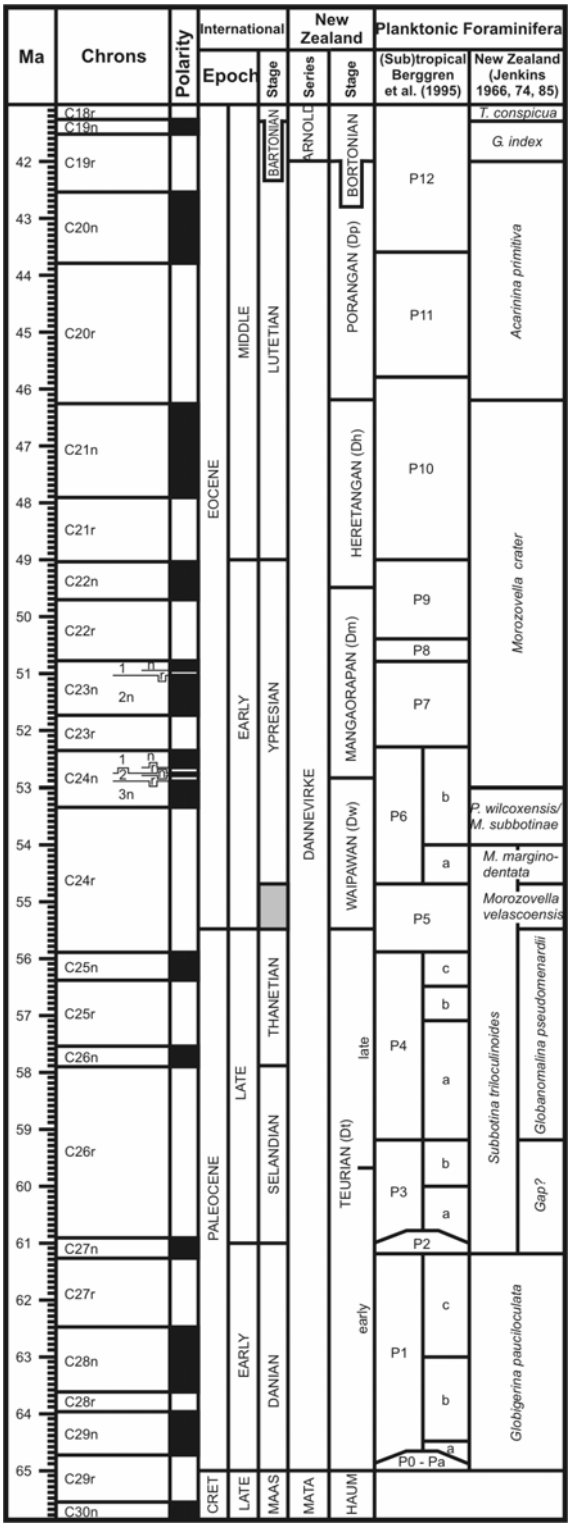

Figure 6. International and New Zealand time scales (Berggren *et al*., 1995; Morgans *et al*., 1996; Jenkins 1966, 1974, 1985). New Zealand subzones identified at Dee Stream are the *Gl. pseudomenardii* to *Ph./M. subbotinae* subzones.

In this article the boundaries between biozones are placed at the level containing the first or last appearance datum (FAD or LAD) of the taxon defining that zone or subzone. We have used Olsson *et al*. (1999) and (Toumarkine and Luterbacher, 1985) for identifications as well as Hornibrook *et al*. (1989) and (Jenkins, 1971, 1985). Benthic foraminifera were also examined, but principally at the genus level, to locate the distinctive BFEE. Benthic foraminifera were identified using the taxonomic descriptions of Tjalsma & Lohmann (1983), van Morkhoven *et al*. (1986), Hornibrook *et al*. (1989) and Bolli *et al*. (1994).

General features of foraminiferal assemblages

Foraminifera comprise 1 to 30% of the sand fraction (>63 μm) in marl layers at Dee Stream (**Table 1**). Planktic foraminifera typically contribute <1% of the sand fraction below the recessive interval at 26.2 m, but 10 to 15% above this horizon. In contrast, benthic foraminifera generally contribute 1 to 5% of the sand fraction over the lower 26.2 m, with a notable decrease at 23.5 m, become extremely rare between 26.2 and 27.5 m, and again comprise 1 to 5% of sand fraction over the remainder of the section. The ratio of planktic to benthic foraminifera thus averages about 1:10 below the recessive interval, exceeds 15:1 within this horizon, and averages 5:1 above 27.5 m.

Twenty-six planktic foraminiferal species and 34 benthic foraminiferal taxa, including 7 agglutinated taxa, were identified (**Table 1**). Poor preservation has limited identifications to below 26.2 m. Most planktic specimens belong to the genera *Acarinina, Subbotina*, and *Morozovella*, whereas most benthic specimens belong to the genera *Eponoides, Gavelinella,* and *Nuttallides*.

PLANKTIC FORAMINIFERAL BIOSTRATIGRAPHY

Planktic foraminifera in the Dee Stream section (**Table 1**; **Fig. 7**) are correlated with Zone P4 through Subzone P6b of the global, tropical-subtropical scheme (Berggren *et al.,* 1995) and *Subbotina triloculinoides* through *Pseudohastigerina wilcoxensis* Zones of the New Zealand scheme (Hornibrook *et al*., 1989; Jenkins, 1971)Jenkins 1966, 1974). An underlying interval of Paleocene strata lacks zonal marker species and therefore cannot be correlated with zones. Not all of these zones are

Table 1. Early Palaeogene foraminiferal biostratigraphy, Dee Stream. Shaded area is Basal Eocene Thermal Maximum (BETM). Faunal assemblages change from benthic to planktic dominated, indicating that either water depth deepened (a biofacies change) or producitivty and/or preservation potential increased. Abundance of foraminifera in each sample: Rare = <1%; Few = 2-5%; Common = 5-10% Abundant = >10%.

PALEOCENE															EOCENE																													Epoch	
Undiff. Paleocene		SELANDIAN - THANETIAN																								YPRESIAN																		European Stages	
		P4													P5											P6a							P6b											Foram Zone Berggren *et al.* (1995)	
TEURIAN															WAIPAWAN																													New Zealand Stages	
Undiff. Teurian		*Subbotina triloculinoides*																																		*Pseudohastigerina wilcoxensis*								Foram Zone Hornibrook *et al.* (1989)	
		Globanomalina pseudomenardii													*Morozovella velascoensis*					*Morozovella marginodentata*																*Pseudohastigerina wilcoxensis/ Morozovella subbotinae*								Subzone	
342	339	337	335	332	322	315	313	311	309	307	305	304	300	299	298	296	294	292	284	279	277	275	273	272	269	267	265	264	261	260	259	258	256	253	252	249	248	247	244	243	242	239	237	NZ Fossil Record # (P30/f1nnn)	
-5.2	-1.2	-0.3	0.0	0.5	5.9	11.0	14.3	17.4	21.8	23.3	23.5	24.3	26.1	26.2	26.5	26.8	27.0	28.7	52.2	59.5	61.5	63.5	64.4	68.3	68.4	68.7	69.1	69.4	70.9	70.94	71.0	71.4	71.9	74.9	75.5	77.2	80.1	83.4	86.3	88.2	89.8	91.7	94.0	Distance (thickness above base) (m)	
x		x	x	x		x	x														x				x	x	x	x			x					x	x		x					*Bolivinopsis* spp.	Agglutinated
	x				x	x				x												x				x				x	x		x											*Bathysiphon* spp.	Agglutinated
		x					x			x																																		*Repmanina charoides carona*	Agglutinated
		x					x			x																																		*Repmanina charoides favilla*	Agglutinated
		x	x	x			x			x													x													x						x		*Glomospira* spp.	Agglutinated
					x																																							*Nodosarella* spp.	Agglutinated
						x			x	x									x			x			x	x					x	x	x		x	x	x							*Ammodiscus* spp.	Agglutinated
x		x		x	x	x	x	x		x	x		x	x																														*Gavelinella beccariiformis*	Benthic
x		x	x		x	x								x																														*Gavelinella* spp.	Benthic
x		x						x						x																														*Allomorphina whangaia*	Benthic
x				x				x								x	x				x										x	x			x									*Bulimina* spp.	Benthic
x		x	x		x	x	x		x	x	x								x		x	x	x		x		x						x			x								*Pullenia* spp.	Benthic
x	x					x				x						x			x						x								x			x		x		x				*Epinoides* spp.	Benthic
x	x	x		x	x	x	x	x		x	x		x	x	x	x		x	x			x	x		x	x	x			x	x	x	x			x	x		x			x		*Anomalinoides* spp.	Benthic
x	x	x			x					x													x									x	x									x	x	*Gyroidina* spp.	Benthic
	x	x																																										*Pyramidulina* spp.	Benthic
		x	x	x	x	x	x			x	x			x							x		x		x							x				x	x		x		x	x	x	*Nuttallides* spp.	Benthic
				x	x	x	x			x	x				x				x			x		x	x	x	x	x	x	x	x			x		x	x	x	x					*Cibicidoides* spp.	Benthic
				x									x			x			x		x	x	x		x		x			x		x							x		x	x	x	*Oridorsilis umbonatus*	Benthic
																x				x											x			x										*Osangularia* spp.	Benthic
														x																														*Valvulineria teuriensis*	Benthic
										x				x		x	x		x		x	x				x	x							x	x	x	x		x					*Pullenia quinqueloba*	Benthic
										x																																		*Nuttallides cretatruempyi*	Benthic
															x	x			x						x												x							*Osangularia mexicana*	Benthic
															x	x		x	x									x					x			x	x	x						*Anomalinoides orbiculus*	Benthic
																x			x			x	x		x	x	x						x	x		x		x	x			x	x	*Bulimina tuxpamensis*	Benthic
																x									x	x						x										x		*Valvulineria advena*	Benthic
																x					x					x	x								x	x		x	x	x	x	x		*Gyroidina girardanus*	Benthic
																x			x																									*Alabamina dissonata*	Benthic
																			x						x			x		x	x		x			x	x	x		x				*Nuttalides carinotruempyi*	Benthic
																						x			x		x	x								x								*Aragonia* spp.	Benthic
																									x											x	x							*Pleurostomella* spp.	Benthic
																																	x			x	x							*Nodosarella* spp.	Benthic
																																					x							*Anomalinoides capitata*	Benthic

Table 1 cont.

Planktic																											Remarks	Distance (thickness above base) (m)	Preservation	Abundance	Dominant Genus
Subbotina cf. triloculinoides	*Acarinina mckannai*	*Subbotina triangularis*	*Acarinina nitida*	*Zeauvigerina teuria*	*Acarinina soldadoensis*	*Zeauvigerina waiparaensis*	*Subbotina velascoensis*	*Chiloguembelina crinita*	*Chiloguembelina trinitatensis*	*Acarinina wilcoxensis*	*Chiloguembelina wilcoxensis*	*Morozovella aequa*	*Acarinina primitiva*	*Acarinina pseudotopilensis*	*Subbotina patagonica*	*Globanomalina reissi*	*Zeauvigerina zealandica*	*Globanomalina australiformis*	*Zeauvigerina parri*	*Acarinina quetra*	*Pseudohastigerina wilcoxensis*	*Morozovella gracilis*	*Morozovella marginodentata*	*Morozovella lensiformis/dolabrata*	*Morozovella subbotinae*	*Acarinina subsphaerica*					
													X		X		X							X				94.0	Mod	Few to Common	*Acarinina*
		X			X								X		X	X		X		X	X							91.7	Mod	Few to Common	*Acarinina*
		X			X								X	X	X			X									*Morozovella* rare	89.8	Mod	Few to Common	*Acarinina, Subbotina*
					X		X					X	X	X								X		X	X		Large *Acarinina*	88.2	Good	Abundant	*Acarinina*
					X	X		X			X		X	X	X	X		X	X		X							86.3	Mod	Few to Common	*Acarinina*
					X	X	X	X		X		X		X	X	X		X			X	X	X	X	X	X	*Morozovella* dominate	83.4	Good	Abundant	*Morozovella*
	X				X		X					X	X						X	X	X	X	X	X	X		Large *Acarinina*	80.1	Mod	Abundant	*Acarinina*
					X	X	X	X			X		X		X	X		X	X		X	X					*Gl. australiformis* & benthics common, no *Morozovella*	77.2	Mod	Abundant	*Subbotina*
		X		X				X			X		X			X			X									75.5	Poor to Mod	Rare	*Acarinina*
					X		X				X		X	X		X		X	X									74.9	Mod	Rare to Common	*Subbotina*
					X		X	X			X	X	X			X		X		X				X				71.9	Mod	Common	*Acarinina*
X					X	X	X		X		X		X	X	X	X											Large benthics	71.4	Mod	Common	*Acarinina*
					X			X			X		X		X	X												71.0	Mod	Few to Common	*Globanomalina*
		X			X		X	X			X		X		X	X			X								Benthics common	70.94	Poor	Few	*Subbotina*
						X			X				X	X	X	X											Benthics common	70.9	Poor	Few	*Acarinina*
X						X		X		X	X		X	X		X		X	X	X								69.4	Poor	Common to Abundant	*Globanomalina*
X		X			X	X		X		X	X	X	X		X	X		X	X	X							*Gl. australiformis*, *Gl. reissi* common	69.1	Mod	Abundant	*Globanomalina*
		X			X	X	X	X	X		X	X	X	X	X	X		X	X								*Z. parri*, *Chiloguembelina* common	68.7	Good	Common	*Zeauvigerina*
					X	X	X	X			X	X	X			X	X										*Subbotina*, *Chiloguembilina* + *Zeauvirigina* common	68.4	Mod	Common	*Subbotina*
														X		X												68.3	Poor	Rare	*Acarinina, Subbotina*
					X	X					X	X		X		X												64.4	Mod	Common	*Subbotina*
	X		X		X		X	X		X	X	X	X	X	X	X							X					63.5	Good	Common	*Acarinina*
X					X	X			X				X			X												61.5	Poor	Common	*Globanomalina*
					X								X			X												59.5	Poor	Few	*Acarinina*
	X	X			X	X	X	X		X	X	X	X	X	X												Oxides, calcite rhombs	52.2	Poor	Few	*Subbotina*
X					X		X					X	X														Deformed, preferential dissolution of *Morozovella*?	28.7	Poor	Few	*Acarinina, Subbotina*
X	X	X			X		X		X			X	X														Deformed, preferential dissolution of *Morozovella*?	27.0	Poor	Common	*Acarinina*
X	X	X	X		X		X		X	X	X	X	X														Benthics return, *Bullimina tuxpamensis* common - low O2	26.8	Mod	Common	*Morozovella*
X		X			X		X		X	X	X	X	X														*Morozovella* abundant - BETM	26.5	Mod	Common	*Subbotina*
X	X	X	X			X	X	X																			Rare benthics	26.2	Poor	Few	*Subbotina*
X																												26.1	Poor	Rare	*Subbotina*
X		X																										24.3	Poor	Rare	*Subbotina*
X	X	X	X			X																					Rare benthics*	23.5	Poor	Rare	*Acarinina*
		X																									Rare planktics	23.3	Poor	Rare	*Nuttallides*
		X																									Very rare benthics	21.8	Poor	Rare	*Subbotina*
																												17.4	Mod	Few	*Gavelinella*
																											No planktics	14.3	Poor	Few to Common	*Gavelinella & Nuttallides*
																											Rare planktics, pyrite	11.0	Poor	Few	*Cibicidoides*
		X																										5.9	Poor	Rare	*Anominaloides*
X		X	X	X	X																						Benthics common, oxides, calcite rhombs	0.5	Poor	Few	*Anominaloides*
X																												0.0	Poor	Rare	*Bolivinopsis*
X	X	X																									Pyrite, glauconite	-0.3	Poor	Rare	*Nuttallides*
																											No planktics, pyrite	-1.2	Poor	Rare	*'Eponoides'*
																											No planktics, pyrite	-5.2	Poor	Rare	*Gavelinella*

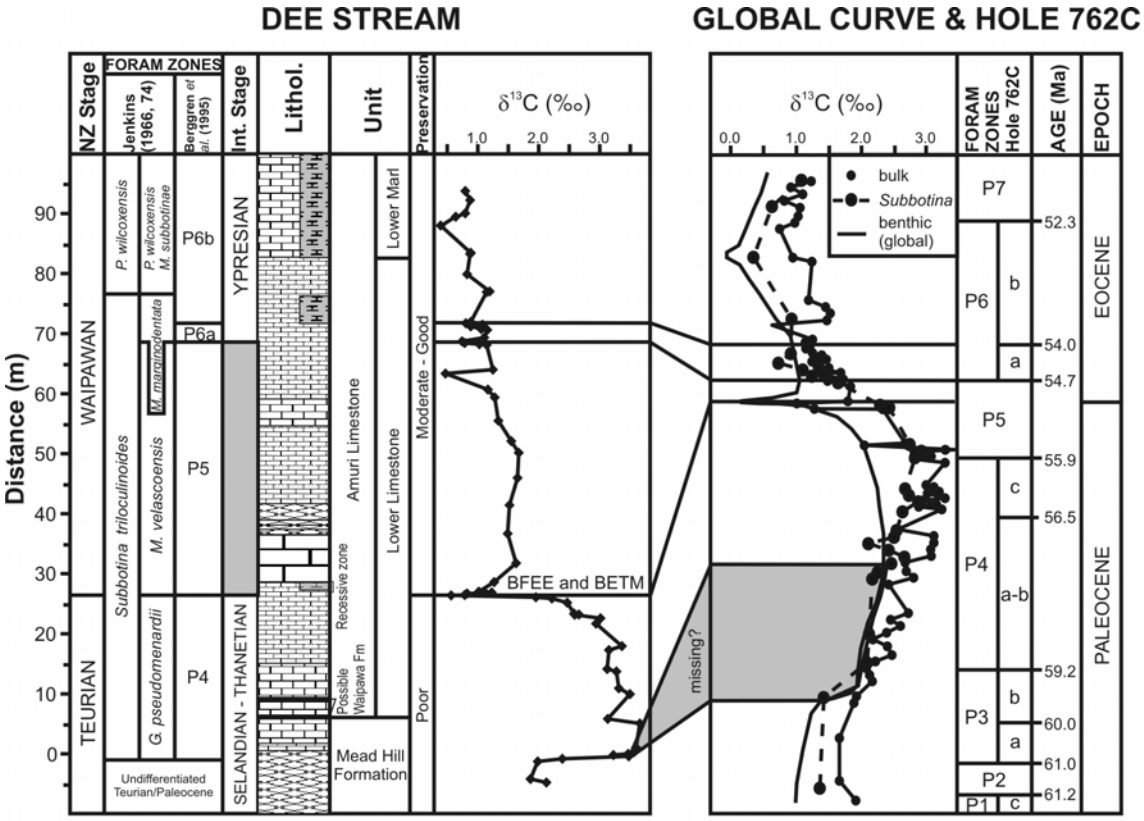

Figure 7. Planktic foraminiferal zones, lithological units and the $\delta^{13}C$ record of bulk carbonate at Dee Stream. Also shown are the planktic foraminiferal zones (Hancock *et al*., 2002) and the $\delta^{13}C$ records of bulk sediment (Thomas *et al*., 1992) and *Subbotina* specimens (Hancock *et al*., 2002) at ODP Site 762, Exmouth Plateau (Northwest Shelf of Australia), one of the few Australasian sites with both foraminiferal and isotopic records for the early Palaeogene. The global benthic foraminiferal $\delta^{13}C$ (‰) curve is shown for comparison (Zachos *et al*., 2001).

recognized with equal confidence. In particular, poor test preservation makes zonal boundaries difficult to locate in the lower 26.2 m using either scheme. Several foraminiferal key species are illustrated and all taxa are listed (**Appendix 1, Plates 1, 2, 3**). Absolute age assignments are estimates from Berggren *et al*. (1995).

Global tropical-subtropical zonation

Undifferentiated Paleocene (<-5.2 to –0.3 m). Unzoned interval above Cretaceous/Tertiary boundary and below Zone P4 characterized by poorly preserved planktics or their absence. It is difficult to refine the stratigraphy of this interval, as planktic foraminifera are absent. However, a chert-rich interval resembling the

Cretaceous/Tertiary boundary at Mead Stream (Strong *et al*., 1995) lies ~50 m below the investigated section, suggesting that the base of Zone P1 lies significantly below our sample set. This, together with the common occurrence of the benthic foraminifera *Gavelinella beccariiformis*, which becomes extinct globally during the BFEE, restricts this part of the section to the Paleocene. Age: 65-59.2 Ma, Early Paleocene to Late Paleocene (Danian-Selandian).

Zone P4 (-0.3 to 26.5 m). In the absence of the primary marker species *Globanomalina pseudomenardii*, the FAD of *Acarinina mckannai* is used to mark the base of Zone P4 at Dee Stream. Olsson *et al*. (1999) place this event at the base of Subzone P4a. Planktic foraminifera are rare in this interval. Typically small and poorly preserved, *Subbotina* and *Acarinina* dominate the planktic faunal assemblage. The most common species are *Subbotina* cf. *triloculinoides*, *S. triangularis*, *S. velascoensis*, and in uppermost Zone P4, *A. nitida*. Because of the generally poor preservation of foraminiferal test surfaces, which aids in species identification within the genus *Subbotina*, we have named those *Subbotina* that have a similar morphology to *S. triloculinoides*, *S.* cf. *triloculinoides*. The Late Paleocene faunal assemblage at Dee Stream is typical of higher latitudes in that it lacks the Late Paleocene *Acarinina* and *Morozovella* radiation found in low and middle latitude successions (Olsson *et al*., 1999). Age: 59.2-55.5 Ma, Late Paleocene (late Selandian-Thanetian).

Zone P5 (26.5-68.7 m). The LAD of *Globanomalina pseudomenardii* is the primary datum for the base of Zone P5. In the absence of this species, the base of the biozone has been placed at the first appearance of an easily identified, although rare taxon, *Acarinina wilcoxensis*, which occurs within upper Zone P5 in the tropical-subtropical global scheme (Berggren *et al*., 1995). In addition to *Acarinina wilcoxensis*, the FADs of *A. primitiva* and *Morozovella aequa* (which coincide with a profound decline in the abundance of benthic species, discussed below) mark the base of this interval. *Morozovella aequa* proliferates at 26.5 m at Dee Stream and elsewhere at the Paleocene-Eocene (P-E) transition, at all latitudes (Berggren *et al*., 1995; Huber, 1991; Lu *et al*., 1995). The FAD's of *Acarinina wilcoxensis* and *Morozovella aequa* are also nearly concurrent at Antarctic ODP Site 690 (Stott & Kennett 1990). In subtropical locations, *Morozovella aequa* first appears well below the P-E transition at the base of Subzone P4c. *Morozovella* spp. other than *M. aequa*, *M. gracilis* and *M. subbotinae* are

extremely rare at Dee Stream compared to their occurrence in lower latitudes. Other species in this interval at Dee Stream include *Acarinina soldadoensis*, *A. nitida*, *A. pseudotopilensis*, *Subbotina* cf. *triloculinoides*, *S. triangularis*, *S. velascoensis*, *S. patagonica*, *Zeauvigerina waiparaensis*, *Z. parri*, *Chiloguembelina crinita*, and *C. wilcoxensis*. These species are typical elements of Zone P5 assemblages elsewhere (Berggren *et al*., 1995; Olsson *et al*., 1999). Age: 55.5 to 54.7 Ma, latest Paleocene to Early Eocene (latest Thanetian to earliest Ypresian). Although the FAD *of Acarinina wilcoxensis* occurs within Zone P5 (Berggren *et al*., 1995), it is not indicated where in the zone. We use this age range because the base of this zone is found to coincide with the CIE excursion and BFEE.

Subzone P6a (68.7-71.9 m). The LAD of *Morozovella velascoensis* defines the base of Subzone P6a (Berggren *et al*., 1995), but this species is conspicuously absent at Dee Stream and at other locations with Eocene latitudes higher than 45° (Olsson *et al*., 1999). The exception is its isolated occurrence at the Mid-Waipara River section on the southern South Island, New Zealand (Jenkins 1965, 1971), an occurrence that has been reconfirmed by the senior author. In the absence of *Morozovella velascoensis*, the base of the subzone has been placed at the FAD of *Globanomalina australiformis*. Although this event occurs earlier in low latitudes (within Zone P5 – Berggren *et al*., 1995), it occurs directly above the LAD of *Morozovella velascoensis* in the mid-Waipara section (Jenkins 1971). For this reason we tentatively use the local first occurrence of *Globanomalina australiformis* as a proxy for the base of Subzone P6a. The base of Subzone P6a is taken as the base of the Ypresian international stage (Berggren *et al*., 1995, Aubry & Berggren 2000). Species common to this subzone at Dee Stream include those species found in Zone P5 (above) and *Globanomalina australiformis*, *Zeauvigerina parri* and *Acarinina quetra*. Age: 54.7-54.0 Ma, earliest Eocene (earliest Ypresian).

Subzone P6b (71.9-94.0 m). The FAD of *Morozovella lensiformis* (= *M. dolabrata* sensu (Hornibrook *et al*., 1989) is the primary datum for the base of Subzone P6b. The species has a well-defined first appearance in moderately preserved assemblages in the upper part of the Dee Stream section. In poorly preserved assemblages, *Morozovella lensiformis* and its predecessor, *M. aequa*, can be difficult to separate as they are distinguished largely by wall texture; although the presence of a

late-formed keel is a distinguishing feature of *M. dolobrata* (Jenkins, 1971). Large specimens of *Acarinina* and *Morozovella* including *M. aequa*, *M. subbotinae*, *M. lensiformis*, *M. marginodentata, M. gracilis, A. soldadoensis, A. primitiva*, and *Globanomalina australiformis* dominate this zone at Dee Stream. Other planktic foraminiferal species common to this zone at Dee Stream include *Subbotina* cf. *triloculinoides, S. triangularis, S. velascoensis, Pseudohasterigina wilcoxensis*, and *Chiloguembelina wilcoxensis*. This assemblage is typical of Subzone P6b elsewhere (Berggren *et al*., 1995) with the exception of *Subbotina velascoensis*, which has its LAD in Subzone P6b at Dee Stream and in Subzone P6a at other localities (Berggren *et al*., 1995). Age: 54.0-52.3 Ma, Early Eocene (early Ypresian).

New Zealand zonation

The New Zealand planktonic foraminiferal zonation was established by Jenkins (1966, 1974) and reproduced by Hornibrook *et al*. (1989). It is important to note that while the zones discussed below have been formally defined (Jenkins 1966), the definition of subzones has not been formalized and identification of primary datums is based on a summary table (Jenkins 1974, Table 2, p. 157). New Zealand species ranges cited below follow Hornibrook *et al*. (1989, Table 4).

Undifferentiated Teurian (-5.2 to –0.3 m). The base of the section cannot be assigned to New Zealand zones because no identifiable planktic foraminifera have been recovered. Age: Paleocene (Teurian).

***Subbotina triloculinoides* Zone, *Globanomalina pseudomenardii* Subzone** (= *Globorotalia pseudomenardii* Subzone, Jenkins 1974) (-0.3 to 26.5 m). The primary datum for the base of this subzone is the FAD of *Globanomalina pseudomenardii* (Jenkins 1974). This species has not been found at Dee Stream and while it is occasionally seen in Teurian samples (CPS observation) as far as is known the species has published records from only two New Zealand sections – mid-Waipara River and Te Uri Stream (Jenkins, 1971). The FAD of *Acarinina mckannai* is used to locate the base of the subzone at Dee Stream. Common species found in this subzone include *Subbotina* cf. *triloculinoides, S. triangularis, S. velascoensis*, and *Acarinina nitida*. The latter three species and *Subbotina triloculinoides s.s.* occur elsewhere in New Zealand

(Hornibrook *et al*., 1989). *Subbotina* cf. *triloculinoides* ranges into the early Eocene at Dee Stream, which is consistent with the upper range limit for *S. triloculinoides* of late-Early Eocene (Heretaungan) indicated by Hornibrook *et al.* (1989), who followed Jenkins (1971) concept of the species. However, it may be that the Dee Stream and other New Zealand records include another similar, but younger morphotype, as Olsson *et al.* (1999) believe that *Subbotina triloculinoides* is restricted to the Paleocene, ranging no higher than uppermost Zone P4. Age: Late Paleocene (late Teurian).

***Subbotina triloculinoides* Zone, *Morozovella velascoensis* Subzone** (= *Globorotalia velascoensis* Subzone, Jenkins 1974) (26.5-68.7 m). The base of this subzone is placed at the FAD of the primary index *Morozovella aequa* at Dee Stream. This event and the FAD of the secondary index *Acarinina primitiva* occur at the BFEE (see discussion below) and Teurian/Waipawan boundary at Dee Stream and elsewhere in New Zealand (Hornibrook *et al*., 1989). In subtropical regions, these two species first appear earlier, together with *Acarinina soldadoensis*, at the base of Subzone P4c (Berggren *et al*., 1995). *Morozovella aequa* proliferates at 26.5 m. Other common species in this subzone at Dee Stream include *Subbotina* cf. *triloculinoides*, *S. triangularis*, *S. velascoensis*, *Acarinina mckannai*, and *Zeauvigerina waiparaensis*. *Acarinina mckannai* ranges into the *Pseudohastigerina wilcoxensis Zone* at Dee Stream and into the Middle Eocene (Bartonian) in other parts of New Zealand (Hornibrook *et al*., 1989). In subtropical areas, it last appears in Subzone P4c (Olsson *et al*., 1999). Age: earliest Eocene (earliest Waipawan).

***Subbotina triloculinoides* Zone, *Morozovella marginodentata* Subzone** (= *Globorotalia marginodentata* Subzone, Jenkins 1974) (68.7-77.2 m). The primary datum for the base of this subzone is the LAD of *Morozovella velascoensis*. In the absence of this species, the base of the subzone is placed at the FAD of *Globanomalina australiformis* at Dee Stream. As discussed above, the latter event occurs directly above the LAD of *M. velascoensis* in the mid-Waipara section (Jenkins 1971). Species common to this subzone include *Morozovella aequa*, *Subbotina* cf. *triloculinoides*, *S. triangularis*, *S. velascoensis*, *S. patagonica*, *Acarinina primitiva*, *A. soldadoensis*, *Chiloguembelina wilcoxensis*, *C. crinita*, and *Zeauvigerina parri*. *Zeauvigerina zealandica* does not make its first appearance near the base of the subzone as recorded

elsewhere in New Zealand (Hornibrook *et al*., 1989), but higher in the subzone. Age: Early Eocene (Waipawan).

Pseudohasterigina wilcoxensis* Zone, *P. wilcoxensis/Morozovella subbotinae (= *Globorotalia rex*, Jenkins 1974) **Subzone** (77.2-94.0 m). The primary datum, the FAD of the nominate taxon, marks the base of this zone at Dee Stream. The FADs of *Pseudohastigerina wilcoxensis* and *Morozovella subbotinae* are approximately concurrent, here and elsewhere in New Zealand (Hornibrook *et al*., 1989). Within this zone at Dee Stream, large *Acarinina* and *Morozovella* dominate faunal assemblages and common species include *Morozovella aequa, M. subbotinae, M. lensiformis, M. marginodentata, Subbotina triangulari*s, *S. patagonica, Acarinina soldadoensis, A. primitiva* and *Chiloguembelina wilcoxensis*. These species are typical of assemblages in the *Pseudohastigerina wilcoxensis* Zone in other New Zealand sections (Hornibrook *et al*., 1989). Benthic foraminifera proliferate at the base of this zone, while *Morozovella* are conspicuously absent and the percentage of terrigenous material increases. Age: Early Eocene (Waipawan).

BENTHIC FORAMINIFERA EXTINCTION EVENT (BFEE)

A marked change in benthic foraminiferal assemblages occurs within the recessive zone at Dee Stream (26-27 m, **Fig. 4; Table 1**). Below 26.5 m, common species include *Gavelinella beccariiformis, Nuttallides* spp. *Gyroidina* spp., *Anominaloides* spp., *Ammodiscus* spp., *Repmanina charoides carona,* and *R. charoides favilla*. Tests of these species generally exceed 250 μm and are thick-walled. An upper bathyal depth ecology (~700–500 m) is inferred (van Morkhoven *et al*., 1986). The highest occurrence of known Teurian species, *Allomorphina whangaia, Valvulineria teuriensis* and *Gavellinella beccariifomis* (Hornibrook *et al*., 1989, Table 3), occurs at 26.2 m. The abundance of benthic foraminifera then plummets at 26.5 m. The first occurrence of benthic species with well-established FADs in the early Waipawan, including *Anomalinoides orbiculus, Osangularia mexicana, Bulimina tuxpamensis, Gyroidina girardanus* and *Alabamina dissonata*, occur within the recessive interval between 26.5 and 26.8 m. Benthic foraminifera increase in abundance and diversity towards the top of the recessive zone, but with a different fauna, dominated by the smaller, thin-walled *Bulimina tuxpamensis, Valvulineria advena, Gyroidina girardanus*

and *Osangularia* spp. Benthic foraminiferal assemblages above the recessive interval are dominated by *Bulimina tuxpamensis*, *Nuttallides carinotruempyi*, *Gyroidina* spp., *Anominaloides* spp., *Eponoides* spp., *Cibicidoides* spp., *Pullenia* spp., and *Pleurostomella* spp. These species have an inferred upper bathyal depth ecology (~700–200 m) (van Morkhoven *et al*., 1986). Agglutinated benthic foraminifera are conspicuously absent from faunal assemblages until at least 5 m above the recessive interval.

COMPARISON WITH MEAD STREAM FORAMINIFERAL SUCCESSION

Overall, the composition and preservation of foraminiferal faunas are similar at Dee Stream and Mead Stream. There are, however, a few differences. *Rzehakina epigona*, a common Paleocene benthic foraminifera in New Zealand assemblages, which became extinct at the BFEE (Hornibrook *et al*., 1989), was observed at Mead Stream (Strong *et al*., 1995) but not at Dee Stream. This may be a consequence of depth ecology, as Dee Stream was closer to the Palaeogene shoreline and perhaps in significantly shallower water. *Bulimina tuxpamenis* is a common species in Waipawan and Mangaorapan assemblages at both Mead and Dee Streams. *Subbotina triangularis* and *Acarinina soldadoensis* are common in Waipawan assemblages at Dee Stream, but have not been recorded at Mead Stream. This may be due to reconnaissance-scale of the Mead Stream foraminiferal study, with only 4 to 5 samples examined over the equivalent Late Paleocene to Early Eocene interval (Strong *et al*., 1995), or it may relate to differences in species concepts. *Morozovella marginodentata*, *M. subbotinae* and *Subbotina patagonica* are common in Mangaorapan assemblages at Dee Stream but were not observed at Mead Stream. This also may reflect the more detailed sampling at Dee Stream as *Morozovella* occur sporadically throughout the section.

CARBON ISOTOPE STRATIGRAPHY

The $\delta^{13}C$ of bulk carbonate varies significantly over the section at Dee Stream (**Table 2**; **Fig. 7**). In the lowest few metres of the section, $\delta^{13}C$ averages ~2.1‰ until it abruptly increases to 3.4‰ at –0.3 m. Carbon isotopic compositions lie between 2.9‰ and 3.6‰ from –0.3 to 22.7 m, where they decline, decreasing by 2.4‰ to a minimum of 0.6‰ at 26.5 m. Almost 2‰ of this decrease occurs within 1 m above the base of the

Table 2. Bulk carbonate $\delta^{13}C$ (‰) contents, Dee Stream. *Shaded areas indicate BETM. L = limestone, M = marl.

NZ Fossil Record #		Distance (m)	$\delta^{13}C$ (‰)		NZ Fossil Record #		Distance (m)	$\delta^{13}C$ (‰)
P30/f1237	M	94.0	0.80		P30/f1292	M	28.8	1.27
P30/f1238	L	92.5	0.88	*	P30/f1293	L	27.1	1.02
P30/f1241	L	90.3	0.80		P30/f1294	M	27.0	1.23
P30/f1242	M	89.8	0.63		P30/f1295	L	26.9	1.13
P30/f1243	M	88.2	0.40		P30/f1296	M	26.8	0.83
P30/f1246	L	83.7	0.89		P30/f1297	L	26.6	0.79
P30/f1247	M	83.4	0.88		P30/f1298	M	26.5	0.57
P30/f1248	M	80.1	0.83		P30/f1299	M	26.2	1.95
P30/f1249	M	77.2	1.20		P30/f1301	L	26.0	2.21
P30/f1250	L	77.1	1.15		P30/f1303	L	25.3	2.46
P30/f1255	L	72.1	0.89		P30/f1305	M	23.5	2.57
P30/f1256	M	71.9	0.81		P30/f1306	L	23.4	2.65
P30/f1257	L	71.7	1.08		P30/f1307	M	23.3	2.58
P30/f1258	M	71.4	0.89		P30/f1308	L	22.7	3.00
P30/f1260	M	70.9	1.06		P30/f1309	M	21.8	2.93
P30/f1262	L	70.8	1.16		P30/f1310	L	18.1	3.35
P30/f1263	L	69.5	1.11		P30/f1311	M	17.4	3.14
P30/f1266	L	68.9	0.75		P30/f1313	M	14.3	3.11
P30/f1268	L	68.6	0.79		P30/f1314	L	13.8	3.26
P30/f1269	M	68.4	1.03		P30/f1315	M	11.0	3.30
P30/f1271	L	68.3	1.15		P30/f1316	L	10.1	3.48
P30/f1274	L	64.2	1.25		P30/f1322	M	5.9	3.12
P30/f1275	M	63.5	0.48		P30/f1327	L	5.2	3.64
P30/f1278	L	60.9	1.17		P30/f1331	L	1.1	3.58
P30/f1279	M	59.5	1.28		P30/f1333	L	0.4	3.55
P30/f1282	L	55.7	1.34		P30/f1334	L	0.1	3.45
P30/f1284	M	52.2	1.55		P30/f1336	L	-0.1	3.21
P30/f1285	L	50.3	1.67		P30/f1337	M	-0.3	3.46
P30/f1287	L	46.1	1.65		P30/f1338	L	-0.7	2.38
P30/f1289	L	41.6	1.52		P30/f1339	M	-1.2	1.98
P30/f1290	L	36.8	1.49		P30/f1342	M	-4.1	1.86
P30/f1291	L	31.9	1.63		P30/f1343	L	-4.7	2.12

recessive interval. Above this pronounced negative excursion, $\delta^{13}C$ increases to 1.7‰ at 50.3 m. The $\delta^{13}C$ then generally decreases over the upper 38 m of section reaching a low of 0.4‰ at 88.2 m. However, a sharp drop to 0.5‰ occurs in a single sample at 63.5 m, which may be anomalous.

Significantly, when coupled with the planktic foraminiferal biozones and benthic foraminiferal turnover, the $\delta^{13}C$ record of bulk carbonate at Dee Stream resembles $\delta^{13}C$ curves of marine carbonate from other global locations (e.g. Bains *et al*., 1999), including Ocean Drilling Program (ODP) Site 762 on the Exmouth Plateau (Northwest Shelf of Australia) (Hancock *et al*., 2002), the only other Australasian location with detailed early Palaeogene foraminiferal and carbon isotope stratigraphies (**Fig. 7**). The $\delta^{13}C$ is relatively low in the Undifferentiated Paleocene and generally high in Zone P4. The abrupt 1.1‰ increase at –0.3 m may correspond to the rapid 0.7‰ rise in global $\delta^{13}C$ curves near the P3/P4 boundary (Zachos *et al*., 2001) or an hiatus (**Fig. 7**). Either interpretation is consistent with observed foraminiferal assemblages. As there is no obvious lithologic break at this level, an hiatus seems less likely. A pronounced 2 to 3‰ drop in $\delta^{13}C$ begins in the uppermost Paleocene, reaching a minimum of 0.6‰ 0.5 m above the base of the recessive interval in Zone P5. During Zone P5 and Zone P6, $\delta^{13}C$ is moderate to low. The prominent lows in $\delta^{13}C$ at 63.5 and 88.2 m may correspond to similar changes in other records, perhaps implying additional releases of light carbon after the BETM, but further work is needed. Importantly, despite burial, uplift and tilting, rocks at Dee Stream clearly contain an easily identifiable, globally significant $\delta^{13}C$ record.

BASAL EOCENE THERMAL MAXIMUM (BETM)

Three features within planktonic foraminiferal Zone P5 characterize the onset of the BETM globally: (1) a major benthic foraminifera extinction event (BFEE), (2) a rapid diversification of *Acarinina* and *Morozovella* (Huber, 1991; Kelly *et al*., 1996; Kelly, 2002; Lu and Keller, 1995) and, (3) a large negative excursion in $\delta^{13}C$. At Dee Stream, all three of these markers lie near the base of the recessive zone. Within the limits of the sample suite all three events can be located within a 30 cm interval above the base of the recessive unit (i.e. between samples P30/f1299 and f1298). Further

detailed sampling of this interval may reveal more information on the relationship between the CIE and foraminiferal assemblage turnover.

The boundary between the Teurian (Dt) and Waipawan (Dw) New Zealand stages traditionally has been defined by a prominent benthic foraminiferal extinction (Hornibrook *et al*., 1989), now termed the BFEE. The well-defined LAD of the common and widespread Paleocene species *Gavelinella beccariiformis* precisely at the onset of the BETM at Dee Stream supports the contention of previous workers (Crouch, 2001; Hollis *et al*., 2000a; Hollis *et al*., 2000b; Kaiho *et al*., 1996; Killops *et al*., 2000) that the Dt/DW boundary coincides with the base of the BETM.

The tendency for the BETM to form a recessive unit in outcrop arises because of an increased ratio of terrigenous clay to biogenic carbonate. Previous workers have noted this phenomenon across the BETM elsewhere, attributing it to enhanced chemical weathering and greater stream discharge along coasts (Schmitz *et al*., 2001; Zachos and Dickens, 2000) or pronounced carbonate dissolution in deep waters (e.g., Dickens, 2000; Dickens *et al*., 1997). Early Eocene benthic foraminiferal assemblages at Dee Stream are generally dominated by *Nuttallides carinotruempyi* and *Cibicidoides* spp., suggesting a slightly shallower, middle to upper bathyal paleodepth (~700–200 m) (Van Morkhoven *et al*., 1986), than during the late Paleocene, and a relative proximity to land and terrigenous supply. Alternatively, the increase in terrigenous material during the BETM interval at Dee Stream may represent a climatic signal and be due to enhanced riverine discharge as suggested for other high-latitude marine sections including other parts of New Zealand (Bains *et al*., 2000; Crouch *et al*., 2001; Kaiho *et al*., 1996; Robert and Kennett, 1992). Moreover, if the higher terrigenous component during the BETM interval is due to increased riverine discharge, then increased surface productivity linked to this phenomenon may be causing the sudden increase in planktic foraminifera during this interval.

The thin-walled and tapering benthic foraminifer, *Bulimina tuxpamensis*, dominates the fauna during the BFEE at Dee Stream. The high abundance of this species probably signifies low dissolved oxygen concentrations during the BETM, which may have been the direct cause of the BFEE (Kaiho *et al*., 1996). Dysoxic bottom waters may also explain the delayed recovery of the agglutinated taxa at Dee

Stream. Assuming the prominent negative $\delta^{13}C$ excursion signifies rapid and massive release of methane from continental margins (Dickens *et al*., 1997; Dickens *et al*., 1995), dissolved oxygen levels should have dropped in waters below the mixed layer (>300 m) as methane was oxidised to CO_2 (Dickens, 2000; Katz *et al*., 1999).

CONCLUSIONS

A relatively thick rock sequence of Upper Paleocene to Lower Eocene, pelagic, siliceous limestone, limestone and marl is well-exposed in Dee Stream, a tributary of the Clarence River. We have measured a 103 m section within this sequence (**Fig. 3)**, documented its lithology (**Fig. 4**) and detailed its biostratigraphy using foraminifera (**Table 1**) and carbon isotope stratigraphy (**Fig. 7**). The section contains a prominent recessive interval at 26.2 to 27.0 m, which consists of alternating marl and marly limestone beds deposited in the earliest Eocene and correlated with the BETM. Foraminifera are poorly preserved below the recessive interval but are somewhat better preserved above it, suggesting a major change in the environment of deposition in the Clarence Valley at the P/E boundary.

It is difficult to rigorously apply the Palaeogene tropical-subtropical planktic foraminiferal zonal scheme (Berggren *et al*., 1995) at Dee Stream, because primary marker species are absent or too poorly preserved for reliable identification. However, using secondary marker species, planktic foraminiferal zones from Zone P4 through Subzone P6b were recognized. The New Zealand foraminiferal zonation (Jenkins 1966, 1974) was easier to apply. The *Subbotina triloculinoides* to *Pseudohastigerina wilcoxensis* Zones were easily recognized and a correlation between the two zonal systems was attempted with some success, in particular the correlation between the onset of the BETM and the Teurian/Waipawan New Zealand stage boundary. The boundary between Subzones P6a and P6b is well-defined by the FADs of *Pseudohastigerina wilcoxensis* and *Morozovella lensiformis* (= *M. dolobrata* of Jenkins, 1971), two events which occur at the base of Subzone P6b in mid to high latitude regions worldwide (Berggren *et al*., 1995).

The $\delta^{13}C$ record of bulk carbonate at Dee Stream shows several prominent rises and falls. When these isotopic changes are aligned using our foraminiferal biozones, the

$\delta^{13}C$ record correlates closely to other $\delta^{13}C$ curves generated from other key early Palaeogene carbonate sequences.

Within the recessive interval, within Zone P5, the three primary diagnostic features of the BETM are identified, namely first abundant appearance of *Morozovella*, a major benthic foraminiferal turnover associated with the BFEE, and a -2‰ $\delta^{13}C$ excursion in bulk carbonate. Evidently, an expanded and apparently complete BETM interval exists at Dee Stream. Immediately following the onset of the BETM, benthic foraminiferal assemblages are dominated by *Bulimina tuxpamensis*, an indicator of low dissolved oxygen levels in deep waters. Overall, the Dee Stream section, with its continuous and thick deposition over the Late Paleocene and Early Eocene, provides an important record for the interval containing the BETM. When combined with current work at Mead Stream and future work at other streams in the Clarence Valley, Dee Stream provides an important site for understanding environmental change on high latitude, continental margins during the early Palaeogene.

ACKNOWLEDGMENTS

The research was supported by the Joseph Cushman Foundation and Mid-American Paleontological Society Awards for student research (HJLH), the Australian Research Council (GRD), and the New Zealand Foundation for Research, Science and Technology (CPS, CJH and BDF). Personal communication with William Berggren regarding Eocene planktic foraminiferal species identification was a great help. We thank Jim Zachos and his laboratory crew for the stable carbon isotope analyses, and Richard and Sue Murray for access to the Dee Stream section.

REFERENCES

Aubry, M.-P. and Berggren, W. A., 2000. The homeless GSSP; the dilemma of the Paleocene/Eocene boundary. *Tertiary Research*, 20 (1-4): 107-112.

Bains, S., Corfield, R. M., and Norris, R. D. 1999. Mechanisms of climate warming at the end of the Paleocene. *Science*, 285: 724-727.

Bains, S., Norris, R. D., Corfield, R. M. and Faul, K. L., 2000. Termination of global warmth at the Palaeocene/Eocene boundary through productivity feedback. *Nature*, 407: 171-174.

Beerling, D. J., 2000. Increased terrestrial carbon storage across the Palaeocene-Eocene boundary. *Palaeogeography, Palaeoclimatology, Palaeoecology*, 161 (3-4): 395-405.

Berggren, W. A., Kent, D. V., Swisher, C. C., III and Aubry, M.-P., 1995. A revised Cenozoic geochronology and chronostratigraphy. In Berggren, W. A., Kent, D. V., Aubry, M. P., Hardenbol, (Eds.), *Geochronology, time scales and global stratigraphic correlation*. J. SEPM Special Publication, 54: 129-212.

Billups, K., Channell, J. E. T, and Zachos, J., 2002. Late Oligocene to early Miocene geochronology and paleoceanography from the subantarctic South Atlantic. *Paleoceanography*, 17 (1): 10.1029/2000PA000568.

Billups, K., Ravelo, A. C., and Zachos, J. C., 1998. Early Pliocene deep water circulation in the western Equatorial Atlantic, implications for high-latitude climate change. *Paleoceanography*, 13 (1): 84-95.

Bolli, H. M., Beckmann, J.-P. and Saunders, J. B., 1994. *Benthic foraminiferal biostratigraphy of the South Caribbean Region*. Cambridge, Cambridge University Press. 408 p.

Bralower, T. J., Zachos, J. C., Thomas, E., Parrow, M., Paull, C. K., Kelly, D. C., Premoli Silva, I., Sliter, W. V., and Lohmann, K. C., 1995. Late Paleocene to Eocene paleoceanography of the Equatorial Pacific Ocean; stable isotopes recorded at Ocean Drilling Program Site 865, Allison Guyot. *Paleoceanography*, 10 (4): 841-865.

Crouch, E. M., 2001. *Environmental change at the time of the Paleocene-Eocene biotic turnover*. Utrecht, Utrecht University. 216 p.

Crouch, E. M., Bujak, J. P., Brinkhuis, H., 2000. Southern and northern Hemisphere dinoflagellate cyst assemblage changes in association with the late Paleocene thermal maximum. *GFF*, 122: 40-41.

Crouch, E. M., Heilmann-Clausen, C., Brinkhuis, H., Morgans, H. E. G., Rogers, K. M., Egger, H. and Schmitz, B., 2001. Global dinoflagellate event associated with the late Paleocene thermal maximum. *Geology*, 29 (4): 315-318.

Dickens, G. R. 2000. Methane oxidation during the late Palaeocene thermal maximum. *Bulletin de la Societe Geologique de France*, 171 (1): 37-49.

Dickens, G. R., 1999. The blast in the past. *Nature*, 401: 752-755.

Dickens, G. R., Castillo, M. M., and Walker, J. C. G., 1997. A blast of gas in the latest Paleocene; simulating first-order effects of massive dissociation of oceanic methane hydrate. *Geology*, 25 (3): 259-262.

Dickens, G. R., O'Neil, J. R., Rea, D. K., and Owen, R. M., 1995. Dissociation of oceanic methane hydrate as a cause of the carbon isotope excursion at the end of the Paleocene. *Paleoceanography*, 10 (6): 965-971.

Field, B. D., and Browne, G. H., 1989. *Cretaceous and Cenozoic sedimentary basins and geological evolution of the Canterbury region, South Island, New Zealand*. New Zealand Geological Survey Basin Studies 2. 94 p.

Field, B. D., Uruski. C. I. *et al.*, 1997. *Cretaceous-Cenozoic geology and petroleum systems of the East Coast region, New Zealand*. Institute of Geological and Nuclear Sciences monograph 19. 301 p, 7 enclosures. Lower Hutt, New Zealand: Institute of Geological and Nuclear Sciences Limited.

Hancock, H. J. L., Chaproniere, G. C., Dickens, G. R., and Henderson, R. A., 2002. Early Palaeogene planktic foraminiferal and carbon isotope stratigraphy, Hole 762C, Exmouth Plateau, northwest Australian margin. Journal of *Micropalaeontology*, 21 (2): 29-42.

Hollis, C. J., Dickens, G. R., Field, B. D., Hancock, H. J. L., Jones, C. M. and Strong, C. P., 2001. *Early Paleogene biosiliceous facies events in the SW Pacific*. Climate and Biota of the Early Paleogene. Northwest College, Powell, Wyoming, Smithsonian Institution. Pp 43.

Hollis, C. J., Field, B. D., Jones, C. M., Killops, S. D., Strong, C. P., and Dickens, G. R., 2000a. New Zealand perspective on global change from late Cretaceous to early Eocene: (a) the Paleocene-Eocene transition at Mead Stream, Marlborough. *GFF* ,122: 71-72.

Hollis, C. J., Jones, C. M., Dickens, G. R., Field, B. D., and Strong, C. P., 2000b. *Age and origin of the Waipawa (black shale) formation*. (2000: Victoria University of Wellington).

Hornibrook, N.de B., Brazier, R. C., and Strong, C. P., 1989. *Manual of New Zealand Permian to Pleistocene foraminiferal biostratigraphy*. Wellington, Department of Scientific and Industrial Research (DSIR). 175 p.

Huber, B. T., 1991. Paleogene and early Neogene planktonic foraminifer biostratigraphy of sites 738 and 744, Kerguelen Plateau (southern Indian Ocean). *Proc. ODP Sci. Res.*, 119: 427-449.

Jenkins, D. G., 1966. Planktonic foraminiferal zones and new taxa from the Danian to lower Miocene of New Zealand. *New Zealand Journal of Geology and Geophysics*, 8: 1088-1126.

Jenkins, D. G., 1971. New Zealand Cenozoic planktonic foraminifera. Wellington, Department of Scientific and Industrial Research (DSIR). 278 p.

Jenkins, D. G. 1974. Paleogene planktonic foraminifera of New Zealand and the Austral region. *Journal of Foraminiferal Research*, 4: 155-170.

Jenkins, D. G., 1985. Southern mid-latitude Paleocene to Holocene planktic foraminifera. *In* Bolli, H. M., Saunders, J. B., Perch-Nielsen, K., (Eds.), *Plankton Stratigraphy*. Cambridge. Pp. 263-283.

Kaiho, K., Arinobu, T., Ishiwatari, R., Morgans, H. E. G., Okada, H., Takeda, N., Tazaki, K., Zhou, G., Kajiwara, Y., Matsumoto, R., Hirai, A., Niitsuma, N., and Wada, H., 1996. Latest Paleocene benthic foraminiferal extinction and environmental changes at Tawanui, New Zealand. *Paleoceanography*, 11 (4): 447-465.

Katz, M. E., Pak, D. K., Dickens, G. R., and Miller, K. G., 1999. The source and fate of massive carbon input druing the latest Paleocene thermal maximum. *Science*, 286: 1531-1533.

Kelly, D. C., Bralower, T. J., Zachos, J. C., Premoli-Silva, I., and Thomas, E., 1996. Rapid diversification of planktonic foraminifera in the tropical Pacific (ODP Site 865) during the late Paleocene thermal maximum. *Geology*, 24 (5): 423-426.

Kelly, D.C., 2002. Response of Antarctic (ODP Site 690) planktonic foraminifera to the Paleocene-Eocene thermal maximum; faunal evidence for ocean/climate change. *Paleoceanography*, 17 (4), 1071, doi:10.1029/2002PA000761.

Kennett, J. P. and Stott, L., 1991. Abrupt deep-sea warming, palaeoceanographic changes and benthic extinctions at the end of the Paleocene. *Nature*, 353: 225-229.

Killops, S. D., Hollis, C. J., Morgans, H. E. G., Sutherland, R., Field, B. D., and Leckie, D. A., 2000. Paleoceanographic significance of late Paleocene dysaerobia at the shelf/slope break around New Zealand. *Palaeogeography, Palaeoclimatology, Palaeoecology*, 156 (1-2): 51-70.

King, P. R., Naish, T. R., Browne, G. H., Field, B. D., and Edbrooke, S. W., 1999. *Cretaceous to Recent sedimentary patterns in New Zealand*. Folio Series 1. Lower Hutt, Institute of Geological and Nuclear Sciences.

Koch, P. L., Zachos, J., and Dettman, D. L., 1992. Correlation between isotope records in marine and continental carbon reservoirs near the Paleocene/Eocene boundary. *Nature*, 358: 319-322.

Lensen., 1962: *Sheet 16 - Kaikoura*. Geological map of New Zeland 1:250 000. Wellington, Department of Scientific and Industrial Research.

Lu, G., and Keller, G., 1993. The Paleocene-Eocene transition in the Antarctic Indian Ocean; inference from planktic foraminifera. *Marine Micropaleontology*, 21 (1-3): 101-142.

Lu, G., and Keller, G., 1995. Planktic foraminiferal faunal turnovers in the subtropical Pacific during the late Paleocene to early Eocene. *Journal of Foraminiferal Research*, 25 (2): 97-116.

Morgans, H. E. G., Scott, G. H., Beu, A. G., Graham, I. J., Mumme, T. C., St. George, W., and Strong, C. P., 1996. *New Zealand Cenozoic timescale (version 11/96)*. Institute of Geological & Nuclear Sciences Science Report: 12.

van Morkhoven, F. P. C. M., Berggren, W. A., and Edwards, A. S., 1986. Cenozoic cosmopolitan deep-water benthic foraminifera. *Pau, France, Societe Nationale Elf Aquitaine*. 421 p.

Norris, R. D., and Röhl, U., 1999. Carbon cycling and chronology of climate warming during the Palaeocene/Eocene transition. *Nature*, 401: 775-778.

Olsson, R. K., Hemleben, C., Berggren, W. A. and Huber, B. T., 1999. *Atlas of Paleocene Planktonic Foraminifera*. Smithsonian Contribution to Paleobiology 85. 252 p.

Peters, R. B., and Sloan, L. C., 2000. High concentrations of greenhouse gases and polar stratospheric clouds: A possible solution to high-latitude faunal migration at the latest Paleocene thermal maximum. *Geology*, 28 (11): 979-982.

Reay, M. B., 1993. *Geology of the Clarence Valley*. Scale 1:50,000. Institute of Geological and Nuclear Sciences geological map 10: 1 sheet + 144 p. Institute of Geological and Nuclear Sciences, Lower Hutt.

Robert, C., and Kennett, J. P., 1992. Paleocene and Eocene kaolinite distribution in the South Atlantic and Southern Ocean, Antarctic climatic and paleoceanographic implications. *Marine Geology*, 103 (1-3): 99-110.

Schmitz, B., Pujalte, V., and Nunez-Betelu, K., 2001. Climate and sea-level perturbations during the Initial Eocene Thermal Maximum, evidence from siliciclastic units in the Basque Basin (Ermua, Zumaia and Trabakua Pass), northern Spain. *Palaeogeography, Palaeoclimatology, Palaeoecology*, 165 (3-4): 299-320.

Stott, L. D., and Kennett, J. P., 1990: Antarctic Paleogene planktonic foraminifer biostratigraphy, ODP Leg 113, Sites 689 and 690. *Proc. ODP Sci. Res.*, 113: 549-565.

Strong, C. P., Hollis, C. J., and Wilson, G. J., 1995. Foraminiferal, radiolarian, and dinoflagellate biostratigraphy of Late Cretaceous to middle Eocene pelagic sediments (Muzzle Group), Mead Stream, Marlborough, New Zealand. *New Zealand Journal of Geology and Geophysics*, 38 (2): 171-209.

Tjalsma, R. C., and Lohmann, G. P., 1983. Paleocene-Eocene bathyal and abyssal benthic foraminifera from the Atlantic Ocean. *Micropaleontology Special* Publication, 4. 1-90.

Thomas, E., and Shackleton, N. J., 1996. The Paleocene-Eocene benthic foraminiferal extinction and stable isotope anomalies. *In* Knox, R. W. O. B., Corfield, R. M., and Dunay, R. E., (Eds.), *Correlation of the early Paleogene in Northwest Europe*. Geological Society Special Publication, 101: 401-441.

Thomas, E., Shackleton, N. J., and Hall, M. A., 1992. Data report; Carbon isotope stratigraphy of Paleogene bulk sediments, Hole 762C (Exmouth Plateau, eastern Indian Ocean). *Proc. ODP Sci Res.*, 122: 897-901.

Toumarkine, M., and Luterbacher, H., 1985. Paleocene and Eocene planktic foraminifera. *In* Bolli, H. M., Saunders, J. B., and Perch-Nielsen, K. (Eds.), *Plankton Stratigraphy*. Cambridge. Pp. 87-154.

Zachos, J. C., and Dickens, G. R., 2000. An assessment of the biogeochemcial feedback response to the climatic and chemical perturbations of the LPTM. *GFF*, 122: 188-189.

Zachos, J., Pagani, M., Sloan, L., Thomas, E., and Billups, K., 2001. Trends, rhythms, and aberrations in global climate 65 Ma to present. *Science*, 292 (5517): 686-693.

APPENDIX 1

List of foraminiferal taxa occurring at Dee Stream.

Planktic Foraminifera

Acarinina mckannai (White 1928)
Acarinina nitida (Martin 1943)
Acarinina primitiva (Finlay 1947)
Acarinina pseudotopilensis Subbotina 1953
Acarinina quetra (Bolli 1957b)
Acarinina soldadoensis (Bronnimann 1952)
Acarinina subsphaerica (Subbotina 1947)
Acarinina wilcoxensis (Cushman & Ponton 1932)
Chiloguembelina crinita (Glaessner 1937b)
Chiloguembelina trinitatensis (Cushman & Renz 1942)
Chiloguembelina wilcoxensis (Cushman & Ponton 1932)
Globanomalina australiformis (Jenkins 1965)
Morozovella aequa (Cushman & Renz 1942)
Morozovella gracilis (Bolli 1957a)
Morozovella lensiformis (Subbotina 1953)
Morozovella marginodentata (Subbotina 1953)
Morozovella subbotinae (Morozova 1939)
Pseudohasterigina wilcoxensis (Cushman & Ponton 1932)
Subbotina patagonica (Todd & Kniker 1952)
Subbotina triangularis (White 1928)
Subbotina triloculinoides (Plummer 1926)
Subbotina velascoensis (White 1928)
Zeauvigerina parri (Finlay 1939)
Zeauvigerina teuria (Finlay 1947)
Zeauvigerina waiparaensis (Jenkins 1965)
Zeauvigerina zealandica (Finlay 1939)

BENTHIC FORAMINIFERA

Alabamina dissonata (Cushman & Renz 1948)

Allomorphina whangaia Finlay 1940

Anomalinoides capitata Guembel 1868

Anominaloides orbiculus (Stache 1865)

Bulimina tuxpamensis (Cole 1928)

Gavelinella beccariiformis (White 1928)

Gyroidina girardanus (Reuss 1851)

Nuttallides carinotruempyi (Nuttall 1930)

Oridorsalis umbonatus (Phleger & Parker 1951)

Osangularia mexicana (Cole 1927)

Pullenia quinqueloba (Reuss 1851)

Valvulineria advena Cushman & Seigfus 1939

Valvulineria teuriensis (Leoblich & Tappan.1939)

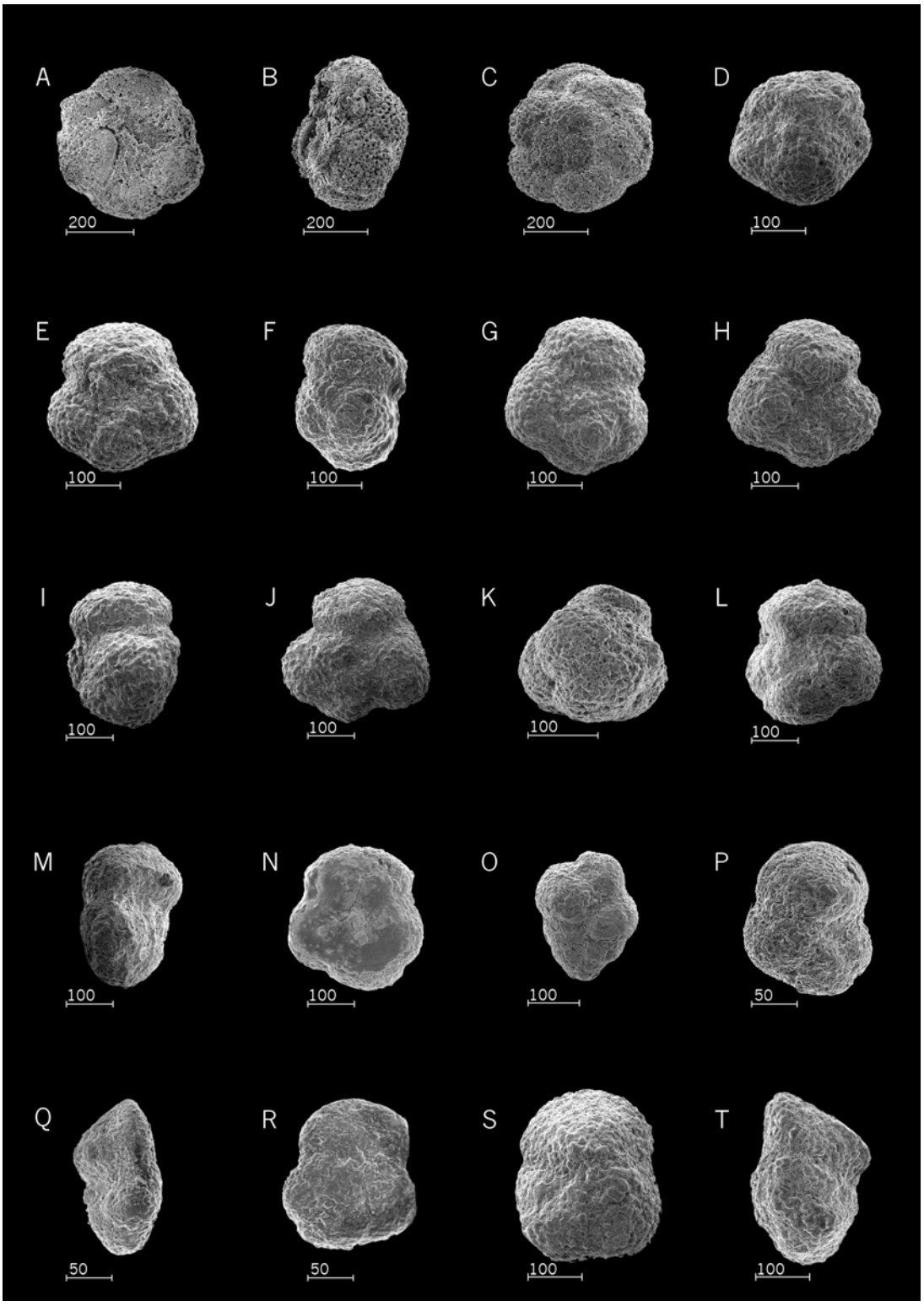

Plate 1. Scanning electron micrographs of Teurian - Mangaorapan foraminifera from the Muzzle Group section at Dee Stream. All scale bars in μm. **A, B, C,** *Acarinina mckannai* (White 1928). A, ventral view; B, side view; C, spiral view. P30/f1337. **D,** *Acarinina primitiva* (Finlay 1947). Ventral view. P30/f1298. **E, F, G,** *Acarinina pseudotopilensis* (Bronnimann 1952). E, ventral view; F, side view; G, spiral view. **H, I, J,** *Acarinina soldadoensis* (Bronnimann 1952). H, ventral view; I, side view; J, spiral view. P30/f1247. **K,** *Acarinina subsphaerica* (Subbotina 1947). Side view. P30/f1247. **L, M, N,** *Acarinina wilcoxensis* (Cushman & Ponton 1932). L, ventral view; M, side view; N, spiral view. P30/f1298. **O,** *Chiloguembelina wilcoxensis* (Cushman & Ponton 1932). Side view. P30/f1248. **P, Q, R,** *Globanomalina australiformis* (Jenkins 1965). P, ventral view; Q, side view; R, spiral view. P30/f1247. **S, T,** *Morozovella aequa* (Cushman & Renz 1942). S, ventral view; T, side view. P30/f1247.

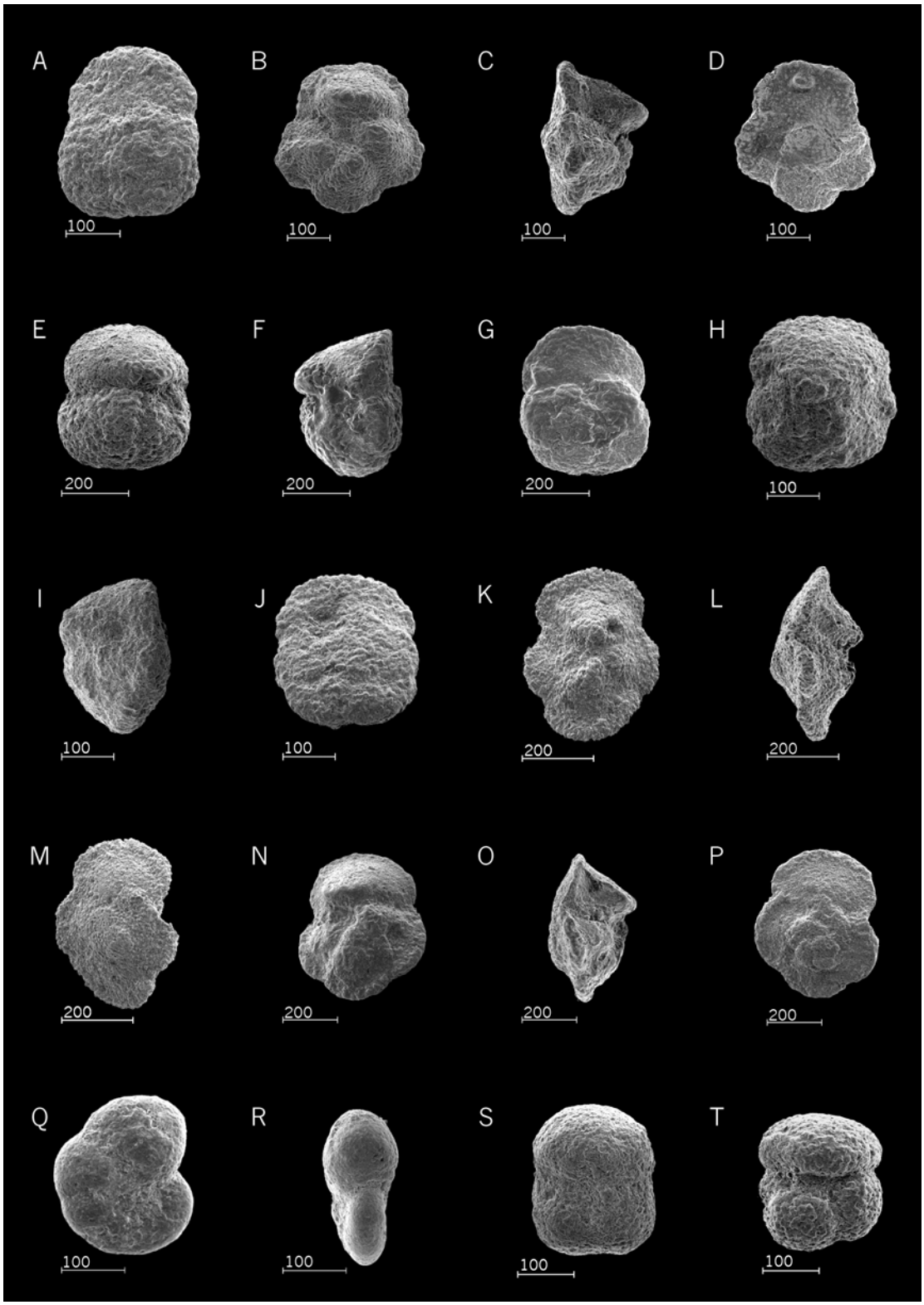

Plate 2. Scanning electron micrographs of Teurian - Mangaorapan foraminifera from Muzzle Group section at Dee Stream. All scale bars in μm. **A,** *Morozovella aequa* (Cushman & Renz 1942). Spiral view. P30/f1247. **B, C, D,** *Morozovella gracilis* (Bolli, 1957a). B, ventral view; C, side view; D, spiral view. P30/f1247. **E, F, G,** *Morozovella lensiformis* (Subbotina 1953), '*dolabrata* type'. E, ventral view; F, side view; G, spiral view. P30/f1248. **H, I, J,** *Morozovella lensiformis* (Subbotina 1953). H, ventral view; I, side view; J, spiral view. P30/f1247. **K, L, M,** *Morozovella marginodentata* (Subbotina 1953). K, ventral view; L, side view; M, spiral view. P30/f1247. **N, O, P,** *Morozovella subbotinae* (Morozova 1939). N, ventral view; O, side view; P, spiral view. P30/f1248. **Q, R,** *Pseudohasterigina wilcoxensis* (Cushman & Ponton 1932). Q, ventral view; R, side view. P30/f1249. **S,** *Subbotina patagonica* (Todd & Kniker 1952). Ventral view. P30/f1247. **T,** *Subbotina velascoensis* (White 1928). Ventral view. P30/f1247.

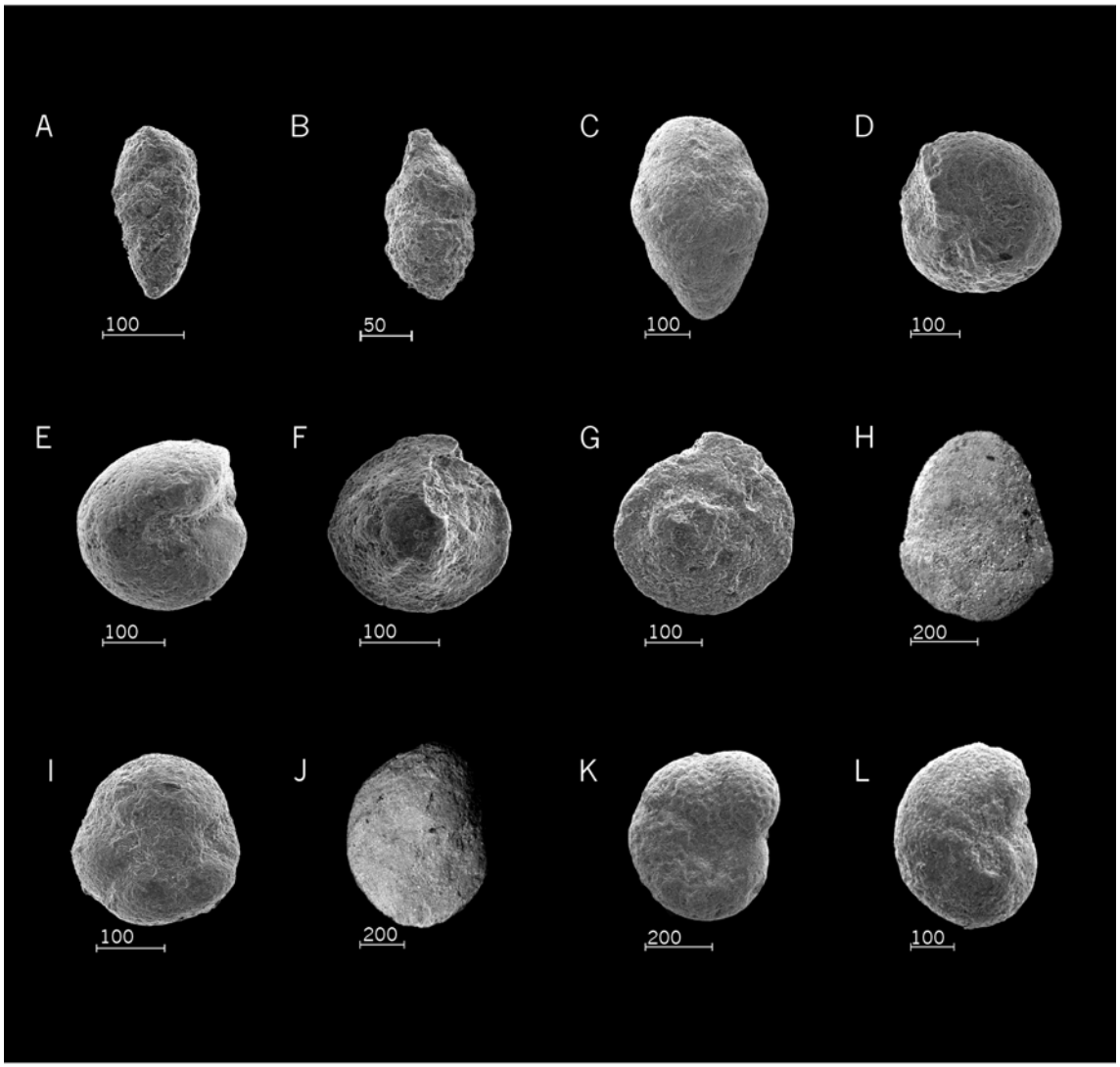

Plate 3. Scanning electron micrographs of Teurian - Mangaorapan foraminifera from Muzzle Group section at Dee Stream. All scale bars in μm. **A,** *Zeauvigerina waiparaensis* (Jenkins 1965). Side view. P30/f1269. **B,** *Zeauvigerina zealandica* Finlay 1939. Side view. P30/f1269. **C,** *Bulimina tuxpamensis* Cole, 1928. Side view. P30/f1247. **D,** *Gavelinella beccariiformis* (White 1928). Ventral view. P30/f1342. **E,** *Gyroidina girardanus* (Reuss, 1851). Ventral view. P30/f1247. **F,** *Nuttallides carinotruempyi* (Nuttall 1930). Ventral view. P30/f1247. **G,** *Oridorsalis umbonatus* (Phleger & Parker 1951). Spiral view. P30/f1247. **H,** *Allomorphina whangaia* Finlay 1940. Ventral view. P30f/1299. **I,** *Valvulineria advena* Cushman & Seigfus 1939. Ventral view. P30/f1296. **J,** *Valvulineria teuriensis* (Leoblich & Tappan.1939). Ventral view. P30/f1337. **K,** *Anomalinoides aotea* (Finlay 1940). Ventral view. P30/f1248. **L,** *Anominaloides orbiculus* (Stache 1865), Ventral view. P30/f1256.

CHAPTER 6

FORAMINIFERAL ASSEMBLAGES AND STABLE CARBON ISOTOPES ACROSS THE PALAEOGENE CARBONATE FACIES OF THE PERTH ABYSSAL PLAIN.

Abstract. This study determines bulk carbonate content, describes planktic and benthic foraminiferal assemblages, stable isotope compositions of bulk carbonate and *Nuttallides truempyi* (benthic foraminifer), and non-carbonate mineralogy across ~30 m of carbonate-rich Palaeogene sediment from Deep Sea Drilling Project (DSDP) Site 259, on Perth Abyssal Plain off Western Australia.. Carbonate content, mostly reflecting nannofossil abundance, ranges from 3 to 80%, generally exceeding 50% between 35 and 57 mbsf. A clay-rich horizon with a carbonate content of about 37% occurs between 55.17 to 55.37 mbsf. The carbonate-rich sequence spans planktic foraminiferal Zones P4c to P6b (~57-52 Ma), with the clay-rich horizon near the base of our Zone P5 (upper) – P6b. Throughout the studied interval, benthic foraminifera dominate foraminiferal assemblages, with scarce planktic foraminifera usually of poor preservation and limited species diversity. A prominent Benthic Foraminiferal Extinction Event (BFEE) occurs across the clay-rich horizon and an influx of large *Acarinina* occurs immediately above it. The $\delta^{13}C$ records of bulk carbonate and *Nuttallides truempyi* exhibit trends similar to those observed in Upper Paleocene-Lower Eocene (~57-52 Ma) sediment from other locations. Two successive decreases in bulk carbonate and *N. truempyi* $\delta^{13}C$ of 0.5‰ and 1.0‰ characterize the interval at and immediately above the BFEE. Despite major changes in carbonate content, foraminiferal assemblages and carbon isotopes, the mineralogy of the non-carbonate fraction consistently comprises expanding clay, heulandite (zeolite), quartz, feldspar (sodic or calcic), minor mica, and pyrolusite (MnO_2). The uniformity of this mineral assemblage suggests that Site 259 received similar non-carbonate sediment before,

during and after pelagic carbonate deposition. The carbonate plug at Site 259 likely represents a drop in the CCD from ~57 to 52-51 Ma recognized at other locations.

INTRODUCTION

Deep ocean temperatures and concentrations of total dissolved inorganic carbonate underwent profound changes during the early Palaeogene (~60-50 Ma), as observed in a characteristic series of shifts in the oxygen and carbon isotopic compositions ($\delta^{18}O$ and $\delta^{13}C$) of benthic foraminiferal carbonate (e.g., Zachos *et al.*, 2001) (**Fig. 1**). The most prominent $\delta^{13}C$ high of the Cenozoic occurred during the Late Paleocene (~59-56 Ma), a time of thermal transition from relatively cool to moderate temperatures. Presumably, this Paleocene Carbon Isotope Maximum (PCIM) reflects massive deposition of organic carbon (Shackleton and Hall, 1984), although the location of this output remains uncertain (Corfield, 1994; Kurtz *et al.*, 2003; Hollis *et al.*, 2005). The PCIM was followed by continued rise in deep ocean temperatures and a decline in $\delta^{13}C$ values in benthic foraminiferal carbonate. At least one brief event marked by extreme warming and a negative Carbon Isotope Excursion (CIE) punctuated these trends during the Basal Eocene Thermal Maximum (BETM), which began at the Paleocene/Eocene (P/E) boundary ~55.5 Ma. The aberrant $\delta^{13}C$ spike signifies a massive injection of ^{13}C-depleted carbon, possibly methane generated by dissociation of gas hydrates (Dickens *et al.*, 1997; Katz *et al.*, 1999). After the CIE and a short, partial rebound to earlier conditions, global $\delta^{13}C$ records plunged to low values over an interval characterized by several P/E-like events or hyperthermals between ~53 to 50 Ma, which coincide with peak Cenozoic temperatures, a time referred to as the Early Eocene Climatic Optimum (EECO) (Thomas and Zachos, 2000; Thomas *et al.*, 2000; Cramer *et al.*, 2003; Lourens *et al.*, 2005).

Oceanic carbonate deposition removes a large fraction of carbon from the ocean and, ultimately, the atmosphere (Kump and Arthur, 1999; Katz *et al.*, 2005). However, this output is spatially heterogeneous because extensive regions of the seafloor lie beneath the calcite compensation depth (CCD), a horizon marking the lower limit of carbonate occurrence in marine sediment, reflecting the saturation state of calcite in deep seawater (Murray and Renard, 1891; Peterson, 1966). Physiochemical conditions

of the deep ocean, especially pressure, temperature and the activities of Ca^{2+} and CO_3^{2-}, regulate the CCD (Valyashko *et al.*, 1989; Pearson and Palmer, 2000; Tyrrell and Zeebe, 2003). The ratio of organic to inorganic carbonate flux also effects preservation of carbonate on the seafloor (Archer and Maier-Reimer, 1994; Mekik *et al.*, 2002). In areas of high surface water productivity carbonate can rapidly build up on the seafloor, as seen in the 'equatorial bulge'. One consequence of these controls is that the modern CCD varies from 4400 m below sea level (mbsl) (and 600 m deeper at the equatorial bulge) in the cold, CO_2-rich bottom waters of the Pacific (van Andel *et al.*, 1975; Berger *et al.*, 1976) to 5200 mbsl in the relatively warm, CO_2-deficient bottom waters of the Atlantic (Berger and von Rad, 1972). The CCD in the Indian Ocean is intermediate between the Atlantic and the Pacific (Farrell and Prell, 1989). It also shoals towards the continental margins and towards polar regions (Berger and Winterer, 1973).

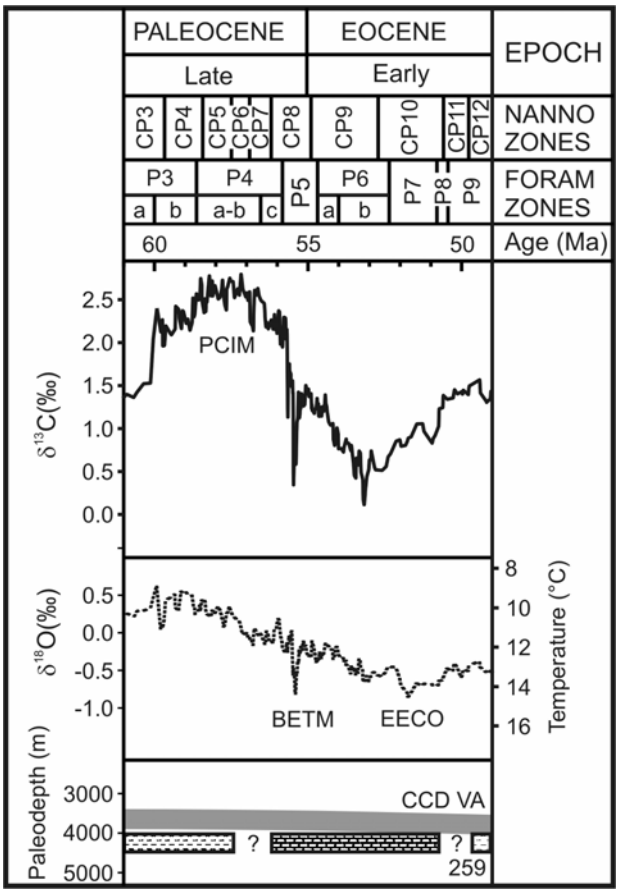

Figure 1. Global carbon and oxygen isotope curves constructed from benthic foraminiferal isotope data (adapted from Zachos *et al.*, 2001, p. 688). Calcite compensation depth (CCD) for the Indian Ocean adapted from van Andel *et al.* (1975) (grey band). Also included is a temporal approximation of the ~30 m thick carbonate sequence bounded by red clays at Site 259.

In a classic paper, van Andel *et al*. (1975) constructed CCD curves for the Pacific and Indian Oceans from Late Jurassic to present-day, and modified a similar curve from the Atlantic Ocean (Berger and von Rad, 1972). These curves, which have remained the standard for models of global geochemical cycling (e.g., Tyrrell and Zeebe, 2003), show the CCD fluctuating by more than 1200 m over the last 50 myr. Given major changes in deep ocean temperature, carbon cycling and the overall environment during the early Palaeogene, one might predict significant fluctuations in the CCD to have occurred between 60 and 50 Ma. However, established compilations (Berger and von Rad, 1972; van Andel *et al.*, 1975) show a fairly shallow (~3.5 km) and relatively unchanging (<200 m) CCD in all oceans during this time (**Fig. 1**).

The long-term CCD curves generated by van Andel *et al*., (1975) used sections recovered by scientific drilling prior to 1975. The palaeodepths of Deep Sea Drilling Project (DSDP) sites were backtracked over time, and dated intervals of carbonate and clay were projected onto these trajectories. However, some intervals of Lower Palaeogene sediment were either not recognized or specifically excluded, and short-term events were not included in the reconstruction. One example is the ~3 m thick carbonate-poor unit at ~150 m below seafloor (mbsf) at DSDP Site 213 in the northeast Indian Ocean. This horizon, perhaps overlooked in 1975 because it lies atop basement, marks the BETM (Ravizza *et al.*, 2001) and a rapid shoaling of the CCD in intermediate waters at this site in response to massive carbon input (Dickens *et al.*, 1997). Of particular interest to this investigation is a 31 m thick section of Lower Palaeogene carbonate sandwiched between clay at DSDP Site 259 in the eastern Indian Ocean. Preliminary interpretations suggested that this section reflected a drop in the CCD (Shipboard Scientific Party, 1974), but it was omitted in the compilations by van Andel *et al*. (1975) because, at the time, "a temporary deepening of the CCD [during the early Palaeogene seemed] unreasonable in the light of other evidence".

Two recent studies highlight a potential problem with the van Andel *et al*. (1975) CCD curve. Zachos *et al*. (2004) have presented Cenozoic records of carbonate accumulation on Walvis Ridge in the southeast Atlantic Ocean, and Hancock and Dickens (2005) have published Palaeogene records of carbonate dissolution on Shatsky Rise in the north Pacific. Both sets of records show an interval of high carbonate accumulation and preservation between ~57 and 51 Ma, suggesting a significant drop in

the CCD during this time and prompting us to re-examine the calcareous interval at Site 259. We establish the nature and timing of this carbonate "plug", and argue that it may represent a deepening of the CCD from the Late Paleocene to the Early Eocene (~57-52 Ma) comparable with records from Walvis Ridge and Shatsky Rise.

SITE 259 AND LOWER PALAEOGENE ABYSSAL CARBONATE

DSDP Site 259 is on Perth Abyssal Plain off the western Australian margin, southern Indian Ocean (**Fig. 2**). At present, the site lies at 29˚37.05'S, 112˚41.78'E, and 4696 m below seal level (mbsl). During the early Palaeogene, however, Site 259 was much farther south, probably at approximately 55ºS (Ocean Drilling Stratigraphic Network (www.odsn.de).

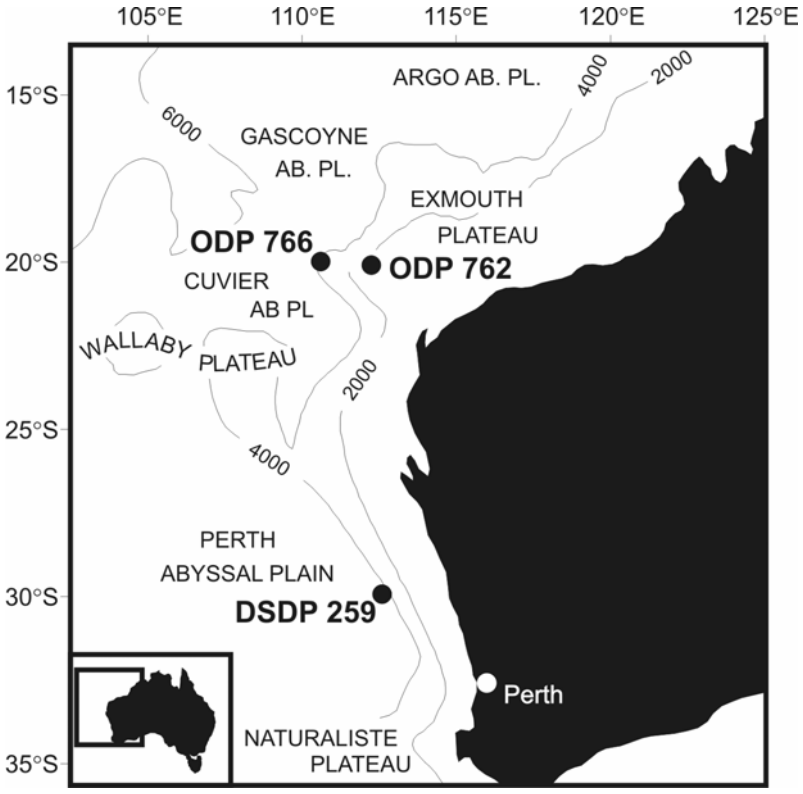

Figure 2. Location of DSDP Site 259 (Perth Abyssal Plain) ODP Sites 762 (Exmouth Plateau) and 766 (Gascoyne Abyssal Plain).

At Site 259, DSDP drilled through 304 m of pelagic sediment and 42 m of basalt (Shipboard Scientific Party, 1974). The basalt is tholeiitic, similar to modern mid-ocean ridges (Robinson and Whitford, 1974; Thompson *et al.*, 1978). It presumably formed at

a ridge in the Early Cretaceous, based on the regional tectonic history and the conformable contact with overlying Aptian sediment (Thompson *et al.*, 1978; Veevers and Tayton, 1985). Assuming normal subsidence and a typical water depth for the center of mid-ocean ridges (2500 m), the site likely lay beneath 4000 m of water during the Late Cretaceous and early Palaeogene (van Andel *et al.*, 1975). Indeed, from the late Albian to the middle Paleocene, the sedimentary sequence comprises zeolitic clay, suggesting a depth below the CCD (Shipboard Scientific Party, 1974). However, yellowish orange lower Palaeogene nannofossil clay and ooze was recovered between 60 and 29 mbsf (**Fig. 3**). Lower Palaeogene nannofossil ooze outcrops on the seafloor 10 km south of Site 259, where the water is about 100 m deeper (Shipboard Scientific Party, 1974). This suggests a regionally extensive deposit of lower Palaeogene pelagic or hemipelagic carbonate. At Site 259, the calcareous section is overlain by 26 m of zeolitic clay and Quaternary foraminiferal-bearing nannofossil ooze.

Initial biostratigraphic work indicated that the calcareous section was deposited in the Late Paleocene through Early Eocene. Five complete Late Paleocene to Early Eocene nannofossil zones were identified (Proto-Decima, 1974, Table 3, p. 593). These include the *Discoaster multiradiatus, Tribrachiatus contortus, Discoaster binodosus, Tribrachiatus orthostylus,*and *Discoaster lodoensis* Zones and correspond to Zones CP8 through CP11 following Berggren *et al*. (1995) (**Fig. 3**). Drilling disturbance or sediment redeposition apparently caused some repetition of zones (Proto-Decima, 1974). The carbonate plug could represent a time of atypical sediment supply from shallower depths. However, the regional extent of Lower Palaeogene carbonate deposition suggests it is *in situ*. Both the nannofossil and planktic foraminiferal assemblages are dominated by dissolution-resistant taxa (Krasheninnikov, 1974; Proto-Decima, 1974). Planktic and benthic foraminifera were examined by Krasheninnikov (1974), but without information on sample depths, a range chart, or photographic documentation of taxa. His main findings of this work were: (1) planktic foraminifera are rare but benthic foraminifera are relatively common, (2) the planktic foraminiferal assemblages comprised the *Globorotalia velascoensis* (= *Morozovella velascoensis*), *Gl. subbotinae* (= *M. subbotinae*), and *Gl. formosa formosa* (= *M. formosa*) Zones, and (3) these assemblages are probably affected by dissolution. The Paleocene/Eocene Boundary, either as originally defined or currently correlated to the start of the BETM

(Aubry *et al.*, 2003), was not located (Krasheninnikov, 1974). To our knowledge, no stable isotope records have been generated for this interval.

Site 259, probably situated between 4000 and 4500 m water depth in the early Palaeogene (van Andel *et al.*, 1975), is one of very few locations drilled to date with core suitable for monitoring changes in deep water conditions and the CCD from 60 to 50 Ma. However, the available information makes it difficult to place the observed record into a palaeoceanographic context.

SAMPLES AND METHODS

Sixty sediment samples of ~20 cm^3 were collected from 20 to 62 mbsf, a section which spans the calcareous interval (**Fig. 3**). Samples were generally collected every 1 m, but after initial examination of foraminiferal assemblages (below), sampling frequency was increased to every 20 cm over the Paleocene-Eocene transition.

All samples were freeze-dried to remove pore water, lightly homogenized, and divided into two portions. A ~5 cm^3 portion was crushed to determine bulk carbonate content and isotopic composition. A ~10 cm^3 portion was wet sieved at 63 μm and dried to examine sediment characteristics and foraminifera.

Carbonate contents were analyzed using the "Karbonate-Bombe" method (Mueller and Gastner, 1971). Approximately 200 mg of dried and crushed sample was placed into a glass beaker along with a vial containing ~10 mL of 10% HCl. The beaker was sealed with a top connected to a water filled hose and graduated cylinder marked at 1 mL gradations. The sample and acid were mixed together, and the liberated CO_2 gas was measured from the displacement of water. Carbonate contents were determined from a calibration curve constructed by measuring the CO_2 evolved from known masses of laboratory grade $CaCO_3$. All samples were analyzed twice to increase precision. A sample of Palaeogene siliceous limestone (JCU sample MS14) with a known $CaCO_3$ content of 72 wt% was also analyzed three times to evaluate accuracy and precision. These analyses rendered a $CaCO_3$ content of 72 wt% ± 1.5 wt%.

The second dried portion was passed through a microsplitter and separated into two aliquots for optical microscope examination of foraminifera. One aliquot was analyzed for sediment characteristics and planktic foraminifera, the other for benthic foraminifera. Because planktic foraminifera are rare (Krasheninnikov, 1974), many specimens were examined using a Jeol JSM 5410LV scanning electron microscope (SEM) at the James Cook University Advanced Analytical Centre (JCU-AAC). Foraminiferal samples were mounted on aluminium stubs and platinum coated. The accelerating voltage was set at 10kV. Secondary electron images were collected using a Jeol slow scan digitizing system.

Planktic foraminiferal species were identified and named in accordance with established Paleocene (Olsson *et al.,* 1999) and Eocene classifications (Toumarkine and Luterbacher, 1985). Eocene species were discussed with Bill Berggren and Dick Olsson in personal communications. To establish sediment age, planktic foraminiferal assemblages were placed into the zonal scheme presented of Berggren *et al*. (1995), with modifications by Olsson *et al*. (1999) and Hancock *et al.* (2002). The latter work details the early Palaeogene planktic foraminiferal assemblages at ODP Site 762 off northwest Australia (**Fig. 2**).

Benthic foraminifera were picked from the >63 µm size fraction and determined to the species level for common or palaeoenvironmentally significant taxa. Generic assignment was made for other taxa. For instance, no species were determined within the group of *Laevidentalina* spp. and unilocular genera. Taxonomy at the generic level follows Loeblich and Tappan (1988); that at the specific level follows Tjalsma and Lohmann (1983), van Morkhoven *et al*. (1986), Thomas (1990), Nomura (1991), Bolli *et al*. (1994), Widmark (1997), and Alegret and Thomas (2001). Data are given in a presence/absence format. We followed van Morkhoven *et al*. (1986) in palaeobathymetric assignments.

Samples of bulk carbonate and *Nuttallides truempyi* specimens were used to determine stable isotope compositions. *Nuttallides* is a common, long ranging benthic foraminiferal genus found throughout the bathyal-abyssal regions of the oceans in the Late Cretaceous through Eocene, and commonly used for isotope work, including recent global compilations (Zachos *et al.*, 2001; Katz *et al.*, 2003). Although *Nuttallides*

truempyi shows little variation in $\delta^{13}C$ across size fractions, only average sized specimens (125 to 250 µm diametre) were used. Thirty to forty specimens from each sample were analyzed. An initial set of samples was analyzed at the Earth Sciences Centre, Gothenburg, Sweden, with a VG Prism Series II mass spectrometer attached to an Isocarb preparation system. A later set of samples was analyzed at the Department of Geological Sciences, University of California, Santa Barbara, with a Finnigan MAT 251 mass spectrometer connected to a carousel-48 automated carbonate preparation device, which has a common reaction vessel (orthophosphoric acid). Analytical precision was less than 0.1‰ for both sets of analyses. Oxygen isotopes were determined for all samples, but are not discussed in this paper.

Some components of the calcareous interval may have arrived via downslope transport (Proto-Decima, 1974). To address this issue the mineralogy of the non-carbonate fraction was examined in six samples that came from below, within and above the carbonate interval. Dried and crushed samples were reacted with 10% HCl to remove $CaCO_3$. Resulting slurries were rinsed with H_2O several times, and dried in an oven at 40˚C for two days. Samples were prepared as powder mounts where approximately 0.5 g of sample was recrushed and packed into a plastic cavity mount. Analyses were conducted using a Siemens D5000 X-ray Diffractometer housed at the JCU-AAC. This instrument is fitted with a Copper tube (Cu Kα = 1.54178 Å), operating at 40 kV and 30 mA, and a post-diffraction graphite monochromator. Samples were scanned from 1.3º to 65º 2θ in steps of 0.02º 2θ at 2.4 s per step.

RESULTS

Carbonate Contents

Carbonate content varies over the studied interval from 3% to 80% (**Table 1**; **Fig. 3**), and generally increased from 29 mbsf to a broad high between 35 and 57 mbsf, where values usually exceed 50%. The carbonate content then declined steadily, dropping to less than 7% by 60 mbsf. Overall, the values and trend agree with the limited measurements made previously (Bode, 1974), and the shipboard descriptions of “light brown nannofossil clay and ooze” (Shipboard Scientific Party, 1974). Crucially, no sample analyzed between 35 and 57 mbsf has a carbonate content less than 37%.

Table 1. Carbonate content (wt%) this study and Shipboard Scientific Party (1974). Grey shaded area is BETM interval.

Sample: Leg, Hole, Core, Section, Interval (cm)	Depth (mbsf)	Carbonate Content (wt%) (this study)	Depth (mbsf)	Carbonate Content (wt%) (ship)
27-259-3R-2, 110-116	20.10	4.19	27.2	1
27-259-4R-1, 60-65	28.06	4.78	30.2	26
27-259-4R-2, 100-105	29.96	23.62	33.2	41
27-259-4R-3, 22-26	30.68	21.43	38.2	39
27-259-4R-4, 60-65	32.56	12.03	39.7	37
27-259-4R-4, 140-144	33.36	46.10	42.7	60
27-259-4R-5, 57-62	34.03	19.66	46.2	59
27-259-4R-6, 61-66	35.57	60.66	49.2	59
27-259-4R-6, 120-124	36.16	62.84	52.2	64
27-259-5R-1, 103-108	37.53	41.30	55.7	61
27-259-5R-2, 61-66	38.61	51.18	58.7	52
27-259-5R-2, 120-124	39.2	55.77	61.7	1
27-259-5R-3, 61-66	40.11	46.12	65.2	1
27-259-5R-3, 120-124	40.7	51.28		
27-259-5R-4, 61-66	41.61	64.83		
27-259-5R-4, 120-124	42.2	58.17		
27-259-5R-5, 56-61	43.06	69.64		
27-259-5R-5, 120-124	43.7	74.76		
27-259-6R-1, 51-56	47.06	56.01		
27-259-6R-1, 120-124	47.75	55.17		
27-259-6R-2, 51-56	48.56	59.95		
27-259-6R-2, 120-124	49.25	70.52		
27-259-6R-3, 51-56	50.06	68.31		
27-259-6R-3, 100-104	50.55	71.70		
27-259-6R-4, 51-56	51.56	57.54		
27-259-6R-4, 66-70	51.71	55.36		
27-259-6R-4, 80-84	51.85	54.82		
27-259-6R-4, 100-104	52.05	66.11		
27-259-6R-4, 120-124	52.25	56.49		
27-259-6R-4, 140-144	52.45	64.07		
27-259-6R-5, 20-24	52.75	61.55		
27-259-6R-5, 51-56	53.06	56.86		
27-259-6R-5, 60-64	53.15	59.07		
27-259-6R-5, 80-84	53.35	59.34		
27-259-6R-5, 100-104	53.55	59.21		
27-259-6R-5, 120-124	53.75	62.28		
27-259-6R-5, 140-144	53.95	68.92		
27-259-6R-6, 20-24	54.25	70.27		
27-259-6R-6, 40-44	54.45	69.88		
27-259-6R-6, 51-56	54.56	62.99		
27-259-6R-6, 60-64	54.65	56.44		
27-259-6R-6, 80-84	54.85	70.46		
27-259-6R-6, 100-104	55.05	70.72		
27-259-6R-6, 112-115	55.17	79.61		
27-259-6R-6, 115-118	55.2	37.94		
27-259-6R-6, 120-124	55.25	40.23		
27-259-6R-6, 140-144	55.45	61.25		
27-259-7R-1, 20-24	55.70	53.92		
27-259-7R-1, 40-44	55.90	49.02		
27-259-7R-1, 60-65	56.10	55.14		
27-259-7R-1, 120-124	56.7	53.35		
27-259-7R-2, 62-65	57.62	56.42		
27-259-7R-2, 120-124	58.2	37.82		
27-259-7R-3, 66-69	59.16	34.11		
27-259-7R-3, 120-124	59.7	25.68		
27-259-7R-4, 52-57	60.52	6.46		
27-259-7R-4, 116-120	61.16	2.70		
27-259-7R-5, 51-56	62.01	21.44		
27-259-8R-1, 80-85	65.80	6.29		

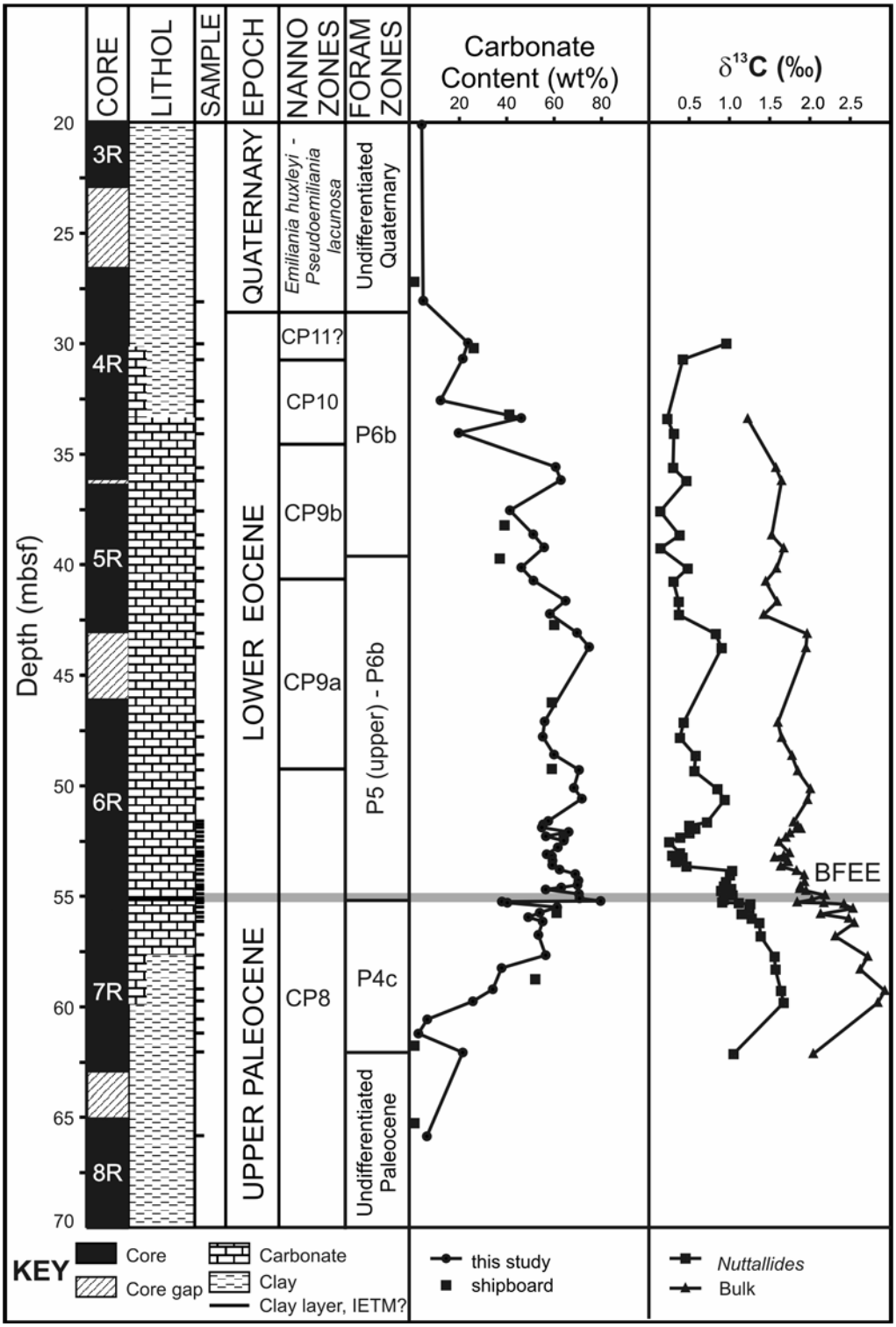

Figure 3. Core lithology, sample location, and shipboard nannofossil biostratigraphy Site 259 (Proto-Decima, 1974), bulk carbonate content, and carbon isotope signatures for Site 259.

Again, this concurs with shipboard descriptions, which do not indicate any clay horizons within this depth interval.

Planktic Foraminiferal Biostratigraphy

Planktic foraminifera are absent in samples from below (>62.01 mbsf) and above (<20.10 mbsf) the calcareous interval. Within the carbonate plug, planktic foraminifera are usually poorly preserved, showing heavy secondary calcite overgrowths and effects of dissolution (**Plates 1, 2**). They consistently comprise <5% of the >63 µm size fraction. Consequently, many samples have no identifiable planktic foraminiferal specimens, and benthic foraminifera typically far outnumber planktic foraminifera (generally 20:1), indicating severe dissolution. Of the impoverished planktic foraminiferal assemblages, the thick-walled *Acarinina* and *Subbotina* generally dominate samples below 50 mbsf, whereas *Chiloguembelina wilcoxensis* dominates samples above 50 mbsf. This generally agrees with Krasheninnikov (1974). The planktic foraminiferal assemblages are too dissolved to resolve the repetition of nannofossil biozones observed by Proto-Decima (1974).

Despite the preservation and rarity of planktic foraminifera, some samples have assemblages with stratigraphically important species (**Plates 1, 2**). On the basis of first appearance datums (FADs) or last appearance datums (LADs) of these species, the calcareous interval ranges approximately from Subzone P4c to Zone P6b of the sub-tropical global scheme, or ~57-52 Ma (Berggren *et al.*, 1995) (**Table 2; Fig. 3**).

Zone P4c (62.01-55.17 mbsf). The FAD of the primary marker species, *Acarinina soldadoensis* occurs at 55.7 mbsf. The FAD of *Acarinina coalingensis*, a secondary marker species, also occurs at this depth. However, it is unlikely that these FADs mark the true first appearance of these species because the preservation of planktic foraminifera is so poor below 55.7 mbsf. *Chiloguembelina wilcoxensis* and *Acarinina nitida* both first occur at 62.01 mbsf. The co-occurrence of these species identifies lowermost Subzone P4c (Olsson *et al.*, 1999). The domination of assemblages by *Acarinina* and *Subbotina* is typical for mid-high latitude locations (e.g., Stott and Kennett, 1990; Quillevere and Norris, 2003).

Table 2. Planktic foraminiferal biostratigraphy, Site 259. Gray shaded area is the BETM interval and black line denotes BFEE.

			Planktic Foraminifera																		
Sample	**Depth (mbsf)**	**Foram Zone (Berggren *et al.*, 1995)**	***Acarinina nitida***	***Subbotina velascoensis***	***Chiloguembelina wilcoxensis***	***Chiloguembelina crinita***	***Subbotina spp***	***Acarinina mckannai***	***Acarinina soldadoensis***	***Acarinina coalingensis***	***Globanomalina spp.***	***Acarinina primitiva***	***Acarinina wilcoxensis***	***?Acarinina subsphaerica***	***Zeauvigerina zealandica***	***Morozovella subbotinae***	***?Globigerinatheka senni***	***Morozovella lensiformis***	***Species 1.***
27-259-3R-2, 110-116	20.10	**?**																	
27-259-4R-1, 60-65	28.06																		
27-259-4R-2, 100-105	29.96						X												
27-259-4R-3, 22-26	30.68																		
27-259-4R-4, 60-65	32.56					X				X									
27-259-4R-4, 140-144	33.36																		X
27-259-4R-5, 57-62	34.03	**P6b**			X		X												
27-259-4R-6, 61-66	35.57				X														
27-259-4R-6, 120-124	36.16				X				X	X			X		X				
27-259-5R-1, 103-108	37.53			X	X		X		X	X									
27-259-5R-2, 61-66	38.61						X												
27-259-5R-2, 120-124	39.20				X	X	X					X			X		X	X	X
27-259-5R-3, 61-66	40.11				X				X										
27-259-5R-3, 120-124	40.70																		
27-259-5R-4, 61-66	41.61				X														
27-259-5R-4, 120-124	42.20				X		X								X				
27-259-5R-5, 56-61	43.06																		
27-259-5R-5, 120-124	43.70				X		X		X	X		X		X	X	X			
27-259-6R-1, 51-56	47.06				X														
27-259-6R-1, 120-124	47.75				X				X										
27-259-6R-2, 51-56	48.56						X												
27-259-6R-2, 120-124	49.25				X	X	X		X	X		X							
27-259-6R-3, 51-56	50.06			X	X						X								
27-259-6R-3, 100-104	50.55																		
27-259-6R-4, 51-56	51.56						X												
27-259-6R-4, 66-70	51.71																		
27-259-6R-4, 80-84	51.85																		
27-259-6R-4, 100-104	52.05																		
27-259-6R-4, 120-124	52.25																		
27-259-6R-4, 140-144	52.45																		
27-259-6R-5, 20-24	52.75																		
27-259-6R-5, 51-56	53.06				X	X													
27-259-6R-5, 60-64	53.15				X														
27-259-6R-5, 80-84	53.35				X														
27-259-6R-5, 100-104	53.55																		
27-259-6R-5, 120-124	53.75				X		X			X			X	X					
27-259-6R-5, 140-144	53.95																		
27-259-6R-6, 20-24	54.25																		
27-259-6R-6, 40-44	54.45																		
27-259-6R-6, 51-56	54.56				X	X	X			X									
27-259-6R-6, 60-64	54.65																		
27-259-6R-6, 80-84	54.85																		
27-259-6R-6, 100-104	55.05																		
27-259-6R-6, 112-115	55.17	**P5 (upper) - P6a**	X						X	X	X	X	X						
27-259-6R-6, 115-118	55.20																		
27-259-6R-6, 120-124	55.25																		
27-259-6R-6, 140-144	55.45																		
27-259-7R-1, 20-24	55.70		X					X	X	X									
27-259-7R-1, 40-44	55.90																		
27-259-7R-1, 60-65	56.10																		
27-259-7R-1, 120-124	56.70						X												
27-259-7R-2, 62-65	57.62	**P4c**																	
27-259-7R-2, 120-124	58.20																		
27-259-7R-3, 66-69	59.16																		
27-259-7R-3, 120-124	59.70																		
27-259-7R-4, 52-57	60.52																		
27-259-7R-4, 116-120	61.16																		
27-259-7R-5, 51-56	62.01		X	X	X	X													
27-259-8R-1, 80-85	65.80	**?**																	

Krasheninnikov (1974) assigned Cores 8, 7 and 6 (and tentatively the bottom of core 5) to the Upper Paleocene *Acarinina acarinata* (= *A. nitida*) Zone, noting, that *A. acarinata* was the most common species below 40 mbsf. Other species identified by this author included *Acarinina mckannai*, *A. primitiva*, *A.* sp., *Globigerina chascanona*, *G. nana*, *Chiloguemblina* aff. *wilcoxensis*, and rare *Globorotalia* aff. *acuta*. These species are representative of Zone P4c (Berggren *et al.*, 1995). A P4c planktic foraminiferal zonation for this depth interval is consistent with the CP8 nannofossil Zone suggested by Proto-Decima (1974).

Zone P5 (upper) – P6a (55.17-39.2 mbsf). The primary marker species for the base of this zone, *Globanomalina psuedomenardii*, is absent at Site 259. However, the FAD of *Acarinina wilcoxensis* occurs within upper Zone P5 in the tropical-subtropical scheme (Berggren *et al.*, 1995). This datum is recognized at 55.17 mbsf, allocating it to Zone P5. Large and robust variants of *A. coalingensis* dominate the foraminiferal assemblages at 55.17 mbsf. An abrupt increase in large and robust variants of *A. coalingensis* and *A. soldadoensis* has been reported at other high southern latitude sites during the BETM (Kelly, 2002). The FAD of *A. primitiva*, which is the more quadrate chambered end member form of the *A .coalingensis - A. primitiva lineage*, occurs at 55.17 mbsf. Although this datum approximates the base of Zone P7 in some locations (Huber, 1991; Kelly, 2002), it marks the P/E boundary at other high southern latitude sites (Hancock *et al.*, 2003; Hollis *et al.*, 2005). *Morozovella subbotinae* was identified in one sample at 43.70 mbsf and this species is a very common constituent of Zone P5 through P6a assemblages elsewhere (Olsson *et al.*, 1999).

The LAD of *Morozovella velascoensis* marks the base of Subzone P6a (Berggren *et al.*, 1995), but this species was not present at Site 259, so that Zones P5 and P6a, cannot be discriminated. *Morozovella velascoensis* is a tropical species, and absent or extremely rare at many high to middle latitude sites (e.g., Hancock *et al.*, 2002; Zachos *et al.*, 2004).

Krasheninnikov (1974) assigned most of this depth interval to the Upper Paleocene *Acarinina acarinata* Zone and could not identify the P/E boundary. On the basis of nannofossils, the boundary was placed at either 36.5 (Shipboard Scientific Party, 1974) or 41.4 mbsf (Proto-Decima, 1974). This is inconsistent with planktic

foraminifera assemblages described in this study (and other information, below), which indicate the P/E boundary is at ~55.17 mbsf. The definition of the P/E boundary in deep-sea sections was generally controversial until the recent definition of this boundary at the base of the CIE (Dupuis *et al.*, 2003), and in most DSDP/ODP sites, nannofossil and planktic foraminiferal defined boundaries did not coincide.

Subzone P6b (39.2-27 mbsf). The FAD of *Morozovella lensiformis* marks the base of this subzone and occurs at 39.2 mbsf. Planktic foraminiferal assemblages are characterized by *Acarinina primitiva, A. soldadoensis*, *Chiloguembelina wilcoxensis*, *Ch. Trinitatensis* and *Zeauvigerina zealandica*, all typically found in P6b assemblages elsewhere (Berggren and Olsson, pers. comm., 2004/2005).

Although we identified very few planktic foraminifera in samples from above Core 5 (i.e., 36.5 msf, **Table 2**), Krasheninnikov (1974) found casts of *Morozovella aequa*, *M. subbotinae* and *M. marginodentata* in Section 3 of Core 4. This core was thus assigned to the *Globorotalia subbotinae* (= *Morozovella subbotinae*) and the *Gl. formosa formosa* (= *M. formosa*) Zones (lower part of Lower Eocene). These observations are in good agreement with the CP9b nannofossil zonal allocation suggested by Proto-Decima (1974).

Undifferentiated. Samples from sediment intervals below and above the calcareous unit are assigned to undifferentiated Upper Paleocene and undifferentiated Upper Quaternary respectively on the basis of nannofossils (Proto-Decima, 1974).

Benthic Foraminifera

The composite faunal list for benthic foraminifera comprises 82 mostly calcareous taxa (**Table 3**), some of which are documented (**Plates 3, 4, 5**). The high diversity is common for the Paleocene (e.g., Nomura, 1991; Thomas and Zachos, 1999). Preservation is generally moderate, but varies strongly between samples. The size of benthic foraminiferal specimens varies significantly within each sample, so that common species such as *Nuttallides truempyi* are represented by moderate (125-250 µm) and very large (>250-300 µm) specimens.

Table 3. Paleocene and Eocene benthic foraminiferal presence/absence data for Hole 259. The BFEE is between 55.25 to 55.17 mbsf.

			Benthic Foraminifera																																								
Sample	**Depth (mbsf)**	**Preservation**	*Abyssamina poagi*	*Abyssamina quadrata*	*Alabamina creta*	*Alabamina dissonata*	*Allomorphina* sp.	*Anomalinoides globosus*	*Anomalinoides spissiformis*	*Anomalinoides* sp.	*Aragonia aragonensis*	*Aragonia velascoensis*	*Arenobulimina* sp.	*Barbysiphon* sp.	*Bolivinoides* sp. (small)	*Bulimina kugleri*	*Bulimina simplex*	*Bulimina thanetensis*	*Bulimina trinitatensis*	*Bulimnella* spp.	*Chrysalogonium tenuicostatum*	*Cibicidoides hyphalus*	*Cibicidoides praemundulus*	*Cibicidoides pseudoperlucidus*	*Cibicidoides proprius*	*Cibicidoides velascoensis*	*Clavulinoides* spp.	*Clinapertina complanata*	*Clinapertina inflata*	*Clinapertina subplanispira*	*Ellipsoidinid species*	*Parsenkoina* sp.	*Globocassidulina subglobosa*	*Gaudryina arenata*	*Gaudryina laevigata*	*Globobulimina* sp.	*Glomospira* spp.	*Gyroidinoides beisselli*	*Gyroidinoides globosus*	*Gyroidinoides quadratus*	*Gyroidinoides* spp.	*Heronallenia* spp.
27-259-4R-5, 57-62	34.03	M-P	X	X				X	X		X		X			X						X		X				X	X	X		X						X	
27-259-5R-3, 61-66	38.61	M	X	X					X	X	X		X			X	X		X		X		X	X			X			X	X		X	X						X
27-259-6R-2, 120-124	49.25	M	X	X			X		X	X			X			X	X				X		X	X					X	X	X	X	X		X		X			X	
27-259-6R-3, 100-104	50.55	P		X					X							X			X	X	X			X						X		X				X			X	X
27-259-6R-4, 66-70	51.71	M		X					X					X		X				X				X					X	X	X	X	X		X					X	
27-259-6R-4, 140-144	52.45	M		X					X				X	X		X					X			X						X	X	X	X								
27-259-6R-5, 100-104	53.55	M	X	X					X					X		X	X						X	X				X		X	X	X	X						X	X	X
27-259-6R-5, 120-124	53.75	M		X					X							X			X					X						X	X	X	X								
27-259-6R-5, 140-144	53.95	M		X					X				X	X		X			X					X						X	X	X	X						X		
27-259-6R-6, 20-24	54.25	M		X					X				X			X	X				X		X	X					X	X	X	X	X								
27-259-6R-6, 40-44	54.45	M		X					X				X			X	X													X	X	X	X								X
27-259-6R-6, 51-56	54.56	M		X					X				X		X	X					X		X					X	X	X	X	X	X								
27-259-6R-6, 60-64	54.65	M		X					X					X		X	X							X						X	X	X	X								
27-259-6R-6, 80-84	54.85	M		X					X				X	X		X														X	X	X	X								
27-259-6R-6, 100-104	55.05	M		X					X				X			X	X					X							X	X	X	X	X						X		
27-259-6R-6, 112-115	55.17	M	X	X					X				X			X	X						X						X	X	X	X	X								
27-259-6R-6, 115-118	55.20	M		X	X				X							X		X				X	X				X		X	X							X			
27-259-6R-6, 120-124	55.25	M		X			X		X			X		X				X				X		X			X		X	X		X					X	X		X	
27-259-6R-6, 140-144	55.45	M		X					X	X		X						X				X		X	X		X		X								X	X			
27-259-7R-1, 20-24	55.70	M		X					X			X	X	X	X	X		X		X	X	X		X			X	X	X	X	X	X	X				X	X		X	
27-259-7R-1, 40-44	55.90	M		X		X		X	X			X	X					X				X	X	X		X	X	X	X	X							X	X			
27-259-7R-1, 60-65	56.10	M		X	X			X	X			X	X				X	X	X	X	X	X			X	X	X	X	X		X						X	X	X	X	
27-259-7R-1, 120-124	56.70	M		X				X	X				X					X	X	X		X		X			X	X		X	X				X		X	X		X	
27-259-7R-2, 62-65	57.62	M		X					X			X						X		X		X		X			X	X		X						X				X	
27-259-7R-2, 120-124	58.20	M		X	X							X						X	X	X		X	X	X			X		X	X	X							X			
27-259-7R-3, 66-69	59.16	M-G		X				X	X			X						X		X		X	X	X			X	X	X								X	X		X	
27-259-7R-3, 120-124	59.70	P-M					X	X	X									X		X		X	X				X		X								X	X			
27-259-7R-4, 52-57	60.52	P-B																																								
27-259-7R-5, 51-56	62.01	M	X	X					X			X		X	X	X	X	X			X	X		X					X	X			X				X		X		X	

Table 3 cont.

Benthic Foraminifera																																									
Laevidentalina, Dentalina spp.	*Lenticulina* spp.	*Marginulina* spp.	*Marssonella oxycona*	*Marssonella trochoides*	*Neoflabellina semireticulata*	*Nodosaria* spp.	*Nonion havanense*	*Nononella robusta*	*Nonionella* sp.	*Nuttallides umbonifera*	*Nuttallides truempyi*	*Nuttallinella florealis*	*Nuttallinella* spp.	*Oridorsalis umbonatus*	*Orthomorphina* spp.	*Paralabamina hillebrandti*	*Paralabamina lunata*	polymorphinid taxa	pleurostomellid taxa	*Pullenia coryelli*	*Pullenia jarvisi*	*Quadrimorphina profunda*	*Rectobulimina carpentierae*	*Rhizammina* spp.	*Rhizehakina epigona*	*Siphogenerinoides brevispinosa*	*Siphonodosaria hispidula*	*Siphonodosaria lepidula*	*Siphonodosaria pomuligera*	*Siphotextularia* spp.	*Spiroplectammina spectabilis*	*Stensioeina beccariiformis*	*Tappanina selmensis*	*Textularia* sp.	*Tritaxia havanensis*	*Turrilina brevispira*	unilocular taxa	*Vaginulina* sp.	sum taxa	**Sample**	**Depth (mbsf)**
X	X						X	X			X			X		X		X	X			X							X					X						27-259-4R-5, 57-62	34.03
X							X	X		X	X			X		X			X			X											X				X			27-259-5R-3, 61-66	38.61
X		X					X	X			X			X		X			X			X				X		X	X				X			X	X			27-259-6R-2, 120-124	49.25
X							X	X			X			X					X			X											X				X			27-259-6R-3, 100-104	50.55
X							X	X		X	X			X			X	X	X			X		X																27-259-6R-4, 66-70	51.71
X							X	X		X	X			X					X			X				X				X			X							27-259-6R-4, 140-144	52.45
X							X	X			X			X					X			X		X		X		X		X			X	X			X			27-259-6R-5, 100-104	53.55
X								X			X			X					X			X				X							X				X			27-259-6R-5, 120-124	53.75
X								X			X			X				X	X			X				X							X				X			27-259-6R-5, 140-144	53.95
X								X			X			X					X			X				X							X				X			27-259-6R-6, 20-24	54.25
X											X			X					X			X				X											X			27-259-6R-6, 40-44	54.45
X								X			X			X				X	X			X				X							X			X	X			27-259-6R-6, 51-56	54.56
X								X			X			X					X			X				X							X				X			27-259-6R-6, 60-64	54.65
X								X			X			X					X			X											X				X			27-259-6R-6, 80-84	54.85
X		X					X	X			X			X		X		X	X			X											X				X			27-259-6R-6, 100-104	55.05
X								X			X			X					X			X				X							X							27-259-6R-6, 112-115	55.17
X							X	X			X			X		X	X		X	X		X										X			X		X			27-259-6R-6, 115-118	55.20
X	X	X		X			X	X			X	X		X		X	X	X		X	X		X					X			X	X			X		X			27-259-6R-6, 120-124	55.25
X	X		X	X			X				X	X		X		X	X	X		X		X				X	X				X	X			X					27-259-6R-6, 140-144	55.45
X			X				X	X			X	X	X	X		X		X	X		X	X				X	X	X			X	X	X		X	X	X			27-259-7R-1, 20-24	55.70
X			X	X			X	X			X	X	X	X		X	X	X	X	X		X			X	X	X	X			X	X			X		X			27-259-7R-1, 40-44	55.90
X				X			X	X			X	X	X	X		X	X	X	X	X	X	X	X			X					X	X			X		X			27-259-7R-1, 60-65	56.10
X	X		X	X		X	X	X			X		X	X		X	X	X		X	X		X			X	X	X			X	X	X		X		X			27-259-7R-1, 120-124	56.70
X			X	X			X	X			X	X	X	X		X	X	X	X	X	X		X			X		X			X	X			X		X			27-259-7R-2, 62-65	57.62
X			X	X	X		X	X	X		X	X	X	X	X	X	X	X	X	X	X		X	X		X	X	X			X	X			X		X			27-259-7R-2, 120-124	58.20
X	X		X	X			X	X	X		X	X	X	X		X	X	X	X	X		X				X		X			X	X			X		X			27-259-7R-3, 66-69	59.16
X			X	X			X	X			X			X		X			X	X						X	X				X	X			X					27-259-7R-3, 120-124	59.70
																																								27-259-7R-4, 52-57	60.52
			X				X	X			X	X		X		X		X	X	X	X	X					X					X	X				X			27-259-7R-5, 51-56	62.01

The benthic foraminiferal extinction is recognized between samples 27-259-6R6, 115-118 (55.20 mbsf) and 27-259-6R6, 112-115 (55.17 mbsf). Across this interval, several cosmopolitan taxa have their LAD including the calcareous *Stensioeina beccariiformis*, *Pullenia coryelli*, *Gyroidinoides globosus* and *Buliminia thanetensis*, and the agglutinated taxa *Tritaxia havanensis* and *Clavulinoides* spp. (**Table 3**). A consequence is a significant drop in species 'richness' defined as the number of species identified per sample (**Fig. 4**). A prominent Benthic Foraminiferal Extinction Event (BFEE) has been observed at many locations, correlated to the base of the CIE, thus the P/E boundary by definition (e.g., Thomas, 1998). Reworking of typically Paleocene species in high samples is relatively common. But reworked specimens can generally be recognized by poor preservation.

Closely spaced samples across the BFEE at other locations often reveal a short (~20 cm) 'post-extinction' interval where benthic foraminiferal assemblages are characterized by extremely low diversity and the occurrence of very small, thin-walled tests (e.g., Thomas, 1998). This succession is not found at Site 259 which may suggest an incomplete record near the start of the BETM. Post extinction faunas at Site 259 are dominated by abyssaminid species, *Quadrimorphina profunda* and *Nuttallides truempyi*, similar to post-extinction faunas at deep sites on Walvis Ridge (e.g., Thomas and Shackleton, 1996; Zachos *et al.*, 2004). The 'missing interval' at Site 259, therefore appears to represent a short duration, possibly a few thousand to <20 kyr (Thomas, 1998).

All samples examined for benthic foraminifera contain large, commonly rounded quartz grains. The occurrence of the large terrigenous grains as well as the wide size variance in benthic foraminifera of the same species suggest that downslope transport, perhaps by turbidity currents, has contributed some material to almost all samples. However, such transport seems to have been largely coeval with deposition, because excluding zones of drilling disturbance, all stratigraphic indicators, including nannofossil assemblages, planktic and benthic foraminiferal assemblages, and carbon isotope variations (below) occur in a systematic and expected order.

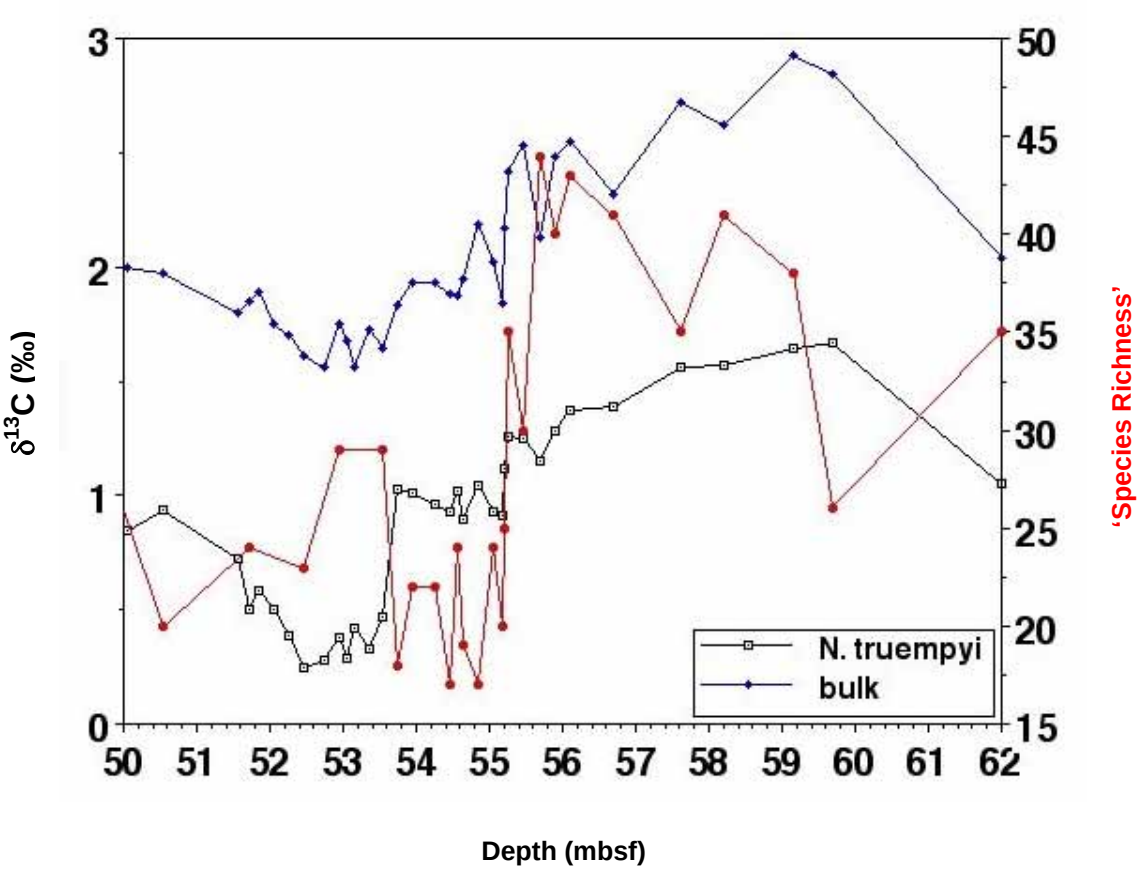

Figure 4. Benthic foraminiferal 'species richness' (sum of different taxa including genera and larger groups) and carbon isotope signatures of bulk sediment and *Nuttallides truempyi*, Site 259.

Carbon Isotopes

Bulk carbonate $\delta^{13}C$ varies from 1.23‰ to 2.93‰, defining a basic curve over the calcareous interval (**Table 4; Fig. 3**). The $\delta^{13}C$ is distinctly high between 59.7 and 55.45 mbsf where values range from 2‰ to 3‰. From 55.45 to 55.17 mbsf, and across the clay-rich horizon and BFEE, $\delta^{13}C$ declines by 0.69‰. After a thin 1.62 m interval of relatively constant $\delta^{13}C$, values drop by another 0.28‰, and reach a minimum of 1.56‰ at 52.75 mbsf. Bulk carbonate $\delta^{13}C$ increases to 2.0‰ at 50.06 mbsf, and then generally decreases over the remainder of the sampled section, reaching a low of 1.23‰ at 33.36 mbsf.

Table 4. Bulk carbonate and *Nuttallides truempyi* carbon and oxygen isotopes, Site 259. Grey shaded area is BETM interval.

Sample: Leg, Core, Section, Interval (cm)	Depth (mbsf)	*N. truempyi* $\delta^{13}C$	*N. truempyi* $\delta^{18}O$	Bulk $\delta^{13}C$	Bulk $\delta^{18}O$
27-259-3R-2, 110-116	20.10	-	-	-	-
27-259-4R-1, 60-65	28.06	-	-	-	-
27-259-4R-2, 100-105	29.96	0.96	-0.76	-	-
27-259-4R-3, 22-26	30.68	0.42	-0.77	-	-
27-259-4R-4, 60-65	32.56	-	-	-	-
27-259-4R-4, 140-144	33.36	0.23	-0.78	1.23	-0.87
27-259-4R-5, 57-62	34.03	0.31	-0.78	-	-
27-259-4R-6, 61-66	35.57	0.30	-0.49	1.58	-0.89
27-259-4R-6, 120-124	36.16	0.46	-0.43	1.65	-0.75
27-259-5R-1, 103-108	37.53	0.14	0.68	-	-
27-259-5R-2, 61-66	38.61	0.38	-0.66	1.53	-0.65
27-259-5R-2, 120-124	39.20	0.14	-0.65	1.67	-0.54
27-259-5R-3, 61-66	40.11	0.48	-0.53	1.58	-0.72
27-259-5R-3, 120-124	40.70	0.31	-0.59	1.45	-0.97
27-259-5R-4, 61-66	41.61	0.37	-0.54	1.59	-0.76
27-259-5R-4, 120-124	42.20	0.37	-0.52	1.43	-0.92
27-259-5R-5, 56-61	43.06	0.83	-0.31	1.97	-0.64
27-259-5R-5, 120-124	43.70	0.90	-0.42	1.95	-0.60
27-259-6R-1, 51-56	47.06	0.43	-0.63	1.60	-0.86
27-259-6R-1, 120-124	47.75	0.39	-0.57	1.65	-0.60
27-259-6R-2, 51-56	48.56	0.58	-0.51	1.78	-0.61
27-259-6R-2, 120-124	49.25	0.57	-0.41	1.85	-0.78
27-259-6R-3, 51-56	50.06	0.85	-0.27	2.00	-0.66
27-259-6R-3, 100-104	50.55	0.94	-0.32	1.97	-0.54
27-259-6R-4, 51-56	51.56	0.72	-0.30	1.80	-0.60
27-259-6R-4, 66-70	51.71	0.50	-0.52	1.85	-0.65
27-259-6R-4, 80-84	51.85	0.58	-0.47	1.89	-0.53
27-259-6R-4, 100-104	52.05	0.50	-0.46	1.75	-0.69
27-259-6R-4, 120-124	52.25	0.39	-0.55	1.70	-0.72
27-259-6R-4, 140-144	52.45	0.25	-0.61	1.61	-0.76
27-259-6R-5, 20-24	52.75	0.28	-0.57	1.56	-0.83
27-259-6R-5, 51-56	53.06	0.29	-0.70	1.68	-0.65
27-259-6R-5, 60-64	53.15	0.42	-0.66	1.56	-0.68
27-259-6R-5, 80-84	53.35	0.33	-0.64	1.73	-0.60
27-259-6R-5, 100-104	53.55	0.47	-0.64	1.64	-0.71
27-259-6R-5, 120-124	53.75	1.03	-0.55	1.83	-0.84
27-259-6R-5, 140-144	53.95	1.01	-0.53	1.93	-0.94
27-259-6R-6, 20-24	54.25	0.96	-0.56	1.93	-0.87
27-259-6R-6, 40-44	54.45	0.93	-0.46	1.88	-0.98
27-259-6R-6, 51-56	54.56	1.02	-0.50	1.87	-0.90
27-259-6R-6, 60-64	54.65	0.90	-0.59	1.95	-0.78
27-259-6R-6, 80-84	54.85	1.04	-0.48	2.19	-0.96
27-259-6R-6, 100-104	55.05	0.93	-0.44	2.02	-0.72
27-259-6R-6, 112-115	55.17	0.91	-0.35	1.84	-0.68
27-259-6R-6, 115-118	55.20	1.12	-0.36	2.17	-0.96
27-259-6R-6, 120-124	55.25	1.26	-0.35	2.42	-0.85
27-259-6R-6, 140-144	55.45	1.25	-0.14	2.53	-0.37
27-259-7R-1, 20-24	55.70	1.15	-0.39	2.13	-0.87
27-259-7R-1, 40-44	55.90	1.28	-0.23	2.48	-0.51
27-259-7R-1, 60-65	56.10	1.37	-0.06	2.55	-0.42
27-259-7R-1, 120-124	56.70	1.39	-0.14	2.31	-0.80
27-259-7R-2, 62-65	57.62	1.56	-0.08	2.72	-0.32
27-259-7R-2, 120-124	58.20	1.57	-0.15	2.62	-0.99
27-259-7R-3, 66-69	59.16	1.64	-0.20	2.93	-0.60
27-259-7R-3, 120-124	59.70	1.67	-0.09	2.84	-0.85
27-259-7R-4, 52-57	60.52	-	-	-	-
27-259-7R-4, 116-120	61.16	-	-	-	-
27-259-7R-5, 51-56	62.01	1.05	-0.56	2.04	-1.03
27-259-8R-1, 80-85	65.80	-	-	-	-

The *Nuttallides truempyi* carbon isotope record shows a broadly similar range and pattern across the calcareous section, although $\delta^{13}C$ is generally lower by ~1‰ than bulk values in the sample samples (**Table 4; Fig. 3**). Between 62.01 and 55.45 mbsf, $\delta^{13}C$ averages 1.5‰. A 0.35‰ drop in $\delta^{13}C$ to 0.91 ‰ then occurs from 55.45 to 55.17 mbsf. Following a short 1.62 m interval of relatively constant $\delta^{13}C$ values, the values drop again from 1.03‰ at 53.57 mbsf to 0.47‰ at 53.55 mbsf. The 0.60‰ magnitude of this drop is greater than that in bulk carbonate values. The $\delta^{13}C$ reaches a minimum of 0.28‰ at 52.75 mbsf, and then rises to 0.94‰ at 50.55 mbsf. Values remain relatively constant at an average of 0.5‰ for the remainder of the sampled section.

The bulk $\delta^{13}C$ values presumably record the $\Sigma\delta^{13}C$ of CO_2 in surface waters, given that nannofossils dominate bulk sediment. The ~1‰ offset between bulk $\delta^{13}C$ and *Nuttallides truempyi* $\delta^{13}C$, therefore, probably reflects the carbon isotope gradient in the water column. Such a gradient occurs today, and seems to have occurred for much of the Paleocene (Corfield, 1994).

Sediment Characteristics

Within the calcareous interval, benthic and planktic foraminifera comprise <5% of the >63 µm sediment fraction and benthic foraminifera far outnumber planktics. Aeolitic aggregates, Fe-Mn micronodules, terrigenous rounded quartz grains (>250 µm) and metamorphic lithic fragments occur in varying amounts in all samples (**Table 5**). Although the core is highly disturbed, interlayered massive and finely laminated dm-scale intervals can be discriminated. Laminae are typically 1-3 mm thick.

Mineralogy

All six samples analyzed for their carbonate-free mineralogy have similar XRD traces (**Table 6; Fig. 5**). Minerals identified include expanding clay, quartz, heulandite (zeolite), pyrolusite (MnO_2), feldspar (sodic or calcic), and mica. Traces of residual calcite were also detected. Similar minerals were identified by Cooks *et al.* (1974). The results indicate that the non-carbonate fraction of sediment remained the same before, during and after deposition of the calcareous interval.

Table 5. Carbonate content (wt%) and sediment characteristics, Site 259. Very minor = <2%; minor = <5%; common = 5-10%; abundant = 10-20% of bulk sediment. Gray shaded area is BETM.

Sample	Depth (mbsf)	Carbonate Content (wt%)	Sediment Characteristics	
			Colour and Bedding	Transported Material*
27-259-3R-2, 110-116	20.10	4.19	red clay, no layering	common
27-259-4R-1, 60-65	28.06	4.78	not determined	abundant
27-259-4R-2, 100-105	29.96	23.62	not determined	abundant
27-259-4R-3, 22-26	30.68	21.43	not determined	abundant
27-259-4R-4, 60-65	32.56	12.03	not determined	abundant
27-259-4R-4, 140-144	33.36	46.10	cream, thick coarse-grained laminae	abundant
27-259-4R-5, 57-62	34.03	19.66	cream, few laminae	abundant
27-259-4R-6, 120-124	36.16	62.84	cream, massive	not determined
27-259-5R-4, 120-124	42.2	58.17	cream, massive	minor
27-259-6R-1, 120-124	47.75	55.17	cream, few laminae	common
27-259-6R-3, 100-104	50.55	71.70	white, massive	not determined
27-259-6R-4, 66-70	51.71	55.36	cream, few laminae	not determined
27-259-6R-4, 80-84	51.85	54.82	cream, few laminae	minor
27-259-6R-4, 100-104	52.05	66.11	creamy white, massive	minor
27-259-6R-4, 140-144	52.45	64.07	cream, massive	minor
27-259-6R-5, 60-64	53.15	59.07	cream, few laminae	minor
27-259-6R-5, 80-84	53.35	59.34	cream, massive	minor
27-259-6R-5, 100-104	53.55	59.21	cream, massive	minor
27-259-6R-5, 120-124	53.75	62.28	white, massive	not determined
27-259-6R-5, 140-144	53.95	68.92	white, massive	very minor
27-259-6R-6, 20-24	54.25	70.27	white, massive	very minor
27-259-6R-6, 60-64	54.65	56.44	cream, massive	not determined
27-259-6R-6, 80-84	54.85	70.46	white, massive	minor
27-259-6R-6, 100-104	55.05	70.72	white, massive	minor
27-259-6R-6, 112-115	55.17	79.61	white, massive	very minor
27-259-6R-6, 115-118	55.2	37.94	cream, thick coarse-grained laminae	abundant
27-259-6R-6, 140-144	55.45	61.25	white, massive	not determined
27-259-7R-1, 20-24	55.70	53.92	white, few laminae	not determined
27-259-7R-1, 40-44	55.90	49.02	cream, massive	minor
27-259-7R-1, 120-124	56.7	53.35	cream, thick coarse-grained laminae	not determined
27-259-7R-2, 120-124	58.2	37.82	cream, massive	not determined
27-259-7R-3, 120-124	59.7	25.68	cream, few laminae	not determined
27-259-7R-4, 116-120	61.16	2.70	dark cream, thick coarse-grained laminae	majority
27-259-8R-1, 80-85	65.80	6.29	dark purple, common brown laminae	common

Table 6. Mineralogy from powder x-ray diffraction analysis for samples below, within and above the carbonate sequence.

Sample: Leg, Core, Section, Interval (cm)	Depth (mbsf)	Mineral
27-259-4R-3, 17-21	30.63	Expanding clay, quartz, feldspar, heulandite, pyrolusite
27-259-4R-3, 41-44	30.87	Expanding clay, quartz, feldspar, heulandite, pyrolusite
27-259-5R-3, 120-124	40.70	Expanding clay, quartz; feldspar, heulandite, mica
27-259-6R-2, 120-124	49.25	Expanding clay, quartz, feldspar, heulandite, pyrolusite, mica
27-259-7R-4, 116-120	61.16	Expanding clay, quartz, feldspar, heulandite, pyrolusite
27-259-7R-5, 120-124	62.70	Expanding clay, quartz, heulandite, pyrolusite

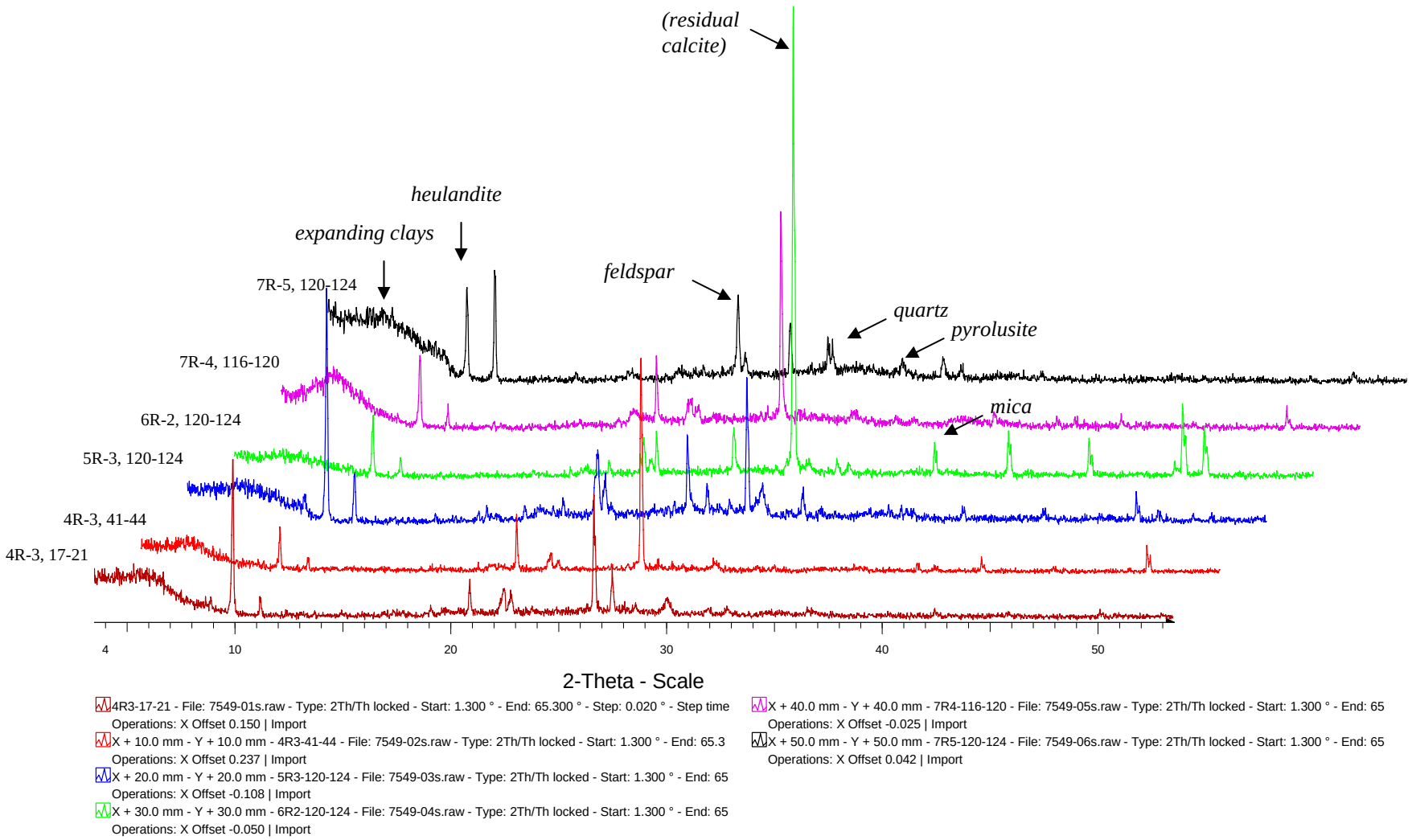

Figure 5. Powder x-ray diffraction analyses of selected samples from Site 259. Two samples are taken from the clay below the carbonate interval, two samples from within the carbonate interval, and two samples from overlying clays

DISCUSSION

A plug of carbonate sediment occurs between 35 and 57 mbsf at Site 259 (**Fig. 3**). Sediment within this interval generally has between 50% and 80 % calcium carbonate, and never drops below 37% (at least in bulk 10 cm^3 samples). Most of this carbonate consists of nannofossils, suggesting a dominantly pelagic origin.

Although planktic foraminifera are generally rare and poorly preserved, their assemblages indicate the calcareous interval was deposited between ~57 and 52 Ma (**Fig. 3**). Carbon isotope curves constructed from bulk carbonate and *Nuttallides truempyi* (**Fig. 3**) exhibit trends that support this timing (**Fig. 1**). Sediment deposited between 62.01 and 55.45 mbsf has foraminiferal assemblages and relatively high $\delta^{13}C$ consistent with Zone P4c and the latter part of the PCIM. Sediment deposited around 55.2 mbsf has an unusual planktic foraminiferal assemblage with large *Acarinina* and a drop in $\delta^{13}C$ consistent with the early stages of the BETM. The BFEE is also recognized at this horizon. Sediment deposited between 55.2 and ~50 mbsf has foraminiferal assemblages and a $\delta^{13}C$ excursion consistent with the main CIE and the following recovery in the latter stage of Zone P5 (upper) - P6a, although this correlation is problematic (below). Sediment deposited from ~50 to 30 mbsf has foraminiferal assemblages and declining, relatively low $\delta^{13}C$ values consistent with Zone P6b, and the drop in $\delta^{13}C$ heading into the low values representative for the EECO.

The 31 m thick Upper Paleocene-Lower Eocene calcareous interval was deposited relatively slowly at accumulation rates averaging 1 cm/kyr. This rate is probably close to the original rate of deposition because the overlying sediment cover is only 29 m so that compaction has been minimal. Slow deposition is consistent with the yellowish orange colour and the presence of pyrolusite (MnO2), which suggests a low flux of organic carbon and oxidized conditions during accumulation.

Calcareous sediment at Site 259 was probably deposited above the CCD but within the lower part of the lysocline. Modern open-ocean locations within this depth interval typically have carbonate contents <70% and sedimentation rates <2 cm/yr, because the relative burial fluxes of biogenic carbonate are similar to those of

background terrigenous aluminosilicate phases (Kennett, 1982). These sites, like the Palaeogene sediment at Site 259, are also characterized by impoverished planktic foraminiferal assemblages dominated by thick-walled species and high ratios of benthic to planktic foraminifera (e.g., Berger, 1968; Thunell, 1976; Williams *et al.*, 1985a; Williams *et al.*, 1985b). We note, however, that planktic foraminiferal assemblages often lack diversity in sediment deposited during the early Palaeogene and at high latitudes (Stott and Kennett, 1990; Huber, 1991). The palaeolocation of Site 259, therefore, may have also contributed to their low diversity.

Site 259 lay beneath 4000 m of water during the early Palaeogene, given the age and composition of basement, and assumptions regarding initial ridge height and thermal subsidence (van Andel *et al.*, 1975). Such a depth cannot be rigorously supported with data from our study, although an abyssal depth for the Paleocene and Eocene is consistent with the benthic foraminiferal assemblages. Irrespective of the absolute palaeodepth, the calcareous interval overlies and underlies carbonate-free zeolitic claystones. There is no evidence for regional tectonism that would have raised the seafloor of Perth Abyssal Plain in the early Palaeogene (Muller *et al.*, 2000). Thus, either some depositional process (e.g., gravity flows) led to preferential accumulation of carbonate-rich sediment during this time, or the CCD dropped between ~57 and 52 Ma. Given evidence for downslope transport at Site 259, one might suggest that the latest Paleocene and earliest Eocene was a time of enhanced delivery of sediment, including carbonate, from shallower locations to Site 259. We re-emphasize the overall pelagic composition and the stratigraphic continuity of the section. Moreover, the non-carbonate fraction of sediment has a similar mineralogical composition before, during, and after the calcareous interval. This suggests similar sediment provenance and transport throughout the early Palaeogene. Overall, the lithological record at Site 259 supports a relatively deep CCD between ~57 and 52 Ma.

The carbonate plug at Site 259 generally correlates in time with an Upper Paleocene-Lower Eocene interval of enhanced carbonate preservation at other locations. ODP Sites 1262 and 1267 lie at 4759 and 4356 mbsl on Walvis Ridge in the southeast Atlantic Ocean (Zachos *et al.*, 2004; Zachos *et al.*, 2005). Calcium carbonate contents are consistently high (>80%) at these sites for sediment deposited from ~57 to 51 Ma, except across the BETM (Shipboard Scientific Party, 2004; Zachos *et al.*, 2005). This

was interpreted to reflect a Late Paleocene-Early Eocene drop in the CCD and lysocline (Zachos *et al.*, 2004) (**Fig. 6**). ODP Sites 1209 and 1211 lie at 2387 and 2907 mbsl on Shatsky Rise in the west central Pacific Ocean (Bralower *et al.*, 2002). Records of carbonate dissolution suggest an interval of high carbonate content and enhanced carbonate preservation from ~57 to 51Ma, again with the exception of the BETM (Hancock and Dickens, 2005; Collosimo in press). This trend has been interpreted as a lowering of the lysocline (Hancock and Dickens, 2005). ODP Site 766 lies at 3997.5 mbsl on the Gascoyne Abyssal Plain off northwest Australia (**Fig. 2**). This site, probably at ~3500 m water depth during the Late Paleocene (Shipboard Scientific Party, 1990) (**Fig. 6**), contains a ~45 m thick calcareous interval deposited between ~57 to 51 Ma. Similar to Site 259, a major hiatus occurs at the upper boundary of this interval, spanning from the upper Lower Eocene to lowermost Pliocene. Sediment from the middle Paleocene is also missing (Shipboard Scientific Party, 1990).

Established Mesozoic-Cenozoic CCD compilations (Berger and von Rad, 1972; van Andel *et al.*, 1975), indicate a relatively shallow (~3500 m) and unchanging CCD in all oceans between 60 and 50 Ma. This view is inconsistent with the lithological record at Site 259 and other locations noted above. We suggest the CCD dropped between nominally ~57 and 52-51 Ma at multiple locations, although the magnitude of this shift cannot be determined with available information. This interpretation, if correct, immediately raises three issues.

First, ODP Leg 199 drilled six sites (1215, 1217, 1219-1222) on the eastern distal flank of East Pacific Rise that terminate in basalt emplaced at a mid-ocean ridge during the latest Paleocene (Lyle *et al.*, 2002). Using Sites 1219 and 1220 and an approach similar to that of van Andel (1975), Rea and Lyle (2005) have recently presented an Equatorial Pacific CCD curve beginning *ca*. 56.5 Ma. Like van Andel (1975), they suggest a shallow (~3200 m) and generally invariant CCD from this age to 42 Ma in direct contradiction to our work. One explanation is that the Late Paleocene-Early Eocene CCD was significantly shallower in the Equatorial Pacific than in the southern Atlantic and Indian Oceans (**Fig. 6**). Such an interpretation, however, is inconsistent with a deepened Late Paleocene-Early Eocene lysocline at Shatsky Rise (Hancock and Dickens, 2005). Alternatively, we note that the “flat” Late Paleocene-Early Eocene portion of the Rea and Lyle (2005) CCD curve is not supported by data.

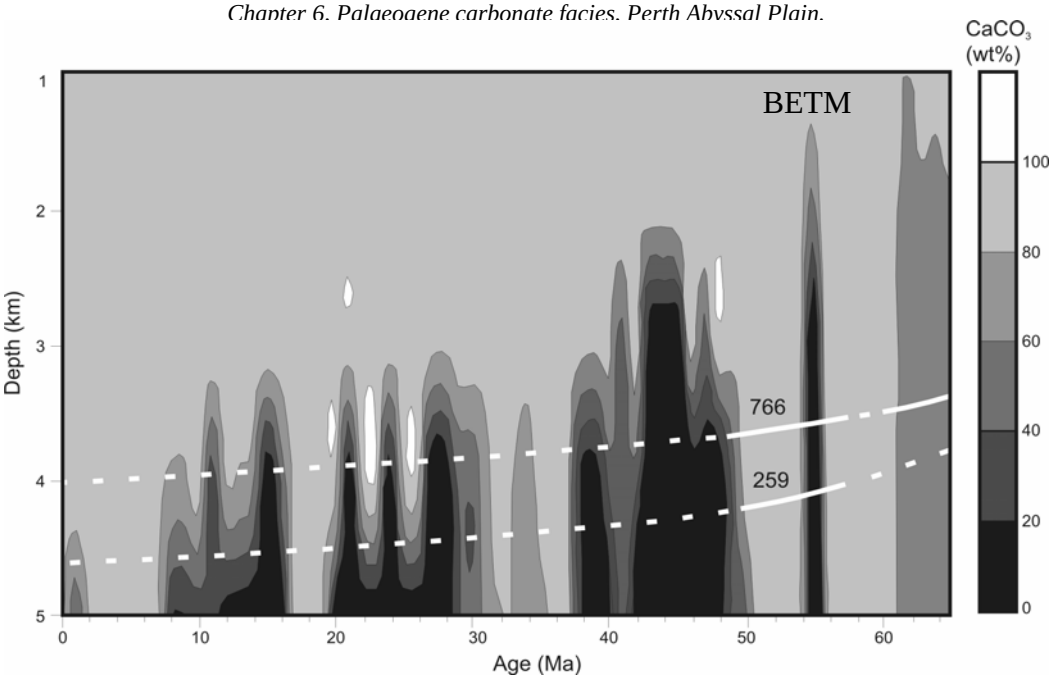

Figure 6. Carbonate (wt%) from Walvis Ridge sites (adapted from Zachos *et al.*, 2004; fig. 45). Subsidence curves for DSDP Site 259 (adapted from van Andel *et al.*, 1975) and ODP Site 766 (adapted from Shipboard Scientific Party, 1990; fig. 28) are also plotted. The white line represents carbonate deposition, and the dashed line when little or no carbonate was deposited.

The six ODP Leg 199 sites of interest contain a succession of Upper Paleocene basalt, Upper Paleocene-Lower Eocene calcareous chalk, and Lower Eocene carbonate-free sediment, with the second transition marking the time when the sites were at 3200-3300 m palaeodepth, and passed under the CCD (Lyle *et al.*, 2002; Rea and Lyle, 2005). Rea and Lyle (2005) indicate an age of 53.4 to 53 Ma for this transition, which occurs in a >5 m coring gap at Sites 1219 and 1220. The age estimate (determined by nannofossils below the gap) thus is a maximum. Cores at Site 1215, which were not used by Rea and Lyle (2005) for constructing their CCD curve, did recover the transition, which occurs some 2-3 m above the FAD of *Discoaster lodoensis* at 52.4 Ma (Lyle *et al.*, 2002). Moreover, given the similarity of basement ages for the sites (56.5-55.0 Ma; Lyle *et al.*, 2002), the depth trajectory of the CCD before the transition is questionable. In short, the sediment records recovered by Leg 199 do not discount a relatively deep Late Paleocene-Early Eocene CCD that rises past 3200-3300 m around 51 Ma.

Second, a significant drop in the CCD at multiple, widespread locations between ~57 and 52-51 Ma necessitates a mechanism. At present, it is difficult to gauge whether the CCD drop occurred only in certain regions, notably the south Atlantic, south Indian

and Pacific, or whether it occurred globally. In the first case, the CCD drop might signify a change in the flow of deep ocean water. Specifically, waters bathing the seafloor at southern latitudes and in the Pacific could have become younger and less corrosive to calcium carbonate. Foraminiferal carbon isotope records may support this interpretation, as they suggest a decrease in the $\delta^{13}C$ gradient between surface water and deep water during the Late Paleocene and the Early Eocene (Corfield, 1994). Neodynium isotope records from Shatsky Rise also suggest that deep waters formed in the north Pacific during the early Palaeogene (Thomas, 2004), although this idea receives little support from benthic foraminiferal carbon isotope records (Corfield, 1994). A global drop in the CCD might instead signify changes in ocean chemistry and higher concentrations of HCO_3^- or Ca^{2+}. Enhanced carbonate accumulation at Site 259 and elsewhere (Fig. 6), roughly coincides with the long-term decrease in $\delta^{13}C$ from the Late Paleocene-Early Eocene (**Fig. 1**). Presumably, this decrease signifies input of ^{13}C-depleted carbon.

Lastly we note some intriguing issues regarding the CIE at Site 259. The CIE signifies a massive injection of ^{13}C-depleted carbon in to the ocean and atmosphere over ~20 kyr, followed by sequestering of this excess carbon into sediments of ~200 kyr (e.g., Dickens *et al.*, 1997; Farley and Eltgroth, 2003). Several authors have noted a stepped drop in bulk carbonate $\delta^{13}C$ at the start of the CIE, perhaps signifying a pulsed input of carbon (Zachos *et al.*, 2005). Such a step occurs in bulk sediment and *Nuttallides* at Site 259 (**Fig. 3**). The major carbon input at the CIE is obvious in sites from the north and central Atlantic (Katz *et al.*, 1999; Zachos *et al.*, 2005), and also occurs at many other locations (Thomas, 1998), but is less prevalent in sites from high southern latitudes and the Pacific (Kelly, 2002) suggesting major carbon input in the north Atlantic and a generally south to north flow of deep water (Dickens, 2000). Our data at Site 259 may confirm this trend, as carbonate contents only drop to 37% at the start of the CIE (Fig. 3). However, the start of the CIE may be missing as noted above. Sediment deposited during the CIE interval, form nominally 55.2 to 50 mbsf, was emplaced about four times faster than the rest of the calcareous section. This may indicate increased delivery of sediment during the CIE as observed at other high southern latitude locations (Crouch *et al.*, 2003), although drilling disturbance could have also stretched the cores.

CONCLUSIONS

1). Approximately 31 m of Upper Paleocene-Lower Eocene abyssal carbonates ($CaCO_3$ >50%) accumulated at Site 259 during planktic foraminiferal Zones P4c through P6b (~57-52 Ma) suggesting a drop in the CCD not presently recognized in global compilations.

2). A partial CIE expressed as a small negative spike in $\delta^{13}C$ of 0.5‰ occurs at 55.17 mbsf and is associated with a clear BFEE, and a rapid influx in large *Acarinina*.

3). The ~5-6 myr duration of the drop in the CCD at several locations may be explained by a higher flux of HCO_3^- and Ca^{2+} and roughly coincides with the long-term decrease in $\delta^{13}C$ from the Late Paleocene-Early Eocene, which signifies input of ^{13}C-depleted carbon.

ACKNOWLEDGMENTS

Thanks go to Dick Olsson and Bill Berggren for their invaluable help with identifications of Eocene planktic foraminiferal species.

REFERENCES

Alegret, L., and Thomas, E., 2001. Upper Cretaceous and lower Paleogene benthic Foraminifera from northeastern Mexico. *Micropaleontology*, 47:269-316.

Archer, D.E., and Maier-Reimer, E., 1994. Effect of deep-sea sedimentary calcite preservation on atmospheric CO2 concentration. *Nature*, 367:260-263.

Aubry, M.P., Berggren, W.A., *et al.*, 2003. Chronostratigraphic terminology at the Paleocene/Eocene boundary. *In* Wing, S.L., Gingerich, P.D., Schmitz, B., *et al.*, (Eds), *Causes and consequences of the globally warm climates in the early Paleogene*, The Geological Society of America, Spec. Paper 369, 551-566.

Berger, W.H., 1968. Planktonic foraminifera; selective solution and paleoclimatic interpretation. *Deep-Sea Research and Oceanographic Abstracts*, 15:31-43.

Berger, W.H., Adelseck, C.G., *et al.*, 1976. Distribution of carbonate in surface sediments of the Pacific Ocean. *Journal of Geophysical Research*, 81:2617-2627.

Berger, W.H., and von Rad, U., 1972. Cretaceous and Cenozoic sediments from the Atlantic Ocean *Init. Repts. DSDP*, 14: Washington US Government Printing Office, 787-886.

Berger, W.H., and Winterer, E.L., 1973. Plate stratigraphy, oceanic fertility, and the paleobathymetry of deep sea carbonate. *European Geophysical Society, Meeting, Abstracts. no.*, 1:8.

Berggren, W.A., Kent, D.V., *et al.*, 1995. A revised Cenozoic geochronology and chronostratigraphy. *In* Berggren, W.A., Kent, D.V., Aubry, M.P., *et al.*, (Eds), *Geochronology, time scales and global stratigraphic correlation,* SEPM Special Publication 54, 129-212.

Bode, G.W., 1974. Carbon and carbonate analyses, Leg 27. *In* Heirtzler, J.R., Veevers, J.J., Bolli, H.M., *et al.*, (Eds), *Init. Repts. DSDP*, 27: Washington US Government Printing Office, 499-505.

Bolli, H.M., Beckmann, J.-P., *et al.*, 1994. *Benthic foraminiferal biostratigraphy of the South Caribbean Region*: Cambridge, Cambridge University Press, 408 p.

Bralower, T.J., Premoli Silva, I., *et al.*, 2002. *Proc. ODP, Init. Repts*, 198 [CD-ROM]. Available from: Ocean Drilling Program, Texas A&M University, College Station, TX 77845-9547, USA.

Cooks, H.E., Zemmels, I., and Matti, J.C., 1974. Eastern Indian Ocean - Leg 27 Deep Sea Drilling Project. *In* Heirtzler, J.R., Veevers, J.J., Bolli, H.M., *et al.*, (Eds), *Init. Repts. DSDP*, 27: Washington US Government Printing Office, 535-548.

Corfield, R.M., 1994. Palaeocene oceans and climate; an isotopic perspective. *Earth-Science Reviews*, 37:225-252.

Cramer, B.S., Wright, A.A., *et al.*, 2003. Orbital climate forcing of $\delta^{13}C$ excursions in the late Paleocene-early Eocene (chrons C24n-C25n). *Paleoceanography*, 18.

Crouch, E.M., Brinkhuis, H., *et al.*, 2003. Late Paleocene - early Eocene dinoflagellate cyst records from the Tethys: further observations on the global distribution of *Apectodinium*. *In* Wing, S.L., Gingerich, P.D., Schmitz, B., *et al.*, (Eds), *Causes and consequences of globally warm climates in the early Paleogene*, The Geological Society of America, Spec. Paper 369, 113-131.

Dickens, G.R., 2000. Methane oxidation during the late Palaeocene thermal maximum. *Bulletin de la Societe Geologique de France*, 171:37-49.

Dickens, G.R., Castillo, M.M., *et al.*, 1997. A blast of gas in the latest Paleocene; simulating first-order effects of massive dissociation of oceanic methane hydrate. *Geology*, 25:259-262.

Dupuis, C., Aubry, M.P., *et al.*, 2003. The Dababiya Quarry Section: lithostratigraphy, clay mineralogy, geochemistry and paleontolgoy. *Micropaleontology*, 49:41-59.

Farley, K.A., and Eltgroth, S.F., 2003. An alternative age model for the Paleocene-Eocene thermal maximum using extraterrestrial ^{3}He. *Earth and Planetary Science Letters*, 208:135-148.

Farrell, J.W., and Prell, W.L., 1989. Climatic change and $CaCO_3$ preservation: an 800 000 year bathymetric reconstruction from the central equatorial Pacific Ocean. *Paleoceanography*, 4:447-466.

Hancock, H.J.L., Chaproniere, G.C., *et al.*, 2002. Early Palaeogene planktic foraminiferal and carbon isotope stratigraphy, Hole 762C, Exmouth Plateau, northwest Australian margin. *Journal of Micropalaeontology*, 21:29-42.

Hancock, H.J.L., and Dickens, G.R., 2005. Carbonate dissolution episodes in Paleocene and Eocene sediment, Shatsky Rise, west-central Pacific. *In*: Bralower, T.J., Premoli Silva, I., and Malone, M.J. (Eds), *Proc. ODP, Sci. Results*, 198 [Online]. Available from World Wide Web: <http://www-odp.tamu.edu/publications/198_SR/116/116.htm>. [Cited 2005-09-04].

Hancock, H.J.L., Dickens, G.R., *et al.*, 2003. Foraminiferal and carbon isotope stratigraphy through the Paleocene-Eocene transition at Dee Stream, Marlborough, New Zealand. *New Zealand Journal of Geology and Geophysics*, 46:1-19.

Hollis, C.J., Dickens, G.R., *et al.*, 2005. The Paleocene-Eocene transition at Mead Stream, New Zealand: a southern Pacific record of early Cenozoic global change. *Palaeogeography, Palaeoclimatology, Palaeoecology*, 215:313-343.

Huber, B.T., 1991. Paleogene and early Neogene planktonic foraminifer biostratigraphy of sites 738 and 744, Kerguelen Plateau (southern Indian Ocean). *Proceedings of the Ocean Drilling Program scientific results*, 119:427-449.

Katz, M.E., Pak, D.K., *et al.*, 1999. The source and fate of massive carbon input druing the latest Paleocene thermal maximum. *Science*, 286:1531-1533.

Katz, M.E., Wright, J.D., *et al.*, 2003. Early Cenozoic benthic foraminiferal isotopes: species reliability and interspecies correction factors. *Paleoceanography*, 18 (2), 1024, DOI:10.1029/2002PA000798.

Katz, M.E., Wright, J.D., *et al.*, 2005. Biological overprint of the geological carbon cycle. *Marine Geology*, 217:323-338.

Kelly, D.C., 2002. Response of Antarctic (ODP Site 690) planktonic foraminifera to the Paleocene-Eocene thermal maximum; faunal evidence for ocean/climate change. *Paleoceanography*, 17 (4), 1071, DOI:10.1029/2002PA000761.

Kennett, J.P., 1982. *Marine geology*: Englewood Cliffs, NJ, Prentice-Hall, 813 p.

Krasheninnikov, G.F., 1974. Cretaceous and Paleogene planktonic foraminifera, Leg 27 of the Deep Sea Drilling Project. *In* Heirtzler, J.R., Veevers, J.J., and Bolli, H.M., (Eds), *Init. Repts. DSDP*, 27: Washington US Government Printing Office, 663-671.

Kump, L.R., and Arthur, M.A., 1999. Interpreting carbon-isotope excursions; carbonates and organic matter. *Chemical Geology*, 161:181-198.

Kurtz, A., Kump, L.R., *et al.*, 2003. Early Cenozoic decoupling of the global carbon and sulfur cycles. *Paleoceanography*, 18(4), 1090, DOI:10.1029/2003PA000908.

Loeblich, A.R., Jr., and Tappan, H.N., 1988. *Foraminiferal genera and their classification*: New York, Von Nostrand and Reinhold Company, 970 p.

Lourens, L., Sluijs, A., *et al.*, 2005. Astronomical modulation of late Palaeocene to early Eocene global warming events. *Nature*, 435:1083-1087.

Lyle, M.W., Wilson, P.A., *et al.*, 2002. *Proc. ODP Init. Repts.*, 199 [CD-ROM]. Available from: Ocean Drilling Program, Texas A&M University, College Station TX 77845-9547, USA.

Mekik, F.A., Loubere, P.W., *et al.*, 2002. Organic carbon flux and organic carbon to calcite flux ratio recorded in deep-sea carbonates: Demonstration and a new proxy. *Global Biogeochemical Cycles*, 16:1-15.

Mueller, G., and Gastner, M., 1971. The "Karbonate-Bombe", a simple device for the determination of the carbonate content in sediments, soils, and other materials. *Neues Jahrbuch fuer Mineralogie Monatshefte*, 10:466-469.

Muller, R.D., Gaina, C., *et al.*, 2000. Seafloor spreading around Australia. *In* Veevers, J.J., (Ed.) *Billion-year earth history of Australia and neighbours in Gondwanaland – BYEHA*, 18-28.

Murray, J., and Renard, A.F., 1891. *Deep-sea deposits based on the specimens collected during the voyage of H.M.S. Challenger in the years 1872 to 1876*: London, Longmans, 525 p.

Nomura, R., 1991. Paleoceanography of Upper Maestrichtian to Eocene benthic foraminiferal assemblages at sites 752, 753 and 754, Eastern Indian Ocean. *In* Weissel, J., Peirce, J., Taylor, E., *et al.*, (Eds), *Proc. ODP, Sci. Results*: College Station, TX Ocean Drilling Program, 3-29.

Olsson, R.K., Hemleben, C., *et al.*, 1999. *Atlas of Paleocene planktonic Foraminifera*: Washington, DC, Smithsonian Institution, 252 p.

Pearson, P.N., and Palmer, M.R., 2000. Atmospheric carbon dioxide concentrations over the past 60 million years. *Nature*, 406:659-699.

Peterson, M.N.A., 1966. Calcite: rates of dissolution in a vertical profile in the central Pacific. *Science*, 154:1542-1544.

Proto-Decima, F., 1974. Leg 27 calcareous nannoplankton. *In* Heirtzler, J.R., Veevers, J.J., Bolli, H.M., *et al.*, (Eds), *Init. Repts. DSDP*, 27: Washington US Government Printing Office, 589-593.

Quillevere, F., and Norris, R.D., 2003. Ecological development of acarininids (planktonic Foraminifera) and hydrographic evolution of Paleocene surface waters. *In* Wing, S.L., Gingerich, P.D., Schmitz, B., *et al.*, (Eds), *Causes and consequences of globally warm climates in the early Paleogene*, The Geological Society of America, Spec. Paper 369, 223-238.

Ravizza, G., Norris, R.N., *et al.*, 2001. An osmium isotope excursion associated with the late Paleocene thermal maximum; evidence of intensified chemical weathering. *Paleoceanography*, 16:155-163.

Rea, D.K., and Lyle, M., 2005. Paleogene calcite compensation depth in the eastern subtropical Pacific: Answers and questions. *Paleoceanography*, 20, PA1012, doi:10.1029/2004PA001064.

Robinson, P.T., and Whitford, D.J., 1974. Basalts from the eastern Indian Ocean, DSDP Leg 27. *In* Heirtzler, J.R., Veevers, J.J., and Bolli, H.M., (Eds), *Init. Repts. DSDP*, 27: Washington US Government Printing Office, 551-559.

Shackleton, N.J., and Hall, M.A., 1984. Carbon isotope data from Leg 74 sediments. *In* Moore, J., T. C., Rabinowitz, P.D., Boersma, A., *et al.*, (Eds), *Init. Repts. DSDP*, 74: Washington US Government Printing Office, 613-619.

Shipboard Scientific Party, 1974. Site 259. *In* Heirtzler, J.R., Veevers, J.J., Bolli, H.M., *et al.*, (Eds), *Init. Repts. DSDP*, 27: Washington US Government Printing Office, 15-29.

Shipboard Scientific Party, 1990. Site 766. *In* Gradstein, F.M., Ludden, J.N., Adamson, A.C., *et al.*, (Eds), *Proc. ODP Init. Reps*, 123: College Station, TX Ocean Drilling Program, 269-352.

Shipboard Scientific Party, 2004. Leg 208 Summary. *In* Zachos, J.C., Kroon, D., and Blum, P., (Eds), *Proc. ODP, Init. Repts.*, 198: College Station, TX Ocean Drilling Program, 1-112.

Stott, L.D., and Kennett, J.P., 1990. Antarctic Paleogene planktonic foraminifer biostratigraphy; ODP Leg 113, Sites 689 and 690. *In* Barker, P.F., Kennett, J.P., and et al., (Eds), *Proc. ODP, Sci. Results*, 113: College Station, TX Ocean Drilling Program, 549-565.

Thomas, D.J., 2004. Evidence for deep-water production in the North Pacific Ocean during the early Cenozoic warm interval. *Nature*, 430:65-68.

Thomas, E., 1990. Late Cretaceous through Neogene deep-sea benthic foraminifers (Maud Rise, Weddell Sea, Antarctica). *Proc. ODP Sci. Results*, 113:571-594.

Thomas, E., 1998. The biogeography of the late Paleocene benthic foraminiferal extinction. *In* Aubry, M.P., Lucas, S.G., and Berggren, W.A., (Eds), *Late Paleocene-early Eocene climatic and biotic events in the marine and terrestrial records*: New York, NY Columbia University Press, 214-243.

Thomas, E., and Shackleton, N.J., 1996. The Paleocene-Eocene benthic foraminiferal extinction and stable isotope anomalies. *In* Knox, R.W.O.B., Corfield, R.M., and Dunay, R.E., (Eds), *Correlation of the early Paleogene in Northwest Europe*, 101 Geological Society London Special Publication, 401-441.

Thomas, E., and Zachos, J.C., 1999. Deep-sea faunas during the late Paleocene-early Eocene climate optimum; boredom or boredom with short periods of terror? *Geological Society of America, 1999 annual meeting*, 31: Anonymous Geological Society of America (GSA), 122.

Thomas, E., and Zachos, J.C., 2000. The late Paleocene thermal maximum a unique event? *GFF*, 122:169-170.

Thomas, E., Zachos, J.C., *et al.*, 2000. Deep-sea environments on a warm earth: latest Paleocene - early Eocene. *In* Huber, B.T., MacLeod, K., and Wing, S.L., (Eds), *Warm climates in Earth history*, Cambridge University Press, 132-160.

Thompson, G., Bryan, W.B., *et al.*, 1978. Basalts and related rocks from deep-sea drilling sites in the central and eastern Indian Ocean. *Marine Geology*, 26:119-138.

Thunell, R.C., 1976. Calcium carbonate dissolution history in late Quaternary deep-sea sediments, western Gulf of Mexico. *Quaternary Research*, 6:281-297.

Tjalsma, R.C., and Lohmann, G.P., 1983. Paleocene-Eocene bathyal and abyssal benthic foraminifera from the Atlantic Ocean. *Micropaleontology, Special Publication*, 4:1-90.

Toumarkine, M., and Luterbacher, H.-P., 1985. Paleocene and Eocene planktic foraminifera. *In* Bolli, H.M., Saunders, J.B., and Perch-Nielsen, K., (Eds), *Plankton stratigraphy*: Cambridge Cambridge University Press, 87-154.

Tyrrell, T., and Zeebe, R.E., 2003. History of carbonate ion concentration over the last 100 million years. *Geochimica et Cosmochimica Acta*, 68:3521-3530.

Valyashko, G.M., Gorodnitskiy, A.M., *et al.*, 1989. Tectonic evolution of Shatsky Uplift on the geomagnetic survey.

van Andel, T.H., Heath, G.R., *et al.*, 1975. *Cenozoic history and paleoceanography of the central equatorial Pacific Ocean; a regional synthesis of Deep Sea Drilling Project data*: Boulder, CO, Geological Society of America (GSA), 134 p.

van Morkhoven, F.P.C.M., Berggren, W.A., *et al.*, 1986. Cenozoic cosmopolitan deep-water benthic foraminifera. *Bulletin des Centres de Recherches Exploration-Production Elf-Aquitaine, Memoire 11*:421 p.

Veevers, J.J., and Tayton, J.W., 1985. Prominent magnetic anomaly along the continent-ocean boundary between the northwestern margin of Australia (Exmouth and Scott plateaus) and the Argo abyssal plain. *Earth and Planetary Science Letters*, 72:415-426.

Widmark, J., G.V., 1997. Deep-sea benthic foraminifera from Cretaceous-Paleogene boundary strata in the South Atlantic- taxonomy and paleoecology. *Fossils and strata*, 43:1-94.

Williams, D.F., Gribble, D., *et al.*, 1985a. Dissolution and water-mass patterns in the Southeast Indian Ocean; Part II, The Pleistocene record from Brunhes to Matuyama age sediments. *Geological Society of America Bulletin*, 96:190-202.

Williams, D.F., Healy-Williams, N., *et al.*, 1985b. Dissolution and water-mass patterns in the Southeast Indian Ocean; Part I, Evidence from Recent to late Holocene foraminiferal assemblages. *Geological Society of America Bulletin*, 96:176-189.

Zachos, J., Pagani, M., *et al.*, 2001. Trends, rhythms, and aberrations in global climate 65 Ma to present. *Science*, 292:686-693.

Zachos, J.C., Kroon, D., *et al.*, 2004. Proc. ODP, Init. Repts, 208 [Online]. Available from World Wide Web: http://www-odp.tamu.edu/publications/208_IR/208ir.htm. [Cited 2005-30-01].

Zachos, J.C., Rohl, U., *et al.*, 2005. Extreme Acidification of the Atlantic Ocean at the Paleocene-Eocene Boundary (~ 55Mya). *Science*, 308:1611- 1615; doi 10.1126/science.1109004.

APPENDIX 1. Taxonomic list of Paleocene and Eocene calcareous foraminifera, Site 259.

Planktic Foraminifera

Acarinina coalingensis (Cushman & Hanna 1927)
Acarinina mckannai (White, 1928)
Acarinina nitida (Martin 1943)
Acarinina primitiva (Finlay 1947)
Acarinina soldadoensis (Bronnimann 1952)
Acarinina subsphaerica (Subbotina 1947)
Acarinina wilcoxensis (Cushman & Ponton, 1932)
Chiloguembelina crinita (Glaessner 1937)
Chiloguembelina wilcoxensis (Cushman & Ponton 1932)
Globigerinatheka senni (Beckmann 1953)
Subbotina velascoensis (Cushman 1925)
Morozovella lensiformis (Subbotina 1953)
Morozovella subbotinae (Morozova 1939)
Zeauvigerina zealandica (Finlay 1939)

Benthic Foraminifera

Abyssamina poagi Schnitker & Tjalsma 1980
Abyssamina quadrata Schnitker & Tjalsma 1980
Alabamina creta (Finlay) 1940
Alabamina dissonata (Cushman & Renz) 1948
Allomorphina sp.
Anomalinoides globosus Brotzen 1945
Anomalinoides spissiformis (Cushman & Stainforth) 1945
Anomalinoides sp.
Aragonia aragonensis (Nuttall 1930)
Aragonia velascoensis (Cushman 1925)
Arenobulimina sp.
Bathysiphon sp.
Bolivinoides sp.
Bulimina kugleri Cushman & Renz 1942

Bulimina simplex Terquem 1882

Bulimina thanetensis Cushman & Parker 1947, emend. Haynes 1954

Bulimina trinitatensis Cushman & Jarvis 1928

Buliminella spp.

Chrysalogonium tenuicostatum Cushman & Bermudez 1936

Cibidoides hyphalus (Fisher 1969)

Cibicidoies praemundulus Berggren & Miller 1986

Cibicidoides pseudoperlucidus (Bykova 1954)

Cibicidoides proprius (Brotzen 1948)

Cibicidoides velascoensis (Cushman 1925)

Clavulinoides sp.

Clavulinoides trilateral (Cushman 1926)

Clinapertina complanata Tjalsma & Lohmann 1983

Clinapertina inflata Tjalsma & Lohmann 1983

Clinapertina subplanispira Tjalsma & Lohmann 1983

Ellipsoidina spp.

Fursenkoina sp.

Globocassidulina subglobosa (Brady 1881)

Gaudryina arenata (Cushman 1936)

Gaudryina laevigata Franke 1914

Globobulimina sp.

Glomospira spp.

Gyroidinoides beisseli (White 1928)

Gyroidinoides globosus von Hagenow 1842

Gyroidinoides quadratus (Cushman & Church 1929)

Gyroidinoides spp.

Heronallenia spp.

Laevidentalina, Dentalina spp.

Lenticulina spp.

*Marginulin*a spp.

Marssonella oxycona (Reuss 1860)

Marssonella trochoides (d'Orbigny 1852)

Neoflabellina semireticulata (Cushman & Jarvis 1928)

Nodosaria spp.

Nonion havanense Cushman & Bermudez 1937

Nonionella robusta Plummer 1931

Nonionella sp.

Nuttallides umbonifera (Cushman 1933)

Nuttallides truempyi (Nuttall 1930)

Nuttalinella florealis (White 1928)

Nuttalinella sp.

Oridorsalis umbonatus (Reuss 1851)

Orthomorphina spp.

Paralabamina hillebrandti (Fisher 1969) (=*Eponides whitei* von Hillebrandt 1962)

Paralabamina lunata (Brotzen 1948)

Polymorphinid taxa

Pluerostomellid taxa

Pullenia coryelli White 1929

Pullenia jarvisi Cushman 1936

Pyramidina rudita (Cushman & Parker 1936)

Quadrimorphina profunda Schnitker & Tjalsma 1980

Rectobulimina carpentierae Marie 1956

Rhizammina sp.

Rhzehakina epigona (Rjzehak 1895)

Siphogenerinoides brevispinosa Cushman 1939

Siphonodosaria hispidula (Cushman 1917)

Siphonodosaria lepidula

Siphonodosaria pomuligera Stache 1865

Siphotextularia sp.

Spiroplectammina spectabilis (Grzybowski 1898)

Stensioeina beccariiformis (White 1928)

Tappanina selmensis (Cushman 1933), emend. Brotzen 1948

Textularia sp.

Tritaxia havanensis (Cushman & Bermudez 1937)

Turrilina brevispira ten Dam 1944

Unilocular taxa

Vaginulina spp.

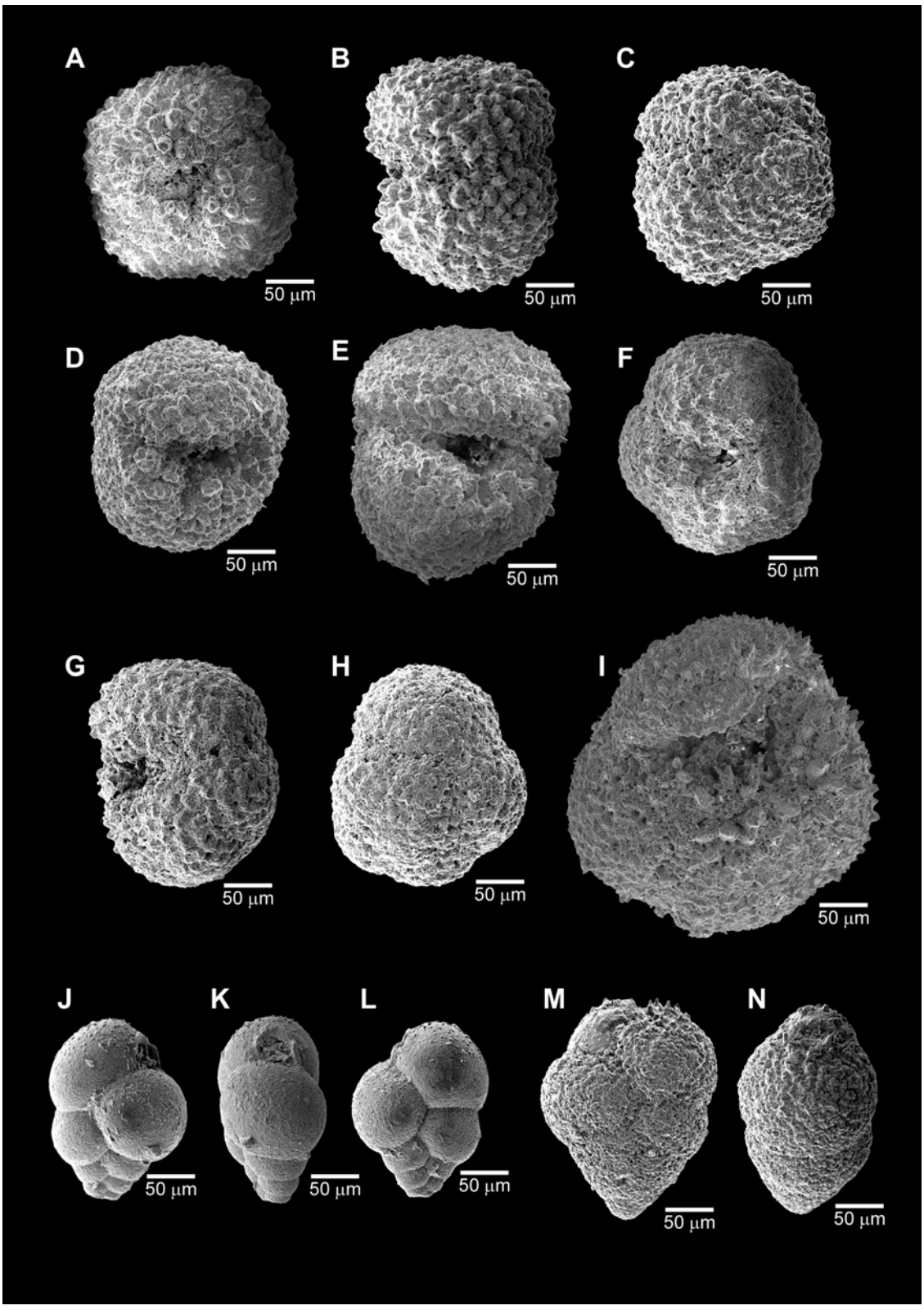

Plate 1. Scanning Electron Microscope (SEM) photographs of Paleocene and Eocene planktic foraminifera, Site 259. **A-E.** *Acarinina coalingensis* (Cushman and Hanna 1927): A, ventral view; B, side view; C, spiral view; D, side view; E, ventral view (259-6R-5, 40-44 cm). **F,G,H.** *Acarinina nitida* (Martin 1943): F, ventral view; G, side view; H spiral view (259-7R-5, 51-56 cm). **I.** *Acarinina soldadoensi* (Bronnimann 1952): ventral view **J, K, L.** *Chiloguembelina crinita* (Glaessner 1937): I, ventral view; J, side view; K, spiral view (259-6R-5, 51-56 cm). **M, N** *Chiloguembelina wilcoxensis* (Cushman and Ponton 1932): M, ventral view; N, side view (259-6R-3, 51-56 cm).

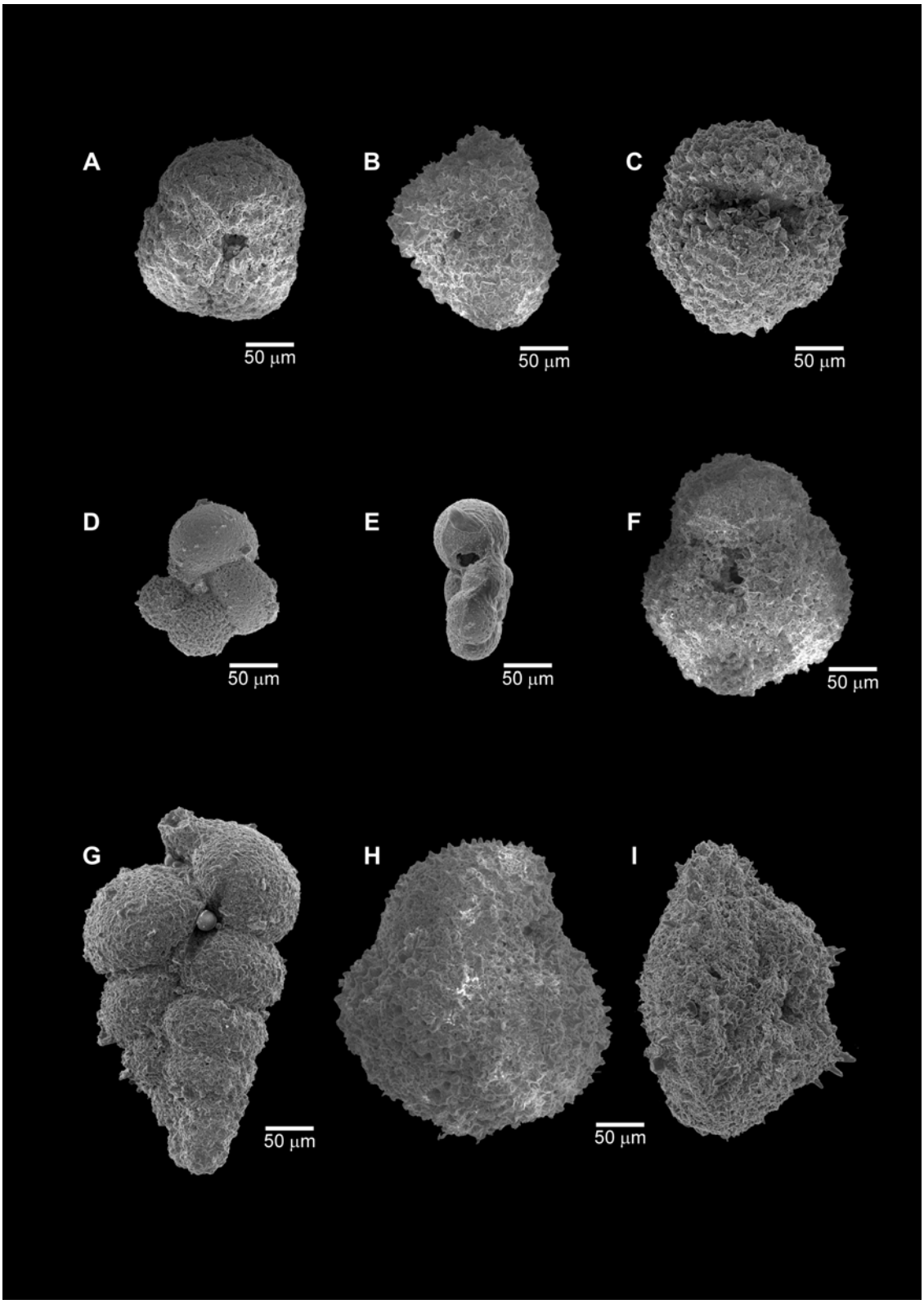

Plate 2. SEM micrographs of Eocene planktic foraminifera, Site 259. **A.** ?*Globigerinatheka senni* (Beckmann 1953): ventral view (259-5R-2, 120-124 cm). **B.** *Morozovella lensiformis* (Subbotina 1953): side view (259-5R-2, 120-124 cm). **C.** *Acarinina primitiva* (Finlay 1947): ventral view (259-6R-5, 40-44 cm). **D, E.** *Species 1* (to be described in forthcoming Eocene atlas, Pearson et al.); D, ventral view (259-5R-2, 120-124 cm); E, side view (259-4R-4, 140-144 cm) **F.** *Acarinina wilcoxensis* (Cushman & Ponton, 1932): ventral view (259-6R-6, 112-116 cm). **G.** *Zeauvigerina zealandica* (Finlay 1939) (259-5R-2, 120-124 cm). **H, I.** *Morozovella subbotinae* (Morozova 1939): N, ventral view; O, side view (259-5R-2, 120-124 cm).

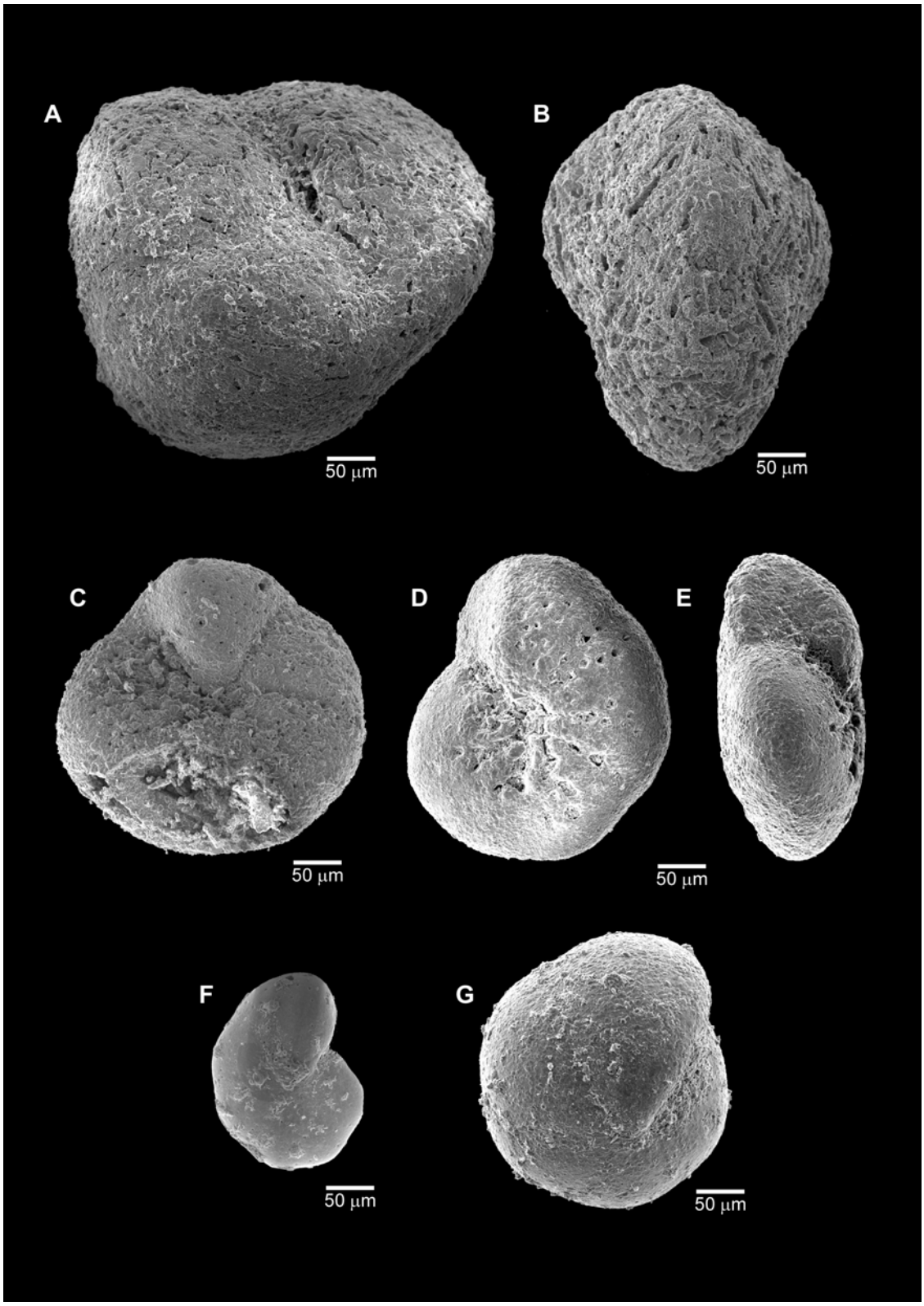

Plate 3. SEM micrographs of Paleocene benthic foraminifera, Site 259. **A.** *Dorothia* sp. (259-6R-6, 140-144 cm). **B.** *Clavulinoides trilatera* (Cushman 1926) (259-6R-6, 120-124 cm). **C.** *Paralabamina hillebrandti* (Fisher 1969): ventral view (259-6R-6, 120-124 cm). **D, E.** *Stensonia beccariiformis* (White 1928): D, ventral view; E, side view (259-7R-3, 66-69 cm). **F.** *Nonionella robusta* Plummer 1931; ventral view (259-6R-6, 120-124 cm). **G.** *Pullenia coryelli* White 1929: ventral view (259-7R-1, 40-44 cm).

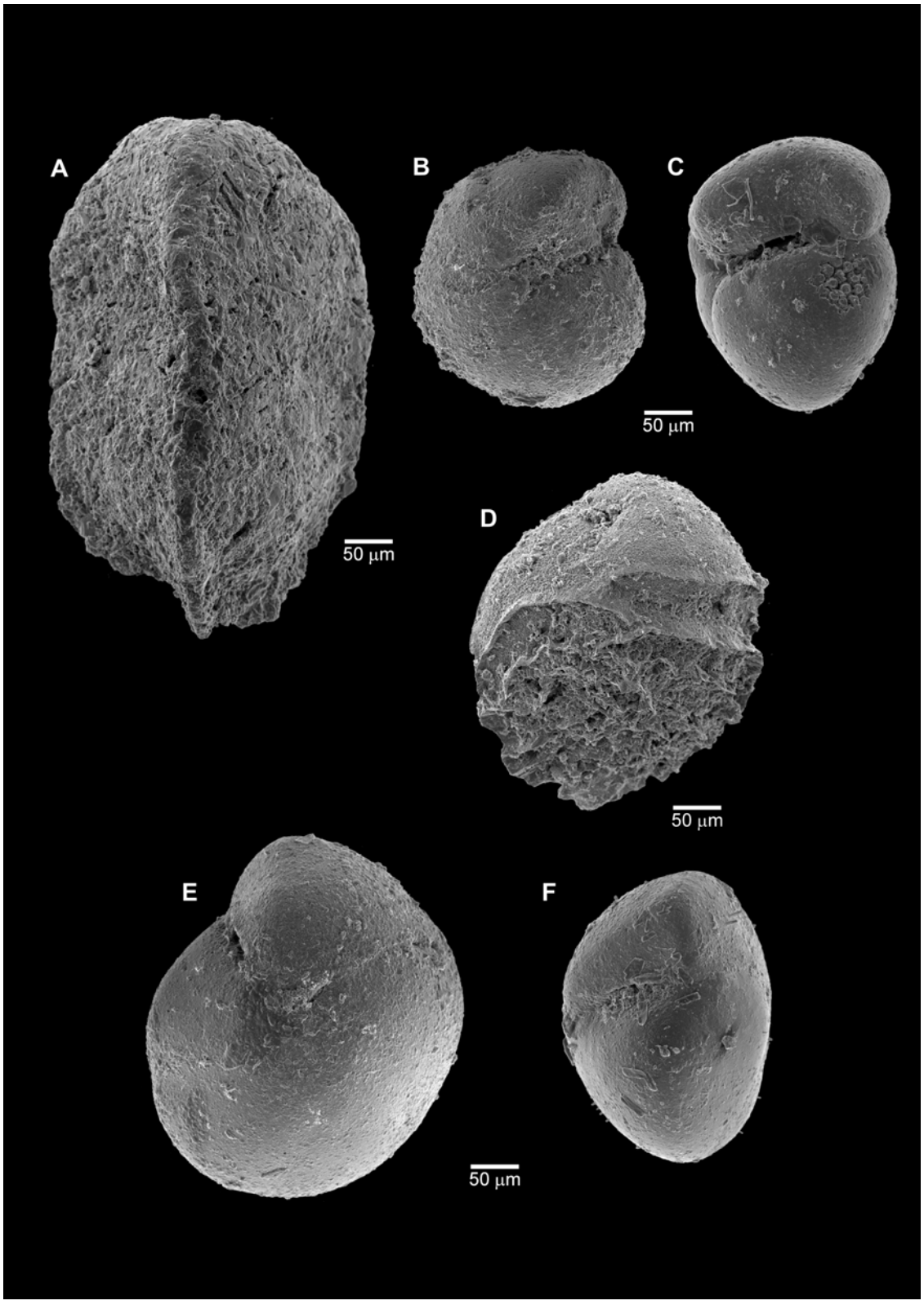

Plate 4. SEM micrographs of Paleocene benthic foraminifera, Site 259. **A.** *Tritaxia havanensis* (Cushman & Bermudez 1937) (259-6R-6, 120-124 cm). **B, C.** *Gyroidinoides globosus* von Hagenow 1842: **B,** ventral view; **C,** side view (259-6R-6, 120-124 cm). **D.** *Aragonia velascoensis* (Cushman 1925) (259-6R-6, 120-124 cm). **E, F.** *Gyroidinoides beisseli* (White 1928): **E,** ventral view; **F,** side view (259-6R-6, 120-124 cm).

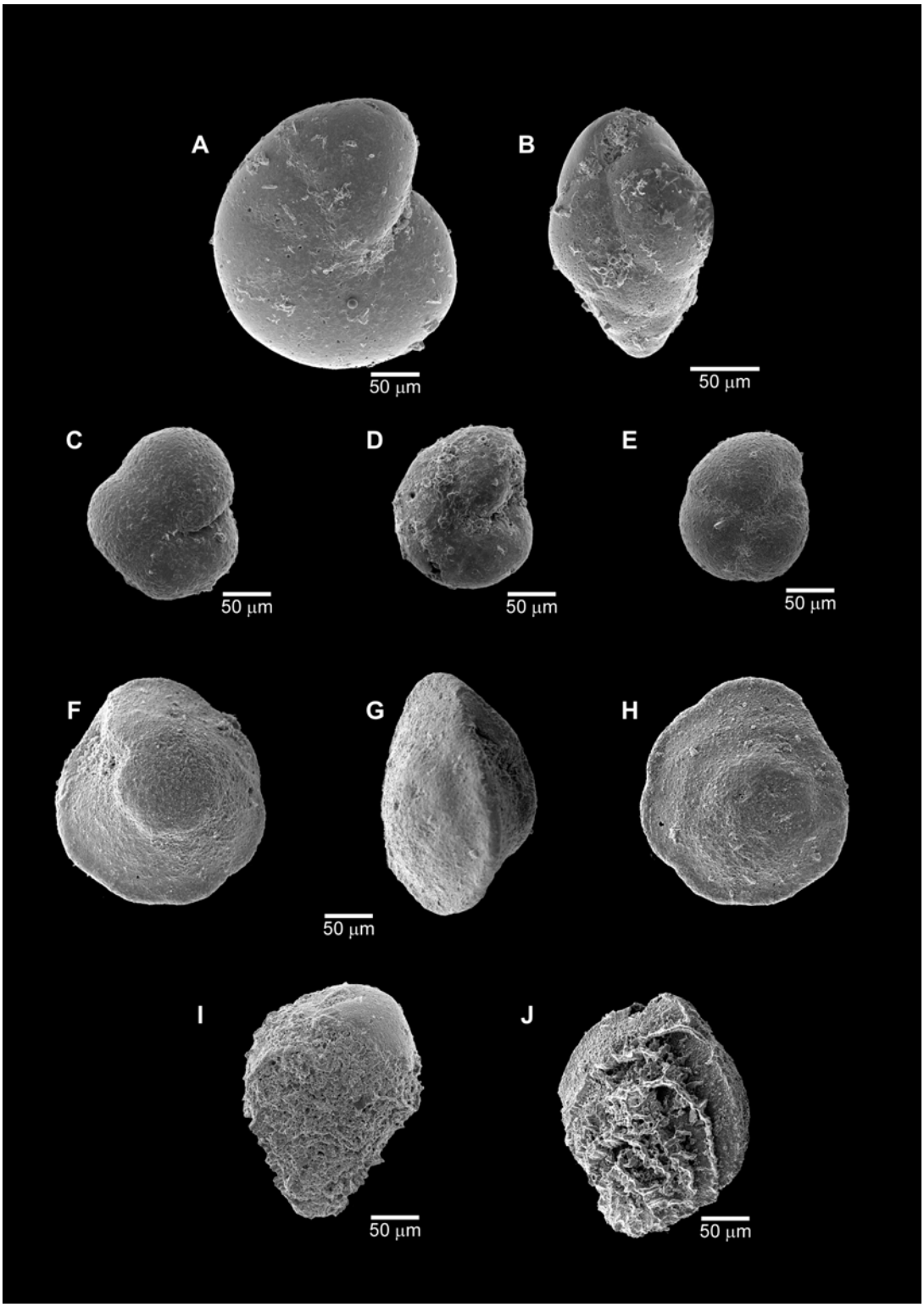

Plate 5. SEM micrographs of Eocene benthic foraminifera, Site 259. **A.** *Nonion havanense* Cushman & Bermudez 1937: ventral view (259-6R-6, 100-104 cm). **B.** *Bulimina kugleri* Cushman & Renz 1942 (259-6R-6, 100-104 cm). **C.** *Abyssamina quadrata* Schnitker & Tjalsma 1980: ventral view (259-6R-6, 112-115 cm). **D.** *Anomalinoides spissiformis* (Cushman & Stainforth) 1945: ventral view (259-6R-6, 112-115 cm). **E.** *Quadrimorphina profunda* Schnitker & Tjalsma 1980: ventral view (259-6R-6, 112-115 cm). **F, G, H.** *Nuttallides truempyi* (Nuttall 1930): F, ventral view; G, side view; H, spiral view (259-6R-6, 51-56 cm). **I.** *Tappanina selmensis* (Cushman 1933), emend. Brotzen 1948 (259-6R-6, 100-104 cm). J. *Aragonia aragonensis* (Nuttall 1930) (259-4R-5, 57-62 cm).

CHAPTER 7

SUMMARY

CHAPTER SUMMARIES

This thesis contributes a series of high resolution studies focusing on the response of planktic foraminifera and the global carbon cycle to changing global climatic conditions during early Palaeogene. This is a large, detailed and valuable dataset given the paucity of records from the Southern Hemisphere, and enhances our understanding of rapid global change during this interval.

Chapter 2 presents the first, detailed and comprehensive deep-sea $CaCO_3$ dissolution dataset from the central Pacific Holes 1209A and 1211A, Shatsky Rise, which spans the entire Paleocene and Eocene Epochs. Four dissolution indices were used: carbonate content, coarse size fraction (>38 μm), benthic foraminiferal abundance, and planktic foraminiferal fragmentation ratio. Carbonate content is not a sensitive indicator of carbonate dissolution in the studied sections and the proportion of coarse size fraction does not accurately record carbonate dissolution either because the relative abundance of nannofossils largely determines the grain-size distribution. Benthic foraminiferal abundance and fragmentation ratio are the best indicators for carbonate dissolution. Two prominent dissolution episodes occurred within the Paleocene and Eocene. The first occurred during the middle Paleocene (~59-58 Ma), and the second from the late Middle Eocene to the Late Eocene (~40-33.7 Ma). Conversely, at the beginning of the Paleocene and Eocene epochs, dissolution is at a minimum and carbonate preservation at its peak.

In Chapter 3 it was shown that the coiling direction of *Igorina albeari* switches at ~59 Ma for three sites in the central Pacific. Stable isotopes of *I. albeari* specimens suggest that both the sinistrally and dextrally coiled morphotypes occupied similar water masses. Thus, the switch to sinistral coiling mode did not involve a significant

shift in depth ecology or photosymbiosis. The coiling reversal perhaps resulted instead from a relative decline in the dextral morph at the tropical localities, due to a change in some other ecological parameter, for example, nutrient availability, while the dextral morph remained the dominant form at the mid latitude locations. A possibly analogous situation is the modern presence of sinistral *Globotruncana truncatulinoides* within the gyres whereas dextral *G. truncatulinoides* are located in the equatorial oceans. The switch is associated with major changes in water column structure. An ~0.5‰ drop in $\delta^{18}O$ of *Subbotina* spp. indicates a 2˚C cooling of deep thermocline waters which is concomitant with a ramping up in $\delta^{13}C$ of *Morozovella* spp in surface waters, as well as an increase in the $\delta^{13}C$ gradient between surface and deep-dwelling foraminifera, suggesting an increase in surface water productivity and organic carbon burial. The coiling switch at the Pacific sites closely approximates the evolutionary first appearance of *Globanomalina pseudomenardii*, the zonal marker for planktic foraminiferal zone P4 (59.2 Ma) and the lower part of the PCIM. The question of whether the coiling switch is restricted to the central Pacific or widespread for the tropics is unresolved. Palaeogene records from the Blake Ridge, Atlantic Basin and other tropical to subtropical regions need to be examined to answer this question.

In Chapter 4 an unusual Late Paleocene abyssal siliceous-rich carbonate facies within abyssal clays on the abyssal plain adjacent to the Campbell Plateau of the New Zealand region, was documented and attributed to a drop in the CCD not previously registered in global reconstructions. Bulk carbonate concentrations vary widely between 3% and 51%. This siliceous-rich carbonate interval is correlated with the Waipawa Formation, a diachronous (~58-57 Ma), organic-rich formation represented in numerous New Zealand basins and marking the lower part of the PCIM. The middle Paleocene was characterized by cool global temperatures which may have increased upwelling in this area at least, as well as surface water productivity, and hence the thickness of the oxygen minimum zone. The Waipawa Formation is thought to have formed at the intersection of the shelf and the oxygen minimum zone

Chapter 5 documents the Paleocene-Eocene transition in a spectacular, uplifted, tilted and exposed Paleocene/Eocene sedimentary section at Dee Stream, South Island, New Zealand. One hundred metres of strata were logged and sampled for foraminifera

and carbon isotopes, which clearly show the section spans the Late Paleocene to Early Eocene planktic foraminiferal Zones P4 to P6b, and the *Subbotina triloculinoides* to *Pseudohastigerina wilcoxensis* Zones of the New Zealand zonal scheme. The section contains a 1.5 m thick BETM interval at the base of Zone P5 and within the *Morozovella velascoensis* Subzone. This is one of few documented studies of the BETM from high palaeolatitudes of the Southern Hemisphere and contributes significantly to knowledge of global responses to this interval of rapid global warming. During the BETM at Dee Stream, benthic foraminifera underwent significant extinction, the carbon isotope curve shows a negative spike of 2‰ and planktic foraminifera are dominated by an influx of low latitude *Morozovella*. The benthic foraminifer *Bulimina tuxpamensis* dominates benthic assemblages immediately following the onset of the BETM interval, suggesting dysoxic bottom waters during this event.

In Chapter 6, the nature and timing of an unusual ~ 30 m thick carbonate interval deposited within abyssal red clays is investigated at Site 259, Perth Abyssal Plain. This study determined the bulk carbonate content, the planktic and benthic foraminiferal assemblages, and the stable isotope composition of bulk carbonate and the benthic foraminiferal taxon *Nuttallides* spp., and non-carbonate mineralogy across the calcareous interval. Carbonate content ranges from 3 to 80%, and generally exceeds 50% between 35 and 57 mbsf. A distinct 20 cm thick clay-rich horizon exists from 55.17 to 55.37 mbsf, but carbonate content remains moderately high at 37%. The carbonate-rich sequence spans planktic foraminiferal Zones P4c through P6b (~57-52 Ma). A BETM interval occurs across the clay-rich horizon and is characterized by a significant benthic extinction event, including the last appearance of *Stensonia beccariiformis* (White 1928), which is a globally recognizable biomarker, a small negative spike of 0.5‰ in $\delta^{13}C$, an influx of the planktic foraminifera *Acarinina coalingensis*, and carbonate content of the sediment reaches 80%. The mineralogy of the non-carbonate fraction of sediment consistently comprises expanding clay, heulandite (zeolite), pyrolusite (MnO_2), quartz, feldspar (sodic or calcic), mica (minor). The carbonate-rich interval is attributed to a drop in the CCD across planktic foraminiferal Zones P4c to P6b (~57-52 Ma). The uniformity of this assemblage suggests that Site 259 experienced continuity in sediment provenance and that the sediment record reflects a drop in the CCD from ~57 to 52 Ma. Data from other locations suggest that this drop

is global. This palaeoceanographic event has not been previously included in CCD reconstructions for the early Palaeogene.

CORRELATION OF EVENTS

The first prominent episode of global change dealt with in this study occurs during the middle Paleocene (~59-58 Ma) where a widespread dissolution horizon is correlated across several sites in the central Pacific and also to significant perturbations in carbon and oxygen isotope records and the lower part of the PCIM. The dissolution horizon is also associated with evolutionary radiations in the planktic foraminifera across the Indo-Pacific region at the base of planktic foraminiferal Zone P4. It is closely associated temporally with organic-rich sediment deposition on both the New Zealand continental shelf and with deep-water siliceous carbonate deposition offshore. These lithologies can be attributed to a middle Paleocene cooling event. Vigorous upwelling and greater nutrient supply to the surface waters probably resulted in the deposition of siliceous rich carbonate facies offshore. The intersection of an expanded oxygen minimum zone (resulting from an increase in surface water) with the New Zealand shelf perhaps led to the widespread deposition of the organic-rich Waipara Formation.

The second interval of global change occurred in the Late Paleocene (~57 Ma) when Paleocene planktic foraminiferal assemblages reached their peak diversification, and $\delta^{13}C$ reached maximum values, as did $\delta^{13}C$ gradients between surface and deeper water. High $\delta^{13}C$ gradients were maintained into the Early Eocene until ~51 Ma. In the latest Paleocene and earliest Eocene, sediment deposited at central Pacific sites consisted entirely of carbonate (~57-51 Ma). For the earliest Eocene interval of central Pacific cores, sediment is characterized by a high percentage of the coarse fraction comprised of planktic foraminifera, a similar pattern to the earliest Paleocene following the Cretaceous/Tertiary mass extinction event. Palaeogene sediment from the Perth Abyssal Plain is generally carbonate-poor. High carbonate contents also characterize the Late Paleocene and Early Eocene (~57-51 Ma), and the earliest Eocene interval is very carbonate-rich, perhaps reflecting a negative feedback response to the massive shoaling (up to 2 km) of the CCD at the BETM.

This combination of factors suggests that the CCD deepened significantly during planktic foraminiferal Zones P4c to P7 (~57-51 Ma), excepting at the BETM, indicating a significant palaeoceanographic event not previously recognized. The ~6 myr duration of the drop in the CCD may be explained by a higher flux of HCO_3^- and Ca^{2+} to the ocean through enhanced weathering, or alteration in patterning of ocean solutes due to palaeoceanographic change. Warm, humid and wet conditions characteristic of the early Palaeogene were most likely conducive to terrestrial organic carbon burial, and may have led to a relative reduction in atmospheric CO_2, and carbonate deposition in the deep-sea. Furthermore, increased continental run-off and nutrient supply to the oceans could also explain the high $\delta^{13}C$ gradients observed between surface and deep ocean waters.

Additionally, two new Southern Ocean BETM sections, representing the New Zealand continental shelf and Perth Abyssal Plain, have been documented in detail as well as correlative sections from the Shatsky Rise. At all sites the BETM is represented by a dissolution layer, a BFEE, planktic foraminiferal adaptation and radiation and at the high latitude Dee Stream sections and Perth Abyssal Plains, carbon isotope anomalies.

Further research including high resolution carbon and oxygen isotope analysis on the same samples used for dissolution studies on the Shatsky Rise, would provide a better understanding of global carbon cycling and the apparently compensatory nature of deep-sea carbonate dissolution during the early Palaeogene. This is an important research direction that would enhance our understanding of the interplay between atmospheric CO_2 levels and global climate change.

APPENDICES

APPENDIX A

EARLY PALAEOGENE PLANKTIC FORAMINIFERAL AND CARBON ISOTOPE STRATIGRAPHY, HOLE 762C, EXMOUTH PLATEAU, NORTHWEST AUSTRALIAN MARGIN.

Abstract. Although the northwest margin of Australia is an important region for petroleum exploration and palaeoceanographic investigations, its Palaeogene stratigraphy is poorly documented, especially in terms of a foraminiferal biozonation. Early Palaeogene cores from 502.96 to 307.80 metres below sea floor (mbsf) at Ocean Drilling Program (ODP) Site 762 on the Exmouth Plateau were examined in this study for their planktic foraminiferal assemblages and the carbon isotopic compositions of *Subbotina* spp. Planktic foraminifera are generally well preserved and belong to 74 species and 17 genera. In spite of a mid-latitudinal palaeolatitude (~40°S) the sequence, deposited between the early Paleocene and Middle Eocene, contains all planktic foraminiferal Zones P1c through P10 of the current global scheme for tropical locations, except for Subzone P4b. Most zones are well defined by the datums of primary marker species except P3a and P9, which have boundaries that probably occur in core gaps, and the P9 zonal boundaries are defined by secondary marker species. Overall, variations in $\delta^{13}C$ based on sequential samples of *Subbotina* are similar in pattern and magnitude to global summary isotope curves spanning the early Palaeogene. However, the prominent $\delta^{13}C$ excursion that characterizes the Paleocene/Eocene transition is mostly missing and appears to lie in a core gap. The planktic foraminiferal zonation, linked with that based on nannofossils, a recalibrated magnetostratigraphy and carbon isotope records, provides a robust temporal framework for the Early Palaeogene of the northwest margin of Australia.

INTRODUCTION

The Early Palaeogene *ca*. 65 to 49 Ma (**Fig. 1**) is an especially significant interval of time because of profound changes in climate, ecosystems and the global carbon cycle (e.g. Zachos *et al*., 1993; Corfield, 1994; Thomas and Shackleton, 1996; Dickens *et al*., 1997; Norris and Röhl, 1999; Zachos *et al*., 2001). Indeed, documentation of Palaeogene paleoceanography is now a high priority for stratigraphic research. However, to resolve outstanding questions of global change, early Palaeogene marine successions must be located that meet certain criteria. These targets must be: 1) thick so as to maximise the temporal quality of the record and time resolution; 2) buried with little overburden to reduce the logistical demands of drilling and diagenetic effects; 3) rich in well-preserved biogenic carbonate for geochemical evaluation; and 4) hosted in stratal geometries which permit construction of detailed depth and latitudinal transects. To date, one of the few investigated locations which meets these criteria is the recently drilled Blake Nose in the western North Atlantic. Studies of this region have already advanced our knowledge of Palaeogene environmental change significantly (e.g. Bains *et al*., 1999; Katz *et al*., 1999; Norris *et al*., 1999; Norris and Röhl, 1999).

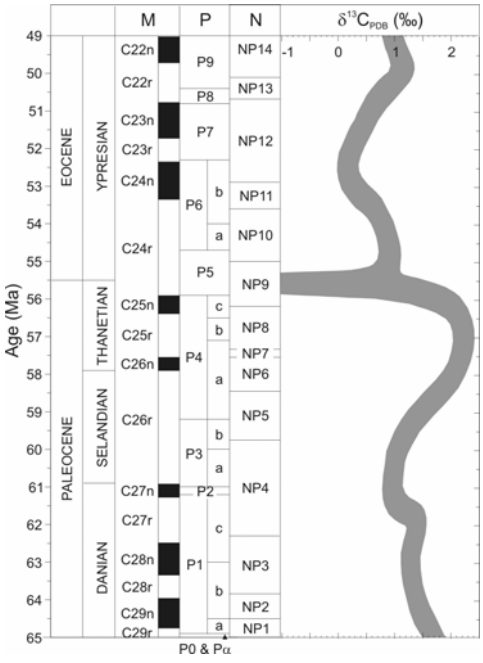

Figure 1. Early Palaeogene global stratigraphy including magnetostratigraphy (M), planktic foraminifera (P) and nannofossil biozones (N) (adapted from Berggren *et al*., 1995) and the global benthic foraminiferal carbon isotope curve (adapted from Shackleton & Hall, 1987 and J. Zachos, unpublished).

The Exmouth Plateau (**Fig. 2**) is a submerged platform extending 150-500 km off northwest Australia that consists of thinned and tilted continental crust with a Phanerozoic sedimentary sequence exceeding 10 km (Barber, 1988; Stagg and Colwell, 1994). The stratigraphic succession on the plateau is particularly interesting because it contains a somewhat expanded Palaeogene sequence deposited in moderate water depths and within the southern subtropical zone (Exon *et al*., 1992). Moreover, unlike many other regions in the world, the Exmouth Plateau has extensive seismic coverage because of petroleum exploration. Seismic records indicate a substantial Palaeogene record which includes thick successions in both offshore and inshore locations making the Exmouth Plateau a potential location for detailed Palaeogene oceanographic reconstructions.

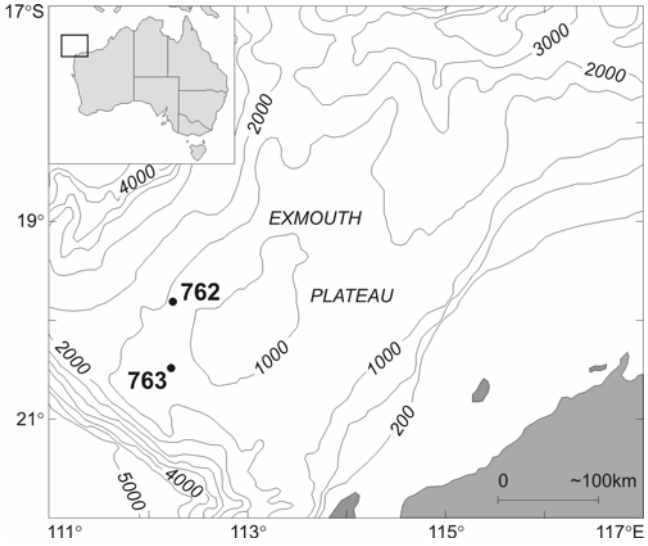

Figure 2. Map of the Exmouth Plateau including ODP Sites 762 and 763 of Leg 122 (adapted from Exon *et al*., 1992). Bathymetry in metres.

Current understanding of Palaeogene stratigraphy for the northwest margin of Australia is mostly a conglomeration of data from sidewall cores and ditch-cuttings mostly held outside of the public domain. Ocean Drilling Program (ODP) Sites 762 and 763 were drilled by Leg 122 in 1988 on the Exmouth Plateau in part to provide an accessible stratigraphic framework for the Tertiary and Cretaceous. Although Neogene and Cretaceous intervals are now well documented for these sites (Wonders, 1992; Zachiariasse, 1992), other than the ranges of calcareous nannofossils (Siesser and Bralower, 1992), and analyses of bulk carbonate carbon isotopes (Thomas *et al*., 1992),

the Palaeogene stratigraphic record has been given little attention. Planktic foraminifera have not been rigorously examined, carbon isotopes have not been measured on foraminiferal species or calibrated against other time markers, and the interpretation of polarity chrons (Galbrun, 1992) is inconsistent with the nannofossil stratigraphy (Siesser and Bralower, 1992). Moreover, the time scale used in previous work (Shipboard Scientific Party, 1990) is now outdated, precluding direct age comparisons with other regions. This study addresses these deficiencies by examining planktic foraminifera and their isotopic composition in sediment from ODP Site 762. The new data set is combined with the results of previous studies to construct the first detailed early Palaeogene record for the Exmouth Plateau.

MATERIALS AND METHODS

Samples

Ocean Drilling Program Hole 762C (**Fig. 2**) was drilled on the central Exmouth Plateau (19°53.24'S, 112°15.24'E) in 1360 m of water depth. Preliminary shipboard work (Haq *et al.*, 1990) and shore-based nannofossil investigations (Siesser and Bralower, 1992) documented 550 m of middle Eocene to lower Campanian nannofossil chalks and oozes from the recovered core. This study investigates 83 samples taken from some 200 m of sediment deposited between the late early Paleocene and the early to middle Eocene. Bulk sediment in this interval consists predominantly of white to pale yellow (5Y 8/2) or grey green (10YR 8/1) carbonate ooze and chalk.

Individual samples of ~20g were collected at ~1.5 m intervals from cores 762C-16X-4 to -37X-4 (307.5- 503.5 mbsf). Portions of each sample were processed for microfossils at the Australian Geological Survey Organization (AGSO) palaeontological laboratory. These samples were treated with hydrogen peroxide to remove organic matter, sieved to remove the <63 µm fraction, and stored in glass vials. The residues were picked for planktic foraminifera, either to completion or to obtain a complete record of taxonomic content. At least 200 and upwards of 500 specimens from each sample were separated and examined as representative of the faunal record.

Biostratigraphy

The identity, relative abundance of individual foraminiferal species, and distribution across the sample set from Site 762 were determined by optical microscopy and scanning electron microscope. Relative abundances of species were classified as dominant (D, >30%), common (C, 10-30%), rare (R, 2-10%) and extremely rare (X, <2%). Most specimens belong to the genus *Acarinina* (*A*), *Subbotina* (*S*), *Morozovella* (*M*), *Globanomalina* (*G*), *Chiloguembelina (C)* or *Parasubbotina* (*P*). The preservation state of the tests also was noted as 'poor', 'moderate' or 'good'. Tests with good preservation show minor secondary calcite growth or dissolution. Tests with moderate preservation are often infilled with calcite or fragmented, but can be classified to species. Tests with poor preservation are moderately to heavily encrusted with secondary calcite, and species identification is less certain.

The current planktic foraminiferal zonal scheme by Berggren *et al*. (1995) is used in this study. Although Site 762 was at southern mid-latitudes (~40°) during the Palaeogene (Veevers *et al*., 1991; Clarke and Jenkyns, 1999), the low latitude biozonation scheme by Berggren *et al*. (1995) best describes the observed faunal assemblages. Paleocene foraminiferal classification, including ranges and zonal boundaries, has been summarized recently by Olsson *et al*. (1999). Boundaries between biozones were placed halfway between the sample containing a defining marker species and the sample above or below it that lacks it.

Stable Isotopes

Specimens of *Subbotina* were separated and analysed for their carbon isotope composition. Although *Subbotina* probably inhabited deep surface waters in the thermocline (Berggren and Norris, 1997) this genus is considered especially appropriate for such work because carbon isotope composition shows little interspecies variation (Berggren and Norris, 1997) and size related variation (D'Hondt *et al*., 1994; Norris, 1996). However, as an added precaution to minimise the effect of ontogenetic changes in depth ecology, we restricted the size range of tests (210-260 µm diameter) and collected 20-30 specimens for each analysis. Although no single *Subbotina* species

spanned the entire early Palaeogene, species with suspected phylogenetic affinities (Olsson *et al*., 1999) and similar morphologies within the genus were collected. The species collected for isotope analyses were *S. triloculinoides* (Zone P1c to the middle of Subzone P4a/b), *S. triangularis* (Subzone P4a/b to Subzone P6a), and *S. patagonica* (Subzone P6a to Zone P10).

Stable isotopes were analysed at the isotope laboratory in the Earth Science Board at the University of California, Santa Cruz (see Billups *et al*., 1998). Samples were subjected to ultrasound whilst bathed in methanol for 3-5 s to remove adhering particles. Samples then were reacted at 90°C in H_3PO_4 on an autocarb common acid bath with the CO_2 generated then analyzed in a Prism gas source mass spectrometer. Carbon isotope values were calibrated to the Peedee belemnite (PDB) standard, and converted to conventional delta notation ($\delta^{13}C$).

RESULTS AND DISCUSSION

Foraminiferal Biostratigraphy

Planktic foraminifera contribute between 10% and 20% of bulk sample volume. The planktic to benthic foraminiferal ratio for the early Palaeogene is approximately 15:1 and the benthic foraminiferal component rarely exceeds 2%. Microfossils are generally complete and unabraded. Secondary recrystallisation or dissolution hampers the identification of species in only a few intervals (**Table 1**), notably within the foraminiferal biozones P4 and P7 (discussed below).

Some 74 species belonging to 17 genera were identified at Site 762, and established biozones can be recognised from the pattern of faunal succession (**Table 1; Fig. 3**). All zones from P1c to P10, with the exception of Subzone P4b, are found at Site 762, spanning the interval from the early Paleocene (Danian) to the early middle Eocene (Ypresian). Absolute age assignments are from Berggren *et al*. (1995). Boundaries between different zones are well defined unless noted otherwise. The zonal scheme adopted here generally follows that of Berggren *et al*. (1995) but some modification is required. Planktic foraminiferal species are listed and key species illustrated in Appendix 1 (Plates 1-3)

Table 1. Distribution of planktic foraminifera in Hole 762C. D = dominant, C = common, R = rare and X = extremely rare. A = *Acarinina*, S = *Subbotina*, M = *Morozovella*, G = *Globanomalina*, C = *Chiloguembelina*, P = *Parasubbotina*.

Period		Planktic Foraminiferal Zones (following Berggren *et al.*, 1995)		Core Section, Interval (cm) (Hole 762C)	Depth (mbsf)	*Eoglobigerina spiralis*	*Rectoguembelina cretacea*	*Subbotina trivialis*	*Praemurica pseudoinconstans*	*Globanomalina compressa*	*Praemurica inconstans*	*Parasubbotina pseudobulloides*	*Subbotina triloculinoides*	*Zeauvigerina waiparensis*	*Chiloguembelina midwayensis*	*Chiloguembelina subtriangularis*	*Subbotina cancellata*	*Parasubbotina varianta*	*Subbotina triangularis*	*Praemurica uncinata*	*Globanomalina ehrenbergi*	*Morozovella conicotruncata*	*Parasubbotina variospira*	*Morozovella angulata*	*Igorina albeari*	*Subbotina velascoensis*	*Morozovella occlusa*	*Globanomalina chapmani*	*Igorina pusilla*	*Acarinina strabocella*	*Morozovella apanthesma*	*Chiloguembelina crinita*	*Morozovella pasionensis*	*Acarinina mckannai*	*Globanomalina pseudomenardii*	*Acarinina subsphaerica*	*Acarinina nitida*	*Zeauvigerina aegyptiaca*	*Morozovella acutispira*	*Morozovella aequa*	*Chiloguembelina wilcoxensis*	*Globanomalina australiformis*	*Globanomalina ovalis*	*Morozovella acuta*	*Morozovella velascoensis*	*Morozovella gracilis*
EOCENE	Mid	P10		16X-4, 30-35	307.80	.	.	.	.	.	.	.	.	.	.	.	.	.	.	.	.	.	.	.	.	.	.	.	.	.	.	.	.	.	.	.	.	.	.	.	.	.	.	.	.	.
	Early	P9		17X-1, 56-61	313.06	.	.	.	.	.	.	.	.	.	.	.	.	.	.	.	.	.	.	.	.	.	.	.	.	.	.	.	.	.	.	.	.	.	.	.	.	.	.	.	.	.	.	.
				17X-2, 50-55	314.50	.	.	.	.	.	.	.	.	.	.	.	.	.	.	.	.	.	.	.	.	.	.	.	.	.	.	.	.	.	.	.	.	.	.	.	.	.	.	.	.	.	.	.
				17X-3, 40-45	315.90	.	.	.	.	.	.	.	.	.	.	.	.	.	.	.	.	.	.	.	.	.	.	.	.	.	.	.	.	.	.	.	.	.	.	.	.	.	.	.	.	.	.	.
				17X-4, 50-55	317.50	.	.	.	.	.	.	.	.	.	.	.	.	.	.	.	.	.	.	.	.	.	.	.	.	.	.	.	.	.	.	.	.	.	.	.	.	.	.	.	.	.	.	.
				17X-5, 49-54	318.99	.	.	.	.	.	.	.	.	.	.	.	.	.	.	.	.	.	.	.	.	.	.	.	.	.	.	.	.	.	.	.	.	.	.	.	.	.	.	.	.	.	.	.
				17X-6, 9-14	320.09	.	.	.	.	.	.	.	.	.	.	.	.	.	.	.	.	.	.	.	.	.	.	.	.	.	.	.	.	.	.	.	.	.	.	.	.	.	.	.	.	.	.	.
				18X-1, 106-111	323.06	.	.	.	.	.	.	.	.	.	.	.	.	.	.	.	.	.	.	.	.	.	.	.	.	.	.	.	.	.	.	.	.	.	.	.	.	.	.	.	.	.	.	.
				18X-2, 90-95	324.40	.	.	.	.	.	.	.	.	.	.	.	.	.	.	.	.	.	.	.	.	.	.	.	.	.	.	.	.	.	.	.	.	.	.	.	.	.	.	.	.	.	.	.
				18X-3, 106-111	326.06	.	.	.	.	.	.	.	.	.	.	.	.	.	.	.	.	.	.	.	.	.	.	.	.	.	.	.	.	.	.	.	.	.	.	.	.	.	.	.	.	.	.	.
				18X-4, 90-95	327.40	.	.	.	.	.	.	.	.	.	.	.	.	.	.	.	.	.	.	.	.	.	.	.	.	.	.	.	.	.	.	.	.	.	.	.	.	.	.	.	.	.	.	.
				18X-5, 106-111	329.06	.	.	.	.	.	.	.	.	.	.	.	.	.	.	.	.	.	.	.	.	.	.	.	.	.	.	.	.	.	.	.	.	.	.	.	.	.	.	.	.	.	.	.
				18X-6, 106-111	330.56	.	.	.	.	.	.	.	.	.	.	.	.	.	.	.	.	.	.	.	.	.	.	.	.	.	.	.	.	.	.	.	.	.	.	.	.	.	.	.	.	.	.	.
				19X-1, 50-55	332.00	.	.	.	.	.	.	.	.	.	.	.	.	.	.	.	.	.	.	.	.	.	.	.	.	.	.	.	.	.	.	.	.	.	.	.	.	.	.	.	.	.	.	.
				19X-2, 50-55	333.50	.	.	.	.	.	.	.	.	.	.	.	.	.	.	.	.	.	.	.	.	.	.	.	.	.	.	.	.	.	.	.	.	.	.	.	.	.	.	.	.	.	.	.
				19X-3, 50-54	335.00	.	.	.	.	.	.	.	.	.	.	.	.	.	.	.	.	.	.	.	.	.	.	.	.	.	.	.	.	.	.	.	.	.	.	.	.	X	.	.	.	.	.	.
				19X-4, 50-55	336.50	.	.	.	.	.	.	.	.	.	.	.	.	.	.	.	.	.	.	.	.	.	.	.	.	.	.	.	.	.	.	.	.	.	.	.	.	.	.	.	.	.	.	.
		P8		20X-1, 40-45	341.40	.	.	.	.	.	.	.	.	.	.	.	.	.	.	.	.	.	.	.	.	.	.	.	.	.	.	.	.	.	.	.	.	.	.	.	R	.	X	.	.	.	.
		P7		20X-2, 50-55	343.00	.	.	.	.	.	.	.	.	.	.	.	.	.	.	.	.	.	.	.	.	.	.	.	.	.	.	.	.	.	.	.	.	.	.	.	.	.	.	.	.	.	.
				20X-3, 50-55	344.50	.	.	.	.	.	.	.	.	.	.	.	.	.	.	.	.	.	.	.	.	.	.	.	.	.	.	.	.	.	.	.	.	.	.	.	.	.	.	.	.	.	.	.
				20X-4, 40-45	345.90	.	.	.	.	.	.	.	.	.	.	.	.	.	.	.	.	.	.	.	.	.	.	.	.	.	.	.	.	.	.	.	.	.	.	.	.	.	.	.	.	.	.	R
				21X-1, 50-55	351.00	.	.	.	.	.	.	.	.	.	.	.	.	.	.	.	.	.	.	.	.	.	.	.	.	.	.	.	.	.	.	.	.	.	.	.	.	.	.	.	.	.	.	.
				21X-2, 48-53	352.48	.	.	.	.	.	.	.	.	.	.	.	.	.	.	.	.	.	.	.	.	.	.	.	.	.	.	.	.	.	.	.	.	.	.	.	X	.	X	.	.	.	.	.
				22X-1, 43-47	360.43	.	.	.	.	.	.	.	.	.	.	.	.	.	.	.	.	.	.	.	.	.	.	.	.	.	.	.	.	.	.	.	.	.	.	.	R	.	C	.	.	.	.	C
				22X-2, 50-55	362.00	.	.	.	.	.	.	.	.	.	.	.	.	.	.	.	.	.	.	.	.	.	.	.	.	.	.	.	.	.	.	.	.	.	.	.	X	R	.	C	.	.	.	R
				22X-3, 49-54	363.49	.	.	.	.	.	.	.	.	.	.	.	.	.	.	.	.	.	.	.	.	.	.	.	.	.	.	.	.	.	.	.	.	.	.	.	.	.	.	R	.	.	.	R
				22X-4, 48-53	364.98	.	.	.	.	.	.	.	.	.	.	.	.	.	.	.	.	.	.	.	.	.	.	.	.	.	.	.	.	.	.	.	.	.	.	.	C	.	.	X	.	.	.	R
				22X-5, 50-55	366.50	.	.	.	.	.	.	.	.	.	.	.	.	.	.	.	.	.	.	.	.	.	.	.	.	.	.	.	.	.	.	.	.	.	.	X	.	R	.	.	.	.	.	.
				22X-6, 47-51	367.97	.	.	.	.	.	.	.	.	.	.	.	.	.	.	.	.	.	.	.	.	.	.	.	.	.	.	.	.	.	.	.	.	.	R	.	.	.	.	.	.	.	.	.
				23X-1, 43-47	369.93	.	.	.	.	.	.	.	.	.	.	.	.	.	.	.	.	.	.	.	.	.	.	.	.	.	.	.	.	.	.	.	.	.	R	.	.	.	.	.	.	.	.	R
		P6	b	23X-2, 50-54	371.50	.	.	.	.	.	.	.	.	.	.	.	.	.	.	.	.	.	.	.	.	.	.	.	.	.	.	.	.	.	.	.	.	.	R	.	.	.	.	.	.	.	.	.
				23X-3, 45-49	372.95	.	.	.	.	.	.	.	.	.	.	.	.	.	.	.	.	.	.	.	.	.	.	.	.	.	.	.	.	.	.	.	.	.	.	.	.	.	.	.	X	.	.	.
				24X-1, 49-53	379.49	.	.	.	.	.	.	.	.	.	.	.	.	.	.	.	.	.	.	.	.	.	.	.	.	.	.	.	.	.	.	.	.	.	.	.	C	R	.	.	.	.	.	.
				25X-1, 49-53	388.99	.	.	.	.	.	.	.	.	.	.	.	.	.	.	.	.	.	.	.	.	.	.	.	.	.	.	.	.	.	.	.	.	.	.	.	C	.	.	.	.	.	.	C
				25X-2, 50-54	390.50	.	.	.	.	.	.	.	.	.	.	.	.	.	.	.	.	.	.	.	.	.	.	.	.	R	.	.	.	.	.	.	.	.	.	.	C	.	.	.	.	.	.	.
				25X-3, 50-54	392.00	.	.	.	.	.	.	.	.	.	.	.	.	.	.	.	.	.	.	.	.	.	.	.	.	.	.	.	.	.	.	.	.	.	.	.	R	C	.	R	.	.	.	R
				25X-4, 49-53	393.49	.	.	.	.	.	.	.	.	.	.	.	.	.	.	C	.	.	.	.	.	.	.	.	.	.	.	.	.	.	.	.	.	.	.	.	.	C	.	R	.	.	.	R
				25X-5, 46-50	394.96	.	.	.	.	.	.	.	.	.	.	.	.	.	.	R	.	.	.	.	.	.	.	.	.	.	.	.	.	.	.	.	.	.	.	.	C	C	.	.	.	.	.	R
				26X-1, 50-54	398.50	.	.	.	.	.	.	.	.	.	.	.	.	.	.	.	.	.	.	.	.	.	.	.	.	.	.	.	.	.	.	.	.	.	.	.	R	R	.	.	.	.	.	.
			a	26X-2, 50-54	400.00	.	.	.	.	.	.	.	.	.	.	.	.	.	.	R	.	.	.	.	.	.	.	.	.	R	.	.	.	.	.	.	.	.	.	.	R	C	.	R	.	.	.
				26X-3, 36-41	401.36	.	.	.	.	.	.	.	.	.	.	.	.	.	.	C	.	.	.	.	.	.	.	.	.	.	.	.	.	.	.	.	.	.	.	.	C	C	.	.	.	.	.	R
				26X-4, 50-55	403.00	.	.	.	.	.	.	.	.	.	.	.	.	.	.	C	.	.	.	.	.	.	.	.	.	.	.	.	.	.	R	.	.	.	.	.	R	C	.	R	.	.	.	C
				26X-5, 46-50	404.46	.	.	.	.	.	.	.	.	.	.	.	.	.	.	C	.	.	.	.	.	.	.	.	.	.	.	.	.	.	.	.	.	.	.	.	C	C	.	R	.	.	.	R
				26X-6, 19-23	405.69	.	.	.	.	.	.	.	.	.	.	.	.	.	.	C	.	.	.	.	.	.	.	.	.	.	.	.	.	.	R	.	.	.	.	.	R	.	.	R	.	.	.	R
				27X-1, 100-104	403.50	.	.	.	.	.	.	.	.	.	.	.	.	.	.	R	.	.	.	.	.	.	.	.	.	C	.	.	.	.	.	.	.	.	.	.	R	C	.	.	.	.	.	C
				27X-2, 104-108	405.04	.	.	.	.	.	.	.	.	.	.	.	.	.	.	C	.	.	.	.	.	.	.	.	.	C	.	X	.	.	R	.	.	.	.	.	C	C	.	.	.	.	.	R
				27X-3, 95-99	406.45	.	.	.	.	.	.	.	.	.	.	.	.	.	.	R	.	.	.	.	.	.	.	.	.	D	.	.	.	.	.	.	.	.	.	.	C	C	.	R	.	.	.	R
		P5		27X-4, 95-99	407.95	.	.	.	.	.	.	.	.	.	R	.	.	R	R	.	.	.	.	.	.	.	C	.	X	.	.	.	C	.	.	.	.	.	.	C	C	.	R	.	X	R	R
				28X-1, 104-107	413.04	.	.	.	.	.	.	.	.	R	.	.	.	.	C	.	.	.	.	.	.	C	R	.	.	.	.	R	.	.	.	.	.	.	.	C	R	.	.	C	R	C	.
				28X-2, 10-12	413.60	.	.	.	.	.	.	.	.	.	R	.	.	R	C	.	.	.	.	.	.	D	C	.	.	.	.	.	.	C	.	.	.	R	.	.	C	R	.	X	R	R	C	.
				29X-1, 48-52	421.98	.	.	.	.	.	.	.	.	R	R	.	.	X	C	.	.	.	.	.	.	C	R	X	.	.	.	R	.	.	.	.	.	.	.	.	.	.	.	.	.	.	C	.
		P4	c	29X-2, 49-53	423.49	.	.	.	.	.	.	.	.	.	.	.	.	R	C	.	.	.	.	.	.	C	R	X	.	.	.	.	R	.	.	.	.	R	.	.	R	.	.	.	.	C
				29X-3, 46-50	424.96	.	.	.	.	.	.	.	.	.	.	.	.	R	C	.	.	.	.	.	.	C	C	R	.	.	.	R	.	.	X	.	C	.	.	R	R	.	.	.	.	R	R
				30X-1, 101-105	432.01	.	.	.	.	.	.	.	.	R	R	.	.	R	C	.	.	.	.	.	R	C	.	R	.	.	.	R	.	R	R	.	.	X	.	.	R	.	.	.	.	.	.
				30X-2, 100-104	433.50	.	.	.	.	.	.	.	.	R	R	.	.	R	C	.	.	.	.	.	C	C	.	C	.	.	.	C	.	R	X	R	.	.	.	.	R	.	.	.	.	R	.
				30X-3, 96-100	434.96	.	.	.	.	.	.	.	.	R	X	.	.	R	C	.	.	.	.	.	R	R	.	.	.	.	.	R	.	C	R	C	.	.	.	.	R	X	.	.	.	.	.
				30X-4, 66-70	437.26	.	.	.	.	.	.	.	.	.	X	.	.	C	C	.	.	.	.	.	R	R	.	R	.	.	.	R	.	C	R	C	R	.	.	.	R	.	R	.	.	.	.
				31X-1, 100-104	441.50	.	.	.	.	.	.	.	.	.	.	.	.	C	C	.	.	.	.	R	C	R	R	C	.	.	R	R	X	C	R	C	C	.	R	.	.	.	.	X	R	C
				31X-2, 100-104	443.00	.	.	.	.	.	.	.	.	R	C	.	.	C	D	.	.	.	.	R	R	R	R	C	.	.	R	R	.	C	R	C	C	.	R	R	R	.	R	R	R	C
				31X-3, 97-101	444.47	.	.	.	.	.	.	.	.	R	R	.	R	R	D	.	.	.	.	.	C	C	R	R	.	.	R	R	R	R	R	C	C	.	R	R	C	R	R	C	R	R
			a/b	31X-4, 97-101	445.97	.	.	.	.	.	.	.	.	R	R	.	C	R	C	.	.	.	C	C	C	R	R	.	.	R	R	X	R	R	C	D	.	C	R	.	X?	X	.	.	.
				31X-5, 101-105	447.51	.	.	.	.	.	.	.	.	R	C	.	C	R	C	.	.	.	R	C	R	R	R	.	.	R	R	X	R	R	C	D	.	C	R	R	.	.	.	.	.	.
				31X-6, 97-101	448.97	.	.	.	.	.	.	.	.	R	C	.	C	R	C	.	.	.	C	C	C	R	C	X	R	R	C	X	C	R	R	D	X	C	.	.	.	.	.	.	.	.
				32X-1, 101-105	451.01	.	.	.	.	.	.	.	R	.	C	.	R	R	C	.	.	.	C	C	R	C	R	.	.	.	C	R	C	R	C	D	.	R	.	.	.	.	.	.	.	.
				32X-2, 100-104	452.50	.	.	.	.	.	.	.	C	R	C	.	R	C	C	.	X	.	R	C	C	C	R	R	R	.	.	R	R	R	C	D	.	C	R	.	.	.	.	.	.	.
				33X-1, 100-104	460.50	.	.	.	.	.	.	.	D	.	R	.	C	C	C	.	R	R	C	C	.	.	C	.	.	C	R	.	R	C	.	C	.	.	.	.	.	.	.	.	.
				33X-2, 100-104	462.00	.	.	.	.	.	.	.	C	R	R	.	R	R	C	.	.	.	C	R	.	.	C	R	.	.	C	X	.	C	.	.	R	.	.	.	.	.	.	.	.	.
				33X-3, 100-104	463.50	.	.	.	.	.	.	.	C	X	C	.	R	D	C	.	.	.	.	R	.	C	C	.	.	.	.	C	.	.	.	.	R	.	.	.	.	.	.	.	.	.
				33X-4, 95-99	464.95	.	.	.	.	.	.	.	D	R	C	.	C	C	.	.	X	R	C	R	C	C	R	C	R	R	C	R	R	C	X	R	.	.	.	.	.	.	.	.	.
				33X-5, 100-104	466.50	.	.	.	.	.	.	.	D	.	C	.	C	R	C	.	R	R	C	.	R	C	R	C	R	.	R	R	C	X	.	.	.	.	.	.	.	.	.	.	.
				33X-6, 46-50	467.46	.	.	.	.	.	.	.	C	.	C	.	C	C	.	.	C	C	C	.	R	.	C	R	.	D	C	R	R	R	R	C	.	.	.	.	.	.	.	.	.	.
				34X-1, 100-104	470.00	.	.	.	.	.	.	R	C	R	C	R	C	R	R	.	.	C	R	C	X	R	.	.	C	R	R	D	R	R	R	R	.	.	.	.	.	.	.	.	.	.
		P3	b	34X-2, 100-103	471.50	.	.	.	.	C	.	X	C	R	C	R	C	C	C	.	.	C	C	D	.	C	.	C	.	.	C	R	.	.	.	.	.	.	.	.	.	.	.	.	.
				34X-3, 97-101	472.97	.	.	.	.	.	.	.	C	.	C	C	R	R	C	.	.	C	C	C	.	R	R	C	R	C	R	R	.	.	.	.	.	.	.	.	.	.	.	.	.	.
				34X-4, 97-101	474.47	.	.	.	.	.	.	R	C	R	C	R	C	C	C	.	R	C	C	C	.	R	C	C	.	.	.	.	.	.	.	.	.	.	.	.	.	.	.	.	.	.
				34X-5, 100-104	476.00	.	.	.	.	C	X	.	D	.	C	.	C	C	C	.	R	C	X	C	.	.	X	.	.	.	.	.	.	.	.	.	.	.	.	.	.	.	.	.	.	.
				35X-1, 90-95	479.40	.	.	.	.	C	R	.	C	R	C	.	C	.	D	.	C	C	C	R	R	X	.	.	.	.	.	.	.	.	.	.	.	.	.	.	.	.	.	.	.	.
				35X-2, 92-96	480.92	.	.	.	.	C	C	R	D	C	C	C	C	C	C	.	R	R	C	C	R	.	.	.	.	.	.	.	.	.	.	.	.	.	.	.	.	.	.	.	.	.
			a	36X-1, 17-21	488.17	.	.	.	.	D	C	R	C	R	C	C	C	C	C	.	C	R	R	R	.	.	.	.	.	.	.	.	.	.	.	.	.	.	.	.	.	.	.	.	.	.
	Early	P2		37X-1, 99-103	498.49	.	R	R	C	C	C	R	C	R	C	C	C	C	C	.	C	.	.	.	.	.	.	.	.	.	.	.	.	.	.	.	.	.	.	.	.	.	.	.	.	.
				37X-2, 97-101	499.97	C	R	R	C	R	R	C	C	C	C		C	D	R	R	.	.	.	.	.	.	.	.	.	.	.	.	.	.	.	.	.	.	.	.	.	.	.	.	.	.	.
		P1	c	37X-3, 97-101	501.47	R	R	C	D	C	C	C	C	R	C	R	C	R	.	.	.	.	.	.	.	.	.	.	.	.	.	.	.	.	.	.	.	.	.	.	.	.	.	.	.	.
				37X-4, 96-100	502.96	R	R	C	C	C	X	R	C	R	C	.	.	.	.	.	.	.	.	.	.	.	.	.	.	.	.	.	.	.	.	.	.	.	.	.	.	.	.	.	.	.	.	.

Table 1 cont.

Morozovella subbotinae	*Acarinina soldadoensis*	*Acarinina pseudotopilensis*	*Acarinina primitiva*	*Chiloguembelina trinitatensis*	*Igorina broedermanni*	*Subbotina patagonica*	*Morozovella marginodentata*	*Acarinina quetra*	*Planorotalites pseudoscitula*	*Subbotina eocaena*	*Acarinina wilcoxensis*	*Morozovella dolabrata*	*Morozovella formosa*	*Morozovella lensiformis*	*Pseudohastigerina wilcoxensis*	*Subbotina hagni*	*Pseudohastigerina micra*	*Morozovella aragonensis*	*Morozovella densa*	*Acarinina collactea*	*Muricoglobigerina senni*	*Catapsydrax unicavus*	*Subbotina inaequispira*	*Morozovella caucasica*	*Acarinina cuneicamerata*	*Subbotina frontosa*	*Acarinina matthewsae*	*Acarinina bullbrooki*	*Morozovella spinulosa*	*Acarinina decepta*	*Subbotina cryptomphala*	*Guembelitrioides lozanoi*	*Guembelitrioides higginsi*	Diversity (No. species)	Dominant Genus	Comments	Foraminiferal Preservation
.	.	C	D	.	.	C	.	.	C	C	.	.	.	R	C	R	R	C	R	C	.	.	C	.	R	C	C	C	.	R	R	C	C	21	*A*		Good
.	.	.	C	.	R	C	.	.	R	D	.	.	.	C	R	R	R	C	R	C	.	.	C	C	.	C	C	C	X	C	R	R	.	21	*M*		Good
.	.	R	C	.	C	C	.	.	.	D	.	.	.	C	R	C	R	C	R	C	X	.	R	C	R	C	R	C	X	C	.	C	.	22	*S,A*		Good
.	R	R	.	.	.	R	.	.	.	C	.	.	.	C	C	C	C	.	R	.	.	.	C	.	.	.	.	.	R	C	R	R	C	.	14	*S*		Good
.	C	.	R	.	R	C	.	.	.	C	.	R	.	.	C	.	.	R	R	C	X	.	R	D	.	C	C	C	R	R	.	.	C	.	19	*S*		Good
.	.	C	.	.	R	C	.	.	.	R	.	R	.	.	C	C	R	R	R	R	X	.	R	C	.	R	C	C	.	.	.	.	R	.	18	*A,S*		Good
.	R	C	C	.	R	R	.	.	.	C	.	.	.	.	C	R	C	C	C	D	.	.	C	C	R	C	C	R	.	R	R	.	.	20	*A,S*		Good
.	C	C	C	.	R	C	.	.	.	C	.	.	.	.	R	R	R	C	C	.	R	C	D	.	R	R	R	R	R	R	X?	.	.	22	*M,A*	Benthics common	Good
.	C	C	C	.	C	C	.	R?	C	D	.	.	.	.	C	C	R	C	C	R	.	R	R	C	R	R	C	C	X	R	R	X	.	25	*A*	Large *Acarinina*, calcite crystals	Good
.	C	C	C	.	C	C	.	R	C	C	.	.	.	.	C	R	C	R	C	C	.	C	C	C	.	.	D	R	.	R	R	.	.	21	*A*	Calcite crystals	Good
.	.	D	R	.	R	R	.	R	R	C	.	.	.	.	C	C	C	R	.	C	.	C	C	C	.	.	R	C	C	R	.	.	.	19	*A,S*		Good
.	C	C	C	.	C	.	.	C	.	C	.	.	.	.	C	C	C	C	.	R	R	R	R	D	C	C	C	R	R	C	.	.	.	21	*A,S*		Good
.	C	C	C	.	R	R	.	.	R	C	.	.	.	.	C	R	D	C	R	C	C	R	C	C	R	C	R	C	R	C	.	.	.	23	*M*	Calcite crystals	Good
.	C	R	C	.	R	C	.	.	C	D	.	.	.	C	C	R	C	D	.	C	X	R	R	R	C	R	C	R	R	C	.	.	.	22	*S*	Calcite crystals	Mod
.	C	C	D	.	C	.	.	.	C	C	C	.	.	C	C	R	R	C	C	C	R	.	R	R	R	.	C	C	X	C	.	.	.	22	*A*	Iron-stained pyrite, calcite crystals	Mod
.	C	.	C	.	R	.	.	.	C	C	.	R	.	C	C	.	X	C	.	C	R	.	C	C	C	.	R	C	C	.	C	.	.	18	*A*	Calcite crystals	Poor
.	.	.	R	.	R	R	.	.	C	X	R	R	.	.	R	.	R	R	R	D	R	.	R	R	R	R	C	C	X	C	.	.	.	21	*A*	*Morozovella* rare, calcite crystals	Mod
.	C	C	D	.	R	R	.	R	C	C	R	R	.	C	C	.	R	R	.	R	C	.	C	.	.	.	.	.	.	.	.	.	.	19	*A*	Calcite crystals	Mod
X	C	R	D	.	R	C	.	C	C	C	.	R	R	R	R	R	.	R	.	R	C	.	C	.	.	.	.	.	.	.	.	.	.	18	*S*	Calcite crystals	Mod
.	D	R	C	.	R	R	.	R	C	C	.	C	.	C	R	.	.	C	.	.	.	.	.	X	.	.	.	.	.	.	.	.	.	16	*A*	Large *Acarinina*	Mod
.	.	R	D	.	R	C	.	.	C	C	.	C	.	R	.	.	.	.	.	R	.	R	.	R	.	.	.	.	.	.	.	.	.	12	*A,S*	Iron-stained pyrite calcite crystals	Poor
.	.	R	R	.	.	R	.	.	C	C	.	C	.	.	.	.	.	.	.	.	.	.	.	.	.	.	.	.	.	.	.	.	.	6?		Heavy recrystallisation	Poor
C	C	C	C	.	X	D	X?	.	R	R	R	C	R	C	C	X	R	R	.	C	C	X	R?	.	.	.	.	.	.	.	.	.	.	23	*S*		Poor
C	C	R	C	.	C	R	.	.	C	C	R?	C	R	C	C	.	.	.	C	R	C	C	.	.	.	.	.	.	.	.	.	.	.	20	*A*	Iron-stained pyrite	Poor
C	C	C	D	.	.	C	.	R	C	C	.	C	C	C	R	.	X	R	R	R	R	R?	.	.	.	.	.	.	.	.	.	.	.	21	*A*	*Subbotina* rare	Good
R	C	R	D	.	.	R	.	.	.	C	.	R	C	C	.	.	.	R	.	R	.	.	.	.	.	.	.	.	.	.	.	.	.	13	*A,S*	*Morozovella* rare	Mod
R	C	R	R	.	.	R	.	.	.	C	.	R	R	C	.	C	.	.	.	.	.	.	.	.	.	.	.	.	.	.	.	.	.	17	*A,S*	Benthics common	Good
.	.	C	D	.	C	R	.	.	D	C	R	.	X	R	R	.	.	.	R	R	.	.	.	.	.	.	.	.	.	.	.	.	.	16	*A,S*	Benthics common	Poor
R	.	R	C	.	C	D	.	R	C	C	.	.	X	R	C	.	.	.	X	R	X	.	.	.	.	.	.	.	.	.	.	.	.	15	*A,S*	Benthics common	Poor
R	D	R	C	.	.	C	.	.	C	C	.	.	.	.	C	R	.	.	R	R	X	.	.	.	.	.	.	.	.	.	.	.	.	14	*A*	Benthics common	Poor
C	C	R	D	.	.	C	R	.	.	C	.	C	R	R	R	.	.	.	.	.	.	.	.	.	.	.	.	.	.	.	.	.	.	12	*M,A*	*Morozovella* common	Mod
R	C	R	R	X	.	C	R	.	C	C	X	C	R	.	C	R	X	.	.	.	.	.	.	.	.	.	.	.	.	.	.	.	.	18	*A,S*		Poor
C	C	R	D	R	.	C	C	C	.	C	R	.	.	R	C	C	.	.	.	.	.	.	.	.	.	.	.	.	.	.	.	.	.	15	*S,A*	Pyrite	Poor
C	C	C	C	C	.	D	C	.	R	C	.	R	X	R	R	C	.	.	.	.	.	.	.	.	.	.	.	.	.	.	.	.	.	16	*A,M*	Pyrite	Good
C	D	C	C	.	X	C	R	R	.	C	C	.	R	R	.	.	.	.	.	.	.	.	.	.	.	.	.	.	.	.	.	.	.	17	*A*		Poor
C	C	.	C	C	.	C	R	.	D	C	R	.	.	.	C	C	R	.	.	.	.	.	.	.	.	.	.	.	.	.	.	.	.	16	*M*		Good
R	C	R	C	.	.	C	C	R	C	D	.	C	.	C	.	C	.	.	.	.	.	.	.	.	.	.	.	.	.	.	.	.	.	17	*S*		Good
C	C	R	C	C	R	C	C	R	R	C	.	C	.	C	.	R	.	.	.	.	.	.	.	.	.	.	.	.	.	.	.	.	.	19	*M*		Good
R	C	R	C	C	.	D	C	R	X	C	R	X	X	C	X	.	.	.	.	.	.	.	.	.	.	.	.	.	.	.	.	.	.	16	*S*		Mod
D	C	R	R	R	C	C	C	R	X	C	R	.	.	.	.	.	.	.	.	.	.	.	.	.	.	.	.	.	.	.	.	.	.	17	*M,S*	Benthics common	Good
R	C	R	C	C	.	D	C	.	X	.	.	.	.	.	.	.	.	.	.	.	.	.	.	.	.	.	.	.	.	.	.	.	.	18	*S,A*		Good
R	C	R	C	C	R	C	C	.	R	.	.	.	.	.	.	.	.	.	.	.	.	.	.	.	.	.	.	.	.	.	.	.	.	15	*S*		Mod
R	C	R	C	C	.	C	R	C	.	.	R	.	.	.	.	.	.	.	.	.	.	.	.	.	.	.	.	.	.	.	.	.	.	14	*S*		Good
R	R	R	R	X	R	C	.	.	R	R	.	.	.	.	.	.	.	.	.	.	.	.	.	.	.	.	.	.	.	.	.	.	.	14	*S*		Good
C	C	R	C	.	R	D	C	C	.	C	.	.	.	.	.	.	.	.	.	.	.	.	.	.	.	.	.	.	.	.	.	.	.	14	*S*	Pyrite, Calcite crystals	Good
C	C	.	C	.	.	D	R	C	X	C	.	.	.	.	.	.	.	.	.	.	.	.	.	.	.	.	.	.	.	.	.	.	.	14	*A*	Benthics rare	Mod
C	R	R	R	.	R	C	C	R	R	R	R	.	.	.	.	.	.	.	.	.	.	.	.	.	.	.	.	.	.	.	.	.	.	16	*A*	Benthics rare	Good
R	C	.	C	X	.	C	.	C	R	R	R	C	.	.	.	.	.	.	.	.	.	.	.	.	.	.	.	.	.	.	.	.	.	20	*A*	*Morozovella* radiate, benthics rare	Good
R	D	R	C	.	C	C	.	C	.	X	.	.	.	.	.	.	.	.	.	.	.	.	.	.	.	.	.	.	.	.	.	.	.	18	*A*	Pyrite, benthics common	Mod
R	C	C	C	X	X	C	R?	R	X	.	.	.	.	.	.	.	.	.	.	.	.	.	.	.	.	.	.	.	.	.	.	.	.	21	*S*	Pyrite, benthics common	Poor
.	C	.	R	R	R	R	.	.	.	.	.	.	.	.	.	.	.	.	.	.	.	.	.	.	.	.	.	.	.	.	.	.	.	14	*S*	Pyrite, benthics common	Mod
.	C	.	R	R	C	C	.	.	.	.	.	.	.	.	.	.	.	.	.	.	.	.	.	.	.	.	.	.	.	.	.	.	.	16	*S*	*Chiloguembbelina* rare	Mod
.	R	.	R	R	R	R	.	.	.	.	.	.	.	.	.	.	.	.	.	.	.	.	.	.	.	.	.	.	.	.	.	.	.	17	*A,S*	*Chiloguembbelina* rare	Mod
.	R	.	.	.	.	.	.	.	.	.	.	.	.	.	.	.	.	.	.	.	.	.	.	.	.	.	.	.	.	.	.	.	.	14	*S,A*	*Morovella* rare	Poor
.	R	.	R	.	.	.	.	.	.	.	.	.	.	.	.	.	.	.	.	.	.	.	.	.	.	.	.	.	.	.	.	.	.	15	*A,S*	*Morovella* rare	Poor
.	C	.	.	.	.	.	.	.	.	.	.	.	.	.	.	.	.	.	.	.	.	.	.	.	.	.	.	.	.	.	.	.	.	13	*A,S*	*Morovella* rare	Poor
.	D	.	.	.	.	.	.	.	.	.	.	.	.	.	.	.	.	.	.	.	.	.	.	.	.	.	.	.	.	.	.	.	.	14	*S*	*Morovella* rare	Mod
C	R	.	.	.	.	.	.	.	.	.	.	.	.	.	.	.	.	.	.	.	.	.	.	.	.	.	.	.	.	.	.	.	.	20	*S*		Poor
C	R	.	.	.	.	.	.	.	.	.	.	.	.	.	.	.	.	.	.	.	.	.	.	.	.	.	.	.	.	.	.	.	.	25	*S*	*Subbotina* very common	Poor
R	C	R	C	.	.	.	.	.	.	.	.	.	.	.	.	.	.	.	.	.	.	.	.	.	.	.	.	.	.	.	.	.	.	29	*A,S*	*G. beccariiformis* common	Mod
.	.	.	.	.	.	.	.	.	.	.	.	.	.	.	.	.	.	.	.	.	.	.	.	.	.	.	.	.	.	.	.	.	.	21	*S*	Benthics common	Mod
.	.	.	.	.	.	.	.	.	.	.	.	.	.	.	.	.	.	.	.	.	.	.	.	.	.	.	.	.	.	.	.	.	.	20	*S*	Benthics common	Poor
.	.	.	.	.	.	.	.	.	.	.	.	.	.	.	.	.	.	.	.	.	.	.	.	.	.	.	.	.	.	.	.	.	.	22	*A*	Benthics common	Mod
.	.	.	.	.	.	.	.	.	.	.	.	.	.	.	.	.	.	.	.	.	.	.	.	.	.	.	.	.	.	.	.	.	.	19	*M,G*		Poor
.	.	.	.	.	.	.	.	.	.	.	.	.	.	.	.	.	.	.	.	.	.	.	.	.	.	.	.	.	.	.	.	.	.	22	*S*		Mod
.	.	.	.	.	.	.	.	.	.	.	.	.	.	.	.	.	.	.	.	.	.	.	.	.	.	.	.	.	.	.	.	.	.	16	*S*	Benthics common	Good
.	.	.	.	.	.	.	.	.	.	.	.	.	.	.	.	.	.	.	.	.	.	.	.	.	.	.	.	.	.	.	.	.	.	16	*P*		Poor
.	.	.	.	.	.	.	.	.	.	.	.	.	.	.	.	.	.	.	.	.	.	.	.	.	.	.	.	.	.	.	.	.	.	11	*S*	Benthics common	Poor
.	.	.	.	.	.	.	.	.	.	.	.	.	.	.	.	.	.	.	.	.	.	.	.	.	.	.	.	.	.	.	.	.	.	23	*S*	Benthics common	Good
.	.	.	.	.	.	.	.	.	.	.	.	.	.	.	.	.	.	.	.	.	.	.	.	.	.	.	.	.	.	.	.	.	.	18	*S*		Mod
.	.	.	.	.	.	.	.	.	.	.	.	.	.	.	.	.	.	.	.	.	.	.	.	.	.	.	.	.	.	.	.	.	.	17	*A,S*	Benthics common	Poor
.	.	.	.	.	.	.	.	.	.	.	.	.	.	.	.	.	.	.	.	.	.	.	.	.	.	.	.	.	.	.	.	.	.	21	*S*		Poor
.	.	.	.	.	.	.	.	.	.	.	.	.	.	.	.	.	.	.	.	.	.	.	.	.	.	.	.	.	.	.	.	.	.	16	*S*		Mod
.	.	.	.	.	.	.	.	.	.	.	.	.	.	.	.	.	.	.	.	.	.	.	.	.	.	.	.	.	.	.	.	.	.	15	*P*		Good
.	.	.	.	.	.	.	.	.	.	.	.	.	.	.	.	.	.	.	.	.	.	.	.	.	.	.	.	.	.	.	.	.	.	15	*S*	Pyrite	Poor
.	.	.	.	.	.	.	.	.	.	.	.	.	.	.	.	.	.	.	.	.	.	.	.	.	.	.	.	.	.	.	.	.	.	12	*S*	Pyrite	Mod
.	.	.	.	.	.	.	.	.	.	.	.	.	.	.	.	.	.	.	.	.	.	.	.	.	.	.	.	.	.	.	.	.	.	13	*S*	Pyrite, calcite crystals	Good
.	.	.	.	.	.	.	.	.	.	.	.	.	.	.	.	.	.	.	.	.	.	.	.	.	.	.	.	.	.	.	.	.	.	15	*P*	Pyrite	Good
.	.	.	.	.	.	.	.	.	.	.	.	.	.	.	.	.	.	.	.	.	.	.	.	.	.	.	.	.	.	.	.	.	.	14	*G*	Pyrite, calcite crystals	Good
.	.	.	.	.	.	.	.	.	.	.	.	.	.	.	.	.	.	.	.	.	.	.	.	.	.	.	.	.	.	.	.	.	.	14	*S*	Benthics common	Good
.	.	.	.	.	.	.	.	.	.	.	.	.	.	.	.	.	.	.	.	.	.	.	.	.	.	.	.	.	.	.	.	.	.	14	*P*	Benthics common	Good
.	.	.	.	.	.	.	.	.	.	.	.	.	.	.	.	.	.	.	.	.	.	.	.	.	.	.	.	.	.	.	.	.	.	14	*P,C*	Benthics common	Good
.	.	.	.	.	.	.	.	.	.	.	.	.	.	.	.	.	.	.	.	.	.	.	.	.	.	.	.	.	.	.	.	.	.	10	*G,C*	Benthics common	Mod

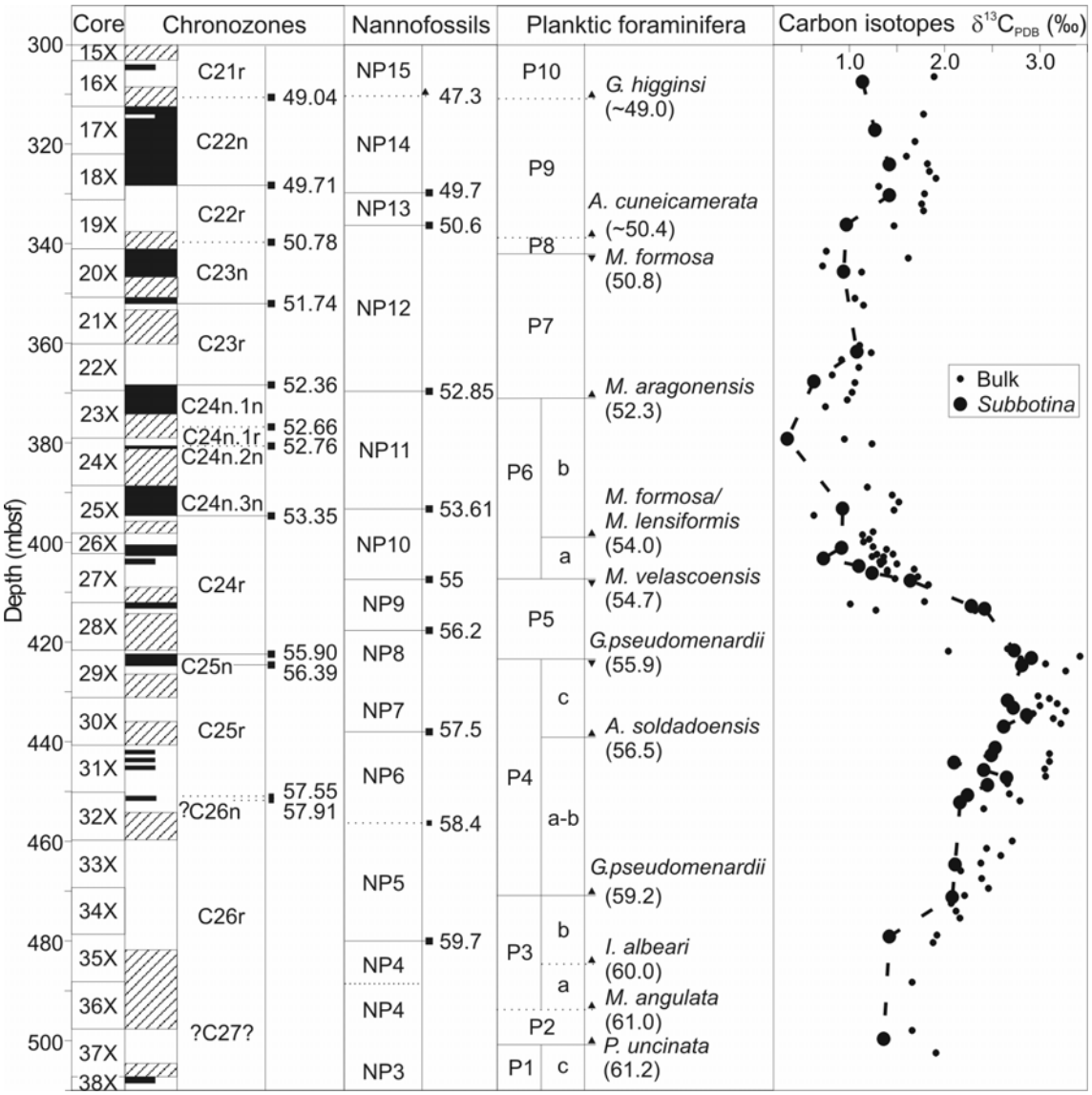

Figure 3. Comparison of planktic foraminiferal biozones (this study), nannofossil biozones (Siesser & Bralower, 1992), recalibrated magnetostratigraphy (this study) and carbon isotope data for *Subbotina* (this study) and the bulk sediment (Thomas *et al.*, 1992) for the early Palaeogene interval at ODP Site 762. Ages follow Berggren *et al*. (1995). Larger circles with dashed lines = $\delta^{13}C$, *Subbotina* specimens; small filled circles = $\delta^{13}C$, bulk sediment.

P1c. FAD of *Globanomalina compressa* and/or *Praemurica inconstans* to FAD of *Praemurica uncinata* (500.72 mbsf). Age: 63.0-61.2 Ma, early Paleocene (Danian). Subzone P1c extends below our sampled interval as only two samples are representative of it. The upper boundary of Subzone P1c is difficult to locate in some sequences because of the short stratigraphic range of its marker species, *Pr. uncinata* (**Plate 1, figs 1-3**). However, this species has been found at Site 762, and is a useful correlation tool. Common species found in uppermost Subzone P1c include *Pr. pseudoinconstans*,

Parasubbotina varianta, Subbotina trivialis, S. triloculinoides, Globanomalina compressa, Chiloguembelina midwayensis and *C. subtriangularis*. Faunal assemblages within this Subzone are consistent with the global scheme (Olsson *et al*., 1999).

P2. FAD of *Praemurica uncinata* (500.72 mbsf) to FAD of *Morozovella angulata* (493.33 mbsf). Age: 61.2-61.0 Ma, late early Paleocene (late Danian). Site 762 contains the transition from *Praemurica inconstans/trinidadensis* to *Pr. uncinata,* which marks the lower zonal boundary. However, an 8m core gap between cores -37X-1 and -36X-1 below the FAD of *Morozovella angulata* (**Plate 1, figs 4-6**) precludes high resolution sampling and accurate placement for the upper boundary. Common species in this zone at Site 762 include *Parasubbotina varianta, P. pseudobulloides, Subbotina triloculinoides, S. cancellata, Praemurica pseudoinconstans* and *Chiloguembelina midwayensis*. This overall assemblage is typical of Zone P2 elsewhere (Olsson *et al*., 1999).

P3. FAD of *Morozovella angulata* (493.33 mbsf) to FAD of *Globanomalina pseudomenardii* (470.75 mbsf). Age: 61.0-59.2 Ma, late Paleocene (Selandian).

P3a. FAD of *Morozovella angulata* (493.33 mbsf) to FAD of *Igorina albeari* (484.55 mbsf*)*. Age: 61.0-60.0 Ma, early late Paleocene (Selandian). The boundaries for this subzone cannot be placed with a high degree of confidence because there is an 8m core gap below the FAD of *Morozovella angulata*, and an 8m core gap below the FAD of *Igorina albeari* (**Plate 1, figs 7-9**). Common species in Subzone P3a at Site 762 include *Globanomalina compressa, Parasubbotina varianta, P. pseudobulloides* and *Subbotina triloculinoides*. The overall assemblage of Subzone P3a at Site 762 is similar to that described elsewhere (Olsson *et al*., 1999), and includes the first appearances of the *Morozovella angulata/conicotruncata* complex, which marks the beginning of the late Paleocene *Morozovella* radiation.

P3b. FAD of *Igorina albeari* (484.55 mbsf) to FAD of *Globanomalina pseudomenardii* (470.75 mbsf). Age: 60.0-59.2 Ma, late Paleocene (Selandian). The upper boundary for Subzone P3b is well defined because *Acarinina subsphaerica*, *A. nitida* and *A. mckannai* have near simultaneous FADs with *Globanomalina pseudomenardii* (**Plate 1, figs 10-12**) at Site 762 and elsewhere (Olsson *et al*., 1999).

Common species in Subzone P3b at Site 762 include *Morozovella angulata*, *M. conicotruncata*, *Parasubbotina variospira*, *Subbotina triloculinoides*, *Globanomalina chapmani*, *G. ehrenbergi* and the first appearance of *Acarinina* with *A. strabocella*. This assemblage is typical of Subzone P3b faunal assemblages (Olsson *et al*., 1999), except that *Morozovella velascoensis* does not make its first appearance here but at the base of Zone P4c.

P4. Total range of *Globanomalina pseudomenardii* (470.75- 423.03 mbsf). Age: 59.2-55.9 Ma, middle late Paleocene (late Selandian-Thanetian). The lower boundary of Zone P4 is placed with moderate conference because *Globanomalina pseudomenardii* has a patchy occurrence at Site 762 and has a similar morphology to both *G. ehrenbergi* and *G. chapmani* (**Plate 1, figs 10-12**). Indeed, preliminary work on the foraminifera at Site 762 (Shipboard Scientific Party, 1990) described *Globanomalina pseudomenardii* as the inflated '*chapmani* type'. However, there is morphological variability within this species with some of the smaller specimens displaying a distinct keel and a sharpened angular periphery. It is one of these more typical *Globanomalina pseudomenardii* morphotypes that marks the P4/P5 zonal boundary.

P4a-b. FAD of *Globanomalina pseudomenardii* (470.75 mbsf) to FAD of *Acarinina soldadoensis* (439.38 mbsf). Age: 59.2-56.5 Ma, middle late Paleocene (late Selandian-Thanetian). In the global scheme, the LAD of *Acarinina subsphaerica* (**Plate 2, figs 14-16**) defines the base of Subzone P4b (Olsson *et al*., 1999). However, at Site 762, this datum occurs in the upper part of Subzone P4c. Consequently, Subzones P4a and P4b cannot be distinguished at Site 762, and they have been combined. Common species of Subzone P4a-b at Site 762 include the *Morozovella angulata-conicotruncata* complex, *M. apanthesma*, *M. acutispira*, *Acarinina subsphaerica*, *A. mckannai*, *A. nitida*, *Igorina albeari*, *Parasubbotina varianta*, *Subbotina triloculinoides*, *S. triangularis*, *S. velascoensis* and *Chiloguembelina midwayensis*. Such an assemblage is characteristic of subzones P4a and P4b in the global scheme (Olsson *et al*., 1999).

P4c. FAD of *Acarinina soldadoensis* (439.38 mbsf) to LAD of *Globanomalina pseudomenardii* (423.03 mbsf). Age: 56.5-55.9 Ma, late Paleocene (late Thanetian). At the base of Subzone P4c at Site 762 the FAD of *Acarinina soldadoensis* (**Plate 1, figs 13-15**) coincides with the FADs of *A. primitiva*, *A. pseudotopilensis*, *Morozovella*

velascoensis, M. acuta and *M. aequa* as found elsewhere (Olsson *et al*., 1999). The interval assigned to this zone at Site 762 is relatively large compared to that of the global scheme (Berggren *et al*., 1995) and its base in particular does not correlate well with the nannofossil zones for the site (Siesser and Bralower, 1992). However, we regard the lower boundary of Subzone P4c as being well defined at Site 762 because so many species make their first appearances at its base, representing a pattern consistent with that of the global scheme.

P5. LAD of *Globanomalina pseudomenardii* (423.03 mbsf) to LAD of *Morozovella velascoensis* (407.23 mbsf). Age: 55.9-54.7 Ma, latest Paleocene-early Eocene (latest Thanetian-earliest Ypresian). The distribution of *Morozovella velascoensis* (**Plate 1, figs 16-18**) is somewhat patchy at Site 762 (**Table 1**) and may not represent its true range. Such a pattern may relate to the higher latitudes and cooler temperatures for the Exmouth Plateau during the time of deposition (due to its location at that time, well to the south), as the species is typical of more tropical areas (Olsson *et al*., 1999). Faunal assemblages in Zone P5 at Site 762 commonly include *Subbotina velascoensis, S. triangularis, S. patagonica, Igorina broedermanni, Morozovella aequa, M. subbotinae, Acarinina soldadoensis* and *A. primitiva,* all typical of other global locations (Berggren *et al*., 1995). The FAD of *Morozovella dolobrata and Acarinina wilcoxensis* occur simultaneously in upper Zone P5, which correlates well with their FAD's in New Zealand at the base of the Waipawan (Hornibrook *et al*., 1989). The LADs of *Morozovella acuta* and *M. occlusa* occur in upper Zone P5, consistent with the global scheme (Olsson *et al*., 1999). However, the distinct morphotypes *Morozovella allisonensis, M. africana* and *Acarinina sibaiyaensis* that developed and diversified during a brief interval of P5 (e.g. Kelly *et al*., 1998; Pardo *et al*., 1999) were not found at Site 762. As discussed later, these species may not have been recovered because of a 5m core gap in uppermost P5 between 762C-28X-1 and -27X-4.

P6. LAD of *Morozovella velascoensis* (407.23 mbsf) to FAD of *Morozovella aragonensis* (370.74 mbsf). Age: 54.7-52.3 Ma, early Eocene (early Ypresian).

P6a. LAD of *Morozovella velascoensis* (407.23 mbsf) to FAD of *Morozovella formosa* or *Morozovella lensiformis* (399.25 mbsf). Age: 54.7-54.0 Ma, earliest Eocene (earliest Ypresian). At Site 762 and elsewhere (Berggren *et al*., 1995) the FADs of

Morozovella formosa (**Plate 1, figs 19-20; Plate 2, fig. 1**) and *M. lensiformis* (**Plate 2, figs 2-4**) coincide. Common species found in this zone at Site 762 include *Subbotina patagonica, S. triangularis, Acarinina soldadoensis, A. primitiva, Morozovella subbotinae, M. marginodentata, Chiloguembelina wilcoxensis and C. crinita*. This overall assemblage is typical for Subzone P6a (Blow, 1979, as Subzone Zone P7; Berggren *et al*., 1995).

There is a problem within the interval containing Subzone P6a at Site 762 with the labelling of core -26X. According to the drilling log, the depth of this core is 398.0 to 402.5 mbsf (4.5m thick). However, there is ~8m of core photographed and illustrated in the lithologic log for core -26X. As the next coring interval, -27X, starts at 402.5 mbsf, there is ~3.5 m of core that has not been accounted for.

P6b. FADs of *Morozovella formosa* or *Morozovella lensiformis* (399.25 mbsf) to FAD of *Morozovella aragonensis* (370.74 mbsf) (Plate 2, Figs 5-7). Age: 54.0-52.3 Ma, early Eocene (early Ypresian). At Site 762 and elsewhere, the FADs of *Morozovella lensiformis* and *M. formosa* coincide, although at Site 762 the latter species is rare. The FAD of *Pseudohasterigina wilcoxensis* also occurs at the base of Subzone P6b at Site 762. In tropical assemblages this datum occurs at the P5/P6 boundary but has a delayed entry in mid-high latitude regions within the P6b-P7 interval (Blow, 1979, as Subzone Zone P7; Berggren *et al*., 1995). Faunal assemblages in Subzone P6a at Site 762 dominantly consist of *Subbotina eocaena, S. patagonica, Acarinina quetra, Acarinina soldadoensis, A. primitiva, Morozovella lensiformis, M. subbotinae, M. gracilis, M. marginodentata, M. aequa* and *Planorotalites pseudoscitula*. These are typical assemblages found elsewhere (Blow, 1979, as Subzone Subzone P8a; Berggren *et al*., 1995). However, at other locations, the LAD of *M. subbotinae* occurs within Subzone P6b (Berggren *et al*., 1995), but at Site 762, this datums occurs later in Zone P7.

P7. FAD of *Morozovella aragonensis* (370.74 mbsf) to LAD of *Morozovella formosa* (342.25 mbsf). Age: 52.3-50.8 Ma, middle early Eocene (mid-Ypresian). The upper boundary of this zone is poorly constrained as the occurrence of *Morozovella formosa* is patchy. Faunal assemblages in Zone P7 at Site 762 are dominated by *Acarinina soldadoensis, A. primitiva, A. quetra, Muricoglobigerina senni, Subbotina*

eocaena, *S. patagonica*, *S. hagni*, *Morozovella aequa*, *M. gracilis*, *M. dolobrata*, *M. lensiformis* and *Planorotalites pseudoscitula*. These assemblages are typical of Zone P7 assemblages found in other parts of the globe (Blow, 1979, as Subzone 8b; Berggren *et al*., 1995). The LAD of *Morozovella aequa* occurs in Zone P7 in the global scheme (Olsson et al., 1999), however, at Site 762, it occurs slightly later in our Zone P8.

P8. LAD of *Morozovella formosa* (342.25 mbsf) to FAD of secondary marker species *Acarinina cuneicamerata* (338.95 mbsf). Age: 50.8-50.4 Ma, late early Eocene (late Ypresian). The top of Zone P8 is defined by the FAD of *Planorotalites palmerae* in the global scheme (Berggren *et al*., 1995). This primary marker species is absent at Site 762. Other authors have noted that *Planorotalites palmerae* has a very patchy geographic distribution (Toumarkine and Luterbacher, 1985). In the absence of *Planorotalites palmerae*, the top of this zone is defined by the FAD of *Acarinina cuneicamerata* (**Plate 2, figs 8-10**) and the common appearance of *A. bullbrooki* (W. A. Berggren, pers. comm., 1999). Common species found in this zone at Site 762 and elsewhere (Toumarkine and Luterbacher, 1985) include *Acarinina primitiva*, *A. pseudotopilensis*, *A. soldadoensis*, *A. collactea*, *A. decepta*, *Muricoglobigerina senni*, *Morozovella aragonensis*, *Subbotina inaequispira*, *S. eocaena* and *Pseudohastigerina wilcoxensis*.

P9. FAD of secondary marker species *Acarinina cuneicamerata* (338.95 mbsf) to FAD of secondary marker species *Guembelitrioides higginsi* (310.91 mbsf). Age: 50.4-49.0 Ma, late early Eocene (latest Ypresian). The FAD of *Hantkenina nuttalli* defines the top of Zone P9 in the global scheme (Berggren *et al*., 1995; Toumarkine, 1981). However, this datum occurs higher in the sedimentary column at Site 762 (section 762C-15X-2) co-existing with taxa characteristic of Zone P11. The placement of this boundary has been problematic elsewhere because of the late arrival and/or rare early appearance of *Hantkenina nuttalli* (e.g. McGowran, 1974). The LAD of *Planorotalites palmerae* is another criterion for the P9/P10 boundary (W. A. Berggren, pers. comm., 1999). Unfortunately, this species was not found at Site 762. The FAD of *Guembelitrioides higginsi* (**Plate 2, figs 11-13**) is close to the P9/P10 boundary at other locations (W. A. Berggren, pers. comm., 1999). We therefore use this datum to mark the top of Zone P9. Common species in Zone P9 at Site 762 and elsewhere (Toumarkine and Luterbacher, 1985; Berggren *et al*., 1995) include *Acarinina primitiva*, *A.*

soldadoensis, A. pseudotopilensis, A. collactea, A. cuneicamerata, A. matthewsae, A. bullbrooki, A. decepta, Morozovella lensiformis, M. densa, M. aragonensis, M. caucasica, Subbotina patagonica, S. eocaena, S. inaequispira, S. frontosa, S. hagni, Pseudohasterigina wilcoxensis, Ph. micra, Planorotalites pseudoscitula, Igorina broedermanni and *Guembelitrioides lozanoi* (in upper P9).

P10. FAD of secondary marker species *Guembelitrioides higginsi* (310.91 mbsf) to FAD of *Globigerapsis kugleri*. Age: 49.0-45.8 Ma, early middle Eocene (early Lutetian). Only one sample within Zone P10 was examined. The top of this zone, therefore, lies above our sampling interval. The sample examined contains *Guembelitrioides higginsi* and *Truncorotaloides* spp., which are characteristic species of Zone P10 (Berggren *et al*., 1995).

Carbon Isotopes

The $\delta^{13}C$ of *Subbotina* tests averages 1.84‰ across our sampled interval but varies significantly between 0.36 and 2.92‰ (**Table 2; Fig. 3**). From the lowest sampled interval in P1 (502.96 mbsf) to the base of Zone P5 (423.49 mbsf) $\delta^{13}C$ gradually increases by about 2.0‰. There is a marked decrease in $\delta^{13}C$ through Zone P5 (423.49 to 407.95 mbsf) by about 2.5‰. From the top of Zone P5 (407.95 mbsf) to the top of the sampled interval in Zone P10 (307.80mbsf) $\delta^{13}C$ is relatively constant, except for a slight drop in upper Zone P6. The *Subbotina* $\delta^{13}C$ curve mirrors the bulk carbonate $\delta^{13}C$ curve at Site 762 (Thomas *et al*., 1992), although *Subbotina* $\delta^{13}C$ values are typically 0.5‰ lower at similar depth. This offset in $\delta^{13}C$ is expected because surface waters are generally enriched in ^{13}C relative to deeper waters of the thermocline.

The exogenic carbon cycle includes all carbon stored in the ocean, atmosphere and biomass reservoirs. Secular changes can occur in this exogenic carbon cycle with variations in carbon inputs or outputs to the ocean or atmosphere (e.g. Kump and Arthur, 1999; Dickens, 2001). Because carbon cycles through all reservoirs of the

Table 2. Carbon isotope composition of *Subbotina* spp.

Core-Section, Interval (cm)	Depth (mbsf)	*Subbotina* spp. Analyzed	$\delta^{13}C$ (‰)
15X-3, 80-85	297.30	*S. patagonica*	1.34
16X-4, 30-35	307.80	*S. patagonica*	1.15
17X-4, 50-55	317.50	*S. patagonica*	1.28
18X-2, 90-95	324.40	*S. patagonica*	1.43
18X-6, 106-111	330.56	*S. patagonica*	1.43
19X-4, 50-55	336.50	*S. patagonica*	0.98
20X-4, 40-45	345.90	*S. patagonica*	0.95
22X-2, 50-55	362.00	*S. patagonica*	1.09
22X-6, 47-51	367.97	*S. patagonica*	0.64
24X-1, 49-53	379.49	*S. patagonica*	0.36
25X-4, 49-53	393.49	*S. patagonica*	0.94
26X-3, 36-41	401.36	*S. patagonica*	0.93
27X-1, 100-104	403.50	*S. patagonica*	0.74
27X-2, 104-108	405.04	*S. patagonica*	1.11
27X-3, 95-99	406.45	*S. triangularis*	1.25
27X-4, 95-99	407.95	*S. triangularis*	1.65
28X-1, 104-107	413.04	*S. triangularis*	2.29
28X-2, 10-12	413.60	*S. triangularis*	2.43
29X-1, 48-52	421.98	*S. triangularis*	2.74
29X-2, 49-53	423.49	*S. triangularis*	2.92
29X-3, 46-50	424.96	*S. triangularis*	2.82
30X-1, 101-105	432.01	*S. triangularis*	2.67
30X-2, 100-104	433.50	*S. triangularis*	2.73
30X-3, 96-100	434.96	*S. triangularis*	2.87
30X-4, 66-70	437.26	*S. triangularis*	2.63
31X-1, 100-104	441.50	*S. triangularis*	2.54
31X-2, 100-104	443.00	*S. triangularis*	2.50
31X-3, 97-101	444.47	*S. triangularis*	2.11
31X-4, 97-101	445.97	*S. triangularis*	2.42
31X-5, 101-105	447.51	*S. triangularis*	2.66
31X-6, 97-101	448.97	*S. triangularis*	2.46
32X-1, 101-105	451.01	*S. triangularis*	2.25
32X-2, 100-104	452.50	*S. triloculinoides*	2.17
33X-4, 95-99	464.95	*S. triloculinoides*	2.12
34X-2, 100-103	471.50	*S. triloculinoides*	2.09
35X-1, 90-95	479.40	*S. triloculinoides*	1.43
37X-2, 97-101	499.97	*S. triloculinoides*	1.37

exogenic carbon cycle over relatively short time intervals, about 2000 years at present day, major perturbations in the isotopic composition of the exogenic carbon cycle will be observed in all carbon reservoirs at nearly the same time (e.g. Dickens *et al*., 1997). The early Palaeogene is especially amenable for correlating widespread locations by this "carbon isotope stratigraphy" because there are a series of prominent $\delta^{13}C$ excursions in the exogenic carbon cycle of long and short duration (e.g. Zachos *et al*., 1993; Corfield, 1994; Dickens *et al*., 1997, Zachos *et al*., 2001). Most key features of the global carbon isotope record for the Palaeogene (**Fig. 1**) can be recognized at Site 762 (**Fig. 3**). Importantly, when the $\delta^{13}C$ variations at Site 762 are placed within the time scale defined by our foraminiferal biozones, they match within 0.5 myr the age

pattern suggested for the global $\delta^{13}C$ record by Berggren *et al*. (1995). This cross-correlation supports the planktic foraminiferal zonation we have developed for Site 762.

Integrated Biostratigraphy

In the previously published nannofossil biostratigraphy for Site 762 (Siesser and Bralower, 1992), nannofossil datums and biozones were calibrated to the time scale of Haq *et al*. (1987). We have recalibrated the nannofossil biozones with the most current global time scale (Berggren *et al*., 1995). The revised nannofossil biostratigraphy at Site 762 agrees reasonably well with both the planktic foraminiferal and carbon isotope stratigraphy. However, there are discrepancies, notably the placement of the NP6/NP7 and NP8/NP9 boundaries, which appear to be too high in the column (**Fig. 3**). There are several possible reasons for such anomalies. First, key nannofossil markers are very rare at Site 762 (Shipboard Scientific Party, 1990) and may have been missed. Second, the high latitude of the Exmouth Plateau in the Early Palaeogene may have put some species at the limits of their biogeographic range (Wonders, 1992) resulting in certain nannofossil and foraminiferal biomarkers at Site 762 being responsive to distribution patterns which applied to the north Australian margin rather than the temporal controls of evolution and extinction. Third, the mismatches could, at least in part, be artefacts of sampling resolution.

Magnetostratigraphy Problem

Galbrun (1992) determined the pattern of polarity reversals for Upper Cretaceous and Lower Tertiary core obtained from Site 762. As noted by Berggren *et al*. (1995, p. 184), the magnetostratigraphy raises a correlation problem. Starting with Chron C22n and continuing back through the Paleocene, there are significant discrepancies between magnetostratigraphic and nannofossil datums at Site 762 (cf. Siesser and Bralower, 1992; Galbrun, 1992). In particular, Chron C22n has been placed within Zone NP12. However, according to global stratigraphic schemes, Chron C22n occurs within NP14 (Berggren *et al*., 1995). Three plausible explanations could account for the miscorrelation. First, the nannofossil zones at Site 762 could be diachronous by some 1.5 myr with the global time scale. Second, recognition of key nannofossil zones could be incorrect. Third, the polarity chrons could have been mislabelled or

misinterpreted. It is noteworthy that the P7/P8 zonal boundary roughly coincides with the top of Chron C23n in global schemes (Berggren *et al*., 1995), but at Site 762 it coincides with the chron labelled C22n (Galbrun, 1992). It is therefore likely that Chron C23n was mistaken for Chron C22n in previous work. Making this correction, and relabelling the chron succession as a consequence, results in a magnetostratigraphy which correlates well with both the planktic foraminiferal zonation and the isotope stratigraphy (**Figs 3, 4**).

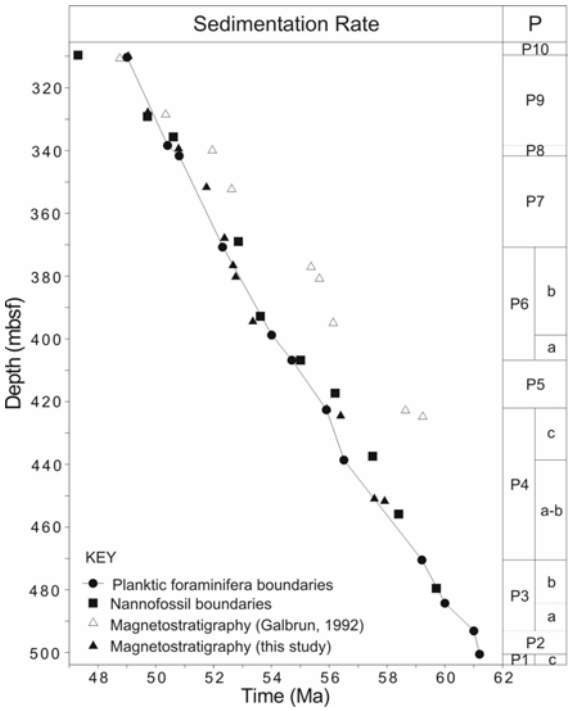

Figure 4. Sedimentation rates calculated from planktic foraminifera (this study) and nannofossils (Seisser & Bralower, 1992) compared with published magnetostratigraphy (Galbrun, 1992) and recalibrated magnetostratigraphy (this study). The original magnetostratigraphy deviates from the other curves, showing where the major adjustment was made for Chron 22n at 49 Ma. Sedimentation rates calculated from the planktic foraminiferal and nannofossil biozonation using the global scheme are 1.5 cm/kyr and 1.4 cm/kyr respectively. P = Planktic foraminiferal biozones (this study).

Paleocene/Eocene Transition

The transition between the Paleocene and Eocene epochs is characterized by a brief warming event *ca*. 55.5 Ma. Globally, this event is recognized in marine sediment

sequences by a pronounced benthic foraminiferal extinction event, the appearance of distinct planktic foraminiferal morphotypes, and a remarkable -2.5 to -3‰ excursion in $\delta^{13}C$ (e.g. Kennett and Stott, 1991; Bains *et al.*, 1999). The distinct morphotypes and abrupt $\delta^{13}C$ anomaly were not observed at Site 762. The simplest explanation is that the warming event lies in a 5m core gap in uppermost Zone P5 between 762C-28X-1 and -27X-4. One check on this interpretation is the occurrence of *Gavelinella beccariiformis*. This species dominates benthic foraminiferal assemblages during the Paleocene but disappears at the warming event. At Site 762 it last occurs in section -28X-1, immediately below the core gap. A -1.3‰ $\delta^{13}C$ excursion is represented in bulk carbonate from section -28X-2 to -28X-1 (Thomas *et al.*, 1992). The start of the warming event may thus be registered in section -28X-1.

Sedimentation Rates

Collectively, all biostratigraphic and revised magnetostratigraphic datums show a near-linear age-depth relationship. Subzone P4c has a greater rate of sedimentation, which may relate to local processes such as uplift. However, the overall coherency permits the accurate calculation of sedimentation rates for the early Palaeogene sequence at Site 762. Sedimentation rates are remarkably constant at about 1.5 cm/kyr, which is typical for carbonate oozes on continental margins (Kennett, 1982) but relatively high compared to known Palaeogene sequences that have not been deeply buried. Continuous sedimentation rates also indicate that significant hiatuses are unlikely to exist at Site 762.

CONCLUSIONS

Site 762 on the Exmouth Plateau contains an expanded Palaeogene sequence with abundant and well-preserved calcareous microfossils, including planktic foraminifera. We have constructed the first detailed early Palaeogene planktic foraminiferal biostratigraphy at this site, and for the region in general (**Tables 1, 3**). Sediment deposited between 307.8 and 502.96 mbsf spans Zones P1c to P10 (Berggren *et al.*, 1995), although Subzone P4b cannot be recognized. Despite a relatively high latitude Palaeogene location for Site 762, planktic foraminiferal biozones are generally

Table 3. Planktic foraminifera, nannofossil and chron (this study) boundary ages at Site 762.

Datum	Age (Ma)*	Sample Core section, interval (cm)		Depth (mbsf)
		Upper	Lower	
FAD *N. fulgens*, NP14/NP15	47.3	16X-3, 99	16X, CC	306.99 - 313.49
FAD *G. higginsi*, P9/P10	49.0	16X-4, 30	17X-1, 56	307.80 - 314.01
C22n/C22r	49.037	16X-4, 16	17X-1, 26	307.67 - 312.76
FAD *D. sublodoensis*, NP13/NP14	49.7	18X-5, 100	18X-6, 100	329.00 - 330.51
C22r/C22n	49.714	18X-4, 110	18X-5, 51	327.60 - 328.51
FAD *A. cuneicamerata*, P8/P9	50.4	19X-4, 50	20X-1, 40	336.50 - 341.40
LAD *T. orthostylus*, NP12/NP13	50.6	19X-2, 101	19X-3, 101	335.51 - 337.01
C23n/C22r	50.778	19X-5, 30	20X-1, 53	337.80 - 341.52
LAD *M. formosa*, P7/P8	50.8	20X-1, 45	20X-2, 55	341.45 - 343.05
C23r/C23n	51.743	21X-1, 107	21X-2, 23	351.57 - 352.23
FAD *M. aragonensis*, P6b/P7	52.3	22X-3, 49	22X-4, 48	369.93 - 371.55
C24n.1n/C23r	52.364	22X-6, 27	22X-6, 81	367.77 - 368.32
C24n.1r/C24n.1n	52.663	23X, CC, 33	24X-1, 61	373.83 - 379.61
FAD *D. lodoensis*, NP11/NP12	52.85	22X-6, 100	23X-1, 100	368.50 - 370.50
C24n.2n/C24n.1r	52.757	24X-1, 124	24X, CC, 25	380.24 - 380.65
C24r/C24n.3n	53.347	25X-4, 139	25X-5, 27	394.40 - 394.76
LAD *T. contortus*, NP10/NP11	53.61	25X-3, 101	25X-4, 101	392.51 - 394.01
FAD *M. formosa/M. lensiformis*, P6a/P6b	54.0	26X-1, 50	26X-2, 50	398.50 - 400.00
LAD *M. velascoensis*, P5/P6a	54.7	27X-3, 99	27X-4, 99	406.46 - 407.99
FAD *T. bramlettei*, NP9/NP10	55.0	27X-3, 99	27X-4, 100	406.49 - 408.00
FAD *D. multiradiatus*, NP7-8/NP9	56.2	28X-1, 100	29X-1, 100	413.00 - 422.50
LAD *G. pseudomenardii*, P4c/P5	55.9	29X-1, 52	29X-2, 53	422.02 - 424.03
C25n/C24r	55.904	29X-1, 48	29X-1, 145	421.98 - 422.95
C25r/C25n	56.391	29X-2, 108	29X-3, 30	424.09 - 424.81
FAD *A. soldadoensis*, P4a-b/P4c	56.5	31X-3, 97	31X-4, 97	437.26 - 441.50
FAD *D. mohleri*, NP6/NP7-8	57.5	30X-3, 139	31X-1, 100	434.00 - 441.50
C26n/C25r	57.554	32X-1, 52	32X-1, 140	450.52 - 451.40
C26r/C26n	57.911	32X-1, 139	32X-2, 50	451.39 - 452.00
FAD *H. kleinpellii*, NP5/NP6	58.4	32X-2, 103	33X-1, 109	452.80 - 459.50
FAD *G. pseudomenardii*, P3b/P4a-b	59.2	34X-1, 100	34X-2, 100	470.00 - 471.50
FAD *F. tympaniformis*, NP4/NP5	59.7	35X-1, 99	35X-2, 12	479.40 - 480.12
FAD *I. albeari*, P3a/P3b	60.0	35X-2, 92	36X-1, 17	480.92 - 488.17
FAD *M. angulata*, P2/P3a	61.0	36X-1, 17	37X-1, 99	488.17 - 498.49
FAD *P. uncinata*, P1c/P2	61.2	37X-2, 97	37X-3, 97	499.97 - 501.47

* Ages from Berggren *et al*., 1995.

in phase and contain representative assemblages with those of the currently used global scheme for sub-tropical locations. However, rare, patchy or non-occurrences of the zonal marker species such as *Globanomalina pseudomenardii*, *Morozovella velascoensis*, *Morozovella formosa*, *Planorotalites palmerae* and *Hantkenina nuttalli*, make some correlations difficult.

The $\delta^{13}C$ record constructed from tests of *Subbotina* spp. is similar to that constructed from bulk sediment. Both records show broadscale excursions which match the global $\delta^{13}C$ curve. However, the large and short-lived negative $\delta^{13}C$ excursion that marks the Paleocene/Eocene transition is at best partially represented at Site 762,

probably because of a core gap. Nannofossil biozonation and magnetic polarity chron records (after adjustment) are consistent with the planktic foraminifera biozonation and the $\delta^{13}C$ curve (**Table 3**). Despite core gaps, the integrated stratigraphy at Site 762 suggests that a complete and expanded Early Palaeogene sediment record exists on the Exmouth Plateau. The relatively shallow subsurface depth of this Palaeogene sequence makes the Exmouth Plateau an ideal location for future scientific drilling to understand Palaeogene oceanography.

ACKNOWLEDGMENTS

We sincerely thank Christian Thun, Tony Watson, Andrew Kelman and Richard Brown at AGSO for sample preparation, and James Zachos at U.C. Santa Cruz for isotope analyses. Personal communications with William Berggren, Richard Norris and Brian Huber have helped us tremendously. This research was funded by AGSO for G. Chaproniere and an ARC small grant to G. Dickens; AGSO provided supplementary funding to H. Hancock. All figured specimens are registered and housed in the Commonwealth Palaeontological Collection (CPC), Australian Geological Survey Organisation, Canberra. The remaining assemblages and samples are stored in the general collections of that organisation.

REFERENCES

Bains, S., Corfield, R. M. and Norris, R. D. 1999. Mechanisms of climate warming at the end of the Paleocene. *Science*, 285:724-727.

Barber, P. M. 1988. The Exmouth Plateau deep water frontier: a case history. *In* Purcell, P. G. and Purcell, R. R. (Eds), *The North West Shelf, Australia:* Proceedings of Petroleum Exploration Society of Australia, Symposium, Perth, 173-187.

Beckmann, J. P. 1953. Die foraminiferen der Oceanic Formation (Eocaen-Oligocaen) von Barbados, Kleine Antillen. *Eclog. Geol. Helvel*., 46: 301-412.

Beckmann, J. P. 1957. *Chiloguembelina* Loeblich and Tappan and related Foraminifera from the Lower Tertiary. *In* Loeblich, A. R. Jr. and Collaborators, Studies in Foraminifera. *Bulletin of the United States National Museum,* 215: 83-95.

Belford, D. J. 1984. Tertiary foraminifera and age of sediments, Ok Tedi-Wabag, Papua, New Guinea. *Bulletin, Bureau of Mineral Resources, Geology and Geophysics, Australia,* 216:1-52.

Berggren, W. A., Kent, D. V., Swisher, III and Aubury, M.-P. 1995. A Revised Cenozoic Geochronology and Chronostratigraphy. *In* Berggren, W. A., Kent, D. V., Aubry, M.-P. and Hardenbol, J., (Eds), Geochronology, Time Scales and Global Stratigraphic Correlations. *Society of Economic Palaeontologists and Mineralogists, Special Publication*, 54:129-212.

Berggren, W. A. and Norris, R. D. 1997. Biostratigraphy, phylogeny and systematics of Paleocene trochospiral planktic foraminifera. *Micropaleontology, Supplement 1,* 43:1-116.

Bermúdez, P. J. 1961. Contribucion al estudio de las Globigerindea de la region Caribe-Antillana (Paleocene-Reciente). *Boletin de Geologia (Venezuela), Pulicacion Especial, 3 (Congres Geologia Venezolano, 3d, Caracas, 1959, Mem.* 3):1119-1393.

Billups, K., Ravelo, A. C. and Zachos, J. C. 1998. Early Pliocene deep water circulation in the western equatorial Atlantic: implications for high-latitude climate change. *Paleoceanography*, 13:84-95.

Blow, W. H. 1979. *The Cainozoic Globigerinida*: Leiden, The Netherlands, 1413 pages.

Bolli, H. M. 1957a. The General *Globigerina* and *Globorotalia* in the Paleocene-Lower Eocene Lizard Springs Formation of Trinidad, B.W.I. *In* Loeblich, A. R. Jr. and Collaborators, Studies in Foraminifera. *Bulletin of the United States National Museum*, 215:61-82.

Bolli, H. M. 1957b. Planktonic Foraminifera from the Eocene Navet and San Fernando Formations of Trinidad, B.W.I. *In* Loeblich, A. R. Jr. and Collaborators, Studies in Foraminifera. *Bulletin of the United States National Museum*, 215:155-172.

Bolli, H. M. and Cita, M. B. 1960. *Globigerine* e *Globorotalie* del Paleocene di Paderno d'Adda (Italia). *Rivista Italiana di Paleontologia e Stratigrafia*, 66:361-408.

Bolli, H. M., Loeblich, A. R. and Tappan, H. 1957. Planktonic foraminifera families *Hantkeninidae, Orbulinidae, Globorotaliidae* and *Globotruncanidae*. *Bulletin of the United States National Museum*, 215:3-50.

Brönnimann, P. 1952. Trinidad Paleocene and Lower Eocene Globigerinidae. *Bulletins of American Paleontology*, 34, 34 pages.

Clarke, L. J. and Jenkyns, H. 1999. New oxygen isotope evidence for long-term Cretaceous climatic change in the Southern Hemisphere. *Geology*, 27:699-702.

Cole, W. S. 1927. A foraminiferal fauna from the Guayabal Formation in Mexico. *Bulletin of American Paleontology*, 14:1-46.

Colom, G. 1954. Estudio de las biozonas con foraminiferos del Terciario de Alicante. *Bol. Espana. Inst. Geol. y Minero*, 66:1-279.

Corfield, R. M. 1994. Palaeocene oceans and climate: an isotopic perspective. *Earth-Science Reviews*, 37:225-252.

Cushman, J. A. 1925. Some new foraminifera from the Velasco Shale of Mexico. *Contributions from the Cushman Laboratory for Foraminiferal Research*, 1:18-23.

Cushman, J. A. 1927. New and interesting foraminifera from Mexico and Texas. *Contributions from the Cushman Laboratory for Foraminiferal Research*, 3:111-119.

Cushman, J. A. 1932. *Rectogüembelina*, a new genus from the Cretaceous. *Contributions from the Cushman Laboratory for Foraminiferal Research*, 8:4-7.

Cushman, J. A. 1940. Midway foraminifera from Alabama. *Contributions from the Cushman Laboratory for Foraminiferal Research*, 16:51-73.

Cushman, J. A. and Bermúdez, P. J. 1949. Some Cuban species of *Globorotalia*. *Contributions from the Cushman Laboratory for Foraminiferal Research*, 25:26-45.

Cushman, J. A. and Ponton, G. M. 1932. An Eocene foraminiferal fauna of Wilcox Age from Alabama. *Contributions from the Cushman Laboratory for Foraminiferal Research*, 8:51-72.

Cushman, J. A. and Renz, H. H. 1942. Eocene Midway foraminifera from Soldado Rock, Trinidad. *Contributions from the Cushman Laboratory for Foraminiferal Research*, 18:1-14.

D'Hondt, S., Zachos J. C. and Schultz, G. 1994. Stable isotopic signals and photosymbiosis in late Paleocene planktic foraminifera. *Paleobiology*, 20:391-406.

Dickens, G. R., Castillo, M. M. and Walker, J. C. G. 1997. A blast of gas in the latest Paleocene: simulating first-order effects of massive dissociation of methane hydrate. *Geology*, 25:259-262.

Dickens, G. R. 2001. On the fate of past gas: What happens to methane released from a bacterially mediated gas hydrate capacitor. *Geochemistry, Geophysics, Geosystems – G3*, 2: 2000GC000131.

Exon, N. F., Haq, U. and Von Rad, U. 1992. Exmouth Plateau revisited: scientific drilling and geological framework. *Proceedings of Ocean Drilling Program, Scientific Results*, 122:3-20.

Finlay, H. J. 1939. New Zealand foraminifera: key species in stratigraphy, No. 2. *Transaction of the Royal Society of New Zealand*, 69:89-128, 327.

Finlay, H. J. 1947. New Zealand foraminifera: key species in stratigraphy, No. 5. *New Zealand Journal of Science and Technology*, 28:259-292.

Galbrun, B. 1992. Magnetostratigraphy of Upper Cretaceous and Lower Tertiary sediments Sites 761 and 762, Exmouth Plateau, Northwest Australia. *Proceedings of Ocean Drilling Program, Scientific Results*, 122:699-716.

Glaessner, M. F. 1937a. Planktonische Foraminiferen aus der Kreide und dem Eozän und ihre stratigraphische Bedeutung. *Studies in Mircopaleontology, Moscow University Laboraties of Paleontology*, 1:27-46.

Glaessner, M. F. 1937b. Studien über Foraminiferen aus der Kreide und dem Tertiär des Kaukasus. *Problems in Paleontology, Moscow University Laboratory of Paleontology*, 2-3:349-410.

Gohrbandt, K. H. A. 1967. Some new planktonic foraminiferal species from the Austrian Eocene. *Mircropaleontology*, 13:319-326.

Gümbel, C. W. 1868. Beiträge zur Foraminiferenfauna der nordalpinen älteren Eocängebilde oder der Kressenberger Nummulitenschichten. *Abhandlungen Bayerische Akademie der Wissenschafen, Math.-Physik Kl*., 10:579-730.

Hagn, H. and Lindenberg, H. G. 1966. Revision of *Globigerina (Subbotina) eocaena* Gümbel from the Eocene of the Bavarian Alps. *Akademy Nauk SSSR Voprosy Mikropaleontologii*, 10:342-50 (in Russian).

Haq, B. U., Hardenbol, J. and Vail, P. R. 1987. Chronology of fluctuating sea level since the Triassic. *Science*, 235:1156-1167.

Haque, A. F. M. M. 1956. The foraminifera of the Ranikot and the Laki of the Nammal Gorge, Salt Range. *Memoirs of the Geological Survey of Pakistan, Palaeontologia Pakistanica*, 1:1-300.

Hornibrook, N. deB., Brazier, R. C.. and Strong, C. P. 1989. Manual of New Zealand Permian to Pleistocene foraminiferal biostratigraphy. *New Zealand Geological Survey paleontological bulletin* 56:1-175.

Jenkins, D. G. 1971. New Zealand Cenozoic planktonic foraminifera. *New Zealand Geological Survey paleontological bulletin*, 42:1-278.

Katz, M. E., Pak, D. K., Dickens, G. R. and Miller, K. G. 1999. The source and fate of massive carbon input during the Latest Paleocene Thermal Maximum. *Science*, 286:1531-1533.

Kelly, D. C., Bralower, T. J. and Zachos, J. C. 1998. Evolutionary consequences of the latest Paleocene thermal maximum for tropical planktonic foraminifera. *Palaeogeography, Palaeoclimatology, Palaeoecology*, 141:139-161.

Kennett, J. 1982. *Marine Geology*: Prentice Hall, New Jersey, 813 pages.

Kennett, J. P. and Stott, L. D. 1991. Abrupt deep-sea warming, palaeoceanographic changes and benthic extinctions at the end of the Paleocene. *Nature*, 353:225-229.

Kump, L. R. and Arthur, M. A. 1999. Interpreting carbon isotope excursions: carbonates and organic matter. *Chemical Geology*, 161:181-198.

Loeblich, A. R. Jr. and Tappan, H. 1957. Planktonic foraminifera of Paleocene and early Eocene age from the gulf and Atlantic coastal plains. Studies in Foraminifera. *Bulletin of the United States National Museum*, 215:173-198.

Martin, L. T. 1943. Eocene foraminifera from the Type Lodo Foramation Fresno County, California. *Stanford University Publications, Geological Sciences*, 3:93-125.

Martini, E. 1971. Standard Tertiary and Quaternary calcareous nannoplankton zonation. *In* Farinacci, A. (Ed), *Proceedings of the Second Planktonic Conference, Roma:* 1970, Rome, 739-785.

McGowran, B. 1974. Foraminifera. *Initial Reports of the Deep Sea Drilling Project*, 22:609-627.

Morozova, V. G. 1939. Foraminiferal superfamily Globigerinidea, superfam. nov. and some of its representatives. *Akademy Nauk SSSR Doklady,* 112:1109-11 (in Russian).

Norris, R. D. 1996. Symbiosis as an evolutionary innovation in the radiation of Paleocene planktic foraminifera. *Paleobiology*, 4:461-480.

Norris, R. D. and Röhl, U. 1999. Carbon cycling and chronology of climate warming during the Palaeocene/Eocene transition. *Nature*, 401:775-778.

Nuttall, W. L. F. 1930 (September). Eocene foraminifera from Mexico. *The Journal of Paleontology*, 4:271-293.

Olsson, R. K., Hemleben, C., Berggren, W. A and Huber, B. T., (Eds). 1999. Atlas of Paleocene Planktonic Foraminifera: *Smithsonian Contributions to Paleobiology*, Washington, D. C., 85, 252 pages.

Pardo, A., Keller, G. and Oberhänsli, H. 1999. Paleoecologic and Paleoceanographic evolution of the Tethyan realm during the Paleocene-Eocene transition. *Journal of Foraminiferal Research*, 29:37-57.

Parr, W. J. 1938. Upper Eocene foraminifera from the deep borings in King's Park, Perth, Western Australia. *Journal of the Royal Society of Western Australia*, 24:69-101.

Plummer, H. J. 1926 (1927). Foraminifera of the Midway formation in Texas. *University of Texas Bulletin*, 2644:1-206.

Said, R. and Kenaway, A. 1956. Upper Cretaceous and Lower Tertiary foraminifera from Northern Sinai, Egypt. *Micropaleontology*, 2:105-173.

Siesser, W. and Bralower, T. J. 1992. Cenozoic calcareous nannofossil biostratigraphy on the Exmouth Plateau, Eastern Indian Ocean. *Proceedings of Ocean Drilling Program, Scientific Results*, 122:601-631.

Shipboard Scientific Party. 1990. Site 762. *Proceedings of the Ocean Drilling Program, Initial Reports*, 122:213-289.

Stagg, H. M. J. and Colwell, J. B. 1994. The structural foundations of the Northern Carnarvon Basin. *In* Purcell, P.G. and R.R. (Eds), *The Sedimentary Basins of Western Australia:* Proceedings of Petroleum Exploration Society of Australia, Symposium, Perth, 349-364.

Subbotina, N. N. 1947. Foraminifers of the Danian and Paleogene deposits of the northern Caucasus. Mocrofauna of the Caucasus Emba region and central Asia. *Trudy VNIGRI*, 39:160 (In Russian).

Subbotina, N. N. 1953. Fossil Foraminifers of the USSR: Globigerinidae, Hantkeninidae and Globorotaliidae, *Trudy VNIGRI*, new series, 76, 296 pages (in Russian). Translated into English by E. Lees, *Fossil foraminifera of the USSR; Globigerinidae, Hantkeninidae and Globorotaliidae*: Collet's Ltd, London and Wellingborough, 321 pages.

Thomas, E., Shackleton, N. J. and Hall, M. A. 1992. DATA REPORT: Carbon isotope stratigraphy of Palaeogene bulk sediments, Hole 762C (Exmouth Plateau, Eastern Indian Ocean). *Proceedings of Ocean Drilling Program, Scientific Results*, 122:897-901.

Thomas, E. and Shackleton, N. J. 1996. The Paleocene-Eocene benthic foraminiferal extinction and stable isotope anomalies. *In* Knox, R. W. O'B., Corfield, R. M. and Dunay, R. E. (Eds), Correlation of the Early Paleogene in Northwest Europe: *Geological Society Special Publication*, London, 101:401-441.

Todd, R. and Kniker, H. T. 1952. An Eocene foraminiferal fauna from the Agua Fresca Shale of Maallanes Province, southernmost Chile. *Special Publication of the Cushman Foundation for Foraminiferal Research*: Washington D.C., 1:28 pages.

Toulmin, L. D. 1941. Eocene smaller foraminifera from the Salt Mountain Limestone of Alabama. *Journal of Paleontology*, 15:567-611.

Toumarkine, M. 1981. Discussion de la validité de l'espèce *Hantkenina aragonensis* Nuttall, 1930. Description de *Hantkenina nuttalli*, n. sp.: *Cahiers de Micropaléontologie*, Livre Jubilaire en l'honneur de Madame Y. Le Calvez, fasc. 4:109-119.

Toumarkine, M. and Luterbacher, H.-P. 1985. Paleocene and Eocene Planktic Foraminifer. *In* Bolli, H. M., Saunders, J. B. and Perch-Nielsen, K., (Eds), *Plankton Stratigraphy:* Cambridge University Press, Cambridge, 87-154.

Veevers, J. J., Powell, C. McA. and Roots S. R. 1991. Review of seafloor spreading around Australia. I. Synthesis of the patterns of spreading. *Australian Journal of Earth Sciences*, 38:373-389.

White, M. P. 1928. Some Index Foraminifera of the Tampico Embayment of Mexico, Part I and Part II. *Journal of Paleontology*, 2:177-215, 280-317.

Wonders, A. A. H. 1992. Cretaceous planktonic foraminiferal biostratigraphy, Leg 122, Exmouth Plateau, Australia. *Proceedings of Ocean Drilling Program, Scientific Results*, 122:587-599.

Zachiariasse, W. J. 1992. Neogene planktonic foraminifers from Sites 761 and 762 off northwest Australia. *Proceedings of Ocean Drilling Program, Scientific Results*, 122:665-681.

Zachos, J. C., Lohmann, K C., Walker, J. C. G. and Wise, S. W. 1993. Abrupt climate change and transient climates during the Paleogene: a marine perspective. *The Journal of Geology*, 101:191-213.

Zachos, J., Pagani, M., Sloan, L., Thomas, E. and Billups, K. 2001. Trends, rhythms, and aberrations in global climate 65 Ma to present. *Science*, 292:686-693.

APPENDIX 1.

TAXONOMIC LIST

The early Palaeogene species represented at Site 762 are listed below alphabetically by genus. Planktic foraminiferal specific and generic concepts used here follow those of Olsson *et al.* (1999) for the Paleocene, and generally follow those of Toumarkine and Luterbacher (1985) and Blow (1979) for the early Eocene.

Acarinina bullbrooki (Bolli 1957*b*)
Acarinina collactea (Finlay 1939)
Acarinina cuneicamerata (Blow 1979)
Acarinina decepta (Martin 1943)
Acarinina matthewsae (Blow 1979)
Acarinina mckannai (White 1928)
Acarinina nitida (Martin 1943)
Acarinina primitiva (Finlay 1947)
Acarinina pseudotopilensis Subbotina 1953
Acarinina quetra (Bolli 1957*a*)
Acarinina soldadoensis (Brönnimann 1952)
Acarinina strabocella (Loeblich & Tappan 1957)
Acarinina subsphaerica (Subbotina 1947)
Acarinina wilcoxensis (Cushman & Ponton 1932)
Catapsydrax unicavus Bolli, Loeblich & Tappan 1957
Chiloguembelina crinita (Glaessner 1937)
Chiloguembelina midwayensis (Cushman 1940)
Chiloguembelina subtriangularis Beckmann 1957
Chiloguembelina trinitatensis (Cushman & Renz 1942)
Chiloguembelina wilcoxensis (Cushman & Ponton 1932)
Eoglobigerina spiralis (Bolli 1957*a*)
Globanomalina australiformis (Jenkins 1965)
Globanomalina chapmani (Parr 1938)
Globanomalina compressa (Plummer 1926)
Globanomalina ehrenbergi (Bolli 1957*a*)

Globanomalina ovalis Haque 1956

Globanomalina pseudomenardii (Bolli 1957*a*)

Guembelitrioides higginsi (Bolli 1957*b*)

Guembelitrioides lozanoi (Colom 1954)

Igorina albeari (Cushman & Bermúdez 1949)

Igorina broedermanni (Cushman & Bermúdez 1949)

Igorina pusilla (Bolli 1957*a*)

Morozovella acuta (Toulmin 1941)

Morozovella acutispira (Bolli & Cita 1960)

Morozovella aequa (Cushman & Renz 1942)

Morozovella angulata (White 1928)

Morozovella apanthesma (Loeblich & Tappan 1957)

Morozovella aragonensis (Nuttall 1930)

Morozovella caucasica (Glaessner 1937)

Morozovella conicotruncata (Subbotina 1947)

Morozovella densa (Cushman 1925)

Morozovella dolobrata (Jenkins 1971)

Morozovella formosa (Bolli 1957*a*)

Morozovella gracilis (Bolli 1957*a*)

Morozovella lensiformis (Subbotina 1953)

Morozovella marginodentata (Subbotina 1953)

Morozovella occlusa (Loeblich & Tappan 1957)

Morozovella pasionensis (Bermúdez 1961)

Morozovella spinulosa (Cushman 1927)

Morozovella subbotinae (Morozova 1939)

Morozovella velascoensis (Cushman 1925)

Muricoglobigerina senni (Beckmann 1953)

Parasubbotina pseudobulloides (Plummer 1926)

Parasubbotina varianta (Subbotina 1953)

Parasubbotina variospira (Belford 1984)

Planorotalites pseudoscitula (Glaessner 1937)

Praemurica inconstans (Subbotina 1953)

Praemurica pseudoinconstans (Blow 1979)

Praemurica uncinata (Bolli 1957*a*)

Pseudohasterigina micra (Cole 1927)

Pseudohasterigina wilcoxensis (Cushman & Ponton 1932)

Subbotina cancellata Blow 1979

Subbotina cryptomphala (Glaessner 1937)

Subbotina eocaena (Gümbel 1868) emended Hagn & Lindenberg 1966

Subbotina frontosa (Subbotina 1953)

Subbotina hagni (Gohrbandt 1967)

Subbotina patagonica (Todd & Kniker 1952)

Subbotina triangularis (White 1928)

Subbotina triloculinoides (Plummer 1926)

Subbotina trivialis (Subbotina 1953)

Subbotina velascoensis (Cushman 1925)

Rectoguembelina cretacea Cushman 1932

Zeauvigerina aegyptiaca Said & Kenawy 1956

Zeauvigerina waiparaensis (Jenkins 1965)

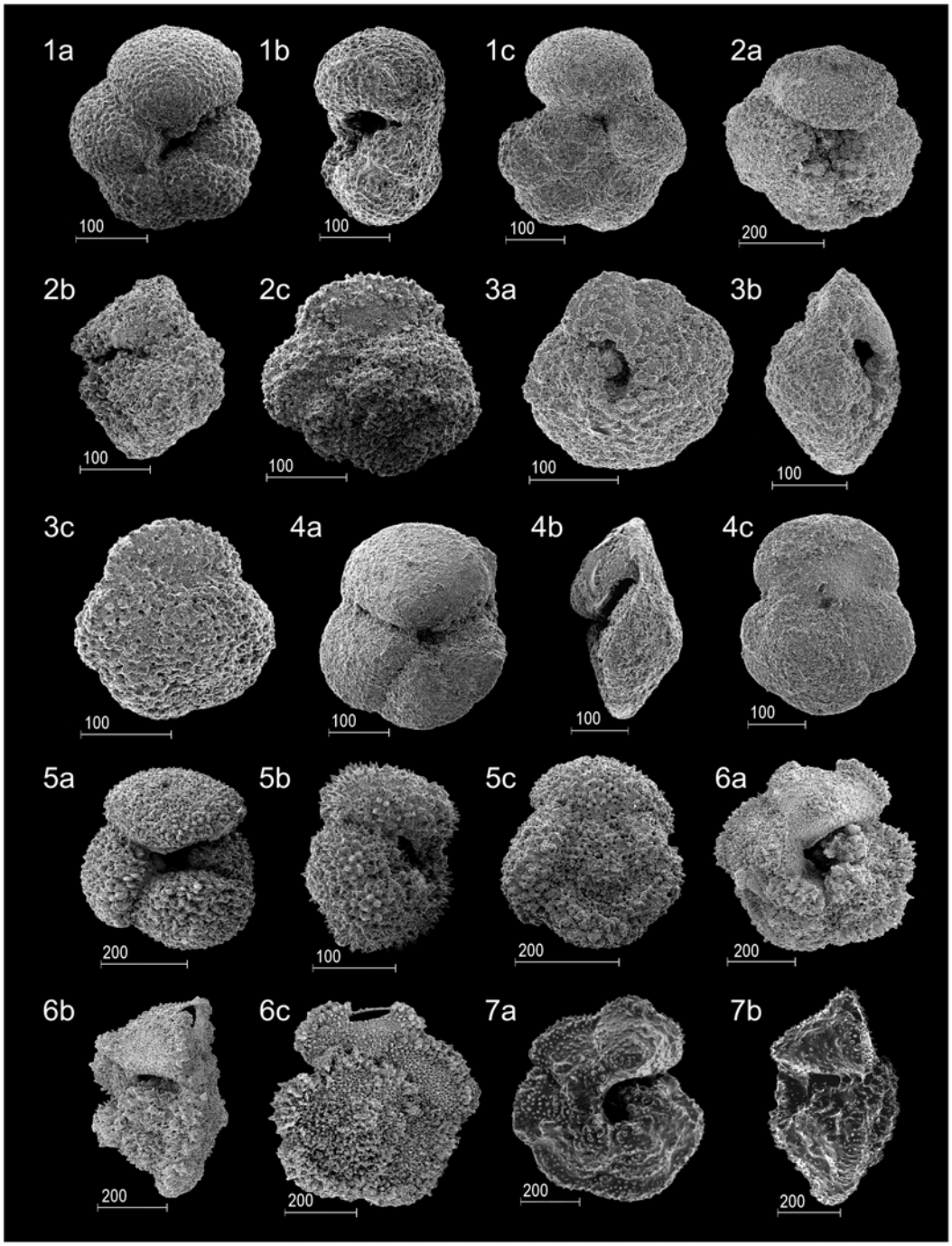

Plate 1. (Scale bars in µm). **Fig. 1).** *Praemurica uncinata* (Bolli, 1957). **a)** Umbilical view, CPC 35739, sample 762-37X-2, 97-100 cm; **b)** side view, CPC 25740, sample 762C-37X-2, 97-100 cm; **c)** spiral view, CPC 35741, sample 762C-37X-2, 97-100 cm. **Fig. 2).** *Morozovella angulata* (White, 1928). **a)** Umbilical view, CPC 35742, sample 762C-33X-1,100-104 cm; **b)** side view, CPC 35743, sample 762C-33X-2, 100-104 cm; **c)** spiral view, CPC 35744, sample 762C-34X-3, 95-99 cm. **Fig. 3).** *Igorina albeari* (Cushman & Bermúdez, 1949). **a)** Umbilical view, CPC 35745, sample 762C-31X-3, 97-101 cm; **b)** side view, CPC 35746, sample 762C-33X-4, 95-99 cm; **c)** spiral view, CPC 35747, sample 762C-31X-2, 100-104 cm. **Fig. 4).** *Globanomalina pseudomenardii* (Bolli, 1957*a*). **a)** Umbilical view, CPC 35748, sample 762C-31X-2, 100-104 cm; **b)** side view, CPC 35749, sample 762C-32X-2, 100-104 cm; **c)** dorsal view, CPC 35750, sample 762C-29X-3, 46-50 cm. **Fig. 5).** *Acarinina soldadoensis* (Brönnimann, 1952). **a)** Umbilical view, CPC 35751, sample 762C-17X-4, 50-55 cm; **b)** side view, CPC 35752, sample 762C-18X-2, 90-95 cm; **c)** dorsal view, CPC 35753, sample 762C-17X-4, 50-55 cm. **Fig. 6).** *Morozovella velascoensis* (Cushman, 1925). **a)** Umbilical view, CPC 35754, sample 762C-31X-3, 97-101 cm; **b)** side view, CPC 35754, sample 762C-31X-3, 97-101 cm; **c)** dorsal view, CPC 35754, sample 762C-31X-3, 97-101 cm. **Fig. 7).** *Morozovella formosa* (Bolli, 1957*b*). **a)** Umbilical view, CPC 35755, sample 762C-22X-3, 49-54 cm; **b)** side view, CPC 35755, sample 762C-22X-3, 49-54 cm.

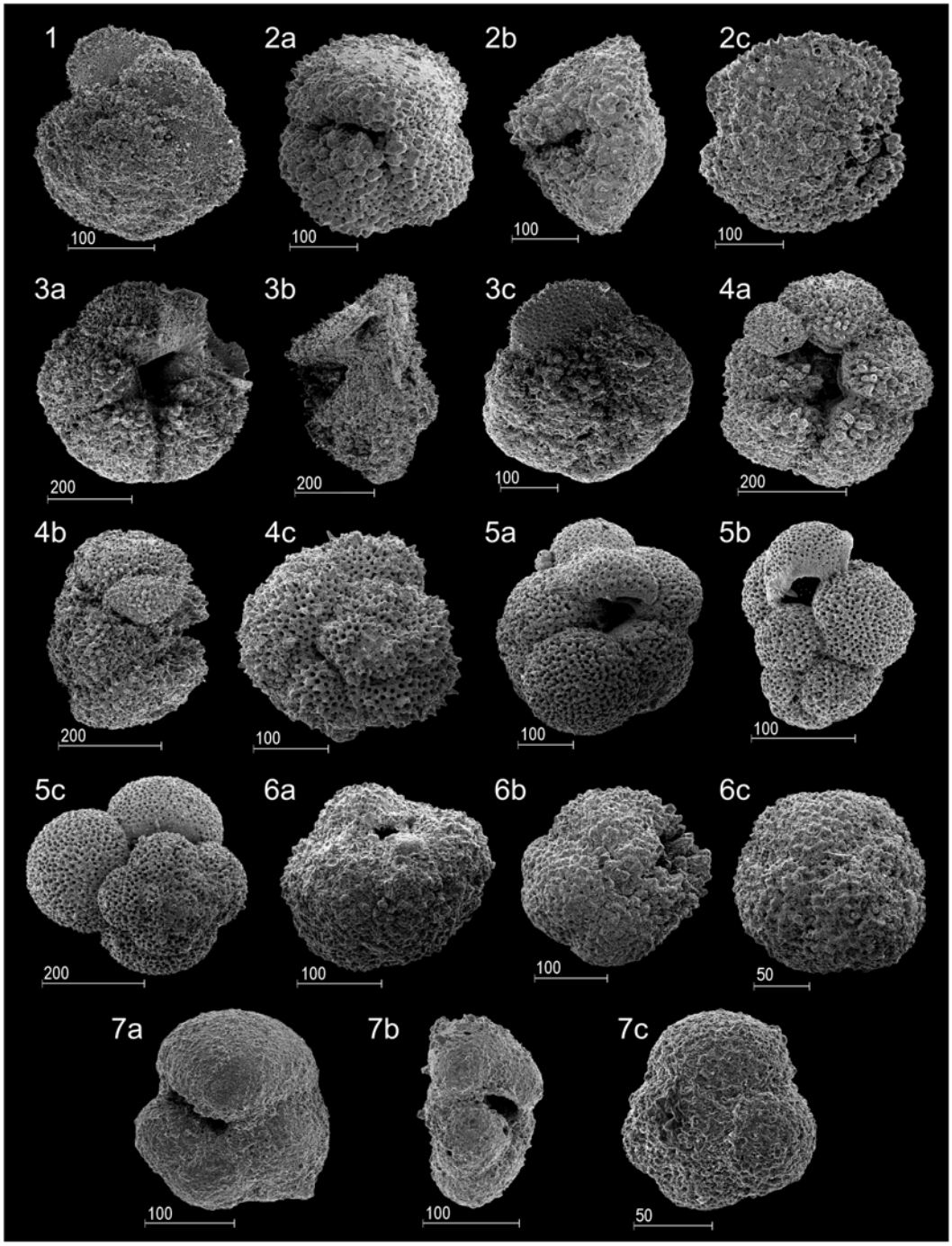

Plate 2. (Scale bars in µm). **Fig. 1).** *Morozovella formosa* (Bolli 1957*b*). Dorsal view, CPC 35756, sample 762C-22X-3, 49-54 cm. **Fig. 2).** *Morozovella lensiformis* (Subbotina, 1953). **a)** Umbilical view, CPC 35757, sample 762C-23X-2, 50-54 cm; **b)** side view, CPC 35758, sample 762C-23X-2, 50-54 cm; **c)** dorsal view, CPC 35759, sample 762C-23X-2, 50-54 cm. **Fig. 3).** *Morozovella aragonensis* (Nuttall, 1930). **a)** Umbilical view, CPC 35760, sample 762C-17X-2, 50-55 cm; **b)** side view, CPC 35761, sample 762C-17X-5, 49-54 cm; c) dorsal view, CPC 35762, sample 762C-17X-5, 49-54 cm. **Fig. 4).** *Acarinina cuneicamerata* (Blow, 1979). **a)** Umbilical view, CPC 35763, sample 762C-19X-4, 50-55 cm; **b)** side view, CPC 35763, sample 762C-19X-4, 50-55 cm; **c)** dorsal view, CPC 35764, sample 762C-19X-3, 50-54 cm. **Fig. 5).** *Guembelitrioides higginsi* (Bolli, 1957*b*). **a)** Umbilical view, CPC 35765, sample 762C-16X-4, 30-35 cm; **b)** side view, CPC 35766, sample 762C-16X-4, 30-35 cm; **c)** dorsal view, CPC 35767, sample 762C-16X-4, 30-35 cm. **Fig. 6).** *Acarinina subsphaerica* (Subbotina, 1947). **a)** Umbilical view, CPC 35768, sample 762C-31X-3, 97-101 cm; **b)** side view, CPC 35769, 762C-31X-6, 97-101 cm; **c)** dorsal view, CPC 35770, sample 762C-32X-2, 100-104 cm. **Fig. 7).** *Globanomalina australiformis* (Jenkins, 1965). **a)** Umbilical view, CPC 35771, sample 762C-31X-3, 97-101 cm; **b)** side view, CPC 35772, sample 762C-31X-3, 97-101 cm; **c)** dorsal view, CPC 35773, sample 762C-30X-3, 96-100 cm.

Table 1. Barium and major elements, Hole 762C

Sample	Depth (mbsf)	Ba ppm	SiO2 %	TiO2 %	Al2O3 %	Fe2O3T %	MnO %	MgO %	CaO %	Na2O %	K2O %	P2O5 %	SO3 %	LOI %	SUM %
762C-17X2 50-55	314.50	913.00	8.97	0.09	1.66	1.69	0.01	0.56	45.99	0.75	0.44	0.07	0.15	39.91	100.30
762C-18X2 90-95	324.40	596.00	5.71	0.05	0.91	0.86	0.01	0.36	48.93	0.83	0.31	0.08	0.12	41.61	99.79
762C-19X2 50-55	333.50	588.00	6.79	0.05	1.11	0.92	0.01	0.37	47.31	0.91	0.37	0.07	0.19	41.19	99.28
762C-20X2 50-55	343.00	1090.00	7.85	0.08	1.14	0.92	0.02	0.39	47.02	0.90	0.41	0.07	0.16	40.82	99.78
762C-20X4 40-45	345.90	703.00	6.89	0.05	0.90	1.58	0.03	0.34	47.48	0.82	0.31	0.06	0.86	39.37	98.70
762C-21X2 48-53	352.48	1154.00	12.54	0.11	2.24	1.63	0.01	0.56	43.18	0.88	0.72	0.10	0.15	38.20	100.32
762C-22X-2 50-55	362.00	782.00	9.41	0.10	1.67	1.19	0.02	0.53	46.28	0.63	0.29	0.08	0.14	39.61	99.96
762C-22X-6 47-51	367.97	617.00	6.26	0.06	1.00	0.73	0.02	0.37	48.75	0.53	0.23	0.06	0.16	41.11	99.29
762C-23X2 50-54	371.50	742.00	13.88	0.16	3.00	1.52	0.01	0.60	41.74	0.87	0.69	0.08	0.13	37.20	99.88
762C-24X1 49-53	379.49	587.00	9.57	0.09	2.05	1.31	0.02	0.45	45.78	0.72	0.47	0.08	0.33	39.16	100.04
762C-25X2 50-54	390.50	552.00	7.83	0.07	1.55	0.95	0.01	0.43	47.69	0.64	0.24	0.06	0.11	40.44	100.02
762C-25X-4 49-53	393.49	716.00	14.25	0.16	3.36	1.97	0.01	0.73	41.29	0.80	0.49	0.08	0.12	36.77	100.02
762C-26X2 50-54	400.00	719.00	9.94	0.09	2.24	1.04	0.03	0.54	45.87	0.65	0.35	0.08	0.12	39.15	100.09
762C-26X-3 36-41	401.36	657.00	11.81	0.09	2.22	1.09	0.02	0.54	44.63	0.63	0.33	0.07	0.12	38.46	100.01
762C-27X-1 100-104	403.50	657.00	18.85	0.19	4.18	2.42	0.01	0.87	37.94	0.89	0.57	0.09	0.39	34.65	101.04
762C-27X-2 104-108	405.04	650.00	13.67	0.14	2.75	1.35	0.03	0.61	42.93	0.64	0.38	0.08	0.10	37.17	99.86
762C-27X-3 95-99	406.45	665.00	13.96	0.14	2.72	1.22	0.03	0.62	43.15	0.63	0.38	0.08	0.11	37.44	100.47
762C-27X-4 95-99	407.95	686.00	15.66	0.12	2.42	1.24	0.02	0.60	42.57	0.61	0.27	0.09	0.12	36.94	100.65
762C-28X1 104-107	413.04	452.00	10.78	0.11	2.74	1.05	0.00	0.66	44.85	0.50	0.29	0.09	0.21	38.74	100.02
762C-28X2 10-12	413.60	495.00	9.89	0.09	1.80	0.65	0.01	0.47	46.57	0.45	0.18	0.07	0.20	39.34	99.71
762C-29X-1 48-52	421.98	598.00	6.21	0.08	1.16	0.48	0.01	0.37	49.70	0.37	0.14	0.06	0.26	41.01	99.84
762C-29X2 49-53	423.49	532.00	8.96	0.08	2.03	0.67	0.01	0.51	47.11	0.51	0.23	0.08	0.14	39.84	100.17
762C-29X3 46-50	424.96	439.00	6.49	0.05	1.33	0.41	0.01	0.33	49.17	0.49	0.17	0.06	0.11	41.19	99.82
762C-30X1 101-105	432.01	358.00	3.14	0.03	0.71	0.23	0.01	0.29	51.78	0.44	0.08	0.05	0.12	42.73	99.61
762C-30X2 100-104	433.50	385.00	5.99	0.02	0.79	0.21	0.01	0.26	49.71	0.51	0.11	0.06	0.08	41.70	99.46
762C-30X-4 66-70	437.26	632.00	11.32	0.13	2.84	1.03	0.01	0.62	44.36	0.67	0.35	0.12	0.36	38.06	99.87
762C-31X-1 100-104	441.50	433.00	10.20	0.08	1.73	0.72	0.01	0.41	46.64	0.55	0.25	0.08	0.14	39.18	99.98
762C-31X2 100-104	443.00	464.00	7.47	0.07	1.50	0.55	0.01	0.38	48.33	0.44	0.19	0.07	0.12	40.55	99.67
762C-31X-3 97-101	444.47	395.00	6.20	0.05	1.19	0.40	0.01	0.29	49.56	0.55	0.18	0.05	0.07	41.16	99.71
762C-32X-2 100-104	452.50	395.00	6.14	0.06	1.29	0.48	0.01	0.31	49.67	0.53	0.24	0.07	0.07	41.08	99.95
762C-33X2 100-104	462.00	617.00	6.04	0.05	1.35	0.49	0.01	0.30	49.18	0.42	0.22	0.07	0.14	41.03	99.30
762C-34X-2 100-104	471.50	478.00	6.74	0.06	1.33	0.45	0.01	0.31	49.33	0.51	0.24	0.06	0.09	40.59	99.70
762C-35X1 90-95	479.40	507.00	9.32	0.10	2.28	0.90	0.01	0.50	46.28	0.55	0.32	0.07	0.33	39.30	99.96
762C-36X-1 17-21	488.17	623.00	8.08	0.07	1.98	0.71	0.01	0.44	48.14	0.54	0.34	0.06	0.18	39.81	100.36
762C-37X3 97-101	501.47	749.00	16.94	0.19	3.87	1.81	0.02	0.77	39.67	0.74	0.54	0.07	0.13	35.36	100.11

Table 2. Barium and major elements, Hole 761B

Sample	Depth (mbsf)	Ba ppm	SiO2 %	TiO2 %	Al2O3 %	Fe2O3T %	MnO %	MgO %	CaO %	Na2O %	K2O %	P2O5 %	SO3 %	LOI %	SUM %
761B-16X-1 (3-7)	122.73	617	9.12	0.05	1.67	2.93	0.009	0.45	44.43	0.77	0.43	0.07	1.40	38.78	100.11
761B-16X-1 (80-84)	123.50	389	8.41	0.08	1.89	0.74	0.009	0.50	46.21	0.95	0.51	0.09	0.18	39.86	99.41
761B-16X-2	124.72	352	8.86	0.07	2.02	0.77	0.013	0.54	46.19	0.89	0.52	0.08	0.16	39.15	99.27
761B-16X-3	126.22	622	6.65	0.07	1.48	0.56	0.010	0.45	48.16	0.72	0.36	0.06	0.17	40.49	99.17
761B-16X-4	127.72	576	7.58	0.07	1.82	0.62	0.007	0.52	47.16	0.80	0.40	0.06	0.16	40.07	99.28
761B-17X-1	132.90	505	8.25	0.06	1.18	0.45	0.005	0.46	47.17	0.81	0.14	0.05	0.18	40.65	99.40
761B-17X-2	134.40	742	10.96	0.05	1.29	0.49	0.008	0.49	45.54	0.83	0.15	0.05	0.19	39.76	99.79
761B-17X-3	136.24	412	7.89	0.03	1.22	0.51	0.009	0.50	47.47	0.84	0.16	0.06	0.19	40.73	99.60
761B-17X-4	137.24	511	6.78	0.04	1.13	0.42	0.007	0.46	48.29	0.80	0.14	0.06	0.18	41.37	99.67
761B-17X-5	138.76	510	7.98	0.06	1.52	0.60	0.008	0.55	47.12	0.83	0.18	0.07	0.18	40.79	99.87
761B-17X-6	140.22	637	7.78	0.07	1.34	0.59	0.006	0.50	47.20	0.81	0.17	0.08	0.19	40.78	99.52
761B-17X-7	141.30	633	7.59	0.07	1.55	0.61	0.009	0.56	47.27	0.73	0.19	0.07	0.18	40.58	99.40
761B-18X-1	142.25	620	8.21	0.07	1.46	0.54	0.010	0.54	46.96	0.77	0.17	0.07	0.18	40.50	99.47
761B-18X-2	144.40	575	7.58	0.07	1.34	0.49	0.006	0.51	47.50	0.76	0.16	0.06	0.18	40.73	99.38
761B-18X-3	145.50	696	9.48	0.08	1.54	0.63	0.007	0.59	45.93	0.80	0.20	0.07	0.18	39.85	99.34
761B-18X-4	146.80	601	8.96	0.08	1.48	0.59	0.007	0.55	46.38	0.77	0.18	0.07	0.17	41.05	100.30
761B-18X-5	148.25	508	6.87	0.08	1.16	0.45	0.004	0.47	48.06	0.75	0.15	0.06	0.17	41.20	99.42
761B-18X-6	149.75	612	7.18	0.07	1.06	0.33	0.006	0.45	48.17	0.71	0.13	0.06	0.17	41.02	99.35
761B-18X-7	150.80	396	7.42	0.05	1.30	0.48	0.010	0.50	47.91	0.70	0.19	0.06	0.15	40.77	99.53
761B-19X-2	153.50	590	5.66	0.08	1.41	0.47	0.010	0.52	48.80	0.66	0.24	0.06	0.16	41.14	99.21
761B-19X-5	157.30	612	7.26	0.07	1.75	0.64	0.013	0.59	47.67	0.65	0.34	0.07	0.17	40.36	99.59
761B-20X-5	167.20	534	21.53	0.10	2.05	0.91	0.011	0.54	38.39	0.95	0.56	0.07	0.16	34.34	99.60

APPENDIX C.

Table 1. Carbonate concentrations (wt%) for Dee Stream. Shaded areas indicate BETM. M = marl, L = limestone.

NZ Fossil Record #		Distance (thickness above base) (m)	Carbonate concentrations (wt%)
P30/f1243	M	88.2	68.4
P30/f1247	M	83.4	75.5
P30/f1248	M	80.1	64.5
P30/f1249	M	77.2	68.2
P30/f1256	M	71.9	72.6
P30/f1268	L	68.6	84.8
P30/f1269	M	68.4	74.0
P30/f1271	L	68.3	88.2
P30/f1274	L	64.2	81.4
P30/f1278	L	60.9	68.2
P30/f1282	L	55.7	75.4
P30/f1284	M	52.2	62.3
P30/f1287	L	50.3	57.6
P30/f1287	L	46.1	60.5
P30/f1289	L	41.6	60.2
P30/f1290	L	36.8	74.6
P30/f1291	L	31.9	80.2
P30/f1293	L	27.1	75.9
P30/f1294	M	27.0	64.8
P30/f1295	L	26.9	73.6
P30/f1296	M	26.8	61.1
P30/f1297	L	26.6	69.9
P30/f1298	M	26.5	52.8
P30/f1299	M	26.2	72.2
P30/f1301	L	26.0	71.1
P30/f1303	L	25.3	73.3
P30/f1305	M	23.5	78.3
P30/f1306	L	23.4	77.4
P30/f1307	M	23.3	75.9
P30/f1308	L	22.7	75.4
P30/f1309	M	21.8	79.8
P30/f1310	L	18.1	72.5
P30/f1311	M	17.4	78.9
P30/f1313	M	14.3	45.2
P30/f1314	L	13.8	78.1
P30/f1315	M	11.0	73.5
P30/f1316	L	10.1	77.1
P30/f1322	M	5.9	85.0
P30/f1327	L	5.2	85.1
P30/f1331	L	1.1	70.7
P30/f1333	L	0.4	60.9
P30/f1334	L	0.1	81.0
P30/f1336	L	-0.1	39.1
P30/f1337	M	-0.3	65.6
P30/f1339	M	-1.2	86.8
P30/f1342	M	-4.1	81.9
P30/f1343	L	-4.7	85.4